Development and Characterisation of HEK293T Cell Expression Systems for Enhanced Production of Recombinant AAV Viral Vectors

2021

Sarah Martin

A thesis submitted to the University of Kent for the degree of Doctor of Philosophy in Biochemistry

University of Kent

School of Biosciences

Declaration

No part of this thesis has been submitted in support of an application for any degree or other qualification of the University of Kent, or any other University or institution of learning.

Sarah Martin **Date: 28/05/21**

Abstract

Viral vectors are a leading method of gene transfer for the delivery of genetic material in gene therapy applications. Although there are a number of different viral vector systems utilised for such applications, in 2020 over 35% of ongoing gene therapy clinical trials utilised recombinant adeno-associated virus (rAAV) vectors for gene transfer. rAAV is particularly attractive for gene therapy applications as there are a number of serotypes which can be used to target different tissues, it does not integrate into the genome and is regarded as safe. Gene therapy treatments utilising rAAV vectors typically require around 10^{15} vectors per treatment and are expensive, in the range of hundreds of thousands of pounds or more per treatment. One of the major contributors to the cost is inefficient production processes with the genome packaging during production of rAAV vectors often being low, resulting in the formation of "empty" or genome lacking viral vectors. Current production methods include the transient co-transfection of three plasmids, a packaging plasmid containing the AAV *Rep* and *Cap* genes, a helper plasmid containing the adenoviral helper genes and the transgene plasmid, whereby the therapeutic gene of interest is flanked by inverted terminal repeats, into a E1a expressing cell line such as HEK293T. There are four Rep proteins, Rep78, Rep68, Rep52 and Rep40, involved in the replication of the virus and three cap proteins, VP1, VP2 and VP3, the structural proteins which form the viral capsid. Assembly activating protein (AAP) is a protein derived from the *Cap* gene too and promotes stability and the interactions between AAV viral proteins. It is essential for the production of AAV capsids from a number of serotypes including serotype 2. The aim of the work in this thesis was to investigate engineering of a HEK293T host cell line to stably and constitutively express rAAV viral proteins and determine the impact on the production and genome packaging of rAAV. Initial investigations looked to generate HEK293T cell pools stably expressing the *Rep* and/or *Cap* genes such that these did not have to be transiently transfected during production. It was not possible to isolate cell pools expressing either, or both, of these genes and proteins, presumably due to the toxic nature of some of the viral proteins. Subsequently, the work describes the generation and characterisation of HEK293T cell pools and clonal cell lines stably expressing AAP and the impact on the production of rAAV2 containing a GFP genome using a triple co-transfection method. Engineered expression of AAP did not impact the growth phenotype of HEK293T cell pools or clones compared to the original host cell line and immunofluorescence analysis showed the AAP localised in the nucleolus. Use of an ATG translation start codon instead of the native CTG resulted in isolation of pools and lines with greater recombinant AAP expression than from the CTG codon. Subsequent packaging of rAAV2 with a model GFP genome in the HEK293T AAP expressing cells compared to the original host was then analysed after production by ELISA and qPCR to determine total particles and viral genome titres, respectively. Of the eight clonal AAP expressing HEK293T cell lines isolated, three that generally had higher AAP expression than the others produced viral vector numbers with similar particle titres to the control host but with statistically significantly increased genome packaging efficiency compared to the HEK293T host control cell line. Transduction assays confirmed the functionality of the particles derived from these cell lines was equivalent to those from the original host, ultimately showing that these particles were able to transduce cells to the same capacity as those generated by the HEK293T cell line. In conclusion, the data presented here shows that the engineering of HEK293T cells to constitutively express AAP from AAV serotype 2 can result in the generation of host cells with enhanced ability to genome package rAAV particles resulting in increased yields of functional rAAV than from the original host cell line.

Acknowledgements

I would first like to give a massive thank you to Prof. Mark Smales for the opportunity to work toward my PhD within the Smales group. I would like to thank him for his constant help, guidance, encouragement, and support over the last few years. I have really valued and enjoyed my time in the Smales lab and gained valuable experience on a project I have thoroughly enjoyed. I would also like to thank Dr. Vera Lukashchuk for all her input, help and support during my PhD and for all her time given to proof reading not only my thesis but every piece of written work to date. It was greatly appreciated. I would also like to thank Dr. Darrell Sleep and Prof. Dan Smith for all the guidance and supervision throughout my PhD; to Cobra Biologics and the University of Kent for funding me and hosting me.

To Mr. Ian Brown, Dr. James Budge, Dr. Emma Hargreaves Dr. Cat Hogwood, Dr. Tanya Knight, Dr. Matt Lee, and Ms. Joanna Roobol at the University of Kent for all their help and advice with immunofluorescence, confocal microscopy, electron microscopy, qPCR, molecular cloning. Without their help and guidance this work would not have been possible. I would like to thank all members, past and present, of the Smales Lab and the School of Bioscience for their support and friendship, throughout my PhD, it has been a pleasure working with you all. I would especially like to thank Laura Dyball, Dr. Emma Hargreaves Dr. Cat Hogwood, Dr. Tanya Knight, Phoebe Lee, Dr. Andy Martin, Dr. Angelica Ozanne, Jo "J Roobs" Roobol, and finally Dr. Natalie Talbot; Thank you all for your kindness and support throughout. Thank you for injecting some fun and nonsense into the days in the lab, into the early morning starts and for continuing to support me and my caffeine addiction. You all made the tough times a little better and the good times great. Thank you for the good times both in the lab and away from the lab. I would also like to thank Liam McCarthy and Louis Darton, we started our PhD journeys together, thank you for joining me on the journey and for the friendship and support through the ups and downs.

I believe my family need a massive shout out here, to Keith, Martina, Amy, Bethan and Steve, for their unconditional love, support and encouragement throughout, I could not have done this without you. Thank you for putting up with the phone calls and too few trips home, for all the care packages and tea bags sent. To Sarah Bowring, Laura Collins and Madeleine Lawler for all the kindness, support and friendship throughout. A massive thank you to Sam Todd, for all the love, care, patience, and encouragement throughout, thank you for being there for me. You have been a rock! I would also like to thank Lynne and David Todd for welcoming me into their home during the first Covid lockdown and for all the support. Thank you all!

In an odd fashion, I would like to thank the coronavirus pandemic, it made the last year and a half of my PhD one of the most stressful experiences to date but I have finished stronger despite it.

This thesis was brought to you by thousands of cups of Lyons Tea supplied by Martina and Keith Martin, Amy Martin and Sam Todd.

Table of Contents

List of Abbreviations

AAP	Assembly Activating Protein
AAV	Adeno-Associated virus
Ad	Adenovirus
AEX	Anion exchange
ALS	Amyotrophic Lateral Sclerosis
BEV	Baculovirus Expression System
bP	Base Pairs
BSA	Bovine Serum Albumen
CAR-T	Chimeric Antigen Receptor T cell
cDNA	Complementary DNA
CF	Cystic Fibrosis
cFIX	Canine Factor IX
CHO	Chinease Hamster Ovary
CRISPR	Clustered Regularly Interspaced Short Palindromic Repeats
DAPI	4',6-Diamidino-2-Phenylindole
ddPCR	Droplet Digital PCR
DMSO	Dimethyl sulfoxide
DNA	Deoxyribonucleic acid
DTT	Dithiothreitol
E. coli	Escherichia coli
EDTA	Ethylenediaminetetraacetic acid
ELISA	Enzyme Linked Immunosorbent Assay
EMA	European Medicines Agency
FDA	US Food and Drug Administration
GFP	Green Fluorescent Protein
GOI	Gene of Interest
gRNA	Guide RNA
hBG	Human Beta globin
HDR	Homology Directed Repair

HEK	Human Embryonic Kidney
HeLa	Henrietta Lacks
HRP	Horseradish Peroxidase
HSC	Hematopoietic stem cells
HSV	Herpes Simplex Virus
IEX	Ion exchange
IgG	Immunoglobin G
ITR	Inverted Terminal Repeats
kDa	Kilo Daltons
LB	Lysogeny Broth
LTR	Long terminal repeats
LV	Lentivirus
MCS	Multiple Cloning Site
MFDS	Ministry of Food and Drug Safety
MLTF	Major late transcription factor
MOI	Multiplicity of Infection
mRNA	Messenger RNA
NHEJ	Non homologous end joining.
NLS	Nuclear localisation signal
NoLS	Nucleolar localisation signal
ORF	Open Reading Frame
OTC	Ornithine Transcarbamylase
PAGE	Polyacrylamide Gel Electrophoresis
PBS	Phosphate Buffered Saline
PCR	Polymerase Chain Reaction
pDNA	Plasmid DNA
PDT	Population doubling time.
PEI	Polyethylenimine
pI	Isoelectric point
PTM	Posttranslational modifications
qPCR	qualitative Polymerase Chain Reaction

rAAV	Recombinant AAV
RBE	Rep Binding Element
rcf	Relative centrifugal force
RNAi	RNA Interface
rpm	Revolutions per minute
SCID	Severe Combined Immunodeficiency
SDS	Sodium Dodecyl sulfate
SEC	Size Exclusion Chromatography
Sf9	Spodoptera frugiperda
siRNA	Short Interfering RNA
SOB	Super Optimal Broth
SOC	Super Optimal Broth with Catabolite Repression
ss	Single Stranded
TALENS	Transcription activator like effector nucleases
TC	Total Cells
TEM	Transmission Electron Microscopy
TGF-B1	Transforming growth factor Beta 1.
TP	Total Particles
TRS	Terminal Resolution site
TSAP	Thermosensitive alkaline phosphate
VA RNA	Viral Associated RNAs
VC	Viable Cells
VCC	Viable cell concentration
VG	Viral Genome
VIP	Vectored immune-prophylaxis
ZFN	Zinc Finger Nucleases

List of Figures

Appendix Figure XV *Schematic showing the vector map for the cloning vector pcDNA3.1 ATGSTOP.*

Appendix Figure XVI *Electron microscopy of purified "Empty" rAAV particles lacking a transgene.*

List of Tables

Chapter 1

Introduction

1.1 Gene Therapy

1.1.1 What is Gene Therapy?

Gene therapy is the introduction of exogenous genetic material, or repair of endogenous genetic material, to treat or cure genetic disorders (Anguela & High, 2019; Gonçalves & Melo Alves Paiva, 2017). This can involve a variety of replacement or repair targeted methods such as replacing a disease-causing gene (usually a mutated/defective gene) with a non-disease causing copy, inactivating a disease-causing gene, or introducing a new functional gene to the body to help treat a disease (Naldini, 2015). This is not a straightforward concept due to the fact that the gene transfer method must overcome cellular defence mechanisms and barriers, all the while not disrupting other 'usual' cellular gene expression or mechanisms that have a regulatory role. The therapeutic must also correct enough cells to reverse the condition and evade an immune response while eliciting a long-term benefit to the patient. The gene should also be targeted to be delivered to those tissues or cells where the gene defect needs correcting. In general, gene therapy is used for the treatment of genetic disorders caused by a faulty or missing gene(s) where the introduction of fully functional copies of an exogenous gene replaces the defective gene. It can be used to introduce nucleic acids, typically DNA and RNA, or other nucleic acid species such as siRNAs to knockdown the effects of over-expressed genes (C. Li & Samulski, 2020). Examples of diseases that gene therapy could/can provide potential treatments for include, but are not limited to, cystic fibrosis, muscular dystrophy, haemophilia, combined immuno-deficiency syndromes and a number of cancers (Cotrim & Baum, 2008).

The definition of a gene therapy therapeutic varies. For example, the European Medicines Agency (EMA) defines gene therapies as '*a biological medicinal product that either (a) contains an active substance which contains/consists of a recombinant nucleic acid used in humans with the aim to regulate, repair, replace, add or delete a genetic sequence, or (b) that its therapeutic effect relates directly to the recombinant nucleic acid sequence it contains or the product of its genetic expression of the sequence*' ("REGULATION (EC) No 1394/2007 OF THE EUROPEAN PARLIAMENT AND OF THE COUNCIL of 13 November 2007 on advanced therapy medicinal products and amending Directive 2001/83/EC and Regulation (EC) No

726/2004," 2007; Wirth, Parker, & Ylä-Herttuala, 2013). On-the-other-hand, the US Food and Drug Administration (FDA) defines them '*as products that mediate their effects by transcriptional or translation of transferred genetic material and/or by integrating into the host genome and that are administered as nucleic acids, viruses or genetically engineered microorganisms*' ("Human Gene Therapy for Rare Diseases- Guidance for Industry," 2020; "REGULATION (EC) No 1394/2007 OF THE EUROPEAN PARLIAMENT AND OF THE COUNCIL of 13 November 2007 on advanced therapy medicinal products and amending Directive 2001/83/EC and Regulation (EC) No 726/2004," 2007; Wirth et al., 2013).

Current gene therapy strategies are generally considered either *in vivo* or *ex vivo* strategies. *In vivo* methods introduce the genetic material directly to the patient target tissue(s). *Ex vivo* strategies involve the harvest of a patients target cells, the cells are then modified prior to being reintroduced to the patient (C. Li & Samulski, 2020). Regardless of which strategy is utilised, gene therapy requires knowledge of both the gene or genes responsible for causing the disease and of a therapeutic "healthy" gene. The therapeutic gene is then produced and delivered to a patient. This can be achieved by direct delivery or, most widely, using viral vector-based vector delivery systems. Direct delivery or non-viral gene delivery systems include the use of electroporation, ballistic gene guns, sonoporation and injection. Viral based methods involve the use of viral vectors (Ramamoorth & Narvekar, 2015; Sung & Kim, 2019).

There are two cell types that gene therapy applications need to consider delivery to: Somatic and Germ line. The difference between these ultimately comes down to whether the Gene of Interest (GOI) is required to be passed on to future offspring (i.e., is heritable). In germ line gene therapy, a GOI is introduced to the patient germ cells so it is passed on to the next generation whereas in somatic gene therapy a GOI is inserted into a target cell, but the change is not passed on to the patients' offspring. This difference is important, as currently it is only somatic gene therapy that has been legislated for and so no country has yet to legislate for germline gene therapies (Boggio, Knoppers, Almqvist, & Romano, 2019; Mourby & Morrison, 2020).

1.1.1.1 History of Gene Therapy

The concept of gene therapy had been circulating for decades prior to any clinical trials using gene therapy. It is thought that the first discussions around what has since become known

as gene therapy was in 1967 by Marshall Nirenberg when he wrote a paper on the possibility of programming cells "with chemically synthesised messages" (J. H. Lee et al., 2019; Nirenberg, 1967). It wasn't long after this that research into this area began and the first human gene transfer was carried out in 1989 (Roberts, 1989). In 1990, the first research involving gene transfer was published. This study involved the use of a retroviral vector to introduce a neomycin resistance gene into lymphocytes that infiltrate tumours. The study involved five metastatic melanoma patients and ultimately showed the feasibility and safety of gene transfer using retroviral vectors (Cotrim & Baum, 2008; Rosenberg et al., 1990).

A

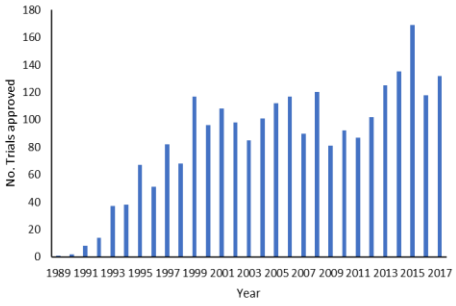

B

Year	Total clinical trial	Haemophilia A	Haemophilia B	rhFVIII	rhFIX	Gene therapy FVIII	Gene therapy FIX
1976-1990	4	0	0	0	0	0	0
1991-2000	17	13	4	3	4	0	0
2001-2005	58	35	13	13	7	0	1
2006-2010	112	71	33	24	8	0	1
2011-2015	195	120	50	40	10	1	5
2016-2019	173	114	58	16	3	10	9

Figure 1.1 A) Number of gene therapy clinical trials yearly up untill 2017, adapted from Ginn et al., 2018. **B)** Distribution of AAV clinical trials between 1976 and 2019, adapted from Pei et al., 2019.

In the last 20-30 years, there has been a rapid increase in the number of gene therapy related clinical trials (Figure 1.1A) looking at inherited diseases, cancers and chronic infections (Ginn, Amaya, Alexander, Edelstein, & Abedi, 2018; Pei, Han, & Zhang, 2019). Haemophilia has been a particularly well investigated disease (Figure 1.1B). However, early trials often showed a lack of therapeutic benefit with patients also experiencing a number of adverse reactions. Such reactions were met with scepticism. One of the major issues in early developments was that the delivery vehicles being used were inefficient, failing to exhibit long term expression (Thomas, Ehrhardt, & Kay, 2003). During this time there was thus an interest in further developing gene therapy research, with large investments into its potential and an increase in research activity. Unfortunately, the optimism in the late 1990's and early 2000's around the application of gene therapies was badly damaged.

One of the major setbacks to the field of gene therapy occurred in 1998 when an 18-year-old patient, Jesse Gelsinger, suffering from a mild form of ornithine transcarbamylase (OTC).

He had mutations in this gene, so partook in a clinical trial to test the safety of an adenovirus serotype 5 vector designed to deliver the OTC gene to the patient's liver (Raper et al., 2003). The patient involved in the trial received the highest dosage of the therapy receiving $3.8x10^{13}$ vector particles. Unfortunately, shortly after receiving the gene therapy treatment, he started experiencing adverse effects, resulting in the patient's death due to multi-organ failure within four days of treatment. It was shown post mortem that the delivery of the viral vectors had trigged a major inflammatory response (Thomas et al., 2003). This case was widely publicised and resulted in the FDA and congress holding hearings on clinical gene therapy trials with a stop being placed on all adenoviral clinical trials. This stop has since been lifted as more of the biology around the use of such vectors, and their consequences, was discovered and led to more stringent regulations on all clinical trials (Cotrim & Baum, 2008).

Research did however, persisted in the area due to the potential benefits and less than a year after the death of Jesse Gelsinger, the results of a successful gene therapy trial were published by Cavazzana-Calvo's group. This study involved the successful treatment of children suffering from X-Linked Severe Combined Immunodeficiency (SCID)-XI syndrome, with the children developing a functioning immune system. The study involved the transfer of the gene ϒc cytokine receptor subunit using a retroviral vector into the children's lymphocytes *ex vivo* and once amplified these cells were returned to the patients (Cavazzana-Calvo, 2000; Cotrim & Baum, 2008; Thomas et al., 2003). Unfortunately, subsequently a number of patients involved in the trial developed a leukaemia like disorder, probably caused by the integration of the vector into the LM02 gene in a non-random manner (Cotrim & Baum, 2008; Thomas et al., 2003). These very unfortunate incidents have resulted in extensive research into the use of viral vectors as gene therapy agents and how such responses can be eliminated, and risk reduced. This is discussed further in Section 1.2.

It was not until 2012, when the first gene therapy product, Glybera, was approved for use in Europe. Glybera was a gene therapy product which utilised Adeno-Associated Virus (AAV) as a method of gene delivery. Glybera was approved for the treatment of Lipoprotein lipase deficiency but has since been withdrawn from the market in 2017. Since Glybera, there have been twenty cell and gene therapies approved for treatment worldwide up until 2019 (Table 1.1-1) (Shahryari et al., 2019).

Table 1.1-1 Approved cell and gene therapies. Adapted from (Shahryari et al., 2019)

Product name	**Type of Therapy**	**Developer**	**Approval Authority**	**Approval Year**
Fomivirsen (Vitravene)	CMV Retinitis	Isis Pharmaceuticals with Novartis Opthalmics	USA FDA EMEA	1998 1999
Gendicine	Head and neck squamous cell carcinoma	Shenzhen SiBionoGeneTech	China FDA	2003
Pegaptanib (Macugen)	Neovascular age-related macular degeneration	Eyetech Pharmaceuticals and Pfizer	USA FDA	2004
H101 (Oncorine)	Nasopharyngeal carcinoma	Shanghai Sunway Biotech	China FDA	2005
Rexin-G	Metastatic solid tumours (pancreatic and breast cancer, Osteosarcoma)	Epeius Biotechnologies	Philippine FDA USA FDA	2007 2010
Neovasculgen (PI-VEGF165)	Atherosclerotic peripheral arterial disease	Human Stem Cells Institute	Russian Ministry of Healthcare	2012
Alipogenetiparvovec (Glybera)	Familial LPDL	Amsterdam Molecular Therapeutics	European commission USA FDA	2012 2013
Mipomersen (Kynamro)	Homozygous familial hypercholesterolemia	ISIS Pharmaceuticals	USA FDA	2013
Imlygic	Melanoma, pancreatic cancer	Amgen	USA FDA	2016
Eteplirsen (Exondys 51)	Duchenne muscular dystrophy	Sarepta Therapeutics	USA FDA	2016
Spinraza (nusinersen)	Spinal muscular atrophy	Biogen Ionis Pharmaceuticals inc.	USA FDA EMA	2016 2016
Defibrotide (defibrotide sodium)	Hepatic veno-occlusive disease, sinusoidal obstruction syndrome	Jazz Pharmaceuticals	USA FDA EMA	2017 2018

Luxturna (Voretigene Neparvovecrzyl)	Inherited retinol dystrophies	Novartis	USA FDA EMA	2017 2018
Patisiran (Onpattro)	Familial amyloid polyneuropathy	Alnylam Pharmaceuticals Inc.	USA FDA EMA	2018 2018
Zolgensma (Onasemnogene abeparvovec-xioi)	Spinal muscular atrophy	AveXis/ Novartis	USA FDA	2019
Strimvelis (GSK2696273)	Adenosine deaminase deficiency Severe combined immunodeficiency	GlaxoSmithKline	EMA	2016
Zalmoxis	Hematopoietic stem cell transplantation	MolMed SPAA	EMA	2016
Kymriah (Tisagenlecleucel CTL019)	B-cell precursor acute lymphoblastic leukemia	Novaritis	USA FDA	2017
Yescarta (Axicabtageneciloleucel)	Non-Hodgkin lymphoma, Bcell lymphoma	Kite Pharma Inc.	USA FDA	2017
INVOSSA (TissueGene-C/Tonogenchoncel-L)	Kellgren-Lawrence Grade 3 knee osteoarthritis	TissueGene/ KolonTissueGene	South Korea's Ministry of Food and Drug Safety (MFDS)	2017

1.1.2 Types of Gene Therapy

1.1.2.1 Gene Replacement Therapy

Gene replacement therapy is perhaps currently the most widely studied and utilised approach to gene therapy. This involves the replacement of a faulty gene with that of a functional copy of the gene in question (Gonçalves & Paiva, 2017). This method usually involves the use of a viral vector as a method of introducing the gene of interest into the body and specific cell/tissue. The most commonly used viral vectors used in gene replacement therapies are Adenovirus, Adeno-Associated virus and retrovirus, such as lentivirus (Shirley, de Jong, Terhorst, & Herzog, 2020). Although viral vectors are widely used, gene delivery can be carried out using non-viral vectored methods. The method utilised for

a given gene therapy needs to consider how to target the correct tissue/cell type, efficient delivery/release of the gene of interest, evasion of the immune system and the ability to produce the therapy at a scale that can meet the market need. Gene replacement therapy also requires the replaced gene to be functional for the patient's entire life. Thus, although these treatments are expensive, in theory they can provide a life-time cure and thus prevent expensive hospital or clinic visits or on-going replacement therapy recombinant proteins (e.g., blood clotting factors such as Factor IX, Factor VIII) that are expensive in themselves and usually required for a lifetime.

As explained earlier in this chapter, gene replacement therapies can deliver the therapeutic gene either *in vivo* or *ex vivo*. *In vivo* methods utilise the direct delivery of a gene, usually via a viral vector, specifically systemic delivery or a local delivery. As outlined above, in 2012 the European Medicines Agency approved its first gene replacement therapy, Alipogene tiparvovec (Glybera), a replacement gene therapy utilised for the treatment of lipoprotein lipase deficiency. This was the first ever gene therapy to gain approval (Burnett & Hooper, 2009; L. J. Scott, 2015; Stroes et al., 2008), but due to the high cost of Glybera and the low demand it never received FDA approval and EMA approval was not renewed for this therapy which was withdrawn from the market (Senior, 2017). In 2017, the FDA approved its first *in vivo* gene replacement therapy Voretigene neparvovec (Luxturna). Luxturna is an AAV2 vectored gene replacement therapy to treat retinal dystrophy used to replace the *RPE65* gene (S. Russell et al., 2017; Smalley, 2017). *Ex vivo* gene therapy involves the harvest of a patient's cells, the cells are then cultured in a lab setting alongside the gene carrying vectors. The cells containing the gene of interest are then transplanted back into the patient. *Ex vivo* gene replacement therapies are of interest as they can target the eye and brain specifically (Gregory-Evans, M.A. Emran Bashar, & Tan, 2012).

1.1.2.2 Gene Silencing or Knockdown Therapy

Gene silencing is described as the suppression of gene expression at either a transcriptional or translational level. Gene silencing can be used on a therapeutic level against cancers, neurodegenerative diseases or infectious diseases. One method of gene silencing or knockdown is RNA interference (RNAi), this is the post-translational silencing of gene expression as a result of double stranded RNA (dsRNA) recognising the complementary sequence on an mRNA and either silencing it or targeting it for degradation (Fire et al., 1998; Mocellin & Provenzano, 2004). RNAi was initially identified in *Caenorhabditis elegans* but has been shown to be an evolutionarily conserved process (Barton & Medzhitov, 2002; Fire et

al., 1998). During the process of RNAi, an immature dsRNA is cleaved into a 21-23 nucleotide length sequence known as a short interfering RNA (siRNA), in an ATP dependent manner (Zamore, Tuschl, Sharp, & Bartel, 2000). Gene silencing therapies have the potential as highly personalised therapies specific for mutations or sequences in individual patients.

Current methods involved in gene silencing via siRNA involve the use of viral vectors or nanoparticles. The use of nanoparticles and viral vectors, such as Adenovirus, Adeno Associated Virus or Retrovirus vectors, circumnavigates the high production costs of synthetic siRNAs and the low or variable transfection efficiency of these strategies (Babu et al., 2016; Barton & Medzhitov, 2002; Shen, Buck, Liu, Winkler, & Reske, 2003; Tomar, Matta, & Chaudhary, 2003).

1.1.2.3 Gene Editing Therapy

Initial gene therapy strategies focused on replacement and silencing therapies. In recent years gene editing techniques have advanced greatly. Gene editing therapy involves the insertion, removal or replacement of specific regions in DNA resulting in a therapeutic effect (Maeder & Gersbach, 2016). The discovery that targeted DNA double strand breaks could be used to stimulate cellular repair had a major impact on the field of gene editing. Breaks in DNA can be repaired by either homology directed repair (HDR) or through nonhomologous end joining (NHEJ) (Maeder & Gersbach, 2016; Takata et al., 1998). While there are a number of methods of gene editing, the most widely used are Zinc Finger Nucleases (ZFNs), transcription activator-like effector nucleases (TALENs) and the clustered regularly interspaced short palindromic repeats (CRISPR)/Cas system (Table 1.1-2) (H. Li et al., 2020).

Table 1.1-2 Comparison of gene editing platforms ZFN, TALEN and CRISPR.

	ZFN	**TALEN**	**CRISPR**
Recognition site	Zinc-finger proteins	Tandem repeats of TALE proteins	Single stranded gRNA
Nuclease	Fok1	Fok1	Cas9
Specificity	Tolerates a small no. positional mismatch	Tolerates a small no. positional mismatch	Tolerates multiple consecutive mismatch
Size (kB)	1 kB	3 kB	4.2 kB
Disadvantages	Time consuming, Highly Expensive, Low success rate, Difficulty targeting non-G rich regions	Time consuming, Relatively Expensive, 5' targeted base must be T for each TALEN monomer	Target site must precede a PAM sequence

Regardless of the method of gene editing used, the nucleases and/or gRNA must be introduced into the patient in a safe but efficient manner. One of the major methods for this is the introduction of the nucleases or gRNA through the transfection of plasmid DNA which carries the expression cassettes required, however as with other gene therapies, transfection of plasmid DNA is not ideal due to low transfection efficiency and DNA related cytotoxicity. One method of *ex vivo* gene therapy is the electroporation of nuclease/gRNA encoded mRNA into primary cells such as T cells or hematopoietic stem cells (HSCs). However, viral vectors are still considered the most efficient method for nuclease or gRNA delivery for *ex vivo* delivery. One such approach is the use of lentiviral vectors (see section 1.2 below for detail on different viral vector systems), capable of efficient transduction of cells such as T cells and HSCs. However, lentiviral vectors have been known to integrate into the genome and so integrase deficient lentiviral vectors have also been generated for use in gene editing therapy (Lombardo et al., 2007). Adenoviral vectors have also been utilised for nuclease or gRNA delivery and achieved high transient expression levels (Holkers et al., 2014, 2013; Lombardo et al., 2007).

In vivo gene editing has a number of outstanding challenges. It requires tissue specific targeting and distribution of the vectors, furthermore there is the potential for immunogenic responses to the vectors. Adeno Associated Viral (AAV) vectors as a delivery vessel for *in vivo*

gene editing therapies can help overcome the targeting as AAV has at least 12 naturally occurring serotypes which can target different tissue types such as the liver, eye, nervous system, skeletal and cardiac tissues (Pillay et al., 2017). Due to the number of serotypes which can target different tissues, AAV is considered a good vehicle for the delivery and transfer of nucleases for gene editing (Asokan, Schaffer, & Jude Samulski, 2012). AAV vectors are also good candidates for gene editing therapy due to their ability to stimulate homologous recombination. AAV-mediated gene targeting can enhance the efficiency of homologous replication by inducing targeted double stranded breaks (Gaj, Epstein, & Schaffer, 2016).

1.1.3 Current Gene Therapy Strategies

As outlined above, generally there are two main strategies for the introduction of a gene into a cell, using either a viral vector or a non-viral vector-based approach. The vectors used to deliver genetic material can vary depending on the target tissue and the size of the gene to be delivered (Ramamoorth & Narvekar, 2015). To date most of the research into gene therapy applications utilise a viral vector approach. This is due to their high transduction efficiency and ability to target specific tissues or cells (depending on viral vector approach). In early developments the viral aspect of these posed potential safety concerns, however the generation of 2nd, 3rd and 4th generation vectors lacking essential viral replication genes/proteins and removal of other high-risk components have dramatically reduced the risk. Non-viral vectors are generally considered to have less of a risk than viral vectors (Cotrim & Baum, 2008). Vectors ultimately function to traffic the gene of interest (GOI) into the required cells, tissues and organs throughout the body, acting as the delivery vehicle of the target nucleic acid.

1.1.3.1 Non-Viral Vectors

Non-viral vectors have been shown to have low pathogenicity in comparison to those of viral vectors, are less costly and easier to produce. Gene therapy is typically an expensive therapy, this is evident with the viral vector therapy Glybera, which was taken off the market in part due to its high cost, $1.2 million per patient (Shahryari et al., 2019) . While there are a number of advantages in using non-viral vectors there are also a number of challenges with their use. Non-viral vectors have been shown to have poor efficiency and low expression of transgenes, these drawbacks have long over shadowed their low pathogenicity (Glover, Lipps, & Jans, 2005; Ramamoorth & Narvekar, 2015). There are a number of methods which can be utilised for nucleic acid transfer. These include the use of naked DNA, particle based

and chemical-based methods. Naked DNA typically refers to plasmid DNA in which the target gene has been inserted. Typically these recombinant plasmids are then introduced into target tissue via direct injection (Mali, 2013). Most often non-viral vectors are used in the transfer of small synthetic DNA, plasmid DNA and RNAs (siRNA, shRNA and miRNA) (Midoux, Pichon, Yaouanc, & Jaffrès, 2009).

1.1.3.1.1 Physical Methods

Physical methods facilitate gene transfer by use of force to cross cell membranes. Physical methods of gene transfer for gene therapy include microinjection, ballistic gene delivery, sonoporation, electroporation and laser irradiation. Most methods of cell entry for nucleic acids utilise endocytosis; once inside the cells the nucleic acids must avoid degradation while moving through the cytoplasm (Khalil, Kogure, Akita, & Harashima, 2006; Mellott, Forrest, & Detamore, 2013). Physical methods of gene delivery have been shown to effectively transfect *in vivo, ex vivo* and *in* vitro primary cells, stem cells and progenitor cells. Unfortunately, physical methods of gene transfer are extremely traumatic to the cells as they force the nucleic acids through the cell membrane and into the cytoplasm, this can result in cell death, via apoptosis.

Microinjection of nucleic acids is a method whereby nucleic acids are injected directly into the nucleus of cells. This is one of the most direct methods of physical entry into the cell. Microinjection via microneedles have been used for drug delivery and can be utilised for gene therapy (Dean, 2006; Mellott et al., 2013; Prausnitz, 2004; Prausnitz & Langer, 2008; Valsalakumari et al., 2013). Microinjection is highly inefficient, transfection of cells on a large-scale format would require more than physically possible via microinjection. Despite this, there are currently a number of therapeutic targets being studied for the treatment of sight loss. One such treatment involves microinjection of sgRNA for the correction of the Pde6b gene in mouse retina (J. H. Lee et al., 2019; Z. Wu et al., 2015)

Ballistic gene delivery involves the nucleic acid been projectiled into the nucleus of the cell using a “gene gun”. This approach was originally described by Sanford *et al* and is a needle-less method of physical gene delivery initially used for the transfection of plant cells using DNA coated metal particles at a velocity of about 1000-2000 ft/sec (Sanford, John, Klein, Wolf, & Allen, 1987). This method has been refined over the years and been commercialised for use in delivering DNA or RNA to mammalian cells (N. S. Yang, Burkholder, Roberts, Martinell, & McCabe, 1990). Genetic material is delivered directly to cells out of a pressurised ballistic device (Gene Gun). In a study by Udvardi *et al.* gold particles coated in a plasmid

expressing the LacZ reporter gene were transported via a gene gun into skin cells such as keratinocytes and single cells in the dermis. Expression was detected 48 h post bombardment. Furthermore, the use of gene gun delivery of nucleic acids such as *Dystrophin* to skeletal muscles *in vivo* has been described (Zelenin et al., 1997). Zelenin *et al.* coated gold/tungsten particles with 20 µg of plasmid *Dystrophin* and projected these into the cells from 10 cm distance. *Dystrophin* was detected 60 days post bombardment via immunohistochemistry. While there is great potential for the use of gene guns in the delivery of genetic material, it also has limitations. Ballistic delivery can only deliver genetic material to a limited tissue depth. Bombardment with particles can also cause damage to tissues along with inflammation (Sohn et al., 2001). Unlike other methods, the use of a gene gun to deliver nucleic acids is unspecific and cells, other than the target cells, can be transfected with the gene of interest. Ballistic guns can also only transfect limited quantities of genes and thus several treatments would be required (Mellott et al., 2013). Finally, it has been shown that while delivery of DNA produces transient expression of the gene of interest in cells, this gene delivery method is extremely variable (Kendall, Rishworth, Carter, & Mitchell, 2004).

Electroporation is one of the most commonly used non-viral delivery methods in gene therapy. It utilises electro-permeabilization to open pores in the cell membrane allowing nucleic acids to enter. Pores are formed when an electrical field is formed across cells. It was first used to transfect mouse lyoma cells with either linear or circular plasmid DNA. Electrical impulses of 8 kV/cm for 5 microseconds were shown to increase uptake of DNA into cells (Neumann, Schaefer-Ridder, Wang, & Hofschneider, 1982). The first incidences of electroporation *in vivo* were published in 1989 describing the use of electrical pulses for the fusion of Hela cells to rabbit corneal cells (Grasso, Heller, Cooley, & Haller, 1989). Since then, electroporation has been used *in vivo* to deliver nucleic acids to a variety of tissues, including skin, skeletal muscle, tumour cells and liver cells (Aihara & Miyazaki, 1998; Bier, Hammer, Canaday, & Lee, 1999; Denet, Vanbever, & Préat, 2004). In one of the first studies into the potential for electroporation for gene delivery *in vivo*, expression of IL-5 was induced in tibialis anterior muscles of mice via electroporation *in vivo* (Aihara & Miyazaki, 1998). As a method, electroporation has the ability to transfect both non dividing and dividing cell. One other advantage of electroporation over other methods such as the gene gun is that electroporation can be used to transfect larger numbers of cells. Electroporation has also been shown to induce expression in progenitor and stem cells. As with other non-viral methods of gene delivery, there are limitations including the impact on viability of electroporated cells. Furthermore, *in vivo* electroporation can result in inflammation due to

cell death. Finally, electroporation can be relatively costly and is an invasive procedure (Mellott et al., 2013).

Sonoporation is similar to electroporation in that it creates pores in the cell membrane allowing nucleic acids to enter the cell. Ultrasonic waves cause microbubbles to form, expand and collapse creating pores which drugs and nucleic acids can enter the cell through. Sonoporation has become a promising method of gene delivery for cancer gene therapies (Al-Bataineh, Jenne, & Huber, 2012; Frenkel & Li, 2006; Yoon & Park, 2010). It has been shown that once the pores have been opened, the length of time they are open for can vary and be controlled. Sonoporation has been shown to be less traumatic to cells than that of electroporation. One of the drawbacks to this method of gene delivery is its inability to control the localisation of the pores. Furthermore, it is not possible to control the uniformity of the pores or the entry of nucleic acids through the pores (Mehierhumbert & Guy, 2005). Large amounts of plasmid DNA needs to be transfected via sonoporation to achieve appropriate delivery and gene expression (Liang, Tang, & Halliwell, 2010).

1.1.3.1.2 Chemical Methods

Chemical methods have been a focus for gene transfer. Such methods can allow for gene transfer both *in vivo* and *in vitro* by way of methods such as cationic polymers, lipid polymers, nanoparticles and exosomes. These chemical methods can be used to overcome a number of the drawbacks associated with the physical methods described in Section 1.1.3.1.1. Chemical transfection via polymers have been widely studied since the 1960s and research has focused on improving the efficiency of gene transfer while reducing toxicity associated with these methods (Jin, Zeng, Liu, Deng, & He, 2014).

Lipids and polymers are used for gene transfer due to their ability to form complexes with plasmid DNA allowing them pass into the cell through the cell membrane. Calcium phosphate precipitation is a well-established method of gene transfer that is cost effective and easy to use (Jin et al., 2014). Calcium phosphate nanoparticles have also been developed, this nanoparticle method has been shown to have a significantly higher transduction efficiency than that of traditional calcium phosphate precipitation methods (Xu et al., 2011). Xu and colleagues developed a method of gene transfer that involved the use of calcium phosphate plasmid DNA nanoparticles encapsulating the transforming growth factor beta 1 (TGF-β1). Ultimately, the team determined that the use of calcium phosphate nanoparticles were an effective, efficient method of gene transfer while exhibiting low cytotoxicity in mesenchymal stem cells (Xu et al., 2011).

Liposomes are another extremely common method of gene transfer. Liposomes are capable of forming complexes with plasmid DNA. These lipid nanoparticles have been shown to have a number of properties that make them an ideal candidate for gene transfer, including low immune responses, easy to manufacture/produce with large payloads. This is a common method used in gene therapy for the knockdown of genes using siRNAs. One such therapy using lipid nanoparticles which has shown success to date is the use of siRNAs to treat transthyretin induced amyloidosis by Alnylam® Pharmaceuticals receiving approval from the FDA in 2018 ((CDER), 2019; Kulkarni, Cullis, & van der Meel, 2018).

Exosomes have also been identified as a potential method of gene transfer. These are extracellular microvesicles which can be engineered for the delivery of therapeutic nucleic acids. Exosomes are an ideal method of transfer due to their tissue tropism and ability to pass through biologic barriers (Luan et al., 2017; Sancho-Albero, Medel-Martínez, & Martín-Duque, 2020). For example, exosomes have been studied for their potential to treat Alzheimer's disease through the delivery of siRNAs for the knockdown of BACE1 via exosomes to dendritic cells by Alvarez-Erviti and colleagues (Alvarez-Erviti et al., 2011)

1.2 Viral Vectors for Gene Delivery and Gene Therapy

Viral vectors can be utilised for the transfer of genetic material for use in vaccines, cancer therapeutics and as a method of gene transfer for gene therapy. One of the main advantages of viral vectors is the natural ability of the virus to infect cells. Viral vectors have a high efficiency of cell transduction, they are highly specific and can deliver genes to target cells and can elicit a robust immune response (Ura, Okuda, & Shimada, 2014). Viral vector-based vaccines have the ability to enhance immunogenicity and illicit an intense cytotoxic T lymphocyte immune response to infected cells. To date several viral vectors have been utilised in vaccine production, this includes viral vectors derived from viruses such as Adenoviruses, Adeno-Associated Viruses, Retroviruses, and Lentiviruses (Ura et al., 2014). In response to the SARS-Cov-2 2019 pandemic there was mass research globally into the development and production of vaccines against SARS-Cov-2 including vaccine development using viral vectors which utilised Adenovirus (Ad) and Adeno-Associated Virus (AAV) among others. These vectored vaccines are replication deficient viral vectors that deliver nucleic acids that encode for the SARS-CoV-2 Spike protein, including the approved Oxford-AstraZeneca vaccine AZD1222 (Amanat & Krammer, 2020; S. P. Graham et al., 2020; Krammer, 2020; Mercado et al., 2020; Poland, Ovsyannikova, Crooke, & Kennedy, 2020; Voysey et al., 2020; Zhu et al., 2020).

Cancer gene therapy, using viral vectors, is a rapidly evolving approach for the treatment and therapeutic intervention of cancer. There are a number of advantages and disadvantages of each virus type utilised for cancer gene therapies. For example, Adenoviruses (Ad) have been shown to have potential to deliver tumour suppressors or suicide gene therapy, facilitating delivery and expression of the target transgene at high amounts with a broad tropism. Adenoviral infection is dependent on the presence of Ad receptors on target cells which are not expressed on all cancer cells, limiting their potential application in this field (Larocca & Schlom, 2011; Sharma, Tandon, Bangari, & Mittal, 2009). Herpes Simplex Virus (HSV) is also a commonly studied viral vector for cancer therapies. As with Ad vectors, it has a broad tropism and can target cells such as dendritic cells. Furthermore, HSV vectors have the capacity to package large transgenes. Indeed, HSV is a known oncolytic vector due to its ability to infect and propagate preferentially in tumour cells. However, transgene expression is limited due to lysis of the target cells (Larocca & Schlom, 2011; Lou, 2003; Varghese & Rabkin, 2002).

The use of viruses in gene therapy as a method of gene transfer has now been extensive, yet still much of the biology and how this impacts their manufacturing and use in the clinic remains to be elucidated. There are 5 main classes of viral vectors, these are grouped based on either their ability to integrate into the host genome or their ability to persist in the nucleus as extrachromosomal episomes (Lundstrom, 2018). The five main types of viral vectors in gene therapy are retrovirus, lentivirus, adenovirus, adeno-associated virus and herpes virus. Virus selection for therapeutic use considers a number of criteria, including, efficiency and targeting of transgene expression, ease of production, safety and toxicity, and stability. As shown in Table 1.2-1, viruses can be either DNA or RNA genome based viruses, single stranded (ss) or double stranded (ds), and enveloped or non-enveloped (Walther & Stein, 2000). The major viral vectors under development and used in gene therapy are discussed below, with a focus on adeno-associated viral vectors, the production and genome packaging of which are investigated during the studies described in this thesis.

Table 1.1-3 Viral vectors used in gene therapy.

	Genome	Enveloped/ Non-enveloped	Capacity (kb)	Advantages	Disadvantages
Adeno-Associated Virus (AAV)	ssDNA	Non-Enveloped	5 kb	Low toxicity, long term expression	Difficult to produce, Low packaging capacity
Adenovirus (Ad)	dsDNA	Non-Enveloped	>8 kb	Clinical phase	Elicits Strong immune response
Herpes Simplex Virus (HSV)	dsDNA	Enveloped	>30 kb	Efficient expression in multiple cell types	No expression during latent expression
Retroviruses	RNA	Enveloped	<8 kb	Effective integration into target cells	Insertional mutagenesis
Lentivirus	RNA	Enveloped	8-10 kb	Efficiently transduce non-dividing cells	Insertional mutagenesis

1.2.1 Adeno-Associated Viral Vectors

Adeno-associated virus (AAV) is one of the most extensively researched viral vector platforms for gene therapy applications to date. As of March 2021, there were 149 clinical trials in process using AAV vectors to a range of indications (Kuzmin et al., 2021). AAV vectors are therefore one of the major delivery vehicles used in *in vivo* gene therapy applications (C. Li & Samulski, 2020). AAV is a small non-pathogenic, non-enveloped parvovirus, consisting of a linear single stranded DNA (ssDNA) genome approximately 4.8 kilobases long and being approximately 25 nm in size (Naso, Tomkowicz, Perry, & Strohl, 2017; D. Wang, Tai, & Gao, 2019). The genome is flanked by inverted terminal repeats (ITRs) at either end which are 145 nucleotides in length (see Figure 1.2). AAV is a dependovirus which means it relies on a helper virus for replication to occur. A helper virus supplies a number of genes essential for replication. The genes required for AAV replication are the E1A, E1B, E2A, E4 and VA RNA. Without these helper genes, AAV will integrate into Chromosome 19 of the host (Daya & Berns, 2008). One of the major benefits in using AAV as a viral vector for gene delivery is its ability to transduce both dividing and non-dividing cells (Berry & Asokan, 2016; Ghosh, Brown, Jenkins, & Campbell, 2020). Furthermore, AAV provides efficient, long term transgene expression in a variety of targetable tissues such as the retina, liver, muscle and CNS. There are a number of serotypes of AAV which can be used to target different tissues (see Table 1.3-1 below) (Domenger & Grimm, 2019; Mietzsch et al., 2021). The wild type AAV genome does not integrate into the host genomic DNA but is maintained as

extrachromosomal episomes in the nucleus. An in-depth description of AAV is provided below in section 1.3.

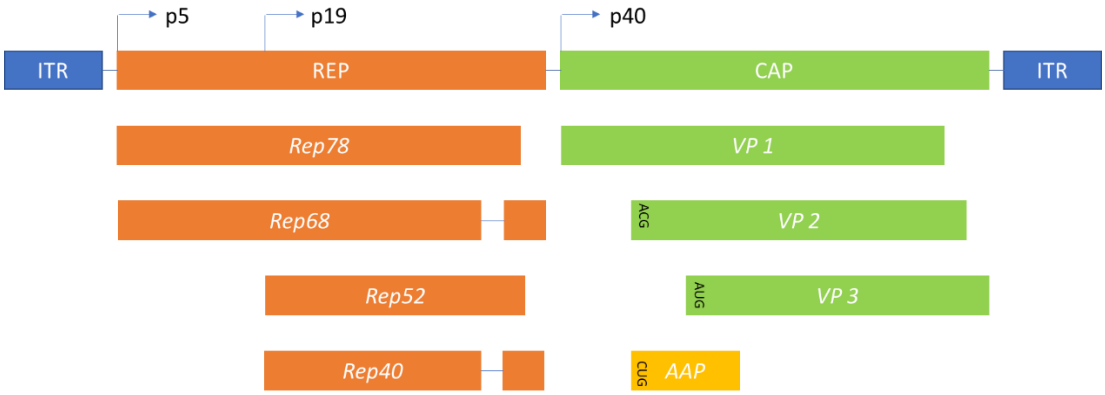

Figure 1.2 Schematic of Adeno-Associated Virus genome. The ITRs flank the genome which consist of wo genes, *REP* and CAP. Rep transcripts are derived from two promoters (p5 and p19) and alternative splicing whilst VP capsid transcripts are driven by the p40 promoter and alternative start codons.

As described previously, recombinant AAV (rAAV) has become a leading viral vector system for gene therapy. Glybera, discussed in section 1.1.2.1, was a rAAV based treatment for lipoprotein lipase deficiency and the first gene therapy approved for use in 2012 by the European Medicines Agency (EMA) (D. Wang et al., 2019; Ylä-Herttuala, 2012). It was not until 2017 when the FDA approved its first AAV gene therapy, Luxturna, used for the treatment of retinal dystrophy. Glybera was an AAV1 based *LPL* gene replacement therapy while Luxturna is an AAV2 based *RPE65* gene replacement therapy. Glybera delivered a hyperactive, Ser(447)X variant of Lipoprotein lipase for the treatment of LPL deficiency (Burnett & Hooper, 2009; S. Russell et al., 2017).

In addition to gene replacement, AAV can be used to deliver gene silencing agents. As described previously, gene silencing therapies can be used to treat monogenetic diseases caused by gain of toxicity mutations. One of the most widely utilised methods to achieve this is RNA interference (RNAi). Unlike gene replacement therapies, the size limitations of rAAV pose less of a limitation with RNAi strategies, as these typically utilise small gene cassettes (Borel, Kay, & Mueller, 2014; Borel & Mueller, 2019). Traditionally, retroviral vectors have been used for transferring siRNAs to a patient, this method requires cells to be actively dividing. Due to their ability to infect both dividing and non-dividing cells, AAV vectors have been designed for the transfer of p53 siRNAs and shown to transfer and efficiently transduce

cells with minimal toxicity (Tomar et al., 2003). Most AAV-based RNAi strategies are still at a preclinical phase (Borel et al., 2014), this is due to a toxicity caused by high levels of shRNAs which can overwhelm endogenous miRNA biogenesis pathways (Dirk Grimm et al., 2006). AAV mediated RNAi strategies have shown great potential for the treatment of disorders such as Amyotrophic Lateral sclerosis (ALS). AAV vectors are also advantageous over other vectors due to their capacity to target different tissues including neuronal. AAV9 vectors have been shown to deliver RNAi against SOD1; it was shown to be possible to reduce mutant SOD1 synthesis, thus delaying the onset of disease and increasing the lifespan of a $SOD1^{G93A}$ mouse model by 39% (Cappella, Ciotti, Cohen-Tannoudji, & Biferi, 2019; Iannitti et al., 2018).

While both gene replacement therapies and gene silencing therapies are utilised for monogenetic diseases, it is possible to utilise viral vectors such as AAV to address more complex genetic diseases, via gene addition therapy. AAV vectors can be used to introduce the genes for recombinant antibodies which can treat viral infections. One such example of antibody gene transfer involves the transfer of genes encoding antibodies which neutralise HIV. This approach has become known as vectored immune prophylaxis (VIP). Mice studies have shown that this method of treatment can result in the lifelong expression of antibodies against HIV strains. This approach has so far only been investigated in phase I clinical trials (Balazs et al., 2012; Balazs & West, 2013; Priddy et al., 2019; Sanders & Ponzio, 2017).

Table 1.1-4 AAV Serotype and tissue tropisms(Srivastava, 2016; Zincarelli, Soltys, Rengo, & Rabinowitz, 2008).

AAV Serotype	Target Tissue Type
1	Neuronal, Skeletal
2	Broad
3	Brain, Liver
4	Brain
5	Neuronal, Retinal pigmented epithelial, Photoreceptors
6	Skeletal, Lung
8	Liver, Skeletal, Pancreas, Heart
9	Liver, Skeletal, Lung

1.2.2 Adenoviral (Ad) Vectors

Adenovirus (Ad) is a class of non-enveloped virus which has a linear 38-43 kb double stranded DNA (dsDNA) genome (Ghosh et al., 2020) which encodes 35 proteins, 20 proteins involved in regulatory and replicatory functions, the remainder are structural proteins (Wold & Toth, 2013). It is the largest non-enveloped virus known and is about 90-100 nm in size with more than 50 serotypes that cause a range of diseases and infections (Table 1.2-2) (Ghebremedhin, 2014; Muruve, 2004). Adenovirus infects cells through endocytosis. Once within the cell the capsid is destroyed and the viral genome is released into the cytoplasm and enters the nucleus (Takahashi & Suzuki, 2011). As for AAV, the adenovirus genome is flanked by two ITR regions, one at each end (Figure 1.3). Another similarity between the Ad and AAV genomes is that they do not integrate into the host genome but remain as an extrachromosomal episome in the nucleus (Ghosh et al., 2020). There are 57 known serotypes of adenovirus, Ad1-57. Most people have been infected with a number of Ad serotypes, most commonly Ad1, 2, 5 and 6, and will have developed a lifelong immunity (Muruve, 2004).

Table 1.1-5 Adenovirus serotypes and associated infections.

Adenovirus subgroup	**Serotype**	**Infection type**
A	12, 18, 31	Gastrointestinal, Respiratory, urinary
B	3, 7, 11, 14, 16, 21, 34 35	Keratoconjunctivitis, gastrointestinal, respiratory, urinary
C	1, 2, 5, 6	Gastrointestinal, respiratory, hepatitis, urinary
D	8-10, 13, 15, 17, 19, 20, 22-30, 32, 33, 36-39, 42-49	Keratoconjunctivitis, gastrointestinal
E	4	Keratoconjunctivitis, Respiratory
F	40, 41	Gastrointestinal
G	52	Gastrointestinal

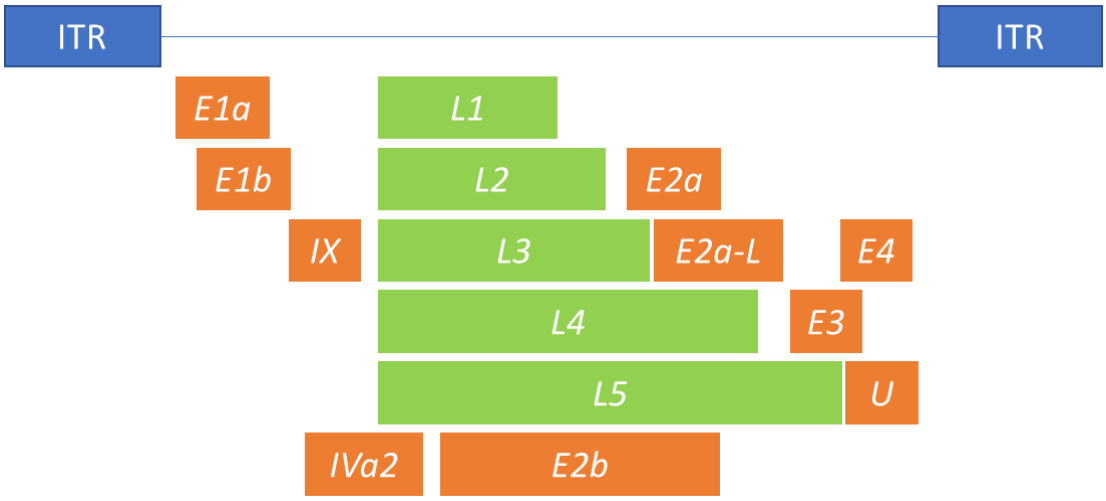

Figure 1.3 Schematic of Adenovirus genome. (E= Early genes, L=Late genes)

Adenovirus vectors have been a major research target with regards to gene therapy and vaccine development (Wold & Toth, 2013; C. Zhang & Zhou, 2016). Currently, Ad based gene therapies account for 50% of gene therapy trials worldwide (Bulcha, Wang, Ma, Tai, & Gao, 2021). While most of these trials focus on cancer gene therapies, there is also a large number of vaccine-based therapies under development whereby the vector contains a transgene for an antigenic protein. One of the most well publicised Ad vector approaches in the vaccine developed in the UK, ChAdOx1 nCoV-19 vaccine (known as AZD1222), developed by AstraZeneca and Oxford University, and approved for use in the UK and other countries against the SARS-CoV-2 virus. This vaccine is a chimp Ad serotype 5 vector vaccine (Folegatti et al., 2020; van Doremalen et al., 2020; Voysey et al., 2020). Most Ad vectors in use or under development have been generated from serotypes 2 and 5 as these are not associated with severe disease states in humans (Walther & Stein, 2000).

Ad vectors are either replication-defective or replication-competent. Replication-defective vectors are utilised largely for vaccine production and have had the essential *E1A* and *E1B* genes removed and a promoter e.g., CMV promoter inserted to replace these genes. The E1A protein is essential for efficient viral encapsulation. To accommodate for the removal of E1A from the genome, host cells such as the human embryonic kidney cell line 293 (HEK293) has been modified to stably express the E1A protein (W. C. Russell, Graham, Smiley, & Nairn, 1977) and are commonly used in the production of Ad vectors. A further advantage

associated with this cell line is its ability to produce and package high titres of vectors (Walther & Stein, 2000; Wold & Toth, 2013).

There are several other advantages to using Ad vectors as gene delivery agents. Adenoviruses have been shown to have genetic stability, shown to be safe and well tolerated in clinical trials, and it is relatively easy (compared to some other viral vector systems) to undertake large scale production. Adenoviruses are larger viruses than AAV and thus are more suited to larger genes of interest than AAV can accommodate, with the ability to package genomes over 30 kb. Nevertheless, although manufacturing can be scaled, the manufacture of high titres of highly efficiently packaged vectors remains a major challenge in Ad vector production (C. S. Lee et al., 2017). Another potential issue that needs to be considered with Adenoviral vectors is that these vectors elicit an inflammatory response to the E2 protein, thus limiting its use for repeated applications of gene therapies (C. S. Lee et al., 2017; Yei, Mittereder, Tang, O'Sullivan, & Trapnell, 1994).

Replication defective and replication competent Ad vectors are commonly used as anti-cancer agents due to their ability to deliver immune related genes to tumour cells which will induce an anti-tumoral immune response. Initial research into Ad vectors as a method of cancer gene therapy focused on replication defective vectors but research has moved into the potential for conditionally replicative Ad vectors. These have the ability to infect and replicate specifically in cancer cells and spread to other cancer cells, while leaving normal host cells untouched (Kimball et al., 2010; LI et al., 2015; Matthews, Alvarez, & Curiel, 2009). One of the methods utilised for this is the deletion, or partial deletion, of either the E1A genome or the E1B genome. This prevents the replication of the vector in normal cells but allows replication in tumour cells which have genetic defects which complement the E1a or E1b genome allowing replication to occur (Matthews et al., 2009).

1.2.3 Herpes Virus (HSV) Vectors

Herpes simplex virus (HSV) is a double stranded enveloped DNA virus with a 150 kb genome encoding 80 genes. This large virus results in vectors with the capacity for packaging genes of interest between 40 and 50 kb (Marconi, Fraefel, & Epstein, 2015). HSV infection is both lytic and latent in nature, the resulting infections are lifelong latent infections of the neurons, thus they provide great potential for long term expression of transgenes in gene therapy (Lundstrom, 2018; Marconi et al., 2015). In general, HSV-1 infection of most cell types results in cell death, however deletion of 40 genes not essential for replication of HSV has resulted in the development of non-pathogenic HSV-1 vectors which can be used for gene transfer

(Fraefel, Marconi, & Epstein, 2011; Marconi, Argnani, Epstein, & Manservigi, 2008). HSV is an appealing method for gene therapy in cases where large amounts of genetic material need to be delivered due to its large genome capacity allowing for the transfer of transgenes up to 50 kB into the nucleus of target cells alongside its ability to infect a number of cell types, both quiescent and proliferating, such as neuronal cells (Epstein, Marconi, Argnani, & Manservigi, 2005; Marconi et al., 2015). Furthermore, HSV can be used for the selective destruction of cancer cells and immunotherapy against oncolytic cells (Marconi et al., 2008; Todo, 2002).

Unfortunately, due to the fact that a high percentage of people have been previously exposed to the herpes simplex virus, many potential patients have an immune response in reaction to these vectors. This pre-existing immune response is responsible for the inactivation and elimination of HSV vectors. It should be noted that HSV vectors also have the opportunity of recombining with latent HSV infected cells, posing a safety risk (Marconi et al., 2008; Vannucci, Lai, Chiuppesi, Ceccherini-Nelli, & Pistello, 2013).

1.2.4 Retroviral Vectors

Retroviruses are enveloped single stranded RNA viruses of approximately 100 nm size, with a genome of 7-11 kB in size, with each virion containing two identical single stranded RNA genomes. The viral genome is flanked by two Long Terminal Repeats (LTR). The LTRs flank three open reading frames, *gag, pol* and *env;* these encode the capsid (matrix protein, capsid protein and nucleocapsid protein) and replication proteins, and the envelope glycoproteins. Retroviral vectors have a packaging capacity of approximately 8 kB. Interest in retroviruses as a gene transfer method stems from their ability to integrate into the genome of the host cell. The integration is permanent, which can be random, posing a safety issue, but that can be overcome using vectors that have targeted integration ability. Unlike other viral vectors, retrovirus vectors, with the exception of lentivirus, cannot infect nondividing cells and for this reason research has tended to focus more on developing lentiviral vectors (Lundstrom, 2018; Vannucci et al., 2013).

Successful production of retroviral vectors initially relied on the transfection of multiple plasmid vectors; a packaging construct which contains the *gag* and *pol* genes, a transgene vector and a plasmid vector expressing the *env* genes. In the transgene plasmid vector, the therapeutic gene is flanked by the LTR regions. While this triple plasmid transfection method successfully produces retroviral vectors the *env* plasmid vector poses a safety risk due to its ability to recombine producing replication competent particles. To combat this, the

production of such viral vectors has evolved to use producer cell lines which express the *env* genes and hence a plasmid with these is not required for their production (Vannucci et al., 2013).

Mason and colleagues have shown that it is possible to utilise retroviral vectors to deliver and express human bone morphogenic protein 7 (BMP-7) in periosteal cells under the control of a CMV promoter and enhancer. Unfortunately, due to the high expression from the CMV promoter, the expression was toxic to the periosteal cells. Replacement of the CMV region with a weaker promoter and enhancer resulted in the successful expression of BMP-7, one of the first studies showing the feasibility of using retroviral vectors for gene therapy (Mason et al., 1998).

1.2.4.1 Lentiviral Vectors

Lentiviral vectors, such as Human immunodeficiency virus (HIV), has been shown to have great potential as gene delivery vectors. They can integrate into host genomes and there is thus prolonged gene expression. Lentiviruses are a part of the *Retroviridae* family; despite being retroviruses, these viruses can infect both dividing and non-dividing cells. HIV-1 has a genome of 9-10 kB in size that encodes for the *gag, pol* and *env* genes as with all retroviruses described in Section 1.2.4. The HIV-1 genome also encodes for the Tat and Rev regulatory proteins along with four accessory proteins (vif, vpr, vpu and nef). Lentiviral vectors have been developed or considered as gene delivery vehicles since 1989, when Terwilliger developed a replication competent HIV-1 vector to express chloramphenicol acetyltransferase (Terwilliger, Godin, Sodroski, & Haseltine, 1989).

Since 1989 there have been at least three generations of lentiviral vectors developed. First generation vectors consisted of a major portion of the HIV genome including the *gag* and *pol* genes along with accessory and regulatory proteins. The envelope gene of another virus was also included instead of the *env* gene of the HIV-1 virus. The second generation of lentiviral vectors were designed without the accessory virulence genes (*vif, vpr, vpu* and *nef),* removal of these genes did not negatively impact delivery of the genes to the host cells. These second generation vectors were safer than the first generation vectors (Vannucci et al., 2013). Third generation vectors initially described by Dull and colleagues (1998) separated the HIV genome across different plasmids, the *gag and* pol genes were encoded on a separate plasmid to that of the *rev* and *env* genes (Dull et al., 1998).

An example of lentiviral vectors in gene therapy is the development of these for the treatment and prevention of cystic fibrosis (CF) lung disease. Primary studies using human CF airway epithelia cells and in animal models have shown that delivery of the *CFTR* gene via lentiviral vectors can correct cystic fibrosis phenotypes long term with low immunogenicity (Stocker et al., 2009). Stocker et al showed that lentiviral vectors containing the gene for *CFTR* produced in HEK293T cells, when targeted to respiratory epithelial cells, can effectively treat CF demonstrating the feasibility and potential for lentiviral vectors for the treatment of CF (Marquez Loza, Yuen, & McCray, 2019; Stocker et al., 2009). Such treatments are yet however, to be successfully used in the clinic.

Lentiviral vectors have become a key player in Chimeric Antigen Receptor T-cell (CAR-T) therapies. CART-T therapy involves the *ex vivo* editing of a patients T-cells to express a chimeric antigen receptor that is specific for a tumour antigen. The edited cells are then re-infused back into the patient. The *ex vivo* editing of the patients T-cells can occur through both viral vector-based methods, in particular lentiviral, and non-viral vector methods (Do Minh, Tran, & Kamen, 2020; Guy, McCloskey, Lye, Mitrophanous, & Mukhopadhyay, 2013; Lana & Strauss, 2020; Miliotou & Papadopoulou, 2018; Moço, de Abreu Neto, Fantacini, & Picanço-Castro, 2020).The FDA approved its first CAR-T cell therapies in 2017, Novartis's tisagenlecleucel and Gilead's axicabtagene ciloleucel for the treatment of acute lymphoblastic leukaemia and large B cell lymphoma respectively. Since 2020, the FDA have approved Gilead's brexucabtagene autikeucel for mantle lymphoma and more recently Bristol Myers Squibb's lisocabtagene maraleucel for the treatment of large Bcell lymphoma (Mullard, 2021)

1.3 Adeno-Associated Virus and Recombinant AAV (rAAV)

As described in section 1.2.1, adeno associated virus, so called as it was initially identified in the 1960s in adenovirus purified samples, is widely used as a gene therapy viral vector. It was first identified by both the Atchison research group and the Rowe group (Atchison, Casto, & Hammon, 1965; Hoggan, Blacklow, & Rowe, 1966), and was initially thought to be contaminants of adenovirus preps. Both Atchison and Rowe showed via electron microscopy that these contaminant virus like particles were approximately 22 nm in diameter and were found in both human and simian Ad serotypes (Hoggan et al., 1966). AAV is a member of the *Parvoviridae* family, this family encompasses small, non-enveloped icosahedral viruses. AAV is a small virus of approximately 20-26 nm in diameter which falls under the genus *Dependovirus* (K. I. Berns & Giraud, 1996). *Dependovirus* are so called due to their reliance,

or dependence, on a second “helper virus”. Without the aid of a helper virus, AAV cannot productively infect cells or replicate. It was the Rowe group that showed that AAV replication was reliant on the presence of the Ad genetic functions and was considered to be a defective virus (Hoggan et al., 1966). The helper genes required are usually supplied by adenovirus, however are not limited to Ad and can be supplied by other viruses including the herpesvirus simplex virus 1 and 2 (Atchison et al., 1965; Buller, Janik, Sebring, & Rose, 1981; Hoggan et al., 1966). While initial studies suggested that AAV was a defective virus, it was later shown that it can induce latent infection in healthy cells (Daya & Berns, 2008).

There have been 13 AAV serotypes (Table 1.3-1) identified from both humans and nonhuman primates to date, AAV 1 to AAV 13, by sequencing and PCR studies (Mietzsch et al., 2021; Schmidt et al., 2006). All AAV serotypes can be separated into two isolates and five clades (A-F), separated based on the VP1 (capsid protein) amino acid sequence. The serotypes have a high structural similarity between 95% and 99%, and range in sequence similarity between 65% and 99%. Despite the similarities in sequence and structure, the serotypes vary in their tissue tropism and different serotypes can be used to target cardiac muscle, skeletal muscle and liver tissues and certain serotypes can even target tissue in the CNS (see Table1.3-1) (Guangping Gao et al., 2004). The natural ability of different serotypes to target different tissue has resulted in great interest in AAV vectors for gene therapy as different serotypes can be utilised for treating different genetic disorders at different tissue sites as long as the limited genome capacity does not preclude this.

1.3.1 The Life Cycle of AAV

The AAV life cycle can be considered as consisting of two phases, one in the presence of a helper virus and the other in the absence. In the presence of a helper virus, AAV replicates productively. When Ad is co-infected with AAV, the infection of Ad can occur prior or at the same time as AAV infection. This is largely the case with herpes simplex virus; a number of herpes simplex serotypes can have lytic effects on the cell and in order for AAV replication to occur, the infection of these lytic serotypes needs to occur simultaneous to that of the AAV infection (K. I. Berns & Giraud, 1996).

In the absence of the helper virus, AAV does not normally undergo infection and replication, it can enter a cell and un-coat its genome. However, the expression of the AAV regulatory proteins is limited and the synthesis of AAV proteins is restricted, this results in the integration of the viral genome into the genome of the host cell where it establishes a latent infection (Handa, Shiroki, & Shimojo, 1977; Hernandez et al., 1999; Leonard & Berns, 1994).

AAV is unique in that it integrates site specifically, into the q arm of chromosome 19 (R M Kotin et al., 1990).

1.3.2 The Genome and Structure of AAV

All AAV serotypes have unique characteristics and properties, and these are based on their viral capsid structure. As previously described, AAV are small non-enveloped icosahedral viruses with a capsid diameter ranging between 20 nm and 26 nm (approximately 260 Å). AAV contains a single stranded DNA (ssDNA) genome that is approximately 4.8 kB in length. This genome is comprised of two open reading frames (ORFs), these are flanked by two inverted terminal repeats (ITRs) (one at each end) which are 145 base palindromic sequences (Rolling & Samulski, 1995). The AAV genome encodes for the *Rep, Cap* and *AAP* genes (Figure 12), the *Rep* ORF encodes the *Rep* gene, that results in the expression of four non-structural proteins, Rep78, Rep68, Rep52 and Rep40. The *Cap* gene encodes for three structural proteins; VP1, VP2 and VP3 that form the capsid structure of the virus in a 1:1:10 ratio (Drouin & Agbandje-McKenna, 2013; Leonard & Berns, 1994). Expression of the *Rep* and *Cap* ORFs is regulated by three promoters: p5, p19 and p40. The p5 and p19 promoters, by way of alternative splicing, are responsible for the expression of the *Rep* ORF generating the Rep78, Rep68, Rep52 and Rep40 proteins, so named due to their apparent molecular weight. The p40 promoter is responsible for directing the expression of the *Cap* ORF resulting in the production of the three structural VP proteins; VP1, VP2 and VP3 via alternative splicing and the use of an alternative ACG start codon (see figure 1.2).

The capsid structures of serotypes 1 to 9 have been determined by x-ray crystallography or cryo-electron microscopy (DiMattia et al., 2012). Such studies have shown that the VP3 region is conserved across serotypes, being composed of a core β-barrel motif which consists of 8 antiparallel strands and a small α-helix. The VP3 protein also contains 9 variable regions which can be found on the capsid surface (Drouin & Agbandje-McKenna, 2013).

The structure of all AAV capsids is formed from the interaction of VP1:VP2:VP3 in a ratio of 1:1:10 (Becerra, Koczot, Fabisch, & Rose, 1988). It was believed for over 25 years that the non-structural Rep and the capsid VP proteins were the only proteins expressed by AAV. However, Sonntag et *al*., in 2010, identified the expression of a protein termed assembly activating protein (AAP). This study showed that the AAP protein was encoded by ORF2 of the *Cap* gene and that it was required for capsid assembly of AAV serotype 2. Furthermore, it was shown that translation of the mRNA to generate the AAP protein was initiated at a

non-conventional CUG start codon resulting in the production of the 23 kDa protein (Sonntag, Schmidt, & Kleinschmidt, 2010).

AAV enters cells through serotype specific glycan receptors prior to endocytotic entry to the cells (Meyer et al., 2019). Bartlett and colleagues described the method of AAV entry into the cell through endocytosis in a receptor mediated manner, through the use of clathrin coated pits, once within the cell AAV escapes the endosomes and enters the nucleus through pores (Bartlett, Wilcher, & Samulski, 2000; Martini, Rocco, & Morales, 2011). The difference in the capsid sequences of the different AAV serotypes influences the transduction abilities of the serotypes in a tissue specific manner. AAV2 binds to heparan sulfate proteoglycans while Serotype 9 has been shown to have a galactose binding domain and it is thought that the preferential galactose binding of AAV9 gives rise to its ability to cross the blood brain barrier and infect the central nervous system (CNS) (Bell, Gurda, Van Vliet, Agbandje-McKenna, & Wilson, 2012; Merkel et al., 2017; Meyer et al., 2019; Hongwei Zhang et al., 2011). Pillay and colleagues recently identified, through genome screening, the cellular protein AAVR, this has been identified as a key receptor for a number of AAV serotypes including AAV2 and AAV5 (Meyer et al., 2019; Pillay et al., 2017).

It is not yet fully understood how the virus capsid is assembled and genome inserted, but it has been shown through radioactive pulse chase labelling experiments that the capsid is rapidly assembled first and the ssDNA genome is then introduced into the empty capsid (Myers & Carter, 1980; Sonntag et al., 2010).

1.3.2.1 Inverted Terminal Repeats

As mentioned in section 1.2.1 and 1.3.2, the wild type AAV genome is flanked by two inverted terminal repeat (ITR) regions, these are 145 bp palindromic sequences which overlap to form a T-shape hairpin structure (Figure 1.4) (Kenneth I. Berns, 2020; Rolling & Samulski, 1995). In a rAAV vector the genome is also flanked by these ITR regions. The ITR regions have been shown to be responsible for the replication and packaging of the AAV genome (Wilmott, Lisowski, Alexander, & Logan, 2019). Furthermore, AAV ITRs have been shown to stimulate gene editing (Hirsch, 2015). There is a high percentage (> 82%) of homology amongst the ITRs of the AAV serotypes 1-9, the exception to this is serotype 5 (58% similarity) (Le Bec et al., 2008). Along with the hairpin structure the ITR regions contain a terminal resolution site (trs) and the Rep binding elements (RBE) (Figure 1.4). The RBE region binds to the p5 promoter Rep proteins, Rep78 and Rep68 (Pereira, McCarty, & Muzyczka, 1997; Young & Samulski, 2001).

ITR presence is essential for the replication and packaging of viral genomes, however, it has been shown that it is possible to produce recombinant AAV with shorter ITR regions of 137 bp. Furthermore, it was shown that AAV genome replication and packaging is possible in the absence of one hairpin structure (Richard J. Samulski, Srivastava, Berns, & Muzyczka, 1983; X. S. Wang, Ponnazhagan, & Srivastava, 1996). The productivity of rAAV is impacted by the ITR regions. The ITR region contains 3 palindromic sequences, A-A', B-B' and C-C' as shown in Figure 1.4. Zhou and colleagues generated truncated ITRs, where the C-C' and B-B' were deleted removing the hairpin structure. This was shown to reduce rAAV productivity but could increase the transgene expression (Q. Zhou et al., 2017).

It is possible to cross packaged the AAV2 genome, containing the ITRs from AAV2, into the capsids of other serotypes. Chao showed that it was possible to package an AAV2 plasmid containing either eGFP or canine Factor IX (cFIX) into rAAV vectors from serotypes 1, 2, 3 and 4. This study showed that it was possible to transduce HEK293 cells with these particles; the AAV2 particles showed the highest percentage of transduced cells while AAV4 was extremely inefficient at transducing human derived HEK293 cells (Chao et al., 2000; Wilmott et al., 2019). In a study carried out by Yan and colleagues, AAV hybrid ITR vectors were generated containing an AAV2-ITR on one end of the viral genome and an AAV5-ITR flanking the other end. It was shown that it was possible to package the hybrid ITR genome into the capsids from both serotype 5 and 2 (Yan, Zak, Zhang, & Engelhardt, 2005).

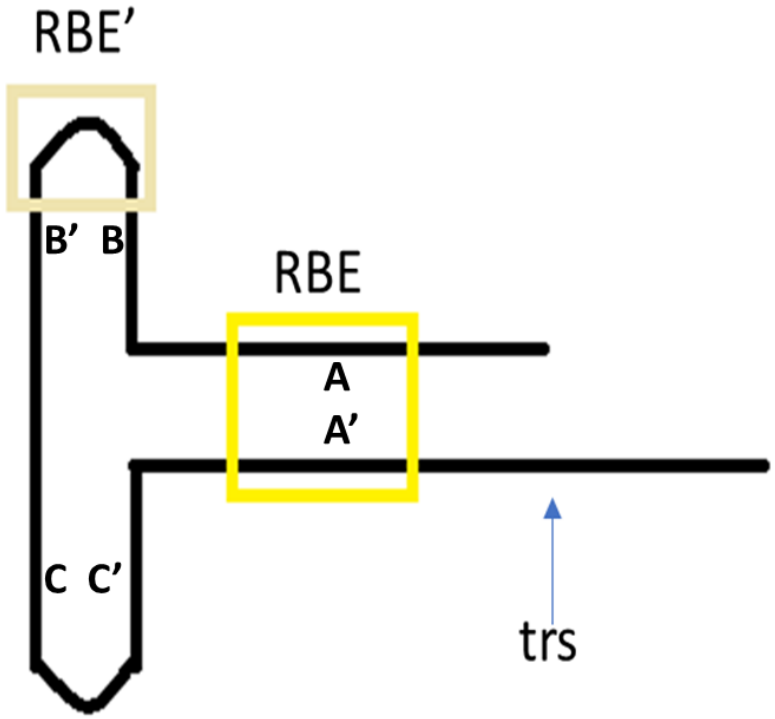

Figure 1.4 Schematic of the ITR regions, including the RBE, RBE' and the terminal resolution site (trs) in the AAV genome along with the three palindromic sequences which make the hairpin loop.

1.3.2.2 The Rep Proteins

As described in the previous section, the AAV genome encodes for the Rep proteins Rep78, Rep68, Rep52 and Rep40 and these are essential for viral replication, integration and assembly. The p5 and p19 promoters are responsible for directing the synthesis of the transcripts that are then translated to generate the respective proteins. The presence of adenoviral helper genes direct p5 and p19 promoter activity. The p5 promoter is induced by the adenovirus E1A gene. E1a activates the p5 promoter via interactions with the Major Late Transcription Factor (MLTF) and YY1 (Chang, Shi, & Shenk, 1989; C A Laughlin, Jones, & Carter, 1982). The p5 promoter initiates the production of the transcripts for *Rep78* and *Rep68* while the p19 promoter is responsible for the production of the smaller *Rep52* and *Rep40* transcripts. Rep68 and Rep40 are translated from spliced mRNAs (Hölscher, Kleinschmidt, & Bürkle, 1995). Rep78 and Rep68 are involved in the regulation of viral transcription, via binding to the ITRs stimulating replication. These two Rep proteins possess

helicase and endonuclease activity required for AAV replication (Ashktorab & Srivastava, 1989; Chiorini et al., 1996; Kyöstiö et al., 1994). Rep78 and Rep68 proteins can also site specifically nick the ITR at the terminal resolution site (trs) (Figure 1.4) allowing the replication of the ITR hairpin structure (Im & Muzyczka, 1990). The smaller Rep52 and Rep40 proteins are involved in the accumulation of ssDNA for packaging. While both Rep78 and Rep68 expression alone has been shown to be sufficient for AAV DNA replication to occur, the smaller Rep proteins (Rep52 and Rep40) are necessary for efficient accumulation and packaging of AAV (Daya & Berns, 2008; Hölscher et al., 1995).

Rep expression is toxic to host cells and negatively impacts the growth phenotype of both insect and mammalian cells. Rep protein expression slows cell growth and can trigger cell death. Schmidt et al showed that Rep-mediated cytotoxicity can be triggered by expression of Rep78 alone. Rep78 causes activation of caspase-3, involved in p53 independent apoptosis, resulting in apoptosis in the G1 and S phase of the cell cycle (Batchu, Shammas, Wang, & Munshi, 1999; Hermonat, 1989; Schmidt, Afione, & Kotin, 2000).

1.3.2.3 The Cap Proteins

As described above, the AAV genome encodes for two ORFs, the *Rep* ORF and the *Cap* ORF. The *Cap* gene encodes for the structural proteins VP1, VP2 and VP3 of molecular weight 87, 72 and 63 kDa, respectively. VP expression is under the control of the p40 promoter. VP3 is the most efficiently translated of the capsid mRNAs due to the presence of a Kozak sequence at the translation start site, VP2 is expressed less than VP3 due to using a non-AUG, ACG, start codon and finally VP1 is the least efficiently expressed capsid protein as it is translated from a minor spliced mRNA species. The three VP proteins all have the same C-terminal sequence, differing at the N-terminal sequence (Becerra et al., 1988; Van Vliet, Blouin, Brument, Agbandje-McKenna, & Snyder, 2008). The mature AAV structure is composed of capsid proteins in a ratio of 1:1:10 (VP1:VP2:VP3) resulting in a 60 subunit capsid approximately 25 nm in diameter. The capsid proteins are arranged in T=1 icosahedral symmetry. VP3 proteins make up approximately 50 out of 60 of the capsid monomers, while it is possible to form capsids from VP3 proteins only (Becerra et al., 1988; Le, Radukic, & Müller, 2019; Venkatakrishnan et al., 2013).

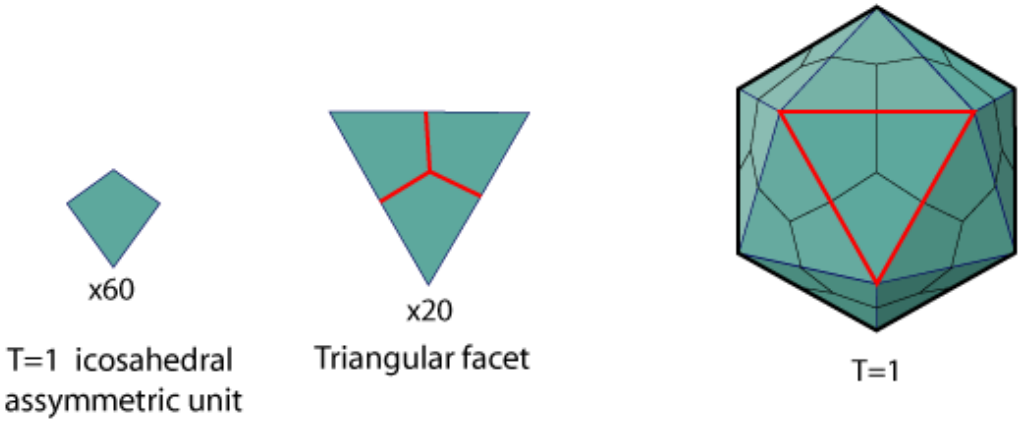

Figure 1.5 Schematic of T1 icosahedral capsid symmetry (taken from ViralZone).

1.3.2.4 Assembly Activating Protein (AAP)

As described in section 1.3.2 above, in 2010 Sonntag et al. identified a new AAV protein encoded by the *Cap* ORF from an alternative reading frame (Sonntag et al., 2010). This protein has become known as the assembly activating protein (AAP) and was shown to be involved in the formation of capsid for some serotypes (Sonntag et al., 2011). AAP expression is initiated at an unconventional CTG start codon. This unconventional start codon is preceded by a weak ACG start codon for VP2, it also contains the ATG start codon of the VP3 protein. The initial study to describe AAP expression was undertaken using AAV serotype 2 and showed that AAP was not just involved in the formation of capsids but for serotype 2, was essential for formation of capsids. AAP is a small protein of approximately 22.6 kDa that initiates the transport of VP proteins to the nucleolus. AAP was shown to rapidly chaperone capsid assembly and this chaperoning prevents the degradation of the unassembled capsid proteins (Grosse et al., 2017; Sonntag et al., 2011, 2010). AAP contains two hydrophobic domains in the N-terminal region of the protein and it is suggested that it is these N-terminal regions that are integral to its assembly promoting activity (Naumer et al., 2012).

Sonntag et al. also showed that AAP, in the absence of VP1 and VP2, can facilitate formation of capsids comprised solely of VP3 proteins. In the absence of AAP, VP3 only serotype 2 capsids cannot be formed. AAP from serotype 2 was also shown to stimulate capsid assembly for a number of other AAV serotypes. As with serotype 2, all AAV serotypes rely on AAP expression for assembly to occur, with the exception of serotypes 4, 5 and 11 which do not rely on AAP for capsid assembly (Earley et al., 2017; Grosse et al., 2017; Sonntag et al., 2011).

It was also demonstrated that AAP is required for the production of recombinant AAV (rAAV) in mammalian cells and insect cells (Grosse et al., 2017).

1.3.2.5 The Role of Adenoviral Helper Genes

Helper genes are essential for efficient AAV replication and propagation, and although these can come from several sources, they are usually from adenovirus. The adenoviral genes required for the production of AAV are *E1A, E1B, E2A, E4* and VA RNA. E1a plays a major role in the activation of the p5 promoter which is responsible for the synthesis of the Rep proteins as described in section 1.2.1. E1a also drives the host cell into S-Phase of the cell cycle for viral DNA replication (Chang et al., 1989; C A Laughlin et al., 1982; Matsushita et al., 2004; Tratschin, West, Sandbank, & Carter, 1984). E1a expression also stabilises p53, leading to apoptosis of cells. Utilising the adenoviral genes, E1b and E4 protects against apoptosis by forming a complex with p53 triggering ubiquitin mediated proteolysis (Lowe, Ruley, Jacks, & Housman, 1993; Steegenga, Riteco, Jochemsen, Fallaux, & Bos, 1998). E1b and E4 are also responsible for preferential export of AAV from the nucleus (Pilder, Moore, Logan, & Shenk, 1986). *E2A* encodes a DNA binding protein that is involved in viral DNA replication, processing of viral mRNAs and regulation of AAV promoters. Viral associated (VA) RNA inhibits the kinase PKR that phosphorylates eIF-2α, preventing the cell from blocking translation of viral mRNAs (Matsushita et al., 2004).

1.4 The Manufacturing of rAAV and Challenges Involved

When determining what AAV serotype is appropriate to use for the intended gene therapy it is important to consider several criteria: (1) The cell or tissue type to be targeted, (2) the safety of the gene of interest, (3) tissue specific or constitutively active promoters, and (4) systemic or local delivery. Production or engineering of rAAV capsids has been a particularly challenging aspect of rAAV vector generation. Methods of production have developed over the years and variations in the rAAV vector production methods are discussed in this section, focusing on the cell lines used to generate the vectors, the number of plasmid vectors transfected, and the transfection methods used. There are a number of challenges in the manufacturing of rAAV that contribute to the high cost of these therapies and make manufacturing processes inefficient. This section also considers the advantages and disadvantages of each production method.

1.4.1 Engineering of rAAV Transgene Cassettes

When producing viral vectors for gene therapy, it is important to consider the genome packaging size. In the case of rAAV, there is limited packaging capacity of approximately 5 kB (Naso et al., 2017). The gene of interest (transgene) to be packaged must be flanked by two ITR regions, and this must be considered within the 5 kB packaging capacity of rAAV. It is worth noting that in the case of self-complementary AAV the packaging capacity is reduced to around 2.4 kB (J. Wu et al., 2007). To overcome this size limitation research into the development of a split AAV approach which allows for the packaging of larger transgenes and its regulatory cassettes has been undertaken (Akil et al., 2019; Nitzahn et al., 2020). As AAV serotype 2 is the most widely studied AAV serotype and was the first to be characterised, the ITR sequence from serotype 2 is the most often used ITR sequence in rAAV work to date. Along with the transgene, the ITR regions also flank mammalian promoters such as the strong CMV promoter and enhancer (Figure 1.7). Use of a strong constitutively active promoter results in high expression levels of the gene of interest. Other strong promoters utilised are the EF1a, SV40, and CAG promoters which, along with the CMV promoter, can deliver high expression levels of the transgene (Powell, Rivera-Soto, & Gray, 2015). To avoid unwanted expression in particular tissue types it is also possible to use promoters specific to the tissue of interest such as the muscle creatine kinase for high expression in skeletal muscle or α-myosin for high expression in cardiac muscle. For high levels of neuronal expression the neuron specific enolase promoter can be used (Dashkoff et al., 2016; B. Wang et al., 2008).

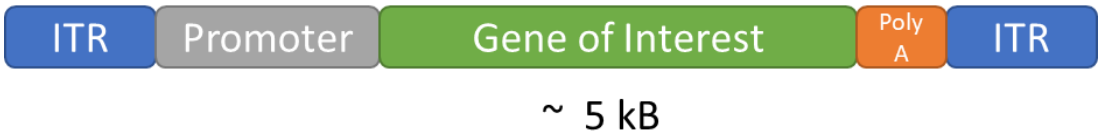

Figure 1.7 Schematic of the components of a packaging cassette for rAAV. AAV is Adeno Associated Virus, ITR is Inverted terminal repeats.

Research has also been carried out over the last two decades studying the link between codon usage in the transcript of the transgene, that partially determines elongation speeds during mRNA translation, and protein expression levels. Codon engineering has been shown to impact mammalian expression and in a tissue specific nature. It is therefore important to understand the implications of codon optimisation of the transgene gene as this impacts the expression of the transgene at the protein level (Carton et al., 2007).

1.4.2 Manufacturing of rAAV

As with many other biotherapeutics, AAV vectors must be produced in living systems and production of rAAV vectors is expensive. Traditionally, rAAV production was carried out in adherently grown cells. Despite larger scale adherent production methods being developed, including cell stacks or roller bottles, production yields of around 10^{14} genome copies (GC) per litre are obtained (R. M. Kotin, 2011; Strobel et al., 2019). Such yields are suitable for generating enough material for early-stage clinical trials but may not be suitable to meet larger scale markets. Furthermore, this platform is not easily scalable and thus suspension cultured cell production systems have received much attention. Both adherent and suspension systems are discussed in more detail in sections 1.4.3.1.2 and 1.4.3.1.3.

1.4.2.1 Methods for Transfection of rAAV Plasmid DNA

One of the most common methods of rAAV vector production utilises a two- or three-plasmid transient transfection of a HEK cell line (R. Jude Samulski & Muzyczka, 2014). One plasmid is the transgene plasmid, containing the therapeutic gene of interest which is flanked by AAV ITRs at each end. The second plasmid transfected contains the AAV *Rep* and *Cap* genes. These two plasmids are co-transfected into a cell line. To produce the vectors, the two plasmids must either be co-infected with a helper virus, such as adenovirus, or be co-transfected with a third "helper" plasmid. The helper plasmid expresses the adenoviral genes *E1B, E2A, E4, VA1* RNA. If co-infection with Ad is used, after production the adenovirus can be heat inactivated at 56°C during rAAV purification (Tenenbaum, Lehtonen, & Monahan, 2003). However, co-infection with a helper-virus plasmid now tends to be favoured, negating the need for co-infection with a helper virus. Xiao et al developed a triple transient transfection method, using the Rep Cap plasmid, the transgene plasmid and a helper plasmid containing the genes E2a, E4 and VA RNA, utilising the E1a expressing HEK293 cell line (Xiao, Li, & Samulski, 1998). This triple transient co-transfection method removes the need to coinfect with a virus and thus is considered a safer method of production. There has also been research into the development of rAAV production systems that are not reliant on the transfection of plasmid DNAs, this is because multi-plasmid transfections are rather inefficient due to the need to ensure multiple plasmids enter each cell and there is no control over the copy number that enters a given cell. Further, it requires large amounts of plasmid DNA rAAV vectors and is difficult to adapt the transient transfection method for large scale manufacturing.

One further aspect that has been studied is the ratio of the plasmid DNA transfected. As mentioned previously, one of the most common methods of rAAV production is the co-

transfection of three plasmids, a plasmid containing the *rep* and *cap* genes, a plasmid containing the ITR regions flanking a GOI and a plasmid containing the helper genes. However, the ratio at which these plasmids get transfected, and the number of plasmids transfected can vary across studies. Xiao and colleagues have studied the effect of altering the transgene/packaging plasmid ratios in their helper free system across a number of packaging plasmids and determined the optimal ratio required to generate a high titre system (Xiao et al., 1998). More recently, Zhao and colleagues used a Design-of-Experiment approach to determine the optimal transgene, packaging and helper plasmid ratios to achieve yields of $3x10^{14}$ vector genomes (VG)/L in a suspension platform, this was carried out by lowering the transgene plasmid concentration with a higher packaging plasmid (Zhao et al., 2020).

Another system has been developed for the production of rAAV vectors which circumnavigates the challenges associated with scalability of AAV production (Discussed in section 1.4.3.1.4). In 2002, Kotin and colleagues established the Baculovirus Expression System (BEV) for AAV production by live baculovirus infection of *Spodoptera frugiperda* (Sf9) cells. Three recombinant baculoviruses are used to infect Sf9 cells, a Rep-baculovirus, a VP-baculovirus and an AAV-ITR baculovirus. Furthermore, the rAAV particles generated in the baculovirus systems have the same physical and biological properties as those produced in mammalian cells. Kotin's team were able to generate yields of $5x10^{4}$ vector genomes per Sf9 cell (Urabe, Ding, & Kotin, 2002)

Work has also been on-going to develop systems that negate the need for transient transfection. For example, the generation of cell lines that have copies of the AAV *Rep* and *Cap* genes integrated into the cells has been reported. More specifically, Lui *et al.* reported on the development of a system which delivers the rAAV genome to a packaging cell line without the need for plasmid transfection. They utilised a HeLa cell line, C12, and engineered this to be under inducible control for the expression of the AAV Rep and Cap proteins when infected with Adenovirus. In this system the rAAV genome is embedded in the E1 region of a replication deficient rAd virus. The HeLa cells are then transduced with the rAd virus resulting in the production of infectious rAAV vectors (K. Reed Clark, Voulgaropoulou, Fraley, & Johnson, 1995; X. L. Liu, Clark, & Johnson, 1999).

1.4.2.1.1 Calcium Phosphate Precipitation Method of Transfection

Calcium phosphate precipitation is one of the most common methods used for transfection of plasmid DNA, including for rAAV production and has been used for transfection of plasmid

DNA co-transfected into HEK293 or HEK293T cell lines (Allay et al., 2011; Zolotukhin et al., 1999). Calcium phosphate co-precipitation has been shown to efficiently transfer DNA into 90% of transfected HEK293 cells. The method works via the formation of a calcium phosphate-DNA precipitate, with the calcium phosphate facilitating binding of DNA to the cell surface and entering the cell by endocytosis ("Calcium phosphate–mediated transfection of eukaryotic cells," 2005). However, calcium phosphate precipitation for the production of rAAV usually requires serum, this is not recommended for clinical use. Furthermore, calcium phosphate precipitation is not easily scalable. AAV production using calcium phosphate mediated transfection has been shown to generate 100,000 vector genomes per cell in HE293 cells (J. Fraser Wright, 2009).

1.4.2.1.2 Polyethylenimine (PEI) Coprecipitation Transfection

Polyethylenimine (PEI) mediated plasmid DNA transfection into cells was first described in 1995 by Boussif and colleagues (Boussif et al., 1995). PEI forms ionic interactions with DNA resulting in the formation of a polyplex which can enter the cells through endosomes. PEI is favourable over calcium phosphate coprecipitation due to the fact that cells can be grown in serum free media and is more efficient at delivering plasmid DNA. PEI is moderately cytotoxic and is non-biodegradable but nevertheless represents a preferred method of transfection of plasmid DNA and can be used in suspension cultures easily. Durocher et al. (2007) reported production of AAV2 vectors of 10^{14} vector genomes per 3.5 L bioreactor culture under serum free conditions and PEI mediated transfection (Durocher et al., 2007). Huang and colleagues, generated AAV2 vectors utilising a triple plasmid co-transfection, using PEI co-precipitation in HEK293T cell lines, reporting titre yields ranging from $2x10^{12}$ vector genomes (VG)/ml to $2x10^{13}$ VG/ml (Huang et al., 2013). PEI transfection offers a cost-effective method of producing high titre AAV vectors in both adherent and suspension culture (Reed, Staley, Mayginnes, Pintel, & Tullis, 2006; J. Fraser Wright, 2009). Chahal and colleagues utilised HEK293SF cells grown in serum free suspension to produce AAVs of serotypes 1-9 using a PEI transfection reagent. This production method generated yields of 10^{13} VG/L cell culture (Chahal, Schulze, Tran, Montes, & Kamen, 2014).

1.4.3 Industrial Manufacture of rAAV Vectors

Production of biologics can be broken down into upstream and downstream processing. AAV manufacturing involves the upstream processes of cell line development, cell culture and harvest of AAV, while the downstream processes consist of purification, formulation and fill

finish. Successful manufacturing of rAAV results in a consistent high titre pure product that meets the safety and efficacy that is required for regulation (Rooij et al., 2019).

1.4.3.1 Upstream Processing

Upstream processing is the first step in the production of biomolecules and generally refers to the entire cell culture process from cell expansion to the harvest of the culture. The main steps of upstream processing are dependent on both the product and the cell line used. All upstream steps can vary and be process and target specific, including harvesting which as described earlier for the case of rAAV may require recovery of material from within the cell or from the supernatant (Lindskog, 2018). Production of rAAV at scale to meet the demands is a continuing challenge with gene therapy vector production. Generally, in order to produce clinical grade rAAV for trial, cultures of between 10 and 200 litres are required (W. Qu, Wang, Wu, & Xu, 2015). Upstream processing specifically focuses on the host cell, transfection, production of the virus (including culturing conditions, feeding/media) and the virus harvest. The host cell refers to the thawing and expansion of the master cell bank, there can be variability associated with this step, from the cell line used to the media. Furthermore, the cell concentration and growth phase of the cell can also cause variability during this phase. During rAAV upstream processing, transfection methods (as described in section 1.4.2.1) can vary from the reagent used, the plasmid size, number of plasmids transfected and the plasmid ratio. Virus production can vary due to time cultured, exchange of media and the temperature the cultures are grown at. If produced in suspension in bioreactors, the control of these and other parameters can be much more stringent than in other systems. The final stage in rAAV upstream processing is particle harvest, how this is achieved, and the time post transfection can vary from process to process.

1.4.3.1.1 Cell Lines

Production of protein therapeutic substances, such as recombinant proteins, monoclonal antibodies (mAbs) and viral vectors can be produced using a variety of methodologies and expression systems. This includes non-mammalian systems, such as bacterial, insect, yeast and plant cell systems, or by using mammalian cell expression production platforms (human and non-human mammalian cell lines)(Dumont, Euwart, Mei, Estes, & Kshirsagar, 2016). The choice of production system can vary based on the protein or target biologic to be expressed. Mammalian cell lines are a preferred method for protein production in the biopharmaceutical industry to make recombinant protein based ‘drugs’, due to their ability to produce, fold and assemble complex proteins with human like post-translational

modifications (PTMs) such as glycosylation patterns similar to those produced in humans (Ghaderi, Taylor, Padler-Karavani, Diaz, & Varki, 2010). Some of the most common cell lines used for biotherapeutic protein production includes the use of the non-human cell lines Chinese Hamster Ovary (CHO) and baby hamster kidney (BHK21) cells among others. The human mammalian cell lines used include, but are not limited to, Human Embryonic Kidney (HEK) and HeLa (after Henrietta Lacks from which the original biopsy of cells was taken) cells. The human cell lines generally produce recombinant proteins most like those synthesised naturally in humans, with their post-translational N-glycansin particular being similar in structure, number and location which plays a role in the biologic activity, stability and immunogenicity of therapeutic proteins (Dumont et al., 2016; Swiech, Picanço-Castro, & Covas, 2012). However, CHO cells in particular are indeed the commercial go to cell line for production of human like recombinant proteins as these can produce human-like PTMs at higher yields and are more robust than other cell line options. Despite this, for commercial viral vector production, human cell lines such as HEK293 and HeLa are of particular interest and HEK cells in particular are the favoured platform at present.

HeLa Cells

HeLa cells were the first *in vitro* continuously cultured human cell line, established in 1953. These cells were derived from a cervical epidermoid carcinoma from Henrietta Lacks (Scherer, Syverton, & Gey, 1953). Unfortunately, these cells were harvested without knowledge or consent, and this has led to much debate on medical ethics and controversy surrounding this cell line. Despite the controversy, HeLa cells are one of the major cell lines used in general cell biology study across the world and has been investigated and used for the production of recombinant AAV vectors. Historically AAV production using a HeLa cell line was carried out using a two plasmid transfection system where the cells were co-transfected with a transgene plasmid and a rep-cap containing plasmid and the HeLa cells were coinfected with wild type Adenovirus (wtAd) (Merten, Geny-Fiamma, & Douar, 2005). Liu and colleagues have reported the development of a HeLa cell line for high titre AAV production using the coinfection of Ad. This method of AAV production is an advantageous system for large scale production as AAV production in HeLa cells occurs in suspension, furthermore, this research showed that increasing the Ad moi to greater than 10 viruses caused a 10 fold increase in the particle titre (X. Liu, Voulgaropoulou, Chen, Johnson, & Clark, 2000).

Research into the development and use of HeLa cell producer cell lines for AAV production has been extensive and a number of HeLa derived cell lines have been generated for the production of high titres of rAAV. One method for the production of rAAV particles reported involves the use of cell lines stably expressing the *Rep* and *Cap* genes, for example the HeLaRC32 cell line. The parental cell lines of these rep/cap expressing cells are typically HeLa cells and generally require the coinfection of Ad for the production of AAV (Chadeuf et al., 2000; G.-P. Gao et al., 1998; Salvetti et al., 1998; Q Yang, Chen, & Trempe, 1994b). Unfortunately, due to the potential for Ad viral genome contaminants in the rAAV stocks produced, rAAV production has largely moved away from the co-infection of cells with wild type Ad due to safety concerns.

HEK293 cells

Human Embryonic Kidney (HEK) cells, like HeLa cells, are an immortalised cell line. The cell line was originally derived from an aborted female foetus in the 1970s and immortalised by the transfection of the cells with Ad5 DNA containing the *E1A* and *E1B* genes (W. C. Russell et al., 1977). There have been a number of sub-cell lines derived from the HEK293 cell line including the HEK293T and HEK293F cell lines. The HEK293T cell line contains the large T antigen of the SV40 virus (Bae et al., 2020; DuBridge et al., 1987). HEK cells are frequently used in the production of rAAV at the bench and commercial scale and are currently the cell line of choice for AAV production.

As with HeLa cells, rAAV was initially produced from HEK293 cells by the co-infection of cells with wtAD, this posed the same safety risks of Ad contaminants (Merten et al., 2005). Further developments moved from use of wtAd to a replication defective Ad which was missing the *E1* genes. HEK cells were a natural choice for the production of AAV using E1 deleted Ad due to the expression of Ad5 E1 genes in the HEK cells (Merten et al., 2005). The most widely used method of rAAV production currently is the triple transient transfection approach using a transgene plasmid, a *Rep/Cap* plasmid and a Ad Helper virus suppling the helper genes *E2*, *E4* and *VA* RNA. Using the helper plasmid negates the risk of Ad contaminants in AAV products (Nguyen et al., 2021).

Typical rAAV production using HEK cells is still undertaken in adherent culture mode; this method is typically a time consuming and challenging production method with a major issue being scalability of adherent HEK293 based rAAV production. While there has been improvement in the scale up of adherent culture systems, such as the development of technologies such as the iCellis system (Strobel et al., 2019) there is still a limitation upon

production using this approach. Nevertheless, Strobel and colleagues utilised high density frozen cell stocks by seeding directly into CELLdiscs for the upscale of HEK 293 cell line derived rAAV production yielding rAAV Serotype 2 post purification titres of 10^{15} vector genomes per batch in the presence of FBS (Strobel et al., 2019).

The limitations of adherent culture means inevitably research has moved towards the development of suspension based HEK cell lines for the production of AAV. Process development advances have yielded titres of up to $1x10^{14}$ vg/L of culture post purification (Blessing et al., 2019; Grieger, Soltys, & Samulski, 2016; Nguyen et al., 2021). Despite the advances in the suspension cells, much improvement is needed to achieve high genome packaged rAAV yields for the treatment of disorders.

A549 cells

One further human cell line which has been utilised for AAV cell line production is the A549 cell line; this is an adenocarcinomic human alveolar basal epithelial cell line developed in the early 1970s (Giard et al., 1973). This cell line is typically used in the study of lung cancer or for the development of drug therapies for the treatment of lung cancer(Han Zhang, Feng, Gong, & Ma, 2018). However, this cell line has been used in research to develop rAAV producer cell lines. Gao and colleagues developed an A549 producer cell line stably expressing *rep/cap*, named K209. A549 cells were transfected with an AAV serotype 2 p5 *rep/cap* cassette. Upon adenoviral infection the K209 producer cell line amplifies the *rep/cap* genes, resulting in a high level of AAV production(Guang-ping Gao et al., 2002). Farson and colleagues also reported development of an A549 producer cell line stably expressing R*ep* and *Cap* genes capable of generating $>10^4$ AAV particles per cell (Farson et al., 2004) . Unfortunately, in order for AAV production to occur these cells must be coinfected with Ad virus for Rep/Cap expression to occur.

CHO cells

The Chinese hamster ovary (CHO) cell system grown in fed-batch suspension is the expression system of choice for complex biopharmaceutical production, however it is not currently used for rAAV production. The CHO cell system has been highly evolved for the production of high titres of recombinant biotherapeutic proteins and therefore an opportunity might exist for this system to be explored to determine if it is able to support high titre and packaging production of rAAV. The advantage to this is that high efficient bioprocess conditions and scale-up approaches have been developed for CHO cells that could

be directly applied to rAAV production if this cell system can support rAAV production in suspension at appropriate titres and packaging efficiencies.

1.4.3.1.2 Producer Host Cell Line

New approaches are continually being investigated and developed to increase rAAV yields and quality while reducing costs. One of the major considerations when producing rAAV for clinical use is the producer cell line used. Human production cell lines have become a key focus in the therapeutics industry, they act as expression systems for the production of recombinant proteins and viral vectors allowing for human post-translational modifications (Malm et al., 2020).

To date rAAV research has largely focused on a number of mammalian cell lines including HEK293 and HEK293T although other host systems including insect and fungi cells have also been explored (Negrete & Kotin, 2007). One of the major advantages of using a HEK cell line, such as HEK293 or HEK293T, is its expression of the adenoviral genes *E1a* and *E1b,* these genes being required for replication of AAV to occur. HEK293 is one of the most commonly researched and utilised cell lines in recombinant protein and viral vector research. The cell line originated in 1973 from an aborted human embryo. The cell line was immortalised by the introduction and integration of a portion of the Ad5 genome containing the *E1A* and *E1B* genes, expression of E1a and E1b allows for the continuous culturing of the cells and inhibits apoptosis (W. C. Russell et al., 1977). Furthermore, E1a and E1b are essential helper proteins for the production of AAV and therefore HEK293 and its derivatives have become key cell lines used in rAAV production to date (Clément & Grieger, 2016; Malm et al., 2020). A number of other cell lines have been derived from the HEK293 parental cell line with the aim of improving the production of recombinant proteins in particular, the HEK293T and the HEK293E cell lines (Kimura et al., 2019; Malm et al., 2020).

1.4.3.1.3 Adherent Culture Production of Viral Vectors

Production of rAAV has long used adherent HEK293 cells, however this method lacks scalability. Scale up of adherent cell cultures involves using a larger number of flasks and the increase in the surface area required (Clément & Grieger, 2016). While adherent cultures are not ideal when it comes to scalability, they are still a well-studied and utilised method of vector production. Allay and colleagues have shown that adherent cultures can be used to generate titres suitable for the production of AAV8 vectors for phase I and II clinical trials for

the treatment of haemophilia B. They used an adherent HEK293T cell line and a two plasmid transfection method using CellSTACKS to sufficient post purification yields (Allay et al., 2011). Microcarriers and the iCellis® system are both used in the scale up and culture of adherent cells for the production of AAV vectors (Cherian, Bhuvan, Meagher, & Heng, 2020; Lennaertz, Knowles, Drugmand, & Castillo, 2013; Powers, Piras, Clark, Lockey, & Meagher, 2016). Most recent systems have investigated scale in suspension culture that can not only be scaled more easily but allows more robust control of parameters during culture in bioreactors such as pH, dissolved oxygen and feeding strategies.

1.4.3.1.4 Suspension Culture Production of Viral Vectors

To overcome the scalability issues associated with adherent cell lines, suspension cell lines have been developed. HEK293 is traditionally an adherent cell line, however it has since been adapted to suspension culture and for the safety and regulatory issues this move has included a move away from serum containing culture media, and hence free from animal components. Such cell lines include the industrially relevant HEK293F and HEK293H (Côté, Garnier, Massie, & Kamen, 1998; F. L. Graham, 1987; Schwarz et al., 2020). Grieger and colleagues developed one of the first suspension cell lines successfully used in the production of rAAV vectors. Their work adapted an adherent HEK293 cell line. The cells were adapted to serum and animal component free media in both shake flasks and WAVE bioreactors. Using the triple transient transfection method to produce AAV vectors, Grieger et al were able to generate vectors with a titre of $1x10^{14}$ VG/L of culture media 48 h post transfection for a number of different AAV serotypes (1-6, 8 and 9). This method of rAAV production is one of the most commonly used methods in the manufacture of GMP phase 1 clinical trial rAAV material for a variety of serotypes (Grieger et al., 2016).

A suspension HEK293T cell line was also used by Zhao and colleagues for the development of a high yield AAV vector production system using a design of experiment approach (DOE). DOE allows one to study a multitude of variables at the same time. This study showed that by lowering the concentration of the transgene plasmid while increasing the concentration of the packaging plasmids it was possible to achieve pre-purification yields of approximately $3x10^{14}$ VG/L of culture supplemented with 2% FBS and 50 µg/mL G418 for 13 serotypes of AAV, 48 h post transfection (Zhao et al., 2020). HEK293T cells are a human cell line derived from HEK293 that express the SV40 T antigen. Typically, this cell line is grown adherently but has been adapted to grow in suspension in chemically defined, protein free media (DuBridge et al., 1987).

Blessing and colleagues have recently described the development of a scalable AAV production system using the suspension HEKExpress cell line. The HEKExpress cell line is a fully characterised and suspension adapted cell line that can be grown in serum free conditions in orbitally shaking bioreactors. rAAV vectors were generated using a two plasmid PEI transfection system and were harvested 72 h post transfection. This study showed that it was possible to obtain similar yields of rAAV for a number of serotypes when grown in suspension and in comparison to adherently grown cells, with post purification yields determined to be between $2.5x10^{10}$ and $1.5x10^{11}$ vector genomes (Blessing et al., 2019).

1.4.3.1.5 Baculovirus Production Systems

As mentioned in section 1.4.2.1, baculovirus is another system used for the production of rAAV viral vectors. This system has been established for the manufacture of human and animal vaccines and human therapeutics including the rAAV-based gene therapy, Glybera®. The BEV system was first used for rAAV production by Kotin and colleagues and involves the infection of Sf9 cells with three baculoviruses, a Rep-baculovirus, a VP-baculovirus and an AAV-ITR-baculovirus to produce rAAV particles that are biologically similar to those produced in mammalian cells. Unlike mammalian cell production, the BEV system does not require addition of any of the adenoviral helper genes (Dirk Grimm, Kern, Rittner, & Kleinschmidt, 1998; Urabe et al., 2002). This system is advantageous over other rAAV production systems due to its fast production and its scalable nature (Felberbaum, 2015).

Mena and colleagues were able to produce yields of 10^{14} vector genomes per litre by infecting Sf9 cells at a low multiplicity of infection (MOI). Using a fed batch approach they were able to achieve a seven-fold increase in rAAV yields, furthermore, they were able to show that production in a bioreactor resulted in a 25% increase on what was achieved in shake flasks (Mena, Aucoin, Montes, Chahal, & Kamen, 2010)

Research continues into the use of the BEV expression system and Sf9 cells. An important aspect of this research is on the safety and efficacy of rAAV generated in the BEV system. Rumachik and colleagues carried out a comparative analysis of the vectors produced in human cells compared to insect cells. This study identified differences at both the genomic and proteomic levels. One of the major differences between the use of insect cells and mammalian cells is post translational modifications (PTMs). For example, insect cells are cannot generate complex N-glycans to the same level as mammalian cells (Kost, Condreay, & Jarvis, 2005). PTMs are known to influence therapeutic proteins by altering their stability, functional activity and immunogenicity. Using mass spectrometry, the study determined that

there are in fact differences between the PTMs of rAAV8 vectors produced in mammalian cells and insect cells, with the Sf9 produced rAAV8 capsids having more PTMs than their mammalian counterparts (Rumachik et al., 2020).

1.4.3.2 Harvesting of rAAV

Following the transfection of plasmids for rAAV production, it is important to harvest the rAAV particles from the culture media, or in the case of a number of AAV serotypes, from the producer cells themselves. This step in the production of AAV particles can vary, from the number of days between transfection of plasmids and the harvest, to how the rAAV particles are harvested (from culture media to the cell lysate). With regards to the time between transfection and harvest, there are a number of studies which harvest the cells after 48 h and others which harvest after 72 h (Blessing et al., 2019; Grieger et al., 2016; Zhao et al., 2020) and the 'best' time is likely to be process specific.

In situations where AAV particles are retained in the cells, this adds another challenge to the production and purification of particles as delivery vectors, as the cells need to be lysed before the AAV particles can be collected and purified. A number of AAV serotypes, including the most commonly used AAV2, are retained inside the producer cell line. Vandenberghe et al., showed that a mere 9% of AAV2 particles were secreted into the culture media from the HEK293 producer cell line, this is in stark comparison to that of serotypes such as AAV8 in which more than 85% of the total particles are secreted from the cells. The difference in the secretory amounts of the serotypes is thought to be due to the serotype affinity for heparin. Removal of AAV2s ability to bind to heparin increases the secretion of AAV into the culture media, while increasing AAV8s ability to bind heparin results in an increase in the number of retained particles in the cell (Summerford & Samulski, 1998; Vandenberghe et al., 2010; Xiao, 2010).

Harvest and purification of AAV particles from the cell begins with the cell lysis, this can be either chemical lysis, through detergent containing lysis buffers, or mechanical lysis, via freeze thaw or microfluidization methods. Once freed, any residual viral or cellular nucleic acids, host cell proteins, lipids or other impurities are removed by downstream purification. Using HEK293T cells to produce AAV vectors in a 10-layer HYPERFlask®, Dias Florencio developed a method of detergent cell lysis using Triton X to detach and lyse the adhered cells. Their method showed that the HEK293T cells treated with 0.5% Triton X-100 for 1 h resulted in the release of rAAV from the cells while maintaining structure and functionality. This method treats the producer cells and the supernatant at the same time, other traditional

methods separate the cells from the supernatant before recombining together. The study showed that treatment of producer cells with Triton X-100 resulted in an increased recovery of AAV in comparison to traditional harvest methods (Dias Florencio et al., 2015). One of the most commonly used protocols for the removal of nucleic acids uses the endonuclease Benzonaze to remove any endogenous DNA from the preparations (Clément & Grieger, 2016).

AAV extraction from the producer cell lines can be achieved by a number of other methods. Negrini et al developed a method of AAV vector extraction utilising chloroform. This method harvested AAV particles 6 days post transfection with the AAV particles being harvested and purified in 4-6 h with titres between 10^{12} and 10^{13} vector genomes per ml from two 175 cm^2 flasks (Negrini, Wang, Heuer, Björklund, & Davidsson, 2020; X. Wu et al., 2001). Unfortunately, this is not an operator safe method of AAV manufacture.

1.4.3.3 Downstream Purification and Polishing of rAAV

Downstream processing is the recovery and purification of the rAAV, the aim being to separate the rAAV from impurities and to formulate for use in patients. In order for viral vectors to be suitable to patient administration they must meet regulatory standards in terms of their critical quality attributes (CQAs) that define the quality of the product. In viral vector production, downstream processing begins with the material harvested either from the cell lysate or from the culture media. It is important and a requirement to remove impurities as they can pose unknow risks to the patient, particular immunogenicity, can impact stability, and can reduce transduction efficiency of the rAAV vectors. Removal of impurities relies on approaches such as ultracentrifugation or chromatography systems. One of the key impurities to be removed from AAV products is empty/incorrectly packaged capsids, that are biologically 'inactive' (i.e. do not carry transgene) and this is a key challenge in downstream processing of rAAV (W. Qu et al., 2015).

1.4.3.3.1 Ultracentrifugation

Ultracentrifugation is used in the purification of rAAV, using differences in the density of rAAV differing from other impurities. rAAV has an approximate density of 1.40 g/cm^3 and ultracentrifugation can be used to separate rAAV from cellular organelles, soluble proteins and nucleic acid. Furthermore, empty particles have a density of 1.32 g/cm^3 (G. Qu et al., 2007), this difference in densities allows for the separation of packaged particles from empty particles. Density gradient ultracentrifugation is suitable for all AAV serotypes (W. Qu et al.,

2015). Caesium chloride ultracentrifugation reduces the number of impurities on the first round of centrifugation, however, multiple rounds of ultracentrifugation results in a higher level of purity. Following $CsCl_2$ ultracentrifugation, the rAAV containing solution undergoes dialysis, a step which ultimately reduces the infectious titres. While there are advantages to the use of ultracentrifugation it is a time-consuming method of purification which takes approximately 30 hours to undergo two rounds of ultracentrifugation. In addition to this it is not currently an easily scalable method of purification.

Iodixanol gradient ultracentrifugation is a preferable method of purification to $CsCl_2$ ultracentrifugation due to its ability to recover higher yields of material. The improved ultracentrifugation method developed by Hermens et al showed a rapid and reproducible method of rAAV purification and concentration. The method is based on the iodixanol gradient described by Ford et al. (1994). Unlike $CsCl_2$, iodixanol gradient ultracentrifugation purification and centrifugation can be carried out in less than 24 h (Hermens et al., 1999).

1.4.3.3.2 Size Exclusion Chromatography (SEC)

Size exclusion chromatography (SEC) is a method that can separate large biologics by size and weight/shape in solution. The total mass of rAAV has been estimated at over 600 kDa, the packaged capsid is approximately 170 kDa heavier than its empty counterparts. If used it is usually as a polishing step although ion exchange chromatography methods are now generally preferred as chromatographic separations for rAAV.

1.4.3.3.3 Ion Exchange Chromatography (IEX)

rAAV particles can bind to ion exchangers, IEX is therefore a useful tool for purification that has received much interest as a scalable approach, making it advantageous over ultracentrifugation methods. The isoelectric point of rAAV serotypes have been calculated for serotypes 1-12. The overall net capsid pI does not vary greatly across the serotypes with the serotypes having an isoelectric point around pI 6. The isoelectric points of the VP3 protein, the most abundant, remains constant across the serotypes. However, there is some variance across the isoelectric point of VP1 and VP2. While most serotypes have a pI between 5 and 7, serotypes AAV2, AAV7, AAV8, AAV10 and AAV12 have a pI of approximately 8, 10, 10, 10, and 8 respectively (Venkatakrishnan et al., 2013). Venkatakrishnan and colleagues also showed that empty capsids have a slightly higher isoelectric point than packaged capsids, this knowledge gives rise to the use of anion exchange chromatography for the separation of full particles from empty particles.

There has thus been considerable focus on the use of anion exchange chromatography for the purification of rAAV. In a study by Kaludov et al, it was shown that ion exchange chromatography can purify AAV serotypes 2, 4 and 5 in a highly efficient and rapid manner, effectively removing the empty AAV capsids with 90 % of purified particles containing the gene of interest. This study utilised both weak AEX and strong AEX columns (Kaludov, Handelman, & Chiorini, 2002). It was later shown in a study by Urabe that anion exchange chromatography can separate packaged AAV1 capsids from empty capsids using the same strong and weak AEX columns as the Kaludov study. Furthermore, this study determined that upon removal of the empty capsids efficiency of AAV1 transduction increased (Urabe et al., 2006)(Dickerson, Argento, Pieracci, & Bakhshayeshi, 2020)

1.4.3.3.4 Affinity Chromatography

Affinity chromatography is a method of separating biomolecules from other contaminants that utilises the specific binding interactions between the biomolecule and a ligand. Research using mutant CHO-K1 cell lines deficient in heparin sulfate has shown that AAV2 contains binding sites specific to heparin sulfate (Summerford & Samulski, 1998). Affinity chromatography utilising Heparin has been used to successfully purify rAAV from the cell lysate of large culture volumes (Anderson, Macdonald, Corbett, Whiteway, & Prentice, 2000). Unfortunately, not all serotypes show affinity for heparin sulfate and some AAV serotypes show greater affinity to heparin sulfate than others, with AAV5 being the most successful (Nass et al., 2018a; W. Qu et al., 2015) and thus this cannot be used as a generic rAAV purification approach.

1.4.4 AAV Analysis Methods and Limitations

A major issue with rAAV process development is the ability to scale up the process for large scale production. All stages of rAAV production; upstream processing, downstream processing and analytics must be suitable for large scale production of AAV. Treatment doses in the clinic require accurate methods for titre analysis from genome titre to capsid/particle titre.

1.4.4.1 Genome Titre Analysis

The key method of determining dosing of rAAV therapeutics in the clinic relies on accurately determining vector genome titre (vg per ml). This can be achieved using a number of analytical methods including quantitative real-time PCR (qPCR) or digital droplet PCR. While

qPCR is the most widely used method of genome quantification due to its simple and well-established protocol, there are a number of limitations to its use. DNA amplification efficiency can be hindered by a number of factors, including poor primer design, presence of inhibitors and the requirement of a standard curve. Currently there are only two reference standards available, for serotypes AAV2 and AAV8. qPCR relies on the use of calibration curves from reference plasmid DNA (D'Costa et al., 2016; Dobnik et al., 2019; Moullier & Snyder, 2008). Aurnhammer et al were one of the first groups to determine the genome titre of AAV2 using qPCR. This group used qPCR and primers specific to the inverted terminal repeats (ITRs) of the packaged genome/transgene. This was an ideal method of quantifying the genome titre of AAV2 particles due to its requirement in AAV2 packaging. (Aurnhammer et al., 2012). However, the use of such an ITR qPCR approach has been shown to produce titres up to eight-fold higher than when targeting other regions of the transgene and packaged DNA which could be overcome by linearisation of plasmids outside the ITR region (D'Costa et al., 2016). The approach was therefore modified by using plasmid standards that had been linearised just outside the ITR region to give more accurate titre values (D'Costa et al., 2016). There are a number of other common sequence regions in the transgene plasmid that are targeted inside a capsid for qPCR analysis that allow general analysis of genomes (as opposed to target specific sequences for the transgene of interest). These include the CMV promoter region, the poly A region and the human beta globin intron (hBG) region. For example Rohr and colleagues utilised primers against the CMV region to determine genome titre (Rohr et al., 2005, 2002). Wang and colleagues also investigated regions away from the ITR regions due to potential issues with the palindromic sequences and over estimation, designing primers which targeted the cytomegalovirus enhancer/chicken β-actin promoter (CAG), the GFP transgene, a woodchuck hepatitis B virus posttranscriptional regulatory element (WPRE), and bovine growth hormone (BGH) polyA element (CAG, EGFP, WPIRE and pBGH, respectively) (F. Wang, Cui, Wang, Xiao, & Xu, 2013).

A new method that is a variation on traditional qPCR for quantifying genome titres has been developed utilising droplet digital PCR (ddPCR). This is a powerful technique that allows for absolute quantification of AAV. ddPCR is an improved PCR method which can separate a single PCR into approximately 20,000 droplets. ddPCR is advantageous to qPCR in that it does not require a standard curve for quantification(Furuta-Hanawa, Yamaguchi, & Uchida, 2019; Lock, Alvira, Chen, & Wilson, 2014; Mostrom et al., 2019). Research by Furuta-Hanawa and colleagues showed that ddPCR is capable of producing reproducible genome titres regardless of the sequence targeted (Furuta-Hanawa et al., 2019)

1.4.4.2 Capsid Particle Titre Analysis

While rAAV dose is usually based on the number of genomes given to a patient it is important to also understand the number of capsid particles present in a sample and how many of these particles are packaged correctly (contain genome). Quantification of particles is generally carried out using enzyme linked immunosorbent assay (ELISA). There are a number of commercial ELISA kits available for the quantification of AAV particles. These kits have been designed to detect fully formed rAAV capsids and are based on the work by Grimm and colleagues. They developed a sandwich ELISA assay which utilised the monoclonal antibody, A20 generated by Wistuba and colleagues, that has the ability to bind specifically to fully formed capsids but not single VP proteins present in the samples (Wistuba, Kern, Weger, Grimm, & Kleinschmidt, 1997). Along with generating an easy to use method of quantifying AAV, this study also determined that rAAV2 preps they investigated contain approximately 80% empty capsids (D Grimm et al., 1999). Since the development of the ELISA AAV2 assays, development of antibodies against serotypes 1, 3, 4, 5 and 6 have also been developed (D Grimm et al., 1999; Kuck, Kern, & Kleinschmidt, 2007; Wistuba et al., 1997).

Total viral particles can also be semi-quantified by separating AAV samples by SDS-PAGE and Coomassie Brilliant Blue staining. Once stained, the gels are subjected to scanning and densitometry analysis. Coomassie Brilliant blue fluoresces in the infrared spectrum if bound to proteins, this knowledge, along with the availability of AAV reference standards led to the development of a method to quantify viral particles while also determining purity of the samples. This method is advantageous due to its low cost and simplicity (Kohlbrenner et al., 2012).

Optical density is a tried and tested method of quantifying Adenovirus, this has since been used for the quantification of AAV. It has been shown to accurately quantify empty and fully packaged capsids, however it is recommended that optical density should be used in association with qPCR and ELISA assays to account for any variability when determining the empty to full ratio. Furthermore, this method has one major limitation, it requires high concentrations of purified AAV particles in the rage of $5x10^{11}$ vector genomes per ml or higher for accurate measurement (Sommer et al., 2003).

1.4.4.3 Transduction Assay and Analysis

As previously mentioned, rAAV can be used as a gene delivery vehicle with the potential to target a number of tissue types. Due to the potential uses, it is vital to study rAAV

transduction. Studies have been carried out to analyse the transduction efficiency of the rAAV generated from different serotypes (Schultz & Chamberlain, 2008). One of the most common methods to study AAV transduction is the use of a GFP transgene packaged inside the rAAV particles. Due to the fluorescent nature of GFP, cells successfully transduced with an AAV particle containing the GFP transgene can be visualised by fluorescent microscopy and flow cytometry. Unfortunately, this method is only suitable in research and would not be commonly used in the clinic (Rodriguez-Estevez, Asokan, & Borrás, 2020; Virella-Lowell, Poirier, Chesnut, Brantly, & Flotte, 2000)

1.4.4.4 Product Quality Attributes

Characterisation of the critical quality attributes of rAAV is important to confirm the authenticity of the material produced. Critical quality attributes are measurements of the product that confirm it is of the required standard for use, such as confirmation of the genome sequence, confirmation of the VP proteins and that these are intact and any post-translational modifications that are considered important. For this, analytics are of high importance when it comes to process development, characterisation and GMP manufacturing. Indeed, characterisation of viral vectors is of high importance in GMP production and product release to ensure product quality and patient safety. Each batch must be tested for identity, purity, safety and potency. Impurities can remain following purification and can be both process related or product related and can include host cell proteins (HCPs), nucleases and other components as outlined in Table1.1-6. Process related impurities refer to impurities derived from the manufacturing process including cell culture medium, HCPs, helper components (plasmid DNA and viruses), and purification related process components, while product related impurities refers to the vector products structurally related to the desired product e.g. Empty capsid vectors(J. Wright, 2014). The complexity of rAAV, consisting of 3 capsid proteins and the encapsulated genome mean that further analytic developments and standards are still required to establish a defined set of critical quality attributes for rAAV preparations.

HCPs are one of the major process contaminants and would be considered a critical quality attribute (CQA). HCPs are of concern due to their potential to induce an immune response, furthermore, HCPs can impact the quality, stability and activity of the drug product(Bracewell, Francis, & Smales, 2015; Bracewell, Smith, Delahaye, & Smales, 2021). Much research has gone into developing methods for the analysis of host cell proteins (HCPs), much of this research has been developed in the monoclonal antibody field but it is

likely that much of this knowledge can be transferred to the viral vector and gene therapy fields. There are a number of methods which can be used to assess HCPs including ELISA, SDS-PAGE, and Mass Spectrometry (Table 1.1-6). Commercial ELISA products are available to detect and quantify HCPs in viral vectors produced in HEK, HeLa, BHK and SF9 cells (Bracewell et al., 2021; J. Wright, 2014). Dong and colleagues have published work describing the co-purification of 13 proteins with rAAV using a combination of Gel LC-MS and 2D gel electrophoresis (Dong et al., 2014). Satkunanathan and colleagues showed using an LC-MS/MS approach that 44 HCPs co purified with AAV (Satkunanathan, Wheeler, Thorpe, & Zhao, 2014).

Table 1.1-6 Process and Product Related Impurities in rAAV Production.

Process Related Impurities	**Methods of Analysis**	**Issues Associated**
Residual Host Cell Protein (HCPs)	ELISA Mass Spectrometry SDS-PAGE	Immunotoxicity
Residual Host Cell Nucleic Acids	qPCR	Genotoxicity
Residual Plasmid DNA	qPCR	Genotoxicity
Residual Helper Viruses (Nucleic acids and proteins)	qPCR Infectious titre of helper virus ELISA Western blot	Immunotoxicity, Infectious Risk, Genotoxicity
Product Related Impurities	**Methods of Analysis**	**Issues Associated**
Empty Capsids	Ultracentrifugation, Electron Microscopy, IEX chromatography	Immunotoxicity
Encapsidated host cell nucleic acids	qPCR	Genotoxicity, Immunotoxicity
Encapsidated helper components	qPCR	Genotoxicity, Immunotoxicity
Replication competent AAV	Ad dependent amplification	Immunotoxicity
Aggregated, degraded and oxidised AAV vectors	Size Exclusion Chromatography, DLS, Electrophoresis	Immunotoxicity

1.5 Aims of this Study

During the production of AAV vectors, it has been widely reported that empty capsids form first and the transgene is then packaged inside these. Unfortunately, rAAV packaging is not efficient and so empty capsid particles remain (Kleinschmidt, Wistuba, Steinbach, & Bock, 1997). Empty particles are a common trait across all AAV serotypes. These empty vectors lack the transgene and thus have no therapeutic benefit. While AAV does not illicit a major immune response, high doses of capsids have the potential to trigger anti-capsid T cell responses (Federico Mingozzi & High, 2007) increasing the innate or adaptive immune response. Introduction of high empty to full particle ratio in a drug product has been shown to reduce transduction efficiency and high doses of rAAV capsids are therefore required (Dickerson et al., 2020; K. Gao et al., 2014). Thus, generally there is a need and drive to increase the packaging efficiency of processes to reduce the number of empty capsids from a process. It is noted that empty AAV vectors are not always undesirable and can in fact be used as decoys. Neutralising antibodies to AAV are present in a number of humans, these hinder rAAV ability to deliver the therapeutic and transduce. Mingozzi and colleagues showed that in the presence of empty AAV particles the neutralising antibodies target the empty particles instead of the transgene containing particles allowing for the delivery of the therapeutic gene (F. Mingozzi et al., 2013). Nevertheless, reducing the number of empty particles manufactured during the upstream culture remains a drive in the industry.

The work in this thesis therefore set out to address this issue by engineering of the HEK293T host cell. Specifically, the aims of the work were to:

1. Establish a rAAV production system using the suspension adapted HEK293T host cell line.
2. Assess the feasibility of generating a HEK293T host cell line stably expressing the four Rep proteins alongside the three VP proteins.
3. Generate and characterise HEK293T cell lines stably expressing Assembly Activating Protein. Determine what impact, if any, this has on rAAV2.GFP packaging.
4. Generate and characterise high, medium and low AAP expressing clonal cell lines, determine the impact these cell lines have on AAP packaging. Assess the functionality of the rAAV capsids.

Chapter 2

Materials & Methods

2.1 General Methods

All materials used in this study were of analytical grade or higher unless otherwise stated.

2.2 Mammalian Cell culture

2.2.1 Revival of Cell Lines

Cryovials containing 1 mL of cells were thawed in a water bath at 37°C before being aliquoted into a 15 mL falcon tube. 9 mL of chilled Gibco™ FreeStyle™ 293 Expression Medium (ThermoFisher Cat. No. 12338026) was then added dropwise to the falcon tube. The cells were centrifuged at 200 x g for 10 mins, the supernatant was then discarded, and the remaining pellet was then resuspended in 10 mL of prewarmed Gibco™ FreeStyle™ 293 Expression Medium (ThermoFisher Cat. No. 12338026). The cell concentration and viabilities were determined using the ViCell XR (Beckman Coulter). The cells were then seeded at a concentration of 3 X 10^5 vc/mL with a final culture volume of 25 mL in a 125 mL Erlenmeyer flask with a vented cap and incubated at 37°C in a shaking incubator at 140 rpm with 5% CO_2.

2.2.2 Routine Subculture of Cell Lines

Cell lines were sub-cultured in prewarmed Gibco™ FreeStyle™ 293 Expression Medium (ThermoFisher Cat. No. 12338026). Routine subcultures were carried out every 3-4 days. Cells were counted using the ViCell (Beckman Coulter). Flasks were seeded at a concentration of 2 X 10^5 vc/mL with a final culture volume of 25 mL. The cells were returned to the shaking incubator at 140 rpm at 37°C.

2.2.3 Cryopreservation of Cell Lines

Cells were cryopreserved at 1 X 10^7 vc/mL. The cell numbers and viability were determined, using these values the volume of cell culture required to bank down a number of vials was calculated, and the culture was centrifuged at 200 x g for 10 mins. The supernatant was then removed, and the pellet was resuspended in the required volume of 1X freeze mix (10%DMSO, 90% Gibco™ FreeStyle™ 293 Expression Medium (ThermoFisher Cat. No. 12338026)); this was then aliquoted at 1 mL per cryovial. The cryovials were then placed in a Mr Frosty containing the appropriate volume of isopropanol and stored at -80°C for 24 h prior to being stored long term in liquid nitrogen.

2.2.4 PEI Transfections

24 h prior to transfections PEI transfections Corning® CellBIND® T25 flasks were seeded at $1.8x10^5$ viable cells (vc) /cm^2. On the day of transfection, the media was carefully removed and replaced with fresh freestyle media. All transfections were carried out using PEIpro (Polyplus transfections). A known number of DNA copies per cell was added to an Eppendorf tube containing 250 µL volume of freestyle media and a volume of PEIpro equal to that of the total mass of DNA to be transfected was added to an Eppendorf containing 250 µL of freestyle media. The media: DNA mix was then added to the media:PEI mix and incubated at room temperature for 10 min prior to being added to the cells in the T25 flasks. Cells were incubated in a static incubator at 37°C for either 48 or 72 h prior to harvesting cells.

2.2.4.1 PEI transfections for the production of rAAV particles

Recombinant AAV vectors were produced as per Methods section 2.2.4 above. A triple transient transfection was carried out by transfecting 200,000 copies of the AAV plasmids, pAAV-RC-Kan, pAAV-GFP-Kan and pHelper-Kan (All supplied by Cobra Biologics). rAAV particles were harvested 72h post transfections. pAAV-RC-Kan contains the *Rep* and *Cap* genes, the pAAV-GFP-Kan plasmid contains the GFP transgene flanked by the ITR regions and the pHelper-Kan plasmid contains the adenoviral helper genes *E2a, E4* and VA RNA.

2.3 Molecular Biology

2.3.1 Cloning of DNA Sequences in Plasmid DNA

All DNA was diluted in either nuclease free water (Promega), EB buffer (From QIAprep Spin Miniprep kit, Cat. No. 27104, Qiagen) or TB buffer (HiSpeed Plasmid Maxi Kit, Cat. No. 12662, Qiagen). All restriction digests were carried out using FastDigest enzymes, restriction enzymes (both ThermoFisher) or High-Fidelity restriction enzymes (NEB) following manufactures protocols. Both gel extracted and digested DNA was purified using the Wizard® SV Gel and PCR Clean-Up System (Promega, Cat No. A9281) according to the manufacturers protocol. Annealed oligos were purified using the QIAquick Nucleotide Removal Kit (Qiagen, Cat. No. 28304). Plasmid DNA was prepped using Plasmid Miniprep or Maxiprep kits (Qiagen, Cat No. 27106 and 12162).

2.3.2 Preparation of Ca^{2+} Competent DH5α *E. coli*.

5 mL of LB media was inoculated with a single colony of DH5α and incubated at 37°C at 200 rpm overnight. 1 mL of overnight starter culture was used to inoculate 50 mL of SOB medium

in a 500 mL conical flask, which was then grown to an A600 of 0.4-0.6. Once at the appropriate A600 nm measurement, the culture was centrifuged in a pre-chilled falcon tube at 3500 rpm at 4°C for 15 min. The pellet was then resuspended in 10 mL filter sterilised 100 mM $CaCl_2$ and incubated on ice for 30 min. This was then centrifuged for a further 15 min at 35000 rpm at 4°C. This pellet was then re-suspended in 100 mM $CaCl_2$ and 80% glycerol before dispensing as 50 µL aliquots on dry ice prior to long term storage at -80°C.

2.3.3 Purification of Plasmids from *E. coli*

5 mL DH5α cultures were grown in LB overnight at 37°C at 200 rpm. Following incubation, these cultures were pelleted by centrifugation at 4000 rpm for 15 min (4°C). Plasmids were purified from the pellets using the QIAprep© Spin Miniprep Kit (Qiagen) as per the manufacturer's protocols and eluted in Nuclease Free water or TB buffer. The plasmid DNA was then quantified using a Nanodrop 1000 Spectrophotometer (ThermoFisher Scientific™) and stored at -20°C. For Larger quantities of DNA, 250 mL cultures were grown and pelleted in the same manner as above, followed by purification using the HiSpeed™ Plasmid Maxi kit (Qiagen) as per the manufactures protocol and quantified as above.

2.3.4 Amplification of Target Genes by Polymerase Chain Reaction

Target genes were amplified from original plasmids supplied by Cobra Biologics using Phusion Hi-Fidelity DNA Polymerase (ThermoFisher Scientific™, Cat No. F530S). Primers and oligos were designed based on the gene of interest sequence and incorporated restriction sites to facilitate cloning into expression vectors. These primers and oligos were synthesised by Eurofins Genomics (**Table 2.2-1 and Table 2.2-4**). Standard Phusion reaction components and conditions are outlined in **Table 2.2-2** and **Table 2.2-3.**

Table 2.2-1 Pimers designed for the amplification of target genes and restriction sites used.

Gene	Forward Primer	Reverse Primer	Restriction sites (fwd/rev)	Annealing Temp (°C)	Insert size (kB)
ATG-AAP	TATGGTACCGGAAAGGCGGGCCAG	ATACTCGAGGGGTGAGGTATCCATACTGTGGCAC	KpnI/XhoI	58	669
ATG-AAP STOP	TATGGTACCGGAAAGGCGGGCCAG	ATACTCGAGTCAGGGTGAGGTATCCATACTGTGGCAC	KpnI/XhoI	58	672
CTG-AAP	TATGGTACCCCTGGTTGAGGAACCTGTTAAGACGG	ATACTCGAGGGGTGAGGTATCCATACTGTGGCAC	KpnI/XhoI	58	751
CTG-AAP STOP	TATGGTACCCCTGGTTGAGGAACCTGTTAAGACGG	ATACTCGAGTCAGGGTGAGGTATCCATACTGTGGCAC	KpnI/XhoI	58	754
Rep	TATGCTAGCATGCCGGGGTTTTAC	ATACTCGAGTTGTTCAAAGATGCAGTCATCC	NheI/XhoI	57.7	1872
Rep+ Cap	TATGCTAGCATGCCGGGGTTTTAC	ATATCTAGACAGATTACGAGTCAGGTATCTGGTG	NheI/XbaI	57.7	4988

Table 2.2-2 Reaction components used with Phusion Hi-Fidelity DNA Polymerase

Component	**Volume (µL)**
DNA Template	1 (10 ng DNA)
Nuclease free water	33.5
5X HF buffer	10
Forward Primer	2
Reverse Primer	2
10 mM dNTP mix	1
Phusion Polymerase	0.5
Total Volume	**50**

Table 2.2-3 Conditions for PCR reactions with Phusion Hi-Fidelity DNA Polymerase.

Step	**Times (m:s)**	**Temperature (°C)**	
Initial Denaturation	0:30	98	
Denaturation	0:10	98	30 Cycles
Annealing	0:30	Primer Specific (Table #)	
Extension	1:00 /kb	72	
Final Extension	10:00	72	
Hold		4	

Table 2.2-4 Oligos ordered for additional sequences.

	Forward Sequence	**Reverse Sequence**	**Restriction Site**
MCS1	TATACGCGTTTAATTAAGCGGCCGCATC GATAGCGCTGATATCTGGCCAGGCCGG CCACCGGTCTTAAGGCTAGC	ATAGCTAGCCTTAAGACCGGTGGCCGG CCTGGCCAGATATCAGCGCTATCGATGC GGCCGCTTAATTAAACGCGT	MluI/NheI
MCS2	TATATTTAAATGCGGCCGCGCTAGCCAT ATGTTAATTAAACGCGTTGGCCAGCTAG CCAGCTGCCTCGAGGAGATCTTACGTA	ATATACGTAAGATCTCCTCGAGGCAGCT GGCTAGCTGGCCAACGCGTTTAATTAAC ATATGGCTAGCGCGGCCGCATTTAAAT	SwaI/SnaBI

2.3.5 Restriction Digests of DNA

Restriction digests for the cloning of the genes of interest were carried out using restriction enzymes supplied by ThermoFisher Scientific™, New England BioLabs or Promega. Digests were carried out according to the manufacturer's guidelines. Digested DNA was separated by gel electrophoresis using a 1% agarose gel for 1 h at 100 V with SYBR™ Safe DNA Gel Stain (ThermoFisher Scientific™, Cat. No. S33102). Agarose gels were visualised under ultraviolet light and the bands of DNA were excised from the agarose gel by a sterile razor blade. The DNA (Digested or PCR product) was purified from the agarose gel using Wizard® SV Gel and PCR Clean-Up system (Promega), in accordance with the manufacturer's protocol.

2.3.6 Dephosphorylation of Backbone and Ligation

Linearised pDNA backbone was dephosphorylated using thermosensitive alkaline phosphatase (Promega) via incubation at 37°C for 20 min followed by heat inactivation at 74°C for 30 min. Once the backbones had been dephosphorylated, DNA ligations using T4 Ligase (Promega, Cat. No. M1801) using plasmid: insert rations of 1:0, 1:1 and 1:3. These reactions were incubated at 4°C overnight and followed by transformation into DH5α *E. coli* cells.

2.3.7 Transformation of Plasmids in Calcium Competent DH5α *E. coli*

DNA constructs were transformed in DH5α *E. coli* cells. The ligation mixes or recombinant constructs was added to 100 µL of calcium competent DH5α cells and incubated on ice for 30 min, following this the cells underwent a heat shock at 42°C followed by a further 2 min on ice. 900 µL of sterile SOC media was added to the DH5α cells and incubated in a shaking incubator at 37°C for 1 h prior to plating out on a LB agar plate containing the appropriate antibiotic selection (Ampicillin or Kanamycin).

1.2.2.8 Colony Screen for Successful Ligation of Insert into Backbone

One colony was picked from an LB agar plate generated in Methods section 2.3.7. this colony was placed in 5 µL of nuclease free water. Standard GoTaq polymerase reaction components (Table 2.2-5) were added to the colony mix and the PCR was set up according to the conditions are outlined in **Table 2.2-6.**

Table 2.2-5 Reaction components used with GoTaq® G2 Flexi DNA Polymerase

Component	**µL**
5X Buffer	4
$MgCl_2$	1.6
Fwd primer	0.8
Rev Primer	0.8
dNTPs	0.4
GoTaq Polymerase	0.1
H_2O	7.3
TOTAL	**15**

Table 0-1 PCR conditions for GoTaq G2 Flexi DNA Polymerase

Temperature (°C)	**Time (h:min:sec)**	
94	0:05:00	
94	0:00:30	30 cycles
55	0:00:30	
72	0:01:00 /kb	
72	0:07:00	
4	hold	

2.4 Transient Expression Experiments

Transient expression was carried out using PEIpro® transfection reagent (Polyplus-transfection®, Cat No. 115-0015). T25 flasks were seeded at $1.8x10^5$ vc/cm^2 24 h prior to transfection and incubated at 37°C in a static incubator. Plasmid DNA was transfected at 100,000 copies/cell with the µL PEI reagent being equal to the mass of DNA being transfected. The plasmid DNA to be transfected was added to 250 µL and this was then added to a PEI: Media mix. This was then incubated at room temperature for 10 min prior to being added dropwise to the cells.

2.5 Protein Analysis and Characterisation

Cell pellets were lysed using 400 µL of lysis buffer pH 7.2 (HEPES, NaCl, β-Glycerophosphate, Triton-X). Prior to use, 500 µL NaF and 50 µL Nav were added to the lysis buffer along with 1 cOmplete™ Mini Protease inhibitor tablet (MERCK, Cat #:11836153001) per 10 mL of Lysis buffer) per $1x10^7$ cells. Cells were incubated on ice for 30 min prior to centrifugation at 13,000 rpm for 10 min. Cell pellets were stored at -80°C prior to analysis. Thawing of cell pellets for analysis was carried out on ice and given a clearing spin at 4000 rpm for 10 min.

2.5.1 Determination of Protein Concentration via Bradford Assay

Protein concentrations collected from cell lines and expression experiments were estimated using the Bradford assay. Bradford reagent was made using 50 mg Coomassie Brilliant Blue G250, 15 mL ethanol, 50 mL 85% phosphoric acid and 435 mL ddH_2O. All samples were diluted 1:20 in ddH_2O, 1 mL of Bradford reagent was added to the diluted samples and incubated for 10 min at room temperature. The absorbance was read at 580 nm on a spectrophotometer to determine the protein concentration in µg/mL using BSA as a standard.

On occasion, the Bradford assay was carried out in a 96 well plate. As above the samples were diluted 1:20 and 200 µL Bradford reagent was added to the samples. A standard curve was set up ranging from 0 µg to 400 µg BSA with the plate being read on a plate reader at 595 nm.

2.5.2 Protein Separation via SDS-PAGE

Protein samples were prepared for SDS-PAGE using the estimated protein concentrations determined by the Bradford assay. Samples were prepared in a 4X reducing laemmli buffer which consists of 50 mM Tris-HCl pH 6.8, 2% SDS, 10% glycerol, 1% β-mercaptoethanol, 12.5 mM EDTA and 0.02% bromophenol blue. Once prepped the samples were boiled at 100°C for 10 min. The samples were then loaded on either 8% or 12% poly acrylamide gels and separated at 100 V for 30 min followed by 150 V for 1 h to 1.5 h in a 1X SDS running buffer. The running buffer was prepared from a 10X stock consisting of 200 mM Glycine, 250 mM Tris and 1% SDS). Samples were loaded with PageRuler™ Plus Prestained Protein Ladder (ThermoScientific, Cat. # 26620). Gels were either or blotted (Section 2.5.3) or stained with Coomassie (Section 2.5.4).

Table 2.2.7 Components for resolving gels for SDS-PAGE.

Component	8% resolving gel (mL)	12% resolving gel (mL)
1.5 M Tris-HCl, pH 8.8	1.250	1.575
30% Polyacrylamide	1.325	0.250
10% SDS	0.050	0.063
10% Ammonium Persulfate	0.050	0.063
TEMED	0.003	0.003
ddH_2O	2.330	2.050

Table 2.2-8 Components for stacking gels for SDS-PAGE.

Component	5% Stacking Gel (mL)
ddH_2O	1.36
30% Polyacrylamide	0.34
1 M Tris pH6.8	0.25
10% SDS	0.020
10% Ammonium persulfate	0.020
TEMED	0.002

2.5.3 Western Blotting

Following SDS-PAGE, the polyacrylamide gels containing the separated proteins were transferred to a 0.45 µM Hybond® ECL™ nitrocellulose membrane (Sigma) for 1 h at 0.75 A in a 2051 Midget Multiblot Electrophoretic Transfer Unit at 4°C containing 1X transfer buffer from a 10X stock (100 mM Glycine, 125 mM Tris +/- 0.5% SDS) ensuring Methanol was present in the 1X solution. Following transfer, the blot was blocked with a 5-10 mL of 5% dried milk powder-TBS for 30 min shaking at 100 rpm at room temperature. The blot was then washed in 1% Tween TBS prior to addition of the primary antibodies (Table 2.2-9), which were left shaking at 100 rpm overnight at 4°C. All primary antibodies dilutions were 1 in 1000 in 5% BSA/TBS unless otherwise stated.

Table 2.2-9 Primary antibodies and appropriate secondary antibodies for western blotting.

Antibody	Cat. #	Supplier	Appropriate secondary
Anti-V5	R961-25	Invitrogen	Mouse
Anti-Rep	61071	Progen	Mouse
Anti-VP1,2,3	61058	Progen	Mouse
Anti-Cyclophilin B (HRP conjugate)	208575	AbCam	N/A
Anti-β-actin	A5441	Sigma	Mouse
L7A	Roobol, A et al. 1999		
Anti-Tubulin	Woods, A et al, 1989 (Gifted by Prof. Keith Gull, University of Oxford, UK).		

The primary antibody was removed the following day and following a number of 1% Tween TBS washes the secondary antibody (Table 2.2-10) was added following dilution 1 in 1000 in 5% milk/TBS unless otherwise stated. The blots were in secondary antibody for 1 h with shaking at 100 rpm at 4°C. Upon removal of the secondary antibody the blots were washed in 1% Tween TBS.

Table 2.2-10 Secondary antibodies used for Western Blot.

Antibody	Supplier, Catalog No.	Dilution
Anti-mouse IgG	Sigma, A4416	1:1000
Anti-Rabbit IgG	Sigma, A6154	1:1000

1 mL of ECL reagent 1 and 1 mL of ECL reagent 2 from Pierce™ ECL Western Blotting Substrate (Thermo Scientific) were placed on the blots and incubated for 5 min at RT prior to the blots being developed on Amersham Hyperfilm™ ECL.

2.5.3.1 Densitometry

Blots were scanned and saved, the density of each band was determined using ImageJ 1.8.0 software (Schneider, Rasband, & Eliceiri, 2012).

2.5.4 Coomassie Stain

Polyacrylamide gels were stained with a staining solution comprised of 1% Coomassie Brilliant Blue G250, 50% methanol and 10% glacial acetic acid at room temperature. The

stained gels were then de-stained using a de-staining solution comprised of 24% methanol and 14% glacial acetic acid for 1 h at room temperature.

2.6 Generation of Cell Pools Expressing Assembly Activating Protein (AAP)

2.6.1 Molecular Cloning

ATG-AAP and CTG-AAP were amplified from the pCET901-ATG-AAP and pCET901-AAP plasmids respectively, supplied by Cobra Biologics, using the primers ATG-AAP, ATG-AAPSTOP, CTG-AAP and CTG-AAP STOP as described in Table 2.2-1. A restriction digest was carried out on the backbone plasmid pcDNA3.1 Hygro using the Fast Digest restriction enzymes *KpnI* and *XhoI* (Thermo Scientific). The AAP insert was ligated into the pcDNA3.1Hygro backbone and transformed into DH5α *E. coli* cells (Methods 2.3.7) and grown overnight at 37°C on an LB agar plate containing 100 µg/mL ampicillin. A Colony PCR screen was carried out on a selection of the colonies present using GoTaq® G2 Flexi DNA Polymerase (Promega) as per manufacturers guidelines using the primers for AAP; ATG-AAP, ATG-AAPSTOP, CTG-AAP and CTG-AAP STOP as described in table 2.2-1. Following successful colony PCR, the colonies were re-transformed into DH5α *E. coli* competent cells and the DNA extracted. A restriction digest was then carried out on the colonies to test for band drop out using the Fast digest restriction enzymes *KpnI* and *XhoI* (Thermo Scientific). All colonies showing band dropout were sent for Sanger Sequencing by Genewiz.

2.6.2 Transient Transfection of Plasmid DNA to Confirm AAP Expression

A transient transfection of the ATG-AAP and CTG-AAP (tagged and untagged) plasmids was carried out by PEI transfection using PEIpro® (Polyplus transfection). 100,000 copies of each plasmid were transfected as per Methods 2.2.4. Protein pellets were harvested for protein analysis to test for AAP expression. This was carried out as described in Methods section 2.5. 20 µg of protein wass loaded onto a 12% gel for SDS-PAGE and a western blot was carried out using a monoclonal anti-V5 primary antibody (Cat #: R961-25, Invitrogen) using the anti-mouse secondary antibody (Sigma Aldrich, Cat #: A4416).

2.6.3 Determination of Hygromycin Selection Concentration (Kill Curve) for HEK293T Cells

250 mL Erlenmeyer flasks were seeded at $2x10^5$ vc/mL to a total volume of 50 mL with HEK293T cells in GIBCO® FreeStyle™ 293 Expression Medium (ThermoFisher). The cells were

also grown in the presence of Hygromycin B (Invitrogen) at concentrations ranging from 250 µg/mL to 500 µg/mL. Cells were counted daily on the ViCell XR (Beckman Coulter).

2.6.4 Linearisation of DNA and DNA Precipitation

The plasmids containing the ATG-AAP, ATG-AAP-V5, CTG-AAP and CTG-AAP-V5 were all linearised using the *FspI* restriction enzyme (ThermoFisher, Cat #: 10687010) as per the manufacturers protocol overnight at 37°C. Following digestion, an ethanol precipitation was carried out. A 0.1 volume of 3 M sodium acetate at pH 5.2 was added to the restriction digest followed by a 2.5 volume of ice cold 95% ethanol. This was then centrifuged at 14,000 rpm for 5 min. The ethanol-sodium acetate mix was then decanted off and the DNA pellet washed in 70% ethanol. Once the DNA pellet had dried it was resuspended in 100 µL of sterile H_2O. The concentration of DNA was determined on a Nanodrop instrument.

2.6.5 Stable Cell Pool Set Up

Cell pools stably expressing ATG-AAP, ATG-AAP-V5, CTG-AAP and CTG-AAP-V5 were created. This was achieved using PEI transfections. 24 h prior to PEI transfections Corning® CellBIND® T25 flasks were seeded at $1.8x10^5$ vc/cm^2. On the day of transfection, the media was carefully removed and replaced with fresh GIBCO® FreeStyle™ 293 Expression Medium (ThermoFisher). All transfections were carried out using PEIpro (Polyplus transfections). 100,000 copies of linearised plasmids were transfected into the HEK293T cells and incubated in a static incubator at 37°C. 24 h following transfection the media was refreshed along with 250 µg/mL of Hygromycin B. The cells remained in a static incubator at 37°C until the cells had recovered enough to be passaged on. The cells were moved from static T25 flasks to shaking 125 mL Erlenmeyer flasks. Cells were kept in the presence of Hygromycin B to maintain selection on the cell line. Once the cell pools had undergone 3 passages and had a percentage viability above 90% the cell pools were banked down as per methods 2.2.3.

2.7 Generation of Clonal AAP Cell Lines by Limiting Dilution

2.7.1 Single Cell Cloning by Serial Dilutions

Clonal cell lines were isolated from the ATG-AAP-V5 and CTG-AAP-V5 cell pools using limiting dilutions. This was carried out in GIBCO® FreeStyle™ 293 Expression Medium (ThermoFisher) containing InstiGRO™ HEK (Sal Scientific). Ten 96 well plates were set up per cell line for limiting dilutions. 200 µL of cells at $7.5x10^3$ viable cells/mL were added to well A1 and then serial dilutions down the column followed by serial dilutions across the rows (Figure 2.1.).

The cells were incubated statically at 37°C. Every two days the cells were observed under the microscope and any well containing more than one colony was noted and removed from selection. Cells from the wells containing only one colony were selected and moved from 96 well plates into 24 well plates and when growth allowed these were moved on to 6 well plates, T25 flasks and finally into 125 mL Erlenmeyer flasks.

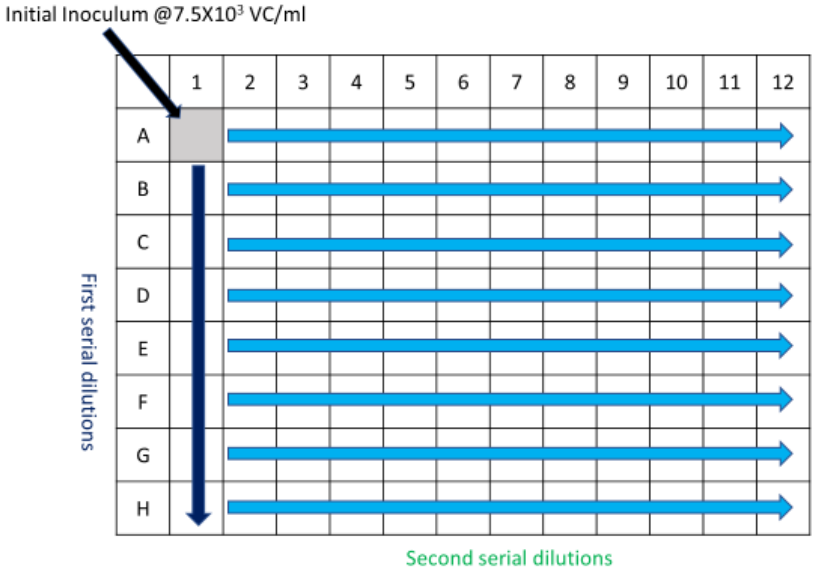

Figure 2.1 Serial dilutions used for single cell cloning via the limiting dilution method.

2.8 Generation of Cell Pools Expressing Replicase Proteins

2.8.1 Molecular Cloning

2.8.1.1 Addition of Rep to pcDNA3.1 Hygro Backbone

The *Rep* gene was amplified from the pAAV-RC-Kan plasmid (supplied by Cobra Biologics) using the forward and reverse primers *Rep* as described in Table 2.2-1. The amplification was carried out using Phusion™ High–Fidelity DNA Polymerase (ThermoFisher). Once amplified the PCR product was cleaned up using the Wizard® SV Gel and PCR Clean-Up System (Promega). A restriction digest was carried out on the backbone plasmid pcDNA3.1 Hygro using the fast digest restriction enzymes *NheI* and *XhoI* (Thermo Scientific). The *Rep* insert was ligated using T4 DNA Ligase (Promega) into the pcDNA3.1Hygro backbone at an insert: backbone ratio of 1:1, 3:1 and 5:1 and transformed into DH5α *E. coli* cells (Methods 2.3.7) and grown overnight at 37°C on a LB agar plate containing 100 µg/mL ampicillin. A colony PCR screen was carried out on a selection of the colonies present using GoTaq® G2 Flexi DNA

Polymerase (Promega) as per the manufacturer's guidelines using the primers for *Rep* as described in Table 2.2-1. Following successful colony PCR, the colonies were re-transformed into DH5α *E. coli* competent cells and the DNA extracted. A restriction digest was then carried out on the colonies to test for band drop out using the Fast digest restriction enzymes *NheI* and *XhoI* (Thermo Scientific). All colonies showing band dropout were sent for Sanger Sequencing with Genewiz. The resulting plasmid was named pcDNA3.1ReHyCMV.

2.8.1.2 Replacement of CMV region with a Multiple Cloning Site

To remove the CMV region of the pcDNA3.1ReHyCMV plasmid a Multiple Cloning Site (MCS) was designed to replace the CMV promotor region. MCS1 forward and reverse oligos were designed as described in Table 2.2-4 and ordered from Eurofins. These primers were amplified using Phusion™ High–Fidelity DNA Polymerase and the resulting PCR product was cleaned up using the QIAquick Nucleotide Removal Kit (Qiagen) as per manufacturer's guidelines. Both the pcDNA3.1ReHyCMV plasmid backbone and MCS1 insert were digested by Fast digest restriction enzymes *MluI* and *NheI*. The MCS1 was then ligated into the backbone using T4 DNA Ligase (Promega) into the pcDNA3.1Hygro backbone at an insert:backbone ratio of 1:1, 3:1 and 5:1 and transformed into DH5α *E. coli* cells (Methods 2.3.7) and grown overnight at 37°C on an LB agar plate containing 100 µg/mL ampicillin. The colonies were re-transformed into DH5α *E. coli* competent cells and the DNA extracted. A restriction digest was then carried out on the colonies to test for band drop out using the Fast digest restriction enzyme *NotI* to check for linearization in the multiple cloning sites. All colonies showing band dropout were sent for Sanger Sequencing with GeneWiz. The resulting plasmid was named pcDNA3.1ReHyMCS.

2.8.2 Transient Transfection to Test for Rep Protein Expression

A transient transfection of the pcDNA3.1ReHyCMV and pcDNA3.1ReHyMCS plasmids was carried out by PEI transfection using PEIpro® (Polyplus transfection). 100,000 copies of each plasmid were transfected as per Methods 2.2.4. Protein pellets were harvested for protein analysis to test for Rep expression. This was carried out as described in Methods section 2.4. 20 µg of protein were loaded onto a 12% gel for SDS-PAGE and a western blot was carried out using the anti-AAV2 Replicase mouse monoclonal antibody (Progen) using the anti-mouse secondary antibody (Sigma, Cat. #: A4416).

2.8.3 Linearisation of DNA and DNA Precipitation

The pcDNA3.1ReHyCMV and pcDNA3.1ReHyMCS plasmids were all linearised using the *FspI* restriction enzyme (ThermoFisher) as per manufacturers protocol overnight at 37°C. Following digestion, an ethanol precipitation was carried out. A 0.1 volume of 3 M sodium acetate at a pH 5.2 was added to the restriction digest followed by a 2.5 volume of ice cold 95% ethanol. This was then centrifuged at 14,000 rpm for 5 min. The ethanol-sodium acetate mix was then decanted off and the DNA pellet was washed in 70% ethanol. Once the DNA pellet had dried it was resuspended in 100 μl in sterile H_2O. The concentration of this DNA was determined on a Nanodrop instrument.

2.8.4 Stable Cell Pool Set Up

In order to attempt setting up stable cell pools using the pcDNA3.1ReHyCMV and pcDNA3.1ReHyMCS plasmids PEI transfections were carried out. 24 h prior to PEI transfections, Corning® CellBIND® T25 flasks were seeded at $1.8x10^5$ vc/cm^2. On the day of transfection, the media was carefully removed and replaced with fresh GIBCO® FreeStyle™ 293 Expression Medium (ThermoFisher). All transfections were carried out using PEIpro (Polyplus transfections). Either 50,000 or 100,000 copies of the linearized plasmids were transfected into the HEK293T cells and incubated in a static incubator at 37°C. 24 h following transfection the media was refreshed with Freestyle media containing 250 μg/mL of Hygromycin B. The cells remained in the static incubator at 37°C until the cells had recovered enough to be passaged on. The cells were monitored regularly to check for the presence of colonies in the flask.

2.9 Generation of Cell Pools Expressing Replicase Proteins and Capsid Proteins

2.9.1 Molecular Cloning

2.9.1.1 Addition of Rep to pcDNA3.1 Hygro Backbone

The *Rep* and *Cap* genes were amplified from the pAAV-RC-Kan plasmid which was supplied by Cobra Biologics using the forward and reverse primers Rep + Cap as described in Table 2.2-1. The amplification was carried out using Phusion™ High–Fidelity DNA Polymerase (ThermoFisher). Once amplified, the PCR product was cleaned up using the Wizard® SV Gel and PCR Clean-Up System (Promega). A restriction digest was carried out on the backbone plasmid pcDNA3.1 Hygro using the fast digest restriction enzymes *NheI* and *XbaI* (Thermo Scientific). The *RepCap* insert was ligated using T4 DNA Ligase (Promega) into the

pcDNA3.1Hygro backbone at an insert:backbone ratio of 1:1, 3:1 and 5:1 and transformed into DH5α *E. coli* cells (Methods 2.3.7) and grown overnight at 37°C on an LB agar plate containing 100 µg/mL ampicillin. A Colony PCR screen was carried out on a selection of the colonies present using GoTaq® G2 Flexi DNA Polymerase (Promega) as per the manufacturer's guidelines using the primers for RepCap described in Table 2.2-1. Following successful colony PCR, the colonies were re-transformed into DH5α *E. coli* competent cells and the DNA extracted. A restriction digest was then carried out on the colonies to test for band drop out using the Fast digest restriction enzymes *NheI* and *BmtI* (Thermo Scientific). All colonies showing band dropout were sent for Sanger Sequencing with Genewiz. The resulting plasmid was called pcDNA3.1ReCHyCMV.

2.9.1.2 Replacement of CMV Region with Multiple Cloning site

To remove the CMV region of the pcDNA3.1ReCHyCMV plasmid, a Multiple Cloning Site (MCS) was designed to replace the CMV promotor region. MCS1 forward and reverse oligos were designed as described in Table 2.2-4 and ordered from Eurofins. These primers were amplified using Phusion™ High–Fidelity DNA Polymerase and the resulting PCR product was cleaned up using the QIAquick Nucleotide Removal Kit (Qiagen) as per manufacturer's guidelines. The both the pcDNA3.1ReHyCMV plasmid backbone and MCS1 insert were digested by Fast digest restriction enzymes *MluI* and *NheI*. The MCS1 was then ligated into the backbone using T4 DNA Ligase (Promega) into the pcDNA3.1Hygro backbone at an insert:backbone ratio of 1:1, 3:1 and 5:1 and transformed into DH5α *E. coli* cells (Methods 2.3.7) and grown overnight at 37 °C on an LB agar plate containing 100 µg/mL Ampicillin. The colonies were re-transformed into DH5α *E. coli* competent cells and the DNA extracted. A restriction digest was then carried out on the colonies to test for band drop out using the Fast digest restriction enzyme *NotI* to check for linearization in the multiple cloning sites. All Colonies showing band dropout were sent for Sanger Sequencing with GeneWiz. The resulting plasmid was called pcDNA3.1ReCHyMCS.

2.9.2 Transient transfection to test for expression of Replicase and Capsid Proteins.

A transient transfection of the pcDNA3.1ReCHyCMV and pcDNA3.1ReCHyMCS plasmids was carried out by PEI transfection using PEIpro® (Polyplus transfection). 100,000 copies of each plasmid were transfected as per Methods 2.2.4. Protein pellets were harvested for protein analysis to test for Rep expression. This was carried out as described in Methods section 2.5. 20 µg of protein were loaded onto a 12% gel for SDS-PAGE and a western blot was carried

out using the anti-AAV2 Replicase mouse monoclonal antibody (Progen) and the anti-AAV VP1/VP2/VP3 mouse monoclonal (Progen) using the anti-mouse secondary antibody (Sigma, Cat. #: A4416).

2.10 Viral Genome Quantification (qPCR)

2.10.1 Extraction of AAV Particles

Following transfection as described in Methods 2.2.4, viral capsids were extracted using AAVpro Extraction Solution (Cat. #6235, Takara). To lift the cells off the CellBIND surface of the culture vessel 1/80 of the total volume of 0.5 M EDTA was added to the culture and the cells were incubated at room temperature for 10 min. The culture was then centrifuged at 1,750 x g at 4°C for 10 min. Once the supernatant was removed the cell pellet was loosened by vortexing and 250 µL of AAV Extraction Solution A. The cells were then suspending by vortexing. The mixture was then incubated at room temperature for 5 min before being vortexed again for 15 s. The cells were then centrifuged at 2000 x g at 4°C for 10 min and the supernatant retained. Finally, 25 µL of AAV Extraction Solution B was then added to the supernatant and the samples were then stored at -80°C until needed.

2.10.2 Extraction of AAV Vector Genome

Harvested AAV Particles were DNase treated for 1 h using the DNaseI supplied in the AAVpro® Titration Kit (for Real Time PCR) Ver.2 (Cat. #6233, Takara) (Table 2.2-11). Once DNase treated the DNaseI was heat inactivated at 95°C for 30 mins.

Table 2.2-11 DNase Treatment of AAV Particles.

	Volume (µL)
10X DNase I Buffer	2
DNase I	1
dH_2O	15
AAV Particle samples	2
Total	**20**

Once heat inactivated, the AAV particles were lysed open. An equal volume of Lysis buffer (Supplied in the Takara AAVpro® Titration Kit) was added to the solution and incubated for 1 h at 70°C. The samples were then diluted 50-fold using the EASY Dilution (supplied in the AAVpro® Titration Kit).

2.10.3 Real-Time PCR

A standard curve was prepared for real-time PCR. The positive control (supplied in the AAVpro® Titration Kit (for Real Time PCR) Ver.2) was diluted in the EASY Dilution buffer. The positive control was serially diluted from $2x10^7$ copies/µL down to $2x10^2$ copies/µL. 5 µL of each standard along with 5 µL of the AAV genome solution (Extracted in Methods 2.10.2) were used as templates for real-time PCR. A primer mix was prepared as per Table 2.2-12.

Table 2.2-12 Preparation of 50X Primer mix for qRT-PCR.

	Volume (µL)
AAV Forward Titre Primer	5
AAV Reverse Titre Primer	5
dH_2O	15
Total	**25**

A master mix was prepared on ice as per table 2.2-13 containing all reaction components listed below with the exception of the template. This 20 µL reaction mix was added to each reaction well of a 96 well plate. The 5 µL templates (Standards, Samples and negative control) were added to the reaction solutions. Real-Time PCR assays were carried out in a 96 well format using non-skirted, white plates (BRAND, Berlin, Germany) in a DNAEngine Peltier thermocycler (BioRad, California, USA) with a Chromo4 real-time PCR detector (BioRad, California, USA) following the protocols outlined in table 2.2-13. TB Green was used to detect the amplified ssDNA using the TAKARA AAVpro® Titration Kit (for Real Time PCR) kit. This was done using the primers supplied in the kit which target to the ITR regions.

Table 2.2-13 Reaction mixtures for real-time PCR

	Volume (µL) per reaction
TB Green Premix Ex Taq (2X conc.)	12.5
50X Primer mix	0.5
dH_2O	7.0
(Template)	(5.0)
Total	**25**

Table 2.2-14 Real-Time PCR instrument cycling set-up.

	Temperature (°C)	Time (s)	Cycles
Initial denaturation	95	120	
2 Step PCR	95	5	35
	60	30	
Melt curve analysis			

The positive ITR control standards were used to extrapolate the ITR copy numbers for each sample and analysed using the Opticon Monitor 3 Software (BioRad, California, USA). Crossing point thresholds were manually set for each plate and the copy numbers were calculated for each sample. Samples were run in both biological triplicate and technical triplicate, unless otherwise stated.

2.11 Viral Capsid Quantification (ELISA)

Capsids were harvested as described in Methods 2.10.1. Once harvested, the samples were prepared for viral capsid quantification using the AAV2 Titration ELISA 2.0R (Cat. #: PRAAV2R, Progen). The samples were diluted 1:5, 1:10, 1:20 using the Assay buffer supplied in the kit. The reconstituted kit control was also serially diluted using the assay buffer. An ELISA assay was carried out using the AAV2 titration ELISA as per the manufacturers protocol with the final colour intensity measured at a wavelength of 450 nm using a plate reader. The viral capsid titre for samples was read off the standard curve created using the kit control supplied.

2.12 AAV Particle Purification

2.12.1 Extraction of AAV Particles

Following transfection as described in Methods 2.2.4, viral capsids were extracted using AAVpro Extraction Solution A Plus supplied as part of the AAVpro Purification Kit Midi (Cat. #6675, Takara). To lift the cells off the CellBIND surface of the culture vessel 1/80 of the total volume of 0.5 M EDTA was added to the culture and the cells were incubated at room temperature for 10 min. The culture was then centrifuged at 1,700 x g at 4°C for 10 min. Once the supernatant was removed and discarded the cell pellet was loosened by vortexing. The cells were resuspended in 2 mL of AAV Extraction Solution A Plus by vortexing. The

mixture was then incubated at room temperature for 5 min before being vortexed again for 15 s. The cells were then centrifuged again at 4000 x g at 4°C for 10 min and the supernatant retained. Finally, 1/10 volume of AAV Extraction Solution B was then added to the supernatant and the samples were then stored at -80°C until needed for purification.

2.12.2 Purification and Concentration of AAV Particles

In order to purify AAV particles, Cryonase Cold-active Nuclease was added to the virus suspension obtained in methods 2.12.1 and was incubated for 1 h at 37°C. Following incubation, 1/10 volume of Precipitator A was added to the particle solution prior to incubation at 37°C for 30 min. 1/20 volume of precipitator B was then added to the mixture and centrifuged at 5000 g for 5 min at 4°C. The supernatant was then filtered using the Millex-HV 0.45 µm supplied. The filtrate was placed in the Amicon Ultra-4 100 kDa filter device and centrifuged for 5 min at 15°C at 2000 g. 1 mL of Suspension Buffer was then added to the filter device and mixed with the solution before centrifugation at 2000 g for 5 min at 15°C, this suspension buffer step was repeated four times to obtain an appropriate volume of solution before the solution remaining in the Amicon Ultra-4 filter device was retained as the purified virus suspension.

2.12.3 Determination of Purity of the Purified Virus Solution

To determine the purity of the particles purified by the AAVpro Purification kit midi, the purified samples were run on an SDS-PAGE gel as described in Methods 2.5.3 and the resulting gel was stained with Coomassie as described in Methods 2.5.4.

2.13 Immunofluorescence and Confocal Microscopy

2.13.1 Adhering, Fixing and Permeabilising Cells on Coverslips

Coverslips used were coated in Poly-D-Lysine (0.01% w/v) and incubated at room temperature for 15 min. The poly-D-Lysine was removed, and the coverslips were washed with sterile H_2O. Cells were seeded at a concentration of $2x10^5$ total cells (tc)/mL and incubated statically at 37°C for 1 h. The media was then removed and washed in PBS. The cells were fixed using 500 µL of ice-cold methanol and incubated on ice for 5 min. The coverslips were then washed in PBS prior to antibody staining.

2.13.2 Antibody Staining of Cells

Cells adhered and fixed to the coverslips were blocked in 250 µL 3% (w/v) BSA in PBS for 20 min at room temperature. Antibodies were diluted as per table 2.2-15 in 3% BSA in PBS. The coverslips were incubated on drops of antibody overnight in a damp box at 4°C. Coverslips were then washed in 100 µL of 0.1% Tween in PBS. Secondary antibodies were prepared in 3% BSA PBS and the coverslips were placed onto drops of antibody and incubated in a dark room for 2 h at room temperature. Following PBS-Tween washes, the coverslips were incubated for 1 min at room temperature in DAPI stain and washed again prior to being mounted on a glass slide using Prolong Diamond mounting reagent.

Table 2.2-15 Antibody dilutions used for immunofluorescence.

Antibody	Supplier, Cat. #	Dilution
Anti-V5	Invitrogen, R961	1:1000
Anti-Mouse IgG FITC	Sigma, F0257	1:100
Anti-Mouse IgG TRITC	Sigma, T5393	1:100

2.13.3 Imaging Cells on the Confocal Microscope

Coverslips were imaged under a Zeiss Confocal microscope. The images were captured using the Zeiss Zen black software.

2.14 Infectivity Assay

2.14.1 Transduction Assay

A 48 well CellBIND plate (Corning) was seeded with suspension adapted HEK293T cells at a cell concentration of $2x10^5$ vc/mL in a total volume of 0.5 mL FreeStyle Media (ThermoFisher). The plate was incubated statically at 37°C for 2 h to allow the cells to settle and adhere to the CellBIND surface. Purified AAV particles were diluted in 250 µL FreeStyle media to a concentration of either 100 vector genomes (vg)/ cell, 250 vg/cell, 500 vg/cell, 1000 vg/cell, 2000 vg/cell or 5000 vg/cell. Purified vectors were harvested from either the HEK293T, ATGV5, A04, A33 or A66 cell lines. Media was removed from the well of the CellBIND plate and retained as a conditioned media. 250 µL of the AAV dilution was added gently to the cells and incubated at 37°C for 3 h. The plate was agitated gently every 30 min. Following this the AAV dilution was removed and replaced with 500 µL of the conditioned media. The plate was then incubated at 37°C for 48-72 h.

2.14.2 Flow Cytometry

$1x10^5$ viable transduced cells were centrifuged at 1000 rpm for 5 min to pellet the cells. The pelleted cells were resuspended in 500 µL of sterile PBS. Samples were loaded onto the probe of a FACScalibur™ instrument (BD biosciences), and fluorescence intensity was measured in relation to the cell count. Data obtained via flow cytometry and presented in figures in Chapter 5 show either the percentage cells exceeding a 10^1, 10^2 or 10^3 fluorescence threshold, termed M1, M2 and M3 respectively, or the mean fluorescence including all recorded cells of a sample.

2.14.3 Florescent Microscopy

Cells transduced with the rAAV2.GFP particles derived from the 293T, ATGV5, ATG04, ATG33 and ATG66 cell lines were visualised on the LEICA microscope to visually observe expression of GFP.

2.15 Electron Microscopy

Visualisation of the rAAV2 particles purified as per Methods Section 2.12 was undertaken on an electron microscope using negative stain and an inhouse microscope facility at the University of Kent by Mr Ian Brown.

Chapter 3

Establishment of AAV HEK293T Expression Systems and the Generation of Molecular Constructs for Rep and RepCap Expressing Cell Pools

3.1 Introduction to the Work Described in this Chapter

As outlined in the introduction chapter of this thesis, adeno-associated virus, so named due to being first identified alongside adenovirus, is a member of the parvovirus family, but it is also a Dependovirus which means it requires co-infection with a "helper" virus, usually Adenovirus or Herpes virus. Without this helper virus there is no expression of AAV genes and the genome integrates into the host chromosome 19 (Dirk Grimm, 2002; Robert M. Kotin, Menninger, Ward, & Berns, 1991; R J Samulski et al., 1991). Thus, to produce recombinant adeno-associated virus it is necessary to provide the host cell with both the required adeno-associated virus genetic material and helper virus genes. This Chapter describes the generation of different constructs and the establishment of a recombinant adeno-associated virus production system using HEK293T host cells.

Again, as outlined in more detail in section 1.3.2 of the introduction, the genome of adeno-associated viruses consists of two open reading frames (ORF), these contain the genes which encode for the structural and replication genes (*Cap* and *Rep*, respectively). The *Cap* gene encodes three capsid proteins, VP1, VP2 and VP3, and *Rep* encodes the four replication genes, *Rep* 78, *Rep* 68, *Rep* 52 and *Rep* 40. The Cap proteins originate by differential splicing of a transcript generated from a p40 promoter; the Cap proteins assemble to make up a non-enveloped protein shell-based capsid which is approximately 25 nm in size (Daya & Berns, 2008). This small viral capsid encapsulates the viral genome which is a single stranded DNA of approximately 4700 bp. The *Rep* genes code for the four Rep proteins which are involved in regulation of gene expression and targeting the viral genome into the capsid (Dirk Grimm, 2002). The two open reading frames are flanked by Inverted Terminal Repeats (ITRs) that facilitate the genome encapsulation into the capsids and allow for replication to occur.

In terms of establishing a recombinant AAV system (rAAV), it is important to note that the AAV capsid can only accommodate a genome up to 5 kB in length. The Helper virus supplies the genes involved in transcriptional regulation that are required for replication to occur; in the case of adenovirus these are *E1*, *E2a*, *E4* and *VA RNA*. To date there have been 12 different AAV serotypes identified each of which have different target tissues making rAAV

and the range of serotypes a useful choice of vector to allow delivery of a target gene to the desired location (Colella, Ronzitti, & Mingozzi, 2018).

In developing a rAAV system, it is important to consider the wildtype control of gene expression in AAV. As outlined in the introduction chapter, there are a number of promoters involved in the regulation of AAV gene expression; p5, p19 and p40. The p5 and p19 promoters are involved directly in the synthesis of the transcript that codes for the four rep proteins, Rep 78, Rep 68, Rep 52 and Rep 40. The p5 promoter is responsible for the transcript that codes for the larger Rep proteins Rep 78 and 68 while the p19 promoter is responsible for the transcript for the smaller Rep proteins Rep 52 and 40. Both of the larger Rep 78 and Rep 68 proteins have been shown to possess helicase and endonucleases required for AAV replication and to bind to DNA in chromosome 19, thus being involved in viral integration of wild-type AAV genomes (Weitzman, Kyostio, Kotin, & Owens, 1994). The larger Rep proteins also bind to the Rep Binding Element (RBE) found within the ITR regions and the p5 promoter. It has been shown that Rep protein interaction with the RBE can act as either a repressor or activator of transcription regulation (Pereira et al., 1997). For rAAV production repression of transcription should ideally be avoided. The p40 promotor is responsible for the production of the transcript that codes for the AAV capsid proteins via alternative splicing. The AAV capsid proteins VP1, VP2 and VP3 differ in their N-terminal structure and are the structural proteins that make up the viral capsid in a ratio of 1:1:10, respectively. A complete AAV capsid is made up of 60 proteins meaning there are 5 VP1 and VP2 proteins in each capsid and 50 VP3 proteins (Kleinschmidt et al., 1997; Le et al., 2019). Controlling the synthesis of the VP proteins to match this ratio in a rAAV system is one aspect of their bioprocessing that has yet to be fully demonstrated.

Finally, in considering a rAAV system the size of the potential transgene needs to be considered. Although adeno-associated virus has a small packaging capacity (around 5 kB) it is one of the most extensively researched vectors to date, with much of this research focused on improving the production of rAAV. Research into the potential for AAV to be used as a gene delivery vector has been around for decades. More detail on this is found in the introduction chapter of this thesis. Briefly, the genome was originally cloned into bacterial plasmid backbones back in the 1980s (Catherine A. Laughlin, Tratschin, Coon, & Carter, 1983; R. J. Samulski, Berns, Tan, & Muzyczka, 1982), this paved the way for future rAAV vector production. All methods for rAAV vector production have specific method relevant advantages and disadvantages. Several different cell lines and host expression systems have been studied for the production of these vectors at a GMP manufacturing level, these include

mammalian cell lines such as HEK293T, HEK293 and HeLa along with Sf9 insect cells. The production in these cell lines varies from two or three plasmid transfection methods utilising PEI or $CaPO_4$ to the Baculovirus infection system as described in Introduction Section 1.4.3.1 (K. Reed Clark et al., 1995; Clément & Grieger, 2016).

HEK293T cells are of much interest when it comes to the production of rAAV. HEK293T cells lines are derived from HEK293 cells which have been engineered to express the large T antigen of SV40 (DuBridge et al., 1987; Pear, Nolan, Scott, & Baltimore, 1993). The HEK293T cell line has been used in research into the production of rAAV2 viral vectors in both academic and industrial settings. HEK293T cell lines have been transformed by the sheared adenovirus E1 gene (Huang et al., 2013).

The estimated therapeutic rAAV particle requirement for gene therapy applications is estimated to be in the region of 10^{14} therapeutic capsids per patient. This number, however, will vary depending on a patients weight, the target tissue and the specific gene therapy and these could in fact be as high as 10^{15} therapeutic capsids (Aucoin, Perrier, & Kamen, 2008; Dirk Grimm & Kleinschmidt, 1999; Urabe et al., 2002). One of the main issues with the production of rAAV vectors is the presence of empty vector particles, which do not contain a (complete) vector genome and therefore do not have any therapeutic benefit. It has been shown that between 50 and 95% of rAAV vectors are either empty or incorrectly packaged (Sommer et al., 2003; J F Wright, 2008). These empty or incorrectly packaged capsids are not pathogenic; however, they can cause the activation of an anti-AAV capsid immune response and can compete for the same surface binding receptors, hence preventing genome-containing particles getting into cells efficiently (Pei et al., 2018; J Fraser Wright, 2014). This has a huge impact on the quality and production costs of rAAV vectors, not just from a scale up point but also from a purification viewpoint.

rAAV vectors are thus usually produced transiently via the co-transfection of a number of plasmids that carry the required genes for their production. Details of approaches that have been used to produce rAAV are outlined in detail in Introduction Section 1.4.3. One of the most widely used methods for rAAV production involves the co-transfection of three plasmids: one plasmid contains both the *Rep* and *Cap* gene for the serotype being used, one plasmid contains the gene of interest (GOI) flanked by ITRs, the third is often referred to as a helper plasmid and contains the adenoviral helper genes, *E2a*, *E4* and *VA RNA* (Balakrishnan & Jayandharan, 2014; Huang et al., 2013). HEK293T cell lines are often used as the host cell for the production of the rAAV particles due to their ability to supply the adenoviral helper

gene, *E1* (Huang et al., 2013). Although a variety of transfection methods are used (see Introduction section 1.4.2.1, when compared to other transfection methods, the PEI mediated transfection method has been found to be a favoured method for the production of rAAV vectors as it is a cost effective method that has a high stability and has the capacity to work at a range of pH levels thus eliminating the need for labour intensive media changes post transfection (Huang et al., 2013).

3.2 Aims of this Chapter

The work presented in this chapter covers the establishment of rAAV serotype 2 vector production using the host suspension HEK293T cell line. Further to this it also determines a baseline for AAV2 vector production and packaging in HEK293T cells as a comparison for results in later work aimed at increasing the production efficiency of rAAV from this host expression system. This chapter also describes investigations into the feasibility of engineering HEK293T cell lines to stably express the *Rep* and *Cap* genes and *Rep* gene only. The overall aims were therefore to:

a. Establish the HEK293T host cell line and characterise its growth characteristics.
b. Establish a rAAV production system in the laboratory based upon a triple co-transfection methodology.
c. Use commercially available PCR and ELISA based assays to determine total vector particle titre and genome-containing particle titre of a model GFP transgene from the HEK293T production system as a baseline for further studies.
d. Generate Rep and Rep/Cap expressing plasmid DNA constructs for HEK293T stable cell line generation in order to reduce the requirement for 3-plasmid co-transfection during AAV production.

3.3 Establishment of a HEK293T rAAV2 Production System

3.3.1 Establishment of the growth profile of the host HEK293T cell line

Growth curves of three biological replicates of the HEK293T host cell line were set up under batch culture conditions with a seeding concentration of $2x10^5$ viable cells/mL. The growth profiles showed a steady growth of cells until day 4, when the cells reached a peak maximum viable cell concentration of approximately $4.16 x10^6$ viable cells per mL (VC/mL) (Figure 3.1A). Based on the growth profiles, the doubling time was calculated across the exponential growth phase and it was determined that the population was doubling every 22.1 hours. The culture viability remained consistently high at this point, above 85% viability. However, by

day 5, the viable cell count had decreased to below 1.35 x10^6 VC/mL with a culture viability of only 52.83% which continued to decrease over the next 2 days (Figure 3.1 A) with the culture viability dropping to 25% by day 7, at which point the study was terminated.

Once the basic batch culture growth profile had been established, the growth of the HEK293T cell line following either a 2-day or 3-day passaging regime was investigated. The passaging regime carried out at collaborators Cobra Biologics involved the passage of cells on a Monday, Wednesday and Friday. Cells were seeded at a concentration of 3x10^5 VC/mL on a Monday and Wednesday, cells were seeded at 2x10^5 VC/mL on a Friday to accommodate the extra day before the next passage. The growth profiles were analysed to determine if there was a difference in the growth characteristics from cultures setup from a two- or three-day passage culture. Based on the cell count data collected over 11 weeks on passage days it was found that the HEK293T cell line generally presented a higher viable cell concentration (VC/mL) and a higher culture viability on a Monday, following a 3-day culture and having been seeded at 2 x10^5 VC/mL the previous Friday. On a Monday, cells reached an average viable cell concentration of 1.9 x10^6 VC/mL (Figure 3.1 B) with an average culture viability of 94% (Figure 3.1 C). However, while the Monday data gave a consistently higher culture viability in comparison to the 2-day growth this was not a large increase; the data for the 2-day passages was consistently above 88%. Nevertheless, in order to ensure the highest viable cell number and culture viability in cultures used to seed rAAV production runs these data established that using cells from a 3-day passage was preferable.

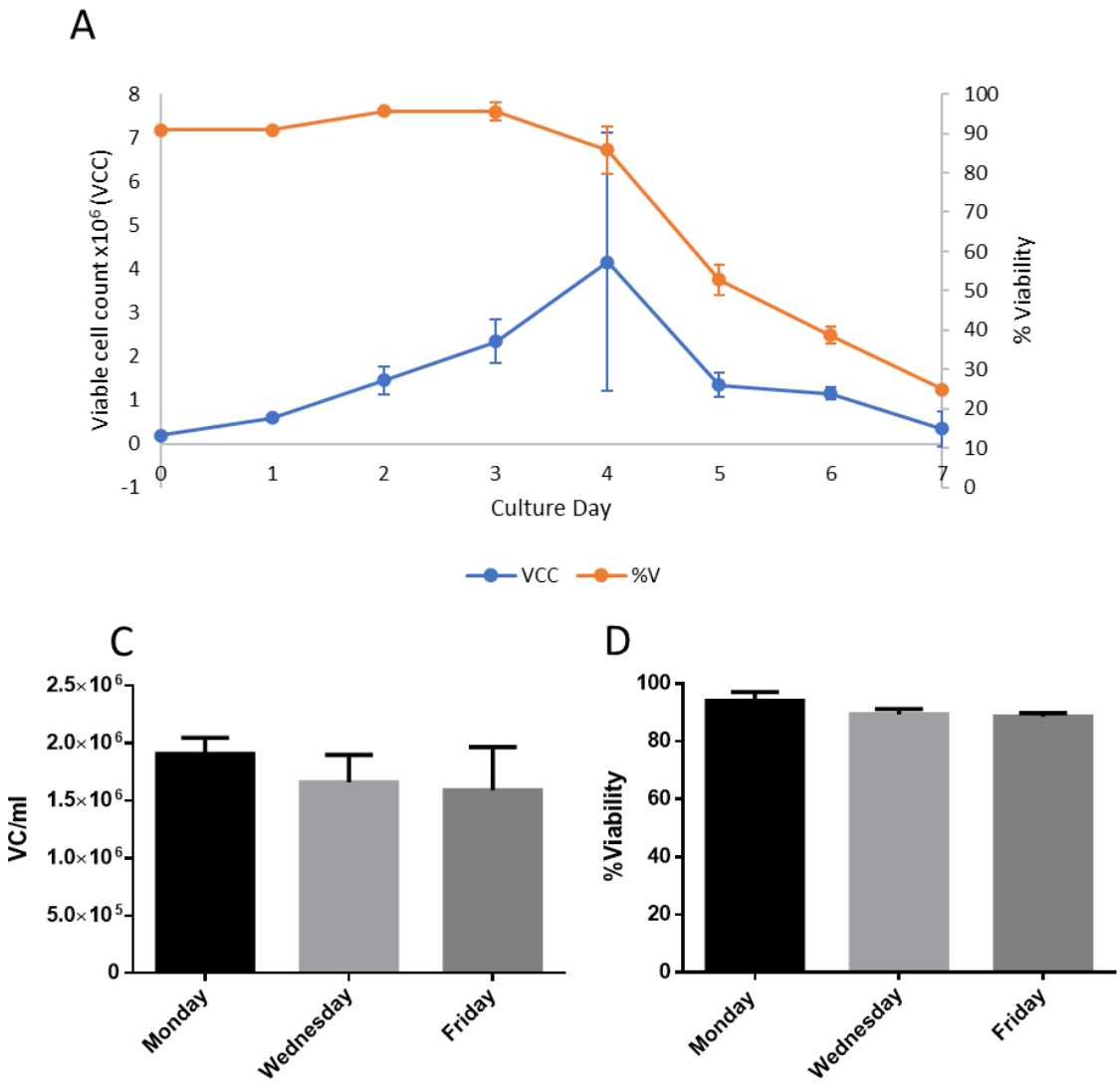

Figure 3.1 Growth profiles of HEK293T host cell line. A) Viable cell concentration per mL of culture and the percentage of cells viable on each culture day for HEK293T cell line grown in 250 mL Erlenmeyer flasks. B) Viable cell concentrations as measured across the different culture passage days. Following either 2 or 3 days of growth. C) Percentage viability as measured across the different culture passage days. Following either 2 or 3 days of growth. Error bars = Standard deviation n=3.

3.3.2 Establishment of a System for the Production of rAAV2 Capsids

Based on the growth results presented in Section 3.3.1, an initial rAAV2 production run in biological triplicate using the HEK293T suspension-adapted cell line (Cobra Biologics) was carried out. rAAV2 vectors were produced as outlined in Methods Section 2.2.4 by PEI co-transfection of three plasmids pAAV-RC-Kan, pAAV-GFP-Kan and pHelper-Kan. The viral capsids were harvested 72 hours post transfection and the total capsid particle and genomic particle titres were determined as described in Methods Sections 2.10 and 2.11 respectively. The error bars were determined based on the standard deviation of the triplicate results obtained. The number of particles secreted into the media was compared to those retained in the cells. Using the Progen ELISA assay, it was determined that the majority of the rAAV2 particles were retained in the cell (as expected) with few particles found in the cell supernatant. Using the HEK293T cell line for rAAV2 particle production, it was determined that the number of capsids produced and retained in the cell was in the region of $1.25x10^9$ particles/mL (Figure 3.2).

In establishing the rAAV system a model GFP transgene was utilised. To determine the number of genome-containing capsids harvested in Section 3.3.1.2 a qPCR assay was carried out using the Takara AAVpro Titration kit (for Real Time PCR) targeting ITR regions of the genome. Following harvest, the viral genomes were extracted as described in Methods section 2.10.1 and the qPCR assay was carried out as per methods sections 2.10.3. Technical triplicates of each sample were loaded into the qPCR plate. The results obtained are shown in Figure 3.2, the genome titre was determined based on the standard curve quantities generated by serial dilution of the Positive Control supplied in the commercial Takara kit. The plasmid control contains plasmid DNA incorporating the ITR regions targeted by the qPCR assay. The standard curve had a range of 2×10^2 to 2×10^7 copies/µL. The copy number of the ITR in the standard was the same as that of the AAV ITR vector genome allowing for relative quantification. This data shows that there was a genome titre of $5.89x10^8$ copies/mL. Through these data the baseline rAAV production from the HEK293T host cell line under the conditions used in this study were established and available to act as a comparator for future studies described in this thesis.

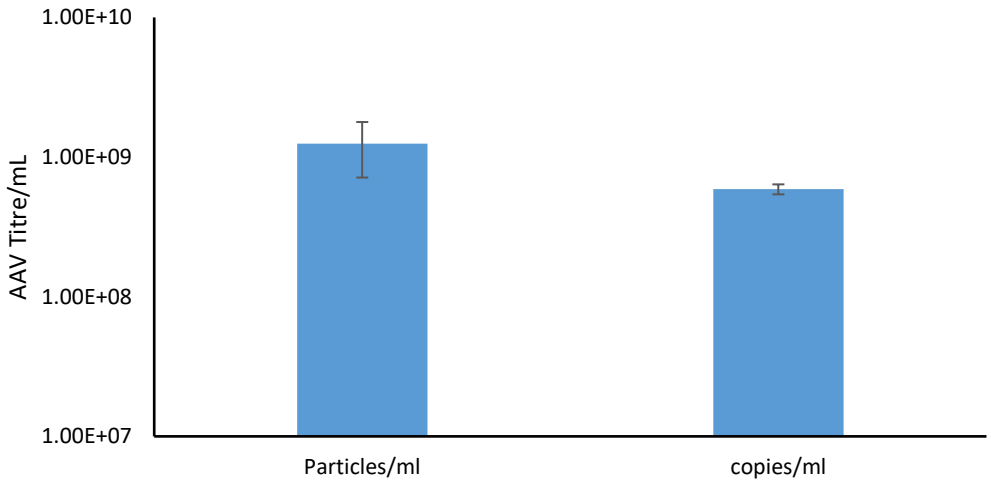

Figure 3.2 AAV2 Titre Analysis 72 h post transfection. Capsid titre (Particles/mL) determined via ELISA assay (Progen) with Genome titre (Copies/mL) determined via Real-Time qPCR (Takara). Error bars were determined from the standard deviation of each experimental repeat n=3.

3.4 Generation of a HEK293T Cell Pool Engineered to Stably Express the AAV Rep Gene

3.4.1.1 Generation of Rep Constructs in Plasmids with an Appropriate Mammalian Cell Selection Marker for Cell Line Development

In order to create HEK293T cells stably expressing the *Rep* gene it was necessary to create a plasmid vector containing a mammalian selection marker (hygromycin) to allow for isolation of cells successfully harbouring the *Rep* gene expression cassette. The methods used for all the different steps of molecular cloning discussed in this chapter can be found in Methods Section 2.3. All detailed plasmid maps can be found in the Appendix and the primer sequences used in the Methods Section.

The first vector constructed was a Rep vector referred to as pcDNA3.1ReHyCMV (or ReHyCMV), as described in Figure 3.3, using the commercially available pcDNA3.1 Hygro backbone. The *Rep* gene was amplified from the pAAV-RC-Kan vector plasmid using the Rep primers described in the Methods Section. Both the *Rep* insert and the pcDNA3.1 Hygro backbone were digested with *NheI* and *XhoI* before being ligated together. Plasmid DNA was isolated from colonies and analysed by a restriction test digest using *BamHI* and *NheI*. Colonies successfully containing the desired gene insert had a backbone band at approximately 6653 bp with a band drop out at 726 bp (representing the required *Rep* gene insert, Figure 3.5 A). Successful colonies were sent for sequencing with GeneWiz for confirmation of the sequence.

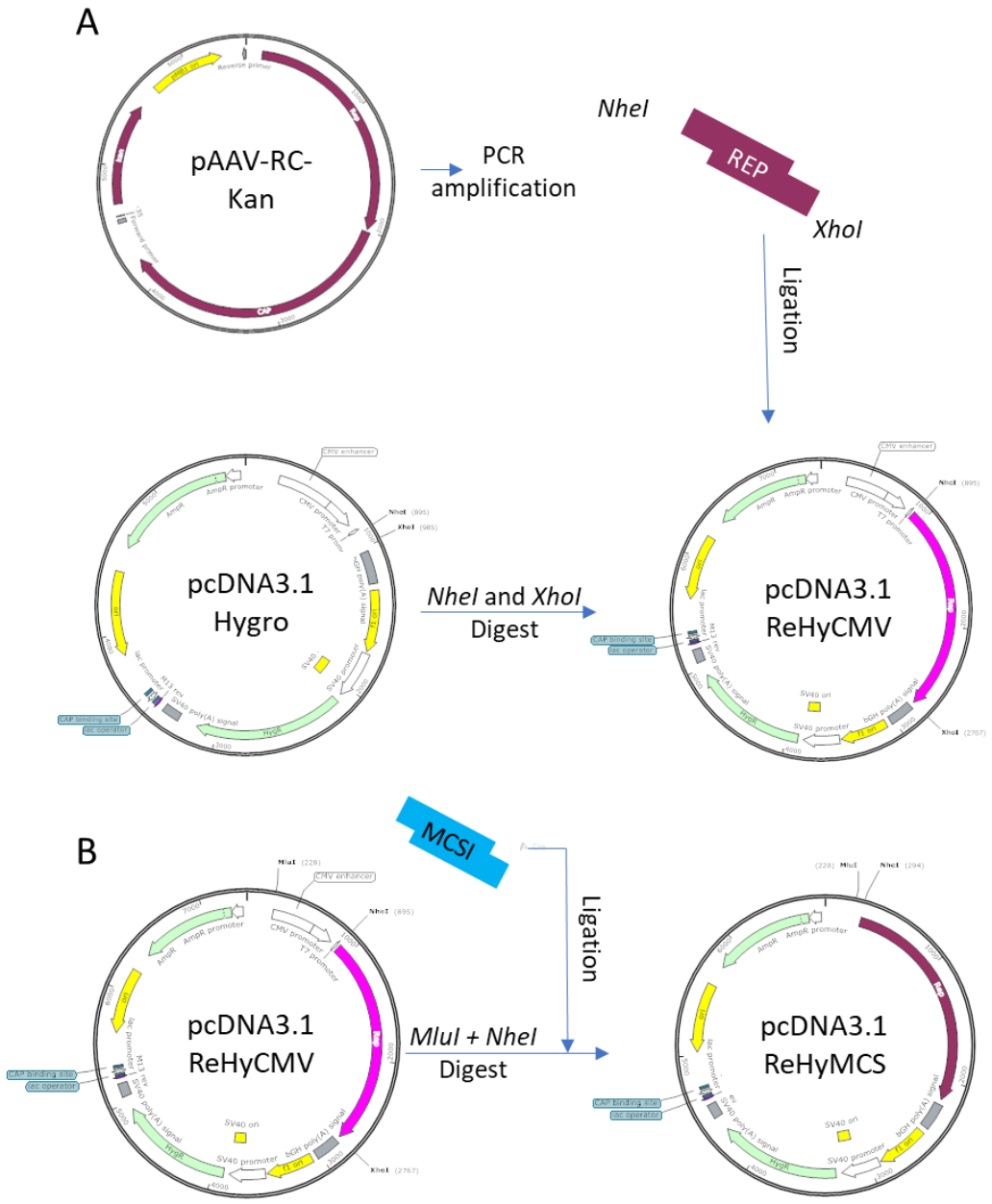

Figure 3.3 Schematic depicting the construction of the Rep Hygromycin vector (A) The *Rep* gene was amplified from the pAAV-RC-Kan plasmid using the Rep primers noted in the Methods Table 2.2-1. The PCR product and the pcDNA3.1 Hygro backbone were then digested with the restriction enzymes *NheI* and *XhoI*. The *Rep* gene was then ligated into the digested backbone to produce the plasmid pcDNA3.1 ReHyCMV. **(B)** To create a version of the *Rep* Hygromycin vector which is lacking in the CMV promotor region, the CMV promotor and enhancer were digested from the pcDNA3.1 ReHyCMV backbone using *MluI* and *NheI.* A short addition oligo sequence, MCS1, was designed as per Methods Table 2.2-4 and annealed together as described in the Methods and ligated into the digested backbone to produce the vector plasmid pcDNA3.1 ReHyMCS.

Figure 3.4 Schematic showing the additional nucleotide region (MCS1) for the replacement of the CMV region.

Following successful generation of the pcDNA3.1 plasmid containing the *Rep* gene, the pcDNA3.1 ReHyMCS vector plasmid was generated which involved the replacement of the CMV promoter region with an additional oligo sequence (MCS1). The MCS1 sequence included the sequences for additional restriction sites to allow for subsequent cloning and is essentially a multiple cloning site (MCS). A schematic of how this was carried out is provided in Figure 3.3. The MCS1 region was commercially synthesised (Figure 3.4). The oligonucleotides were then annealed as per Methods Section 2.3 to produce a double stranded DNA fragment, once annealed the fragment was digested using the restriction enzymes *MluI* and *NheI.* The vector plasmid pcDNA3.1 ReHyCMV was also digested using *MluI* and *NheI* to remove the CMV promoter region, the digested backbone was then ligated with the MCS1 region. The resulting colonies were screened for the presence of the MCS using a test restriction digest using the restriction enzymes *EcoRV* and *BamHI.* All successful colonies when run on a DNA agarose gel showed a band at approximately 6018 bp and a band dropout at 760 bp (Figure 3.5 B). These colonies were then sent for Sanger sequencing to confirm the presence of the desired sequence and insert.

3.4.1.2 Initial Experiments to Investigate Transient Expression of Rep from the Generated Constructs

Prior to using the constructs for the generation of HEK293T cells stably expressing the *Rep* gene, it was necessary to test if the pcDNA3.1 ReHyCMV and pcDNA3.1 ReHyMCS plasmids could be used to successfully produce the Rep proteins in a transient manner. These two constructs were validated via transient PEI transfection into HEK293T cells and subsequent western blot analysis of cell lysates using an anti-Rep protein antibody. HEK293T cells were transfected with 200,000 copies of an appropriate Rep plasmid (either pAAV-RC-Kan,

pcDNA3.1 ReHyCMV or pcDNA3.1 ReHyMCS) and 200,000 copies of the helper plasmid, pHelper-Kan; a mock transfection was also carried out. The transient transfections were set up in biological duplicate. A cell pellet was harvested 48 h post transfection, along with a cell pellet of the untransfected HEK293T cells. The cell pellets were lysed, and the protein samples were prepared as per Methods Section 2.5. After estimating the amount of total protein in cell lysates, 50 μg of total protein sample were loaded and run on an 8% polyacrylamide gel, the proteins were then transferred to nitrocellulose for subsequent western blot analysis as described in Methods Section 2.5.3. The western blot was probed for the presence of the Rep proteins using a commercially available anti-Rep antibody. As seen in Figure 3.5 C, the samples transfected with the Rep plasmids (pAAV-RC-Kan, pcDNA3.1 ReHyCMV or pcDNA3.1 ReHyMCS) produce a band at approximately 40 kDa. This band at 40 kDa is of the expected size for one of the Rep proteins, the expected size of the different Rep proteins being 78 kDa, 68 kDa, 52 kDa and 40 kDa. These data indicate that the vector plasmids pcDNA3.1 ReHyCMV and pc3.1 ReHyMCS do result in the production of the Rep proteins. Furthermore, a band in the Rep plasmid transfected samples at approximately 70 kDa was also observed with those from the ReHyCMV transfected samples appearing to show higher expression of this 70 kDa band. No Rep protein expression was observed in the control HEK293T sample nor in the mock transfected cell line as expected.

3.4.1.3 Attempts to generate HEK293T cell lines stably expressing the Rep proteins

In order to generate HEK293T cell lines stably expressing the Rep proteins it was necessary to set up a transfection using the plasmids that contain the selection marker. Hygromycin B was chosen as an appropriate selection marker for the generation of these Rep expressing cell pools. In order to determine an appropriate concentration of Hygromycin B to use for the establishment of stable cell lines, a kill curve was carried out as described in the Method Section 2.6.3. Based on the kill curves, 250 μg/mL was chosen as an appropriate concentration of hygromycin B to use for stable cell line generation.

Four sets of transfections were initially carried out as described in Methods Section 2.2.4 using 100,000 copies of pcDNA3.1 Hygro, pAAV-RC-Kan, pcDNA3.1 ReHyCMV and pc3.1 ReHyMCS. The transfected cells were then incubated statically at 37°C, then 24 hours post transfection the selection agent Hygromycin B was added to the cells which were then left in the incubator and checked regularly for colonies of cells to emerge in the presence of Hygromycin B. As expected, cells transfected with the pAAV-RC-Kan as a control did not

survive the addition of Hygromycin selection agent due to the fact this plasmid does not contain the selection marker gene. Unfortunately, the cells transfected with pcDNA3.1 ReHyCMV and pc3.1 ReHyMCS did not survive the transfection and selection process either and no colonies grew within one month of the transfections. This could be because the hygromycin gene was not expressed although this is unlikely as others in the laboratory used the same backbone for the successful generation of stable cell lines in the presence of hygromycin (further, this is used in later studies in this thesis successfully to produce stable cell pools and lines). Alternatively, the viral proteins are known to be toxic to the cell (Berthet, Raj, Saudan, & Beard, 2005; Saudan, 2000) and hence their continued expression at high amounts may have resulted in cell death. To try and address this potential outcome, the same transfections were carried out but this time only 50,000 copies of each vector plasmid were transfected to potentially reduce the expression in any stably integrated cells. However, once again, no cells emerged from the selection process and for this reason the work on the Rep expressing cell pools was halted at this point.

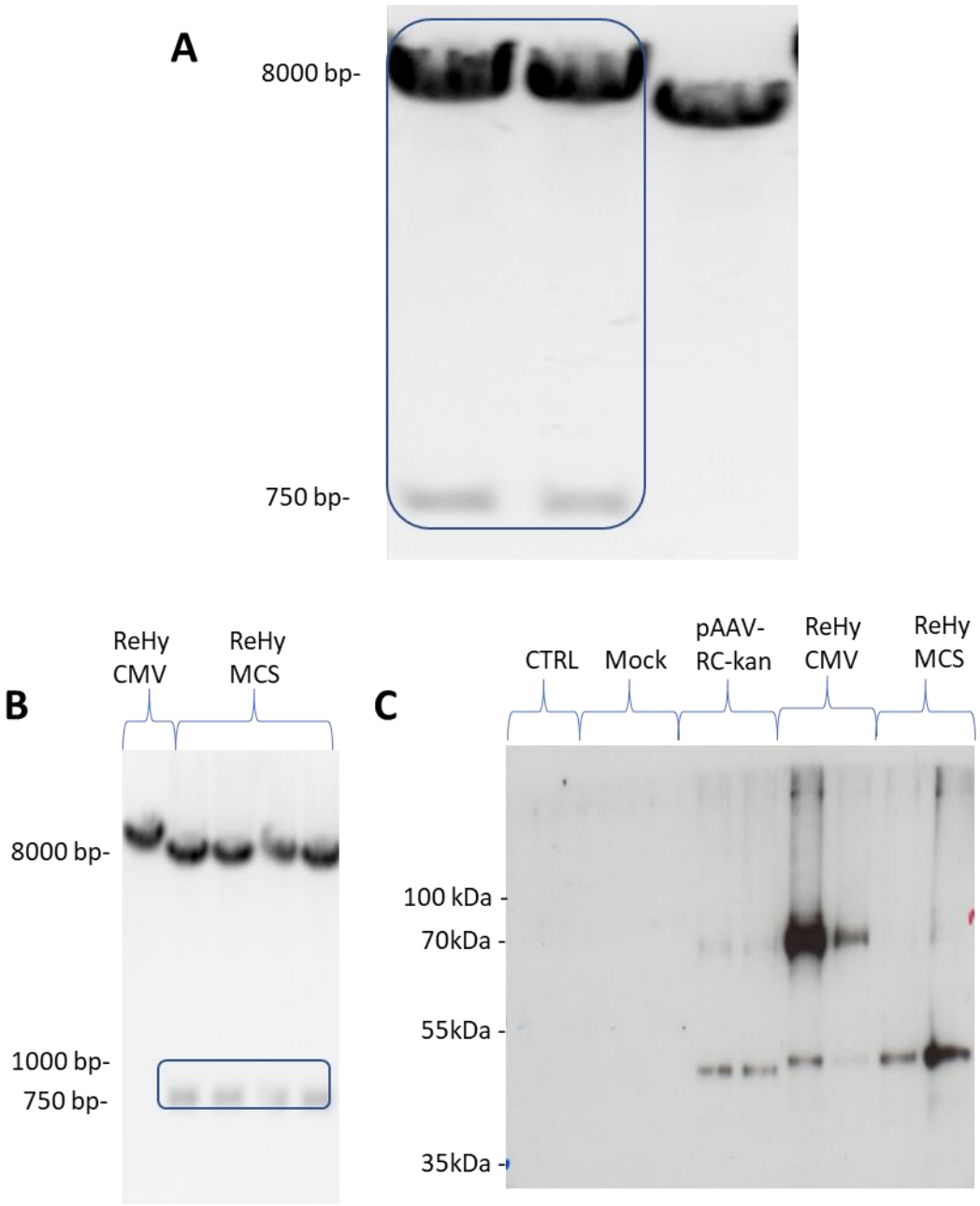

Figure 3.5 A) DNA agarose gel showing a test restriction digest of pcDNA3.1 ReHyCMV using the restriction enzymes *BamHI* and *NheI* with expected bands at approximately 6653 bp and 726 bp. B) DNA agarose gel showing a test digest of pcDNA3.1 ReHyMCS with *EcoRV and BamHI* with a band drop out at approximately 760 bp. C) Western blot following transient transfections of the following plasmids: pAAV-RC-Kan, pcDNA3.1 ReHyCMV,(ReHyCMV) pcDNA3.1 ReHyMCS (ReHyMCS) with an untransfected control (CTRL) and a mock transfected control (Mock) to test for Rep expression using the anti-Rep primary antibody.

3.5 Generation of HEK293T Cell Pools Stably Expressing the *Rep* and *Cap* Genes

3.5.1 Generation of Rep Cap Expressing Constructs

In order to create HEK293T cells stably expressing both the Rep and Cap proteins from a single genomic AAV sequence, it was necessary to create a plasmid vector containing a mammalian selection marker to allow for identification of cells successfully expressing the *Rep* and *Cap* genes as for the *Rep* gene alone described in section 3.4. The methods used for the different steps of molecular cloning discussed are found in Methods Section 2.3. Detailed plasmid maps can be found in the appendix and the primer sequences used in the Methods Section 2.3.

The first vector constructed was the Rep vector referred to as pcDNA3.1 ReCHyCMV (or ReCHyCMV), as described in Figure 3.8 A using the pcDNA3.1 Hygro backbone. The *Rep* and *Cap* genes were amplified from the pAAV-RC-Kan vector plasmid using the RepCap primers as described in the Methods Section 2.34. Both the RepCap insert and the pcDNA3.1 Hygro backbone were digested with *NheI* and *XbaI* before being ligated together and transformed into DH5α cells. A selection of colonies was then subjected to a test restriction digest after growth in culture overnight and purification of the resulting plasmid DNA using a commercially available kit (Methods Section 2.3.3) using the restriction enzymes *NheI* and *BamHI.* A successful band pattern when analysed on a DNA agarose gel showed a band of approximately 8863 bp and a band dropout at approximately 726 bp as seen in lane 8 of the DNA gel in figure 3.9A. The samples showing the correct banding pattern were sent for sequencing with GeneWiz for confirmation of the sequences.

Next it was necessary to generate the pcDNA3.1 ReCHyMCS plasmid which involved the removal of the *Rep* gene from pcDNA3.1 ReHyMCS vector plasmid and replacing it with the *RepCap* insert. The *RepCap* insert was amplified from the vector plasmid pAAV-RC-Kan using the same RepCap primers used for the generation of pcDNA3.1 ReCHyCMV plasmid. Both the RepCap insert and pcDNA3.1 ReHyMCS backbone were digested using the restriction enzymes *NheI* and *XbaI*. A schematic of how this was carried out is shown in figure 3.7B. A selection of transformed colonies was analysed as described above using a test restriction digest and the restriction enzyme *KpnI*. A successful banding pattern contained a band at approximately 6778 bp and a band drop out at approximately 2252 bp (Lane 7, Figure 3.8). The successful colonies were then sent for Sanger sequencing by GeneWiz for sequence confirmation.

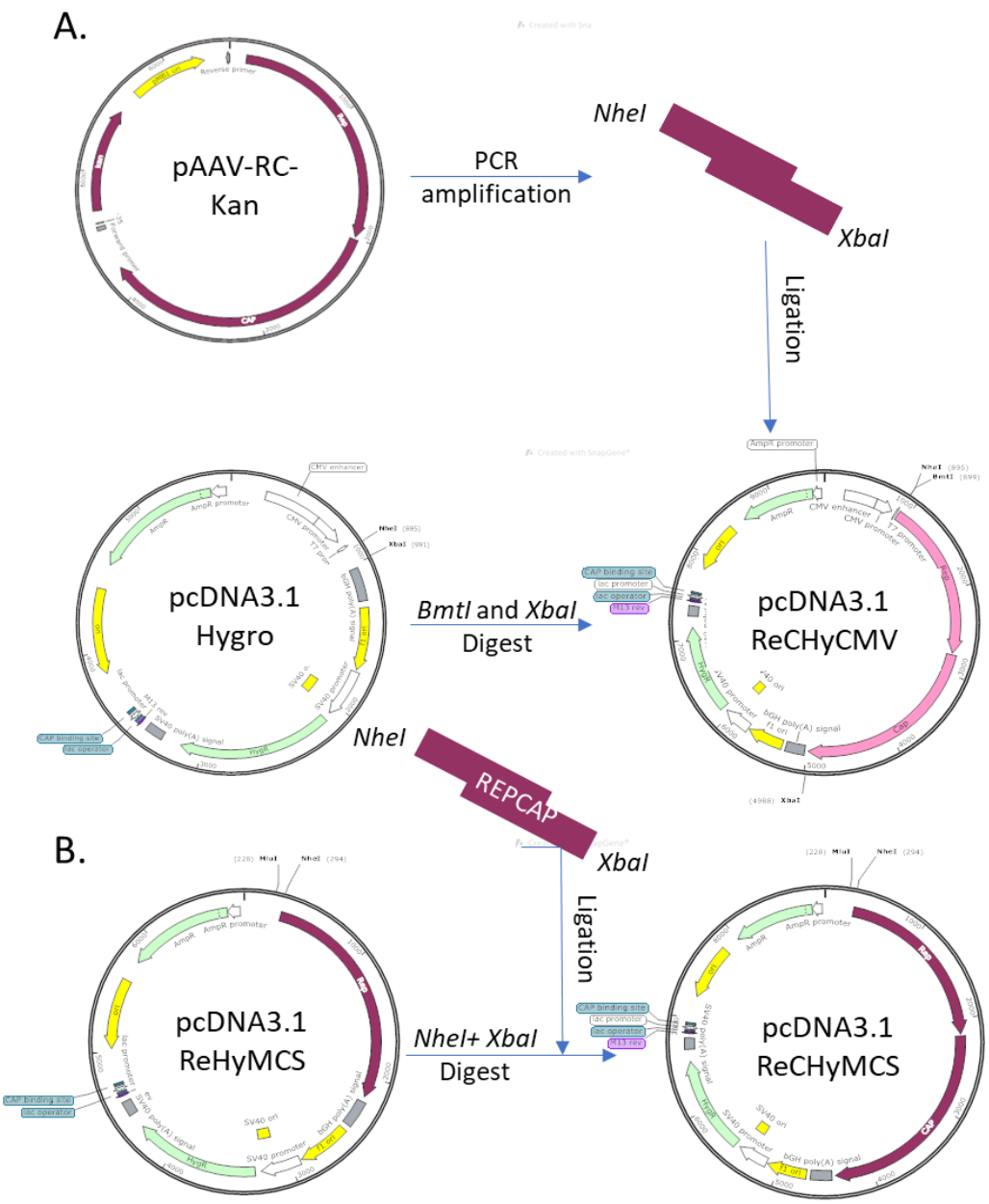

Figure 3.7 Schematic Showing the Construction of the RepCap Hygromycin Vector. (A.) Both the *Rep* and *Cap* genes were amplified out of the pAAV-RC-Kan Plasmid using the RepCap primers noted in the materials and methods Table 2.2-1. The PCR product and the pcDNA3.1 Hygro backbone were then digested with the restriction enzymes *BmtI* and *XbaI*. The *Rep* and *Cap* genes were then ligated into the digested backbone to produce the plasmid pcDNA3.1 ReCHyCMV. **(B.)** To create a version of the Rep Cap Hygromycin vector, which is lacking in the CMV promotor region, the plasmid vector pcDNA3.1 ReHyMCS was digested with the restriction enzymes *XbaI* and *NheI.* The RepCap gene was amplified by PCR and digested with *NheI* and *XbaI* prior to being ligated into the digested pcDNA3.1 ReHyMCS backbone, to produce the vector plasmid pcDNA3.1 ReCHyMCS.

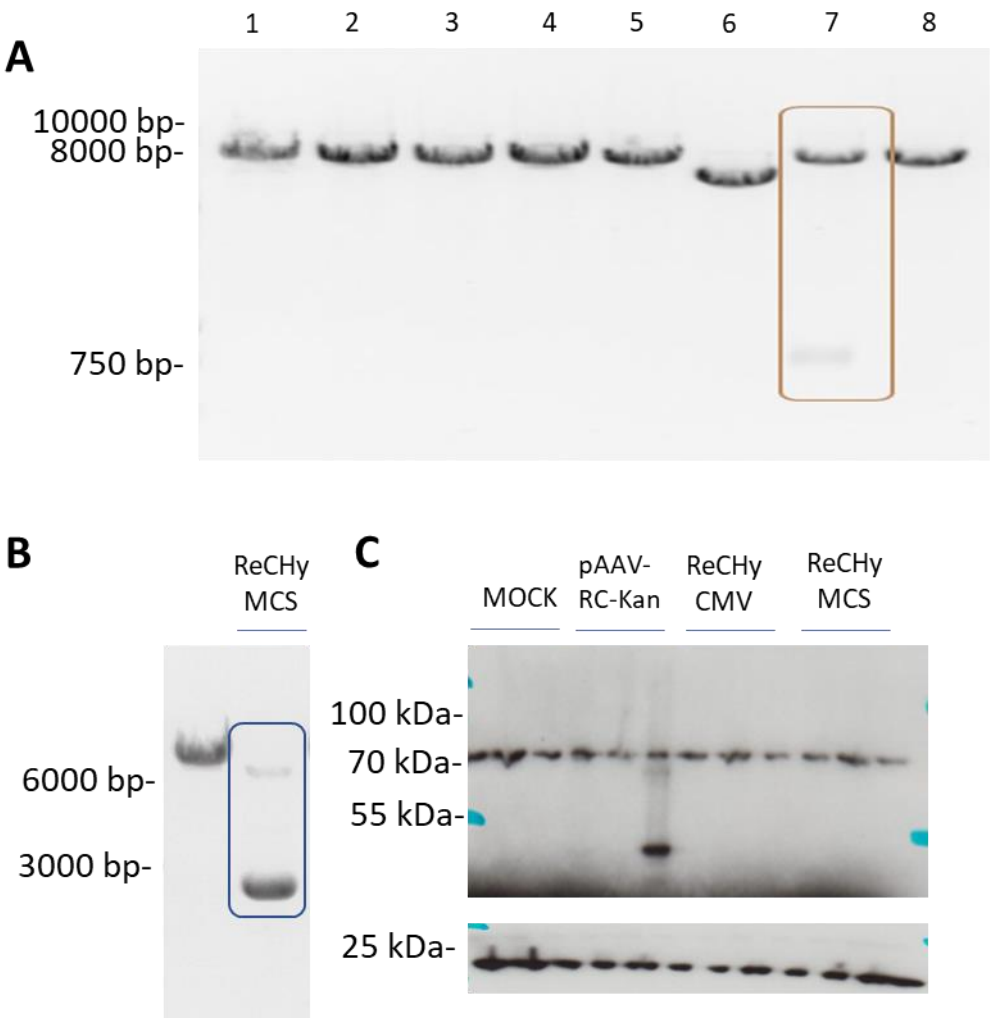

Figure 3.8. A) DNA agarose gel showing a restriction test digest of pcDNA3.1 ReCHyCMV using the restriction enzymes *NheI* and *BamHI.* A successful banding pattern shows bands at 8863 bp with a band drop out at approximately 726 bp. B) DNA agarose gel showing an enzyme digest of pcDNA3.1 ReCHyMCS using the restriction enzyme *KpnI,* with bands at approximately 6778 bp and a band at approximately 2252 bp. C) Western blot following transient transfections of the following plasmids: pAAV-RC-Kan, pcDNA3.1 ReCHyCMV,(ReCHyCMV) pcDNA3.1 ReCHyMCS (ReCHyMCS) with a mock transfected control (Mock) to test for Rep expression using the anti-Rep primary antibody. L7a was used as a loading control for these blots with a band detected approximately 25 kDa.

3.5.2 Initial Experiments to Investigate Transient Expression of Proteins from the RepCap Generated Constructs

Prior to using the constructs for the generation of the HEK293T cell line stably expressing the *Rep* and *Cap* genes, it was necessary to determine if the pcDNA3.1 ReCHyCMV and pcDNA3.1 ReCHyMCS plasmids could successfully transiently produce the Rep or Cap proteins. The aim was to validate these two constructs via transient PEI transfections. HEK293T host cells were transfected with 200,000 copies of the Rep and Cap producing plasmids (pAAV-RC-Kan, pcDNA3.1 ReCHyCMV or pcDNA3.1 ReCHyMCS) and 200,000 copies of the helper plasmid, pHelper-Kan, a mock transfection was also carried out. These transient transfections were set up in biological triplicate. A cell pellet was harvested 48 h post transfection, along with a cell pellet of the host HEK293T cells. The cell pellets were lysed, and the protein samples were prepared as per the Methods Sections 2.5, respectively. Samples containing 50 µg of total protein were loaded and run on an 8% polyacrylamide gel and a western blot was carried out as described in Methods Section 2.5.3. The western blot was probed for the presence of the Rep proteins using the anti-Rep antibody and the protein L7a as a loading control (~30 kDa). A band was observed in all samples including the HEK293T control at just above 70 kDa, however it was not possible to visualise any of the Rep protein bands in any of the samples except one of the biological replicates of the pAAV-RC-Kan transfections. Due to the fact that the presence of the band's indicative of Rep expression in the ReCHyCMV or ReCHyMCS samples were not observed (Figure 3.6 C), this indicates that the vector plasmids pcDNA3.1 ReCHyCMV and pc3.1 ReCHyMCS either do not produce the Rep proteins or do but at amounts not detectable by western blotting and hence were very low. In view of these results, it was decided that work on developing a HEK293T host cell pool stably expressing Rep and Cap genes/protein be halted.

3.6 Discussion

The aim of this Chapter was to establish AAV2 vector production using a suspension adapted host HEK293T cell line. This traditionally adherent cell line was adapted to suspension at Cobra Biologics. Once the host cell line was established it was possible to use this host cell line as a baseline for vector production and as a comparison for future work in Chapter 4 and Chapter 5. Establishment of the suspension adapted HEK293T cell line involved an initial investigation into the growth kinetics of the HEK293T cells by analysing their culture viability and viable cell concentration during batch culture. The HEK293T cell line maintained a high

culture viability (% viability) for the first 4 days following transfection prior to steadily declining. There was a steady increase in the viable cell concentration which peaked on day 4 with a steady decline of viable cells by day 5. The growth profiles reported in figure 3.1 mirror the growth profile of HEK293T cell lines reported in other research (Termini et al., 2017). Based on the growth profiles, the population doubling time (PDT) was also determined across the first four days of culture; the doubling time of the suspension adapted HEK293T cell line was calculated as 22.1 h. While there are very few studies looking at the doubling time of suspension adapted HEK293T cell lines, the doubling time of the suspension adapted HEK293T line can be compared to that of the adherent HEK293T cell line, where the population doubling times range up to 30 h (Pfeifer et al., 1993; Ramboer et al., 2015). Furthermore, the doubling time of the HEK293T cell line used in this research is around that of suspension adapted HEK293 cells which have a reported doubling time of 24 h (Cervera, Gutiérrez, Gòdia, & Segura, 2011). As with the research in this study, the Cevera study did not use serum in the media the cells were grown in (Freestyle).

It was important to determine if there was any impact of subculture length between passaging on the cell culture heath as determined by culture viability and viable cell numbers. Ideally, transient transfections should be set up on a day when the cultures have a high culture viability (>90%) (de los Milagros Bassani Molinas, Beer, Hesse, Wirth, & Wagner, 2014) and in the same growth phase every time so that reproducible methodology is followed and results obtained. Based on the growth data collected on passage days Monday, Wednesday and Friday, it was shown that the cells appeared to maintain a higher culture viability on a Monday following a 3-day culture when compared to Wednesday and Friday following a 2-day culture. Based on this it was determined that the set-up of the transient transfections would occur for experiments undertaken in this thesis following three days in culture to give the most reproducibility possible rather than using a 2-day culture (Figure 3.1). However, research undertaken at Cobra Biologics has shown that the passaging regime is known to marginally improve the robustness of the AAV production, this is due to the variable nature of the production of these viral vectors. Major factors that impact this variability include the transfection efficiency and the cells ability to produce the AAV vectors.

Along with the initial establishment of the HEK293T suspension adapted cells it was also necessary to establish a baseline for rAAV2 vector production using the model system and process to be utilised throughout the remainder of the studies. The initial titre data reported in this results chapter was used as a comparison for further work described in Chapters 4 and 5. rAAV2 vectors were produced by a transient triple PEI transfection of the appropriate

plasmids; pAAV-RC-Kan, pAAV-GFP-Kan and pHelper-Kan. The capsid titres obtained during this preliminary small-scale study are in line with the capsid titres generated in other studies. The study by Hyang et al (2013) yielded capsid titres between $2x10^8$ and $2x10^9$ /mL using PEI transfection reagent. However, previous studies have often been carried out in adherent cells with media containing FBS (D Grimm et al., 1999; Huang et al., 2013). Other large-scale studies such as that by Durocher et al (2007) achieved titres of $4.5x10^{11}$ infectious viral particles in a 3.5 L bioreactor. The Durocher study used a HEK293 suspension cell line along with serum free, Freestyle media and as with the work in this chapter the plasmids were transfected in a triple transfection method and were carried out using PEI transfection reagent (Durocher et al., 2007).

The majority of the particles produced here were retained in the cells, this has been reported in other studies where the lysate titre was compared to that of the supernatant titre. This was an expected result, as it is a well-known that the majority of rAAV2 vectors need to be purified from the cell lysate as AAV2 remains cell associated due to its affinity for heparin (Huang et al., 2013; Vandenberghe et al., 2010). The retention within the cell is not a trait common to all AAV serotypes, indeed many serotypes (e.g., AAV1, AAV8 and AAV9) do in fact release vectors into the culture medium. On-the-other-hand, the study by Vandenberghe et al showed that for AAV2 and AAV5 the majority of capsids are retained within the cell (Vandenberghe et al., 2010). The retention of the viral capsids for certain serotypes adds an extra level to the purification of the capsids as it is necessary to extract them from cells and then purify them from all other intracellular material. This is a major challenge for downstream processing (Morenweiser, 2005). Thus, the choice of serotype can have profound implications on downstream purification demands and secreted or released serotypes might be advantageous for production in this respect although choice of serotype also depends on the tissue to be targeted for the gene therapy. Low packaging efficiency is also a common trait observed in rAAV production (Sommer et al., 2003; J F Wright, 2008) and is one of the major challenges that needs to be overcome in the production of such vectors. This work served as a baseline for the future chapters of this thesis where the aim was to investigate the improved packaging of rAAV2 vectors by engineering of the host cell.

One of the approaches to potentially improve rAAV production explored in this chapter was to look at generating a HEK293T cell line stably expressing the Rep proteins or both the Rep and Cap proteins. Transfection efficiency can be influenced by many factors including cell type, nucleic acid/chemical ratio, pH and cell membrane conditions. It has been shown that the ratio between the molar units of PEI nitrogen to the units of phosphate atoms in DNA,

the N/P ratio, correlates with increased transfection efficiencies (Huang et al., 2013). Furthermore, studies have shown co-transfection can have a negative impact or mutual inhibition of plasmid expression when transiently co-transfected (Stepanenko & Heng, 2017). Therefore, the generation of a cell line stably expressing the *Rep* and *Cap* genes would potentially reduce the strain on the cells producing the vectors as it would reduce the number of plasmids required to be transfected into the HEK293T cells. A further reason for undertaking this work relates to the method behind genome encapsulation. Although this is not fully elucidated, one hypothesis is of "Rep mediated encapsulation" whereby the Rep78 protein is thought to attach to the 5' end of the DNA genome. This complex then binds to a fully formed capsid and the 3' end binds to another Rep protein before binding to the capsid followed by encapsulation of the genome through Rep-Rep interactions. This Rep mediated encapsulation involves the Rep binding to the Rep Binding elements (RBE) within the ITR regions (Bleker, Pawlita, & Kleinschmidt, 2006; R. Jude Samulski & Muzyczka, 2014; Wang Y, Wang L, & Aslanidi GV, 2015). It is for this reason we had a keen interest in manipulation of the Rep proteins and the role they might play in the ratio of empty vector vs packaged vector observed.

Initially, it was necessary to produce Rep and RepCap plasmid DNA vectors that contained a selection marker to allow for selection/isolation of cells stably expressing the Rep or Rep and Cap proteins. The cloning was successful as confirmed by sequencing of the final plasmids produced. Unfortunately, while the Rep proteins have been shown to play a multitude of essential roles including AAV DNA replication, regulation and genome integration it has also been shown that expression of these have a cytotoxic effect on the cells. The expression of Rep78 has been shown to induce apoptotic cell death during the G1 and S phases of the cell cycle (Schmidt et al., 2000; Qicheng Yang, Chen, Ross, & Trempe, 1995). Due to this potentially detrimental impact, and the presence of a CMV region in the plasmid vectors, plasmid vectors were designed and generated that were lacking the CMV region to potentially decrease the expression of the Rep proteins. The hypothesis was that lower Rep protein expression may be tolerated and the stably expressing cell lines would not experience cell death by apoptosis. The CMV promoter is of variable promotor strength, being strong in certain cell lines and weak in other cell lines although generally considered a strong promoter, particularly when the enhancer is present as in the vector used in this study. Thus, the CMV promotor is a strong promotor in the HEK293T cell line (Qin et al., 2010). The plasmid vectors pcDNA3.1 ReHyMCS and the pcDNA3.1 ReCHyMCS were

therefore made whereby they had a multiple cloning site in place of the CMV promotor region.

It was important to test that the plasmid constructs without the CMV promoter did still produce the Rep or the Rep and Cap proteins. This was achieved by transiently transfecting these plasmid vectors into the HEK293T host cells. The Rep plasmids (pcDNA3.1 ReHyCMV and pcDNA3.1 ReHyMCS) did show successful expression of the Rep proteins as seen in figure 3.6C. Unfortunately, it was not possible to detect Rep or Cap expression from the RepCap plasmids pcDNA3.1 ReCHyCMV and pcDNA3.1 ReCHyMCS. However, following the validation that pcDNA3.1 ReHyCMV and pcDNA3.1 ReHyMCS could transiently express the Rep proteins, transfections were carried out and 24 h later the Hygromycin B selection agent was added to the cells to allow selection for stably integrated and surviving cells. The concentration of hygromycin B was determined based on the results seen in a kill curve, the kill curve concentrations are in line with other studies with 250 µg/mL being a commonly used hygromycin B selection concentration with HEK293T cell lines (Reus, Trivino-Soto, Wu, Kokott, & Lim, 2020). Indeed, the concentration of hygromycin B used in HEK293T research generally ranges from 100 µg/mL to 300 µg/mL (Boshtam et al., 2018; Fatahi et al., 2018; Parris, Vizlin-Hodzic, Salmela, & Funa, 2019). Unfortunately, no colonies emerged from these transfections. The transfections were carried out again but using less copies of the plasmid vectors per cell (50,000 copies/cell). These cells did not survive selection either. As mentioned earlier, the expression of Rep proteins has detrimental effects on the cells by slowing cell growth and promoting cell death (Khleif, Myersz, Carter, & Trempe, 1991). We theorise that it is potentially these cytotoxic effects that prevents the emergence of stably expressing Rep protein cell lines.

Due to the data derived from the experiments outlined in this Chapter, work on development of HEK293T stably expressing Rep and Cap protein cell pools was not continued. While this approach was unsuccessful, there has been some work on development of such cell lines expressing the Rep proteins. A dual switch inducible system has been reported for the inactivation and activation of the *Rep* genes in a HEK293 cell line which results in normal growth profiles and high rAAV vector yields (Qiao, Wang, Zhu, Li, & Xiao, 2002). There have also been HeLa cell lines produced that do express both the *Rep* and *Cap* genes (K. Reed Clark et al., 1995). Further, there has also been a non-HeLa cell line developed expressing both the Rep and Cap proteins, this cell line (known as K209) has been designed by stable transfection of A549 with an AAV2 plasmid containing the p5 Rep and Cap cassette. This cell line has been shown to produce a high yield of rAAV2 vectors (G. P. Gao et al., 2002). There is thus evidence

of it being possible to generate Rep and Rep-Cap stably expressing cell lines, but it is likely that for this to give long term stability an inducible system of expression is required such that these are not expressed in the cell in the absence of an inducing agent. This in itself offers some issues for production as an inducer agent would need to be added to the cells after transfection of plasmids containing the target genome and additional helper genes. Thus, one potential way of overcoming the issue in future work would be to develop an inducible Rep system in the host cell lines. This would maintain the Rep genes in an "off" position until an inducer switches it on. This off switch would potentially prevent the cytotoxic effects of the Rep proteins from killing the cells. Inducible systems have been designed using HEK293 cell lines to allow amplification of the helper genes under the control of the tetracycline transactivator system (Inoue & Russell, 1998; Qiao, Li, Skold, Zhang, & Xiao, 2002). The use of a tetracycline inducible system would be a potential next step for the production of the stable cell lines expressing *Rep* and *Cap* genes.

Although it did not prove possible to generate HEK293T stably expressing Rep and Cap cell pools, other cell line engineering approaches can be taken to try and improve rAAV production from HEK293T cells. The following Chapters describe one such approach, whereby HEK293T cells stably expressing a further protein that can arise from the Cap transcript, AAP, were generated and evaluated for their ability to produce rAAV compared to the original HEK293T cells.

Chapter 4

Generation of Molecular Constructs and Assembly Activating Protein (AAP) HEK293T Expressing Cells

4.1 Introduction to the Work Described in this Chapter

As outlined in the Introduction chapter of this thesis, when AAV capsids are generated, reports suggest that the empty capsids are initially formed in a rapid reaction followed by the slow insertion of the single stranded genome into the protein capsid (Myers & Carter, 1980). Despite this, the mechanisms involved in both the formation of the capsid and encapsulation of the genome still remain largely unknown in comparison to what is known about the molecular events involved in the replication of the genome. For over 25 years it was thought that the only proteins expressed by AAV2 were that of the non-structural Rep proteins (Rep40, Rep52, Rep68 and Rep78) and the three capsid proteins (VP1, VP2 and VP3). This remained the case until a small 23 kDa protein was identified which was encoded within an alternative ORF upstream of the VP3 coding sequence. The translation of this mRNA is initiated from an unconventional start codon (CUG) (Sonntag et al., 2010). Due to what was thought initially to be an essential role in capsid assembly, it became known as the Assembly Activating Protein (AAP). Studies on AAP have shown it to have a role in the transport of VP proteins to the nucleolus for capsid assembly, this role being identified partly by the presence of a nucleolar localisation signal (Earley et al., 2015; Sonntag et al., 2010). AAP has been identified in all parvoviruses that are found in the genus *Dependovirus* (Sonntag et al., 2010). Most of the research to date has involved the AAP protein from the AAV serotype 2. While it was initially thought that AAP was vital for capsid assembly, it has since been shown that the importance of AAP in capsid assembly is serotype specific. The initial research was based on the AAP from AAV serotype 2 that showed that AAP plays an essential role in the production of AAV2 capsids, however it has been shown to be less essential in serotypes 4, 5 and 11 (Earley et al., 2017).

Traditionally when discussing protein coding sequences in eukaryotic cells, we think of them as starting with a conventional AUG start codon and ending in one of three stop codons, UAA, UGA and UAG. This is known to be the most efficient method of translation initiation. As far back as the 1980s it was shown that ribosomes can identify/recognise unconventional start codons, albeit in a less efficient manner than that of the conventional AUG start codon (Kearse & Wilusz, 2017; Zitomer, Walthall, Rymond, & Hollenberg, 1984). While it is

abnormal for mammalian cells to utilise non-conventional start codons, initiation at unconventional start codons is a trait that can be found in viruses and a variety of cell types including mammalian cells (Firth & Brierley, 2012; Peabody, 1989). The use of non-conventional start codons in mammalian cells can be divided into two separate groups; IRES-dependent or IRES-independent. It has been shown that CUG initiated translation does not utilise an IRES mechanism of translation initiation and is based on the typical cap-dependent ribosome scanning mechanisms (Gerashchenko, Su, & Gladyshev, 2010).

As mentioned above, translation of AAP is initiated from an funconventional start codon, CUG. It is this ability of the translational machinery of mammalian cells to initiate at non-conventional start codons that allows for the production of AAV serotype 2 capsids. There are a number of start codons responsible for the different proteins expressed from the *Cap* gene. VP2 is initiated by a weak ACG start codon prior to the non-conventional CTG start codon for AAP followed by a standard ATG start codon for the VP3 protein. To ensure that all proteins are expressed from one transcript the cells utilise a translation strategy which engages a leaky scanning or shunting mechanism to produce the proteins (Ryabova, Pooggin, & Hohn, 2002; Sonntag et al., 2010).

4.2 Aims of this Chapter

The work presented in Chapter 3 evaluated expression of *Rep*/*Cap* genes and the possibility of establishing stably expressing cell pools of Rep and Cap. This was found to be difficult to achieve as outlined in Chapter 3. The focus of this Chapter was therefore to begin investigating manipulation of AAP expression in HEK293T cells. Further, the role of the Assembly Activating Protein (AAP) was of particular interest to Cobra Biologics due to the gaps in our understanding regarding AAP and its potential impact on making recombinant AAV. In this chapter is described the production of HEK293T cell pools stably expressing AAP. As AAP has a cryptic start codon (CTG) it was necessary to design AAP constructs that have this cryptic start codon, but alongside side this we investigated using an ATG start codon in the transcript encoding for the AAP protein. This chapter also reports on the characterisation of the AAP cell pools developed, specifically C-terminally V5 tagged AAP cell pools via western blotting and immunofluorescence. The chapter concludes with an investigation into the effect of exogenous AAP expression in HEK293T cell pools on the production of AAV serotype 2 capsids by determining capsid and genome titres from these pools via ELISA and qPCR methods compared to the original HEK293T cell host.

The overall aims of the work described in this chapter were therefore to:

a. Generate constructs containing the AAP gene with either a CTG or ATG start codon and that included within the acceptor plasmid a mammalian selection marker (Hygromycin) in order to produce HEK293T cell lines stably expressing the *AAP* genes
b. Characterise the resulting HEK293T cell pools stably expressing AAP from either a CTG or ATG start codon, looking specifically at:
    i. Expression of AAP from the CTG and ATG constructs
    ii. Growth characteristics
    iii. Localisation of AAP
c. Establish an rAAV2 production system using the CTG and ATG construct AAP expressing cell pools and using commercially available PCR and ELISA based assays, determine the effects of AAP over-expression on capsid formation and genome titre of a AAV2 expressing model transgene GFP.

4.3 Generation of Recombinant AAP Expressing Cell Pools

4.3.1 Generation of AAP Expressing Constructs

In order to generate HEK293T cells stably expressing the AAP proteins it was necessary to create a plasmid vector containing a mammalian selection marker to allow for isolation of cells successfully harbouring the *AAP* gene expression cassettes. Furthermore, due to the lack of commercially available AAP antibodies it was necessary to express the *AAP* gene in frame with a C-terminal V5 tag to allow for visualisation of the protein. To ensure any effects observed on cell phenotype were caused by the AAP protein and not the V5 tag, it was also important to generate a vector plasmid where the *AAP* gene did not read through to the V5 tag, this was achieved via the addition of a TGA stop codon following the *AAP* gene. The methods used for the different stages of molecular cloning are described in Methods Section 2.3. Detailed plasmid maps are located in the Appendix and the primer sequences used are described in Table 2.2-1.

As previously mentioned, *AAP* naturally has a cryptic CTG start codon. A pCET901-AAP plasmid containing the CTG-AAP gene, supplied from Cobra Biologics, was used as a template to amplify the CTG-*AAP* gene using the CTG-AAPV5 primer set or the CTG-AAPSTOP primer set (Table 2.2-1) for the production of the pcDNA3.1 CTGV5 and pcDNA3.1 CTG-AAP STOP vectors using the pcDNA3.1 Hygro V5His backbone, as described in Figure 4.1 and 4.2, respectively. Furthermore, a pCET901-ATG-AAP plasmid containing the synthetically engineered ATG-AAP gene, was also supplied by Cobra Biologics. This pCET901-ATG-AAP

plasmid was used as template to amplify the *ATG-AAP* gene using either the ATG-AAPV5 primer set or the ATG-AAPstop primer set (Table 2.2-1), this resulted in the production of the pcDNA3.1 ATGV5 and pcDNA3.1 ATG-AAP STOP vectors using the pcDNA3.1 Hygro V5His backbone, as described in Figure 4.4 and 4.5, respectively. A schematic of the CTG-AAP plasmid vectors is shown in Fig 4.3 A and the ATG-AAP plasmid vectors is shown in Fig 4.6A. The amplified *AAP* genes and the pcDNA3.1 Hygro V5His backbone were digested using the restriction enzymes *KpnI* and *XhoI*. The backbones and inserts were ligated together and transformed into DH5α cells in the presence of ampicillin. A selection of colonies were chosen to confirm the presence of plasmid DNA containing the required inserts. A restriction test digest using the restriction enzymes *KpnI* and *XhoI* followed DNA extraction. All test digests were then analysed on a DNA agarose gel, colonies containing the desired gene insert had a backbone band at approximately 5599 bp with a band drop out of approximately 751 bp expected and representing the *CTG-AAPV5* gene (Fig. 4.3 B), a band dropout of 754 bp expected representing the *CTG-AAP* STOP gene (Fig. 4.3 C), a band drop out of 669 bp representing the ATGV5 gene(Fig. 4.6 B) or a band dropout of 672 bp representing the ATG-*AAP* STOP plasmid (Fig. 4.6 C) (Table 4.3-1). Colonies that appeared successful based on the restriction test digest were sent for sequencing commercially by GeneWiz for confirmation of the sequence.

Table 4.3-1 Test restriction digest expected DNA band sizes (bp).

Inserted gene	Backbone size (bp)	Insert size (bp)
CTG-AAPV5	5599	751
CTG-AAPstop	5599	754
ATG-AAPV5	5599	669
ATG-AAPstop	5599	672

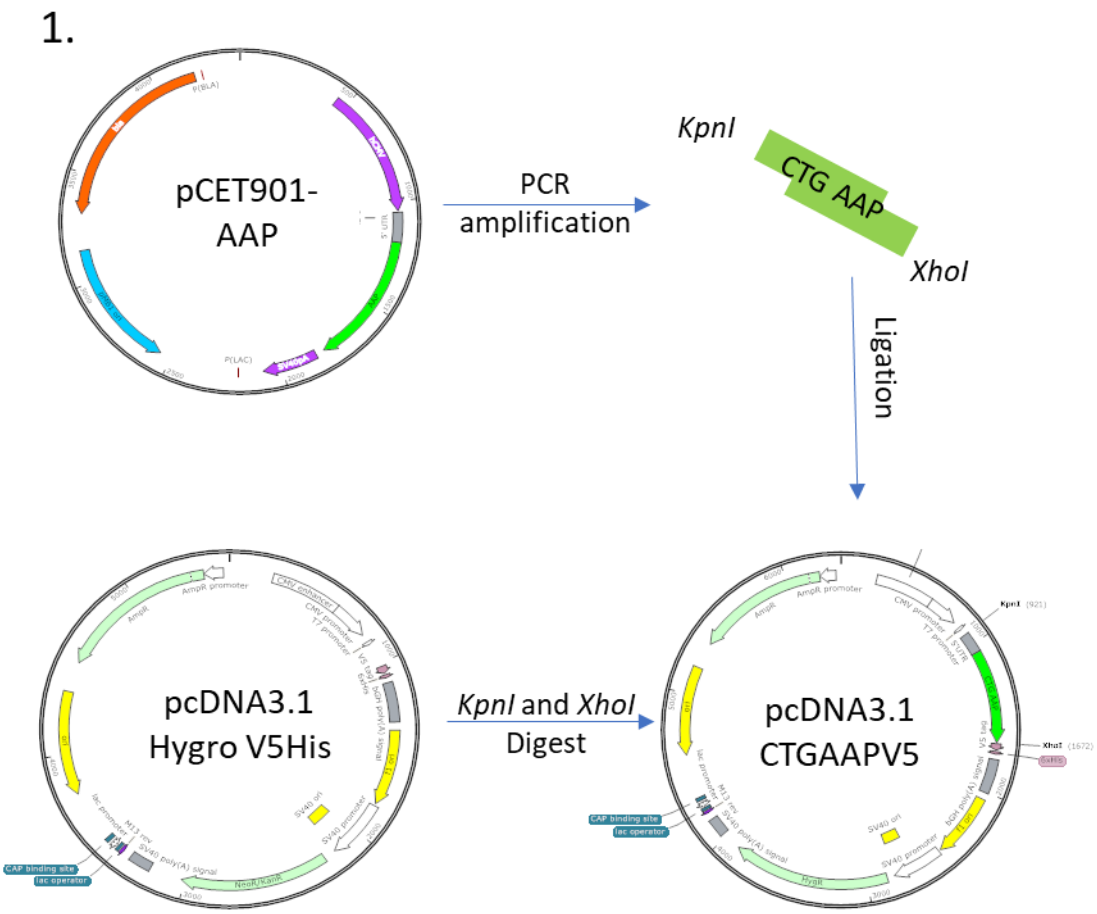

Figure 4.1 Schematic showing the construction of the CTG-AAPV5 tagged vector (pcDNA3.1 CTG-AAP V5). The *AAP* gene with the cryptic start codon, CTG, was amplified out of the pCET901-AAP plasmid using the CTG-AAP primers described in Methods Table 2.2-1. The PCR product and the pcDNA3.1 Hygro V5His backbone were then digested with the restriction enzymes *KpnI* and *XhoI*. The CTG *AAP* gene was then ligated into the digested backbone to produce the plasmid pcDNA3.1 CTG-AAP V5.

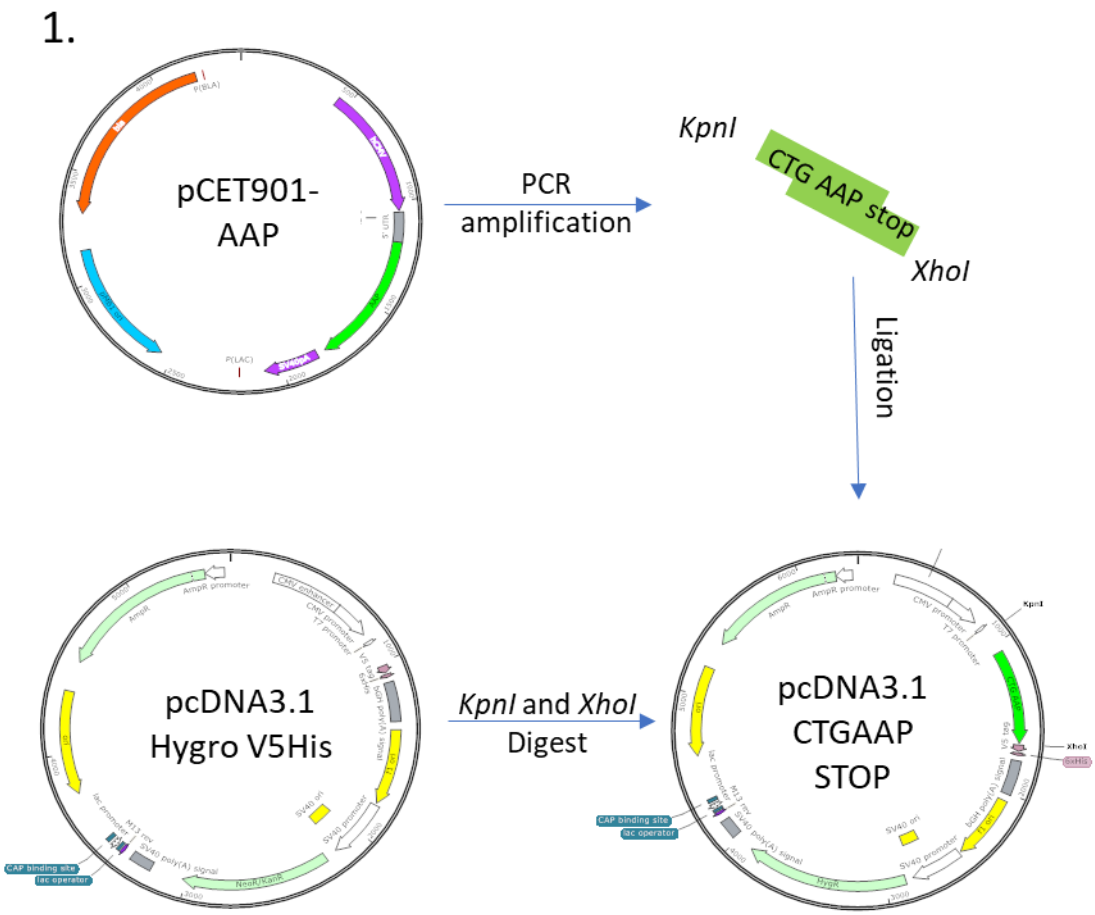

Figure 4.2 Schematic showing the construction of the CTG-AAP vector lacking a tag (pcDNA3.1 CTG-AAP STOP). The *AAP* gene with the cryptic start codon, CTG, was amplified out of the pCET901-AAP plasmid using the CTG-AAP STOP primers described in Methods Table 2.2-1. The PCR product and the pcDNA3.1 Hygro V5His backbone were then digested with the restriction enzymes *KpnI* and *XhoI*. The CTG *AAP* gene was then ligated into the digested backbone to produce the plasmid pcDNA3.1 CTG-AAP STOP.

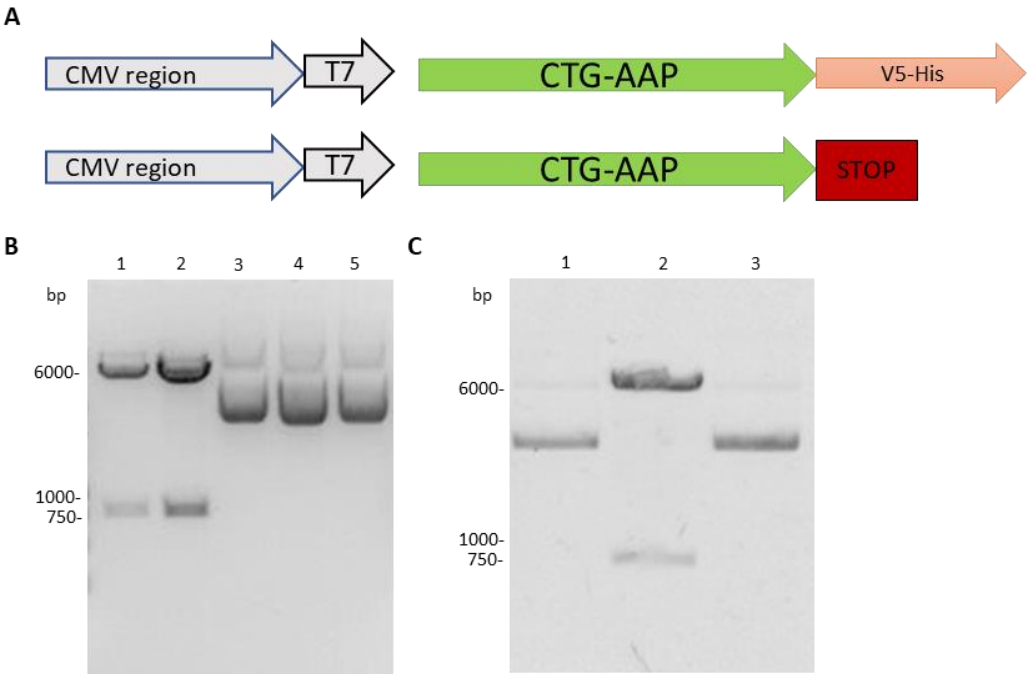

Figure 4.3 Generation of CTG-AAP vector constucts with and without a V5 tag. A) Schematic of the CTG-AAP vector constructs pcDNA3.1 CTG-AAP V5 (upper) and pcDNA3.1 CTG-AAP STOP (lower). **(B)** DNA agarose gel showing a test restriction digest of plasmid DNA thought to be that of pcDNA3.1 CTG-AAP V5 using the restriction enzymes *KpnI* and *XhoI*. Lanes 1 and 2 show bands representative of the predicted fragments 5599 bp and 751 bp. **(C)** DNA agarose gel showing a test restriction digest of plasmid DNA thought to be that of pcDNA3.1 CTG-AAP STOP using the restriction enzymes *KpnI* and *XhoI.* Lane 2 shows bands representative of the predicted fragments at 5599 bp and 754 bp.

Clones 1 and 2 for CTG-AAPV5 and clone 2 for CTG-AAPSTOP, clones 1 and 2 for ATG-AAPV5 and clones 1, 2 and 4 for ATG-AAPSTOP were confirmed for the presence of the correct insert sequence by commercial sequencing via Genewiz. Successfully sequenced AAP vector constructs were extracted on a larger scale for use in the generation of HEK293T cell pools stably expressing AAP as described in Results Section 4.4 following validation of vector constructs by western blot analysis as described in Results Section 4.3.3.

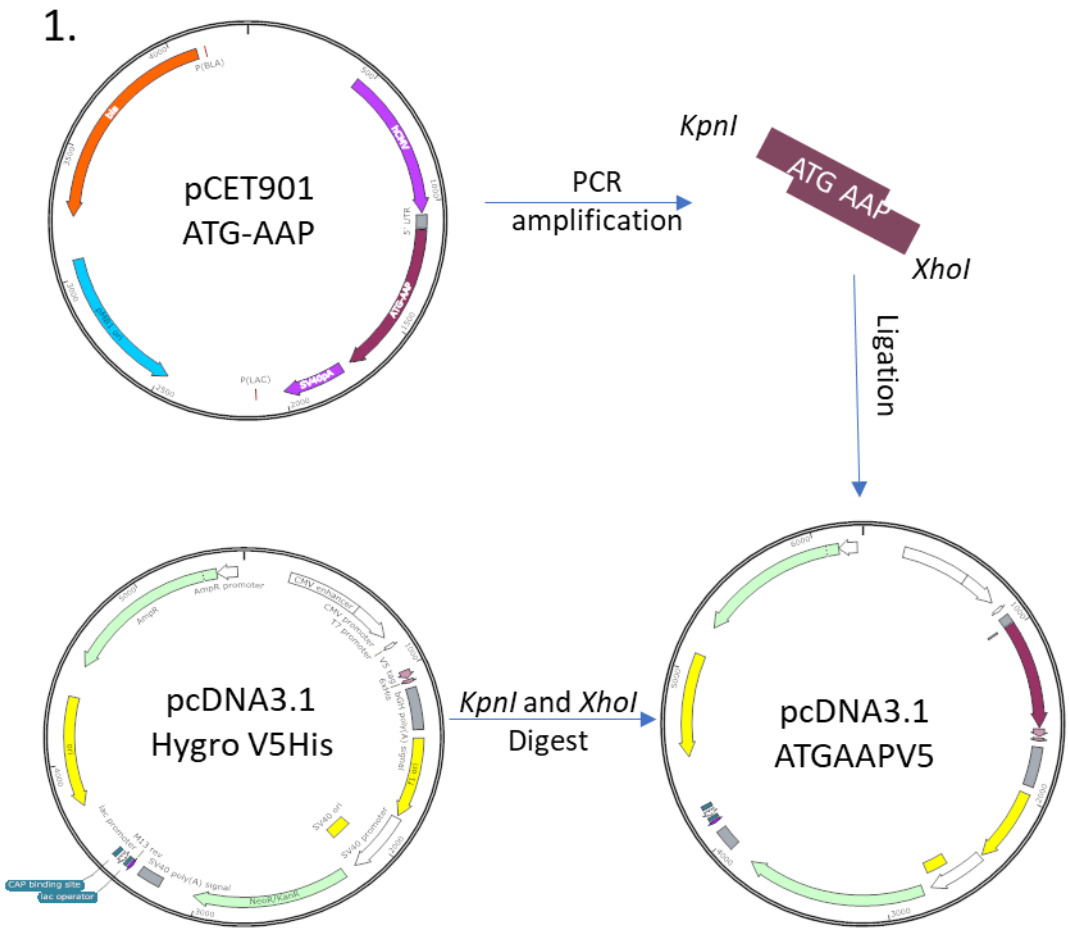

Figure 4.4 Schematic showing the construction of the ATGV5 tagged vector (pcDNA3.1 ATG-AAP V5). The *AAP* gene with the ATG, was amplified out of the Pcet901 ATG-AAP plasmid using the ATG-AAP primers described in Methods Table 2.2-1. The PCR product and the pcDNA3.1 Hygro V5His backbone were digested with the restriction enzymes *KpnI* and *XhoI*. The ATG *AAP* gene was ligated into the digested backbone to produce the plasmid pcDNA3.1 ATG-AAP V5.

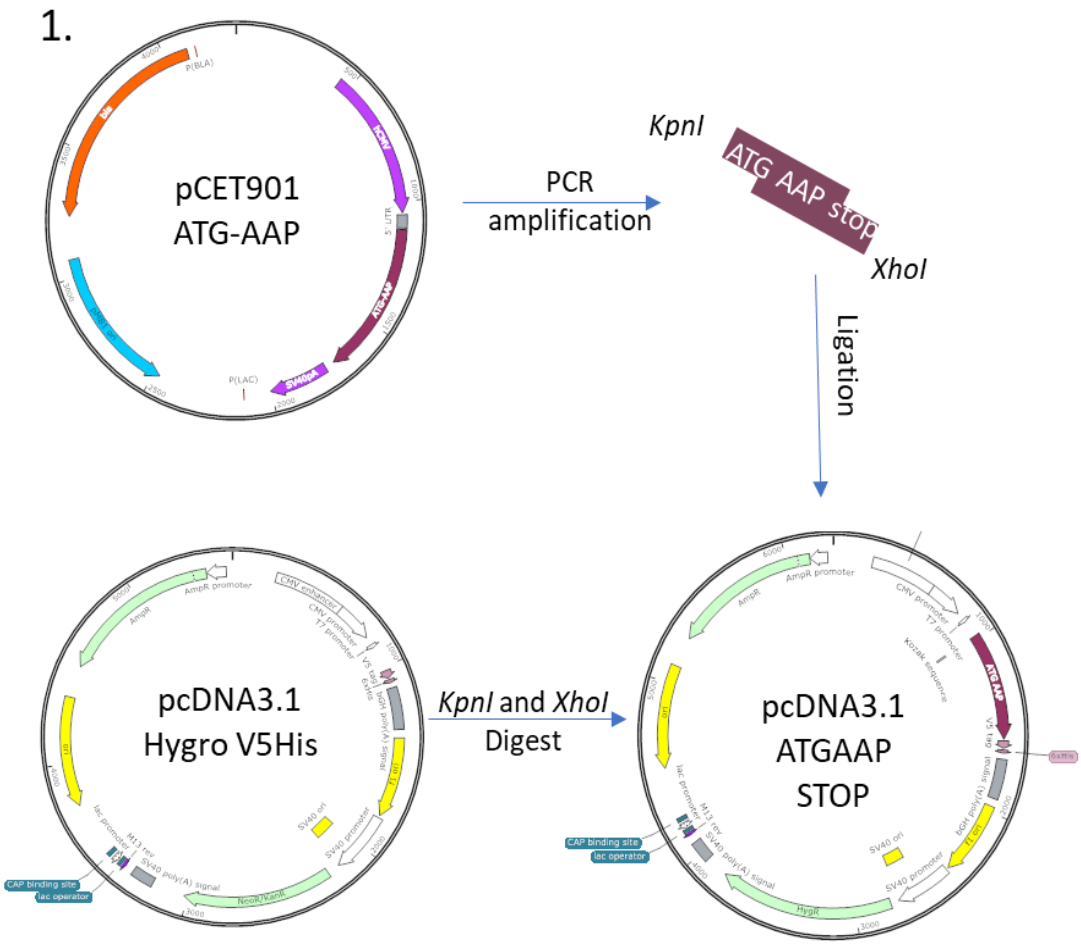

Figure 4.5 Schematic showing the construction of the ATG-AAP un-tagged vector (pcDNA3.1 ATG-AAP STOP). The *AAP* gene with the ATG was amplified out of the pCET901 ATG-AAP plasmid using the ATG-AAP STOP primers described in Methods Table 2.2-1. The PCR product and the pcDNA3.1 Hygro V5His backbone were digested with the restriction enzymes *KpnI* and *XhoI*. The ATG AAP STOP gene was ligated into the digested backbone to produce the plasmid pcDNA3.1 ATG-AAP STOP.

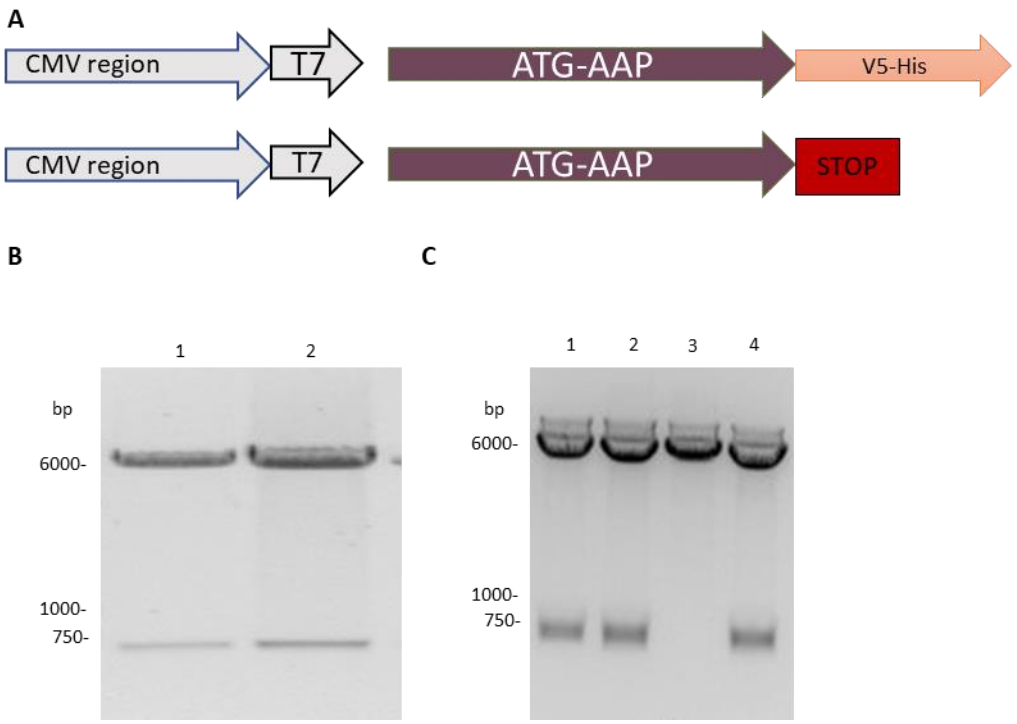

Figure 4.6 Generation of ATG-AAP vector constructs with and without a V5 tag. A) Schematic of the ATG-AAP vector constructs designed pcDNA3.1 ATGV5 (upper) and pcDNA3.1 ATG-AAP STOP (lower). **(B)** DNA agarose gel showing a test restriction digest of plasmid DNA pcDNA3.1 ATGV5 using the restriction enzymes *KpnI* and *XhoI*. Lanes 1 and 2 having bands representative of the predicted fragments 5599 bp and 669 bp. **(C)** DNA agarose gel showing a test restriction digest of plasmid DNA pcDNA3.1 CTG-AAP STOP using the restriction enzymes *KpnI* and *XhoI.* Lanes 1, 2 and 4 having bands representative of the predicted fragments 5599 bp and 672 bp.

4.3.2 Evaluation of Transient Expression of Exogenous AAP from the AAP Constructs

Prior to using the AAP constructs for the generation of the HEK293T cell pools stably expressing the various tagged and untagged versions of the *AAP* gene, it was necessary to ensure that the pcDNA3.1 CTGV5 plasmid and the pcDNA3.1 ATGV5 plasmid successfully produce the AAP proteins in a transient manner. Unfortunately, expression of AAP could not be determined directly due to the lack of any commercially available AAP antibody, meaning plasmids pcDNA3.1 CTG-AAP STOP and pcDNA3.1 ATG-AAP STOP could not be evaluated for AAP expression at the protein level.

The AAP-V5 tagged constructs were validated at the protein level via transient PEI transfections into HEK293T cells and subsequent western blot analysis of the cell lysates using an anti-V5 antibody. To achieve this, the HEK293T host cells were transfected with 200,000 copies/cell of the AAP-V5 plasmids (pcDNA3.1 CTG-AAP V5, pcDNA3.1 ATG-AAP V5, pcDNA3.1 CTG-AAP STOP or pcDNA3.1 ATG-AAP STOP) in duplicate with un-transfected cells as a control. Cell pellets were harvested and lysed 48 h post transfection as per Method Section 2.5 and AAPV5 expression was analysed by western blot as described in Methods Section 2.5.3 using a commercially available anti-V5 antibody.

In the samples transfected with the pcDNA3.1 CTGV5 and pcDNA3.1 ATG-AAP V5, bands were observed at approximately 25 kDa indicating the presence of a protein at the expected sized for the V5 AAP protein and confirming the V5 tag was expressing in frame with the AAP protein. As expected, there was no evidence of V5 expression in the HEK293T un-transfected control samples or the samples transfected with pcDNA3.1 CTG-AAP STOP and pcDNA3.1 ATG-AAP STOP (Fig. 4.7). Collectively, these data provide good evidence that the AAP-V5 constructs could be used to express exogenous AAP in HEK293T cells and were therefore suitable for use in establishing stably expressing HEK293T cell pools.

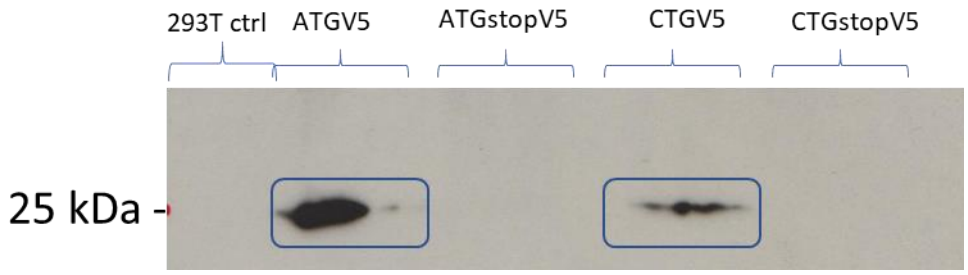

Figure 4.7 Validation of ATG-AAP and CTG-AAP vector constructs ability to express AAP-V5 tagged protein. Protein samples were harvested following the transient transfection of 200,000 copies/cell of each vector plasmid to be validated by western blot to test for the expression of the V5 tag. Samples positive for AAP tagged with V5 show a band at ~ 25 kDa. This confirms the expression of V5 in both the pcDNA3.1 ATGV5and the pcDNA3.1 CTG-AAP V5 plasmids.

4.3.3 Generation of HEK293T Cell Pools Stably Expressing the AAP Protein

In order to generate HEK293T cell pools stably expressing the AAP proteins (V5-tagged and untagged), it was necessary to transfect the cells with AAP-expressing plasmids containing the hygromycin selection marker. Hygromycin B was chosen as an appropriate selection marker for the generation of these AAP expressing cell pools, and based on the results described in Section 2.6.3, 250 μg/mL was chosen as an appropriate concentration of hygromycin B to use for the stable cell line generation.

Five sets of transfections were carried out using the PEI transfection method described in Methods section 2.2.4 using 100,000 copies of pcDNA3.1 Hygro V5His, pcDNA3.1 CTG-AAP V5, pcDNA3.1 ATG-AAP V5, pcDNA3.1 CTG-AAP STOP or pcDNA3.1 ATG-AAP STOP. The transfected cells were then incubated statically at 37°C, and 24 hours post transfection the selection agent Hygromycin B was added to the cells followed by further incubation and regular monitoring of the cells for presence of colonies. Colonies emerged from all transfections in the presence of hygromycin B. Once the cells had grown to a sufficient concentration (judged by visual appearance of colonies), they were moved from a static incubator to a shaking incubator (125 rpm) and an aliquot of cell culture was centrifuged and the pelleted cells were harvested to analyse for the presence of the AAP protein in frame with the V5 tag. The cell pellets were lysed and AAPV5 expression was analysed by western blot as described in Methods Section 2.5.3 using a commercially available anti-V5 antibody. The blot was also probed for the loading control tubulin. Following development for a 30 s exposure there was obvious evidence of V5 expression indicated by the presence of a band at approximately 25 kDa in the cell pool stably expressing ATGV5 as shown in Figure 4.8 A. A 10-minute exposure also revealed evidence of V5 expression indicated by the presence of a band at approximately 25 kDa in both the cell pool stably expressing ATGV5 and the cell pool stably expressing CTG-AAP V5, as shown in Figure 4.8 B. Meanwhile, there was no indication of V5 protein expression across the cell lysate samples from the HEK293T host cell line and the cell lines stably expressing the AAP-STOP proteins as expected and shown in Figure 4.8. Note that from this point on the cell lines are referred to as **CTG-V5** (pcDNA3.1 CTG-AAP V5), **ATGV5** (pcDNA3.1 ATG-AAP V5), **CTGSTOPV5** (pcDNA3.1 CTG-AAP STOP) and **ATGSTOPV5** (pcDNA3.1 ATG-AAP STOP).

Table 4.3.2 List of plasmids used to generate AAP expressing cell pools and corresponding cell pool.

Plasmid	Cell pool name
pcDNA3.1 CTG-AAP V5	CTGV5
pcDNA3.1 CTG-AAP STOP	CTGSTOPV5
pcDNA3.1 ATG-AAP V5	ATGV5
pcDNA3.1 ATG-AAP STOP	ATGSTOPV5

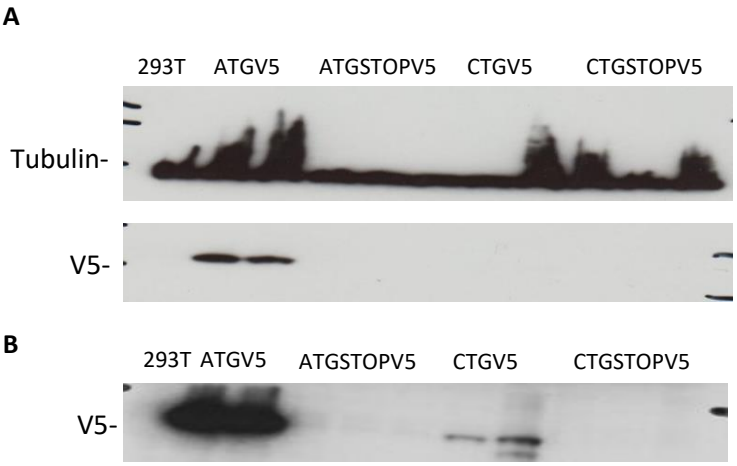

Figure 4.8 Analysis of the generation of ATG-AAP and CTG-AAP expressing HEK293T cell pools with and without a V5 tag. A) Western blot analysis following a short (30 s) exposure. The loading control alpha tubulin can be seen across the blot at ~55 kDa while the AAP-V5 expression can be seen at ~25 kDa. A total of 50 µg of cellular lysate was loaded on SDS-PAGE gels following sample preparation in a reducing buffer. A long (10 min) exposure **(B)** shows expression of both the ATG and the CTG versions of AAPV5.

4.4 Characterisation of AAP expressing HEK293T cell pools

4.4.1 Growth Profiles of HEK293T Cell Pools Stably Expressing AAP Cultured Under Batch Condition

In order to establish growth characteristics of the AAP engineered cell pools, cell pools stably expressing AAP (CTGV5, ATGV5, CTGSTOPV5 and ATGSTOPV5) were cultured under batch conditions in 250 mL Erlenmeyer flasks and incubated in a shaking incubator at 125 rpm at 37°C. The growth profiles of AAP expressing cell pools were characterised in biological triplicate and compared against the growth profile of the HEK293T host cell line.

Three biological repeats were run for all cell pools, with the mean culture viability and cell concentrations reported in Figure 4.9A and B, respectively. To ensure that any changes to growth profiles observed were due to the AAP protein and not the presence of the V5 tag,

the growth profile of the stop codon containing cell pools (CTGSTOPV5 and ATGSTOPV5) were also analysed. When compared with the growth profiles of the HEK293T cell line, the culture viability for the two CTG-AAP cell pools followed a similar trend to that of HEK293T cell line up until day 4. After this time-point, the profiles began to differ with the HEK293T culture viability dropping to 61.1% viable on day 5 while CTG V5 and CTGSTOPV5 pools remained higher at 93.5% and 86.1% viable, respectively. The culture viabilities of the CTG-AAP cell pools remained consistently higher than that of the HEK293T host cell line until day 10 where they were all reduced to a similar level of approximately 20%. In the cell pools expressing the CTG-AAP the decline phase was initiated later than that of the HEK293T cell line. Both the CTGV5 and CTG-AAP STOP cell pools followed a similar trend across the culture days indicating that the increased culture viability observed in figure 4.9 A is likely to be related to the presence of the exogenous AAP and not V5 tag.

The viable cell concentration (VCC) of the CTG-AAP cell pools were also compared to that of the HEK293T host cell line throughout the batch cultures. There were clear differences in the growth profiles observed. The HEK293T host cell line was seen to initially increase in viable cell numbers much more rapidly, reaching a viable cell concentration of 1.44 $x10^6$ viable cells/mL (vc/ml) on day 2 of culture, while the CTGV5 and CTG-AAP STOP reached a VCC of 0.6 $x10^6$ vc/mL and 0.36 $x10^6$ vc/mL, respectively. However, on day 3 the HEK293T cell line obtained a peak viable cell concentration of 2.02 $x10^6$ vc/mL and remained around this VCC until day 8 whereby the VCC dropped from 1.82 $x10^6$ vc/mL to 0.87 $x10^6$ vc/mL on day 9. The CTG-AAP cell pools reached higher VCCs than the HEK293T host, with the CTGV5 pools reaching a peak viable cell concentration of 3.21$x10^6$ vc/mL on day 5 and the CTG-AAP STOP pools reaching a peak viable cell concentration of 2.95 $x10^6$ vc/mL on day 6. As with the culture viability data, the CTG-AAP cell pools followed a similar trend indicating the V5 tag was not likely to be responsible for the increase in viable cell concentrations observed in figure 4.9 B.

As with the CTG-AAP expressing cell pools, the growth profiles of the ATG-AAP expressing cell pools were compared with the growth profiles of the HEK293T host cell line. The culture viability for both the ATG-AAP cell lines maintained a similar culture viability up until day 4 where they started to differ from the HEK293T culture viability profile, with the HEK293T cultures dropping to 61.1% viable on day 5 while the ATGV5 and ATG-AAP-STOP pools remained high at 92.7% and 93.0% viable, respectively. The culture viabilities of the ATG-AAP cell pools remained consistently higher than that of the HEK293T cell line until day 10 where they all decreased to a similar level of approximately 20%. As with the CTG-AAP expressing

pools, the ATG-AAP expressing pools appear to enter the decline phase later than that of the HEK293T cell line. Both the ATGV5 and ATG-AAP STOP pools followed a similar trend across the culture days indicating that the V5 tag is not likely to be responsible for the increased culture viability reported in figure 4.9 A.

The viable cell concentration (VCC) of the ATG-AAP cell pools were compared to that of the HEK293T cell line. Once again, as for the case of the CTG-AAP pools, there were differences in the profiles between the HEK293T and AAP engineered cell pools. The HEK293T cell line reached a viable cell concentration of 1.44 $x10^6$ viable cells/mL on day 2 of culture, while the ATGV5and ATG-AAP STOP reach a VCC of 0.68 $x10^6$ vc/mL and 0.81 $x10^6$ vc/mL, respectively on this day. However, as described in section 4.4.1, on day 3 the HEK293T cell line reached a peak viable cell concentration of 2.02 $x10^6$ vc/mL and remained around this VCC until day 8 where it dropped from 1.82 $x10^6$ vc/mL to 0.87 $x10^6$ vc/mL on day 9. On-the-other-hand, the ATG-AAP cell pools reached higher VCCs, with the ATGV5 pool reaching a peak viable cell concentration of 2.99$x10^6$ vc/mL on day 6 and ATG-AAP STOP reaching a peak viable cell concentration of 2.96 $x10^6$ vc/mL on day 5. As with the culture viability profiles, the ATG-AAP cell pools followed a similar trend indicating that the V5 tag is not likely to be responsible for the increase in viable cell concentrations reported in figure 4.9 B and is likely related to the presence of the exogenous AAP.

It was also important to analyse if there was a difference between the growth profiles of the CTG-AAP cell pools and the ATG-AAP expressing cell pools. Based on both the culture viability and viable cell concentration, as reported in figure 4.9, it appeared that all the AAP cell pools followed a similar growth profile during batch culture. This indicates that even low AAP expression levels, as observed in the CTG-AAP cell pools (Fig. 4.8 C), was sufficient to have a positive effect on the growth of the cells. The population doubling times (Fig. 4.9 C) of the HEK293T cell line was 21.73 h whereas the AAP expressing cell pools were doubling at a slightly slower rate than that of the HEK293T host cell line. The ATGV5 cell pool was doubling every 23.58 h, very similar to that of the ATGSTOPV5 cell pool which was doubling every 25.3 h. Meanwhile, the CTGV5 cell pool and CTGSTOPV5 cell pool have a population doubling time of 23.66 and 22.65 h, respectively. The similarity in the population doubling times of the AAP expressing cell pools would explain the similar growth profiles reported in figure 4.9 .

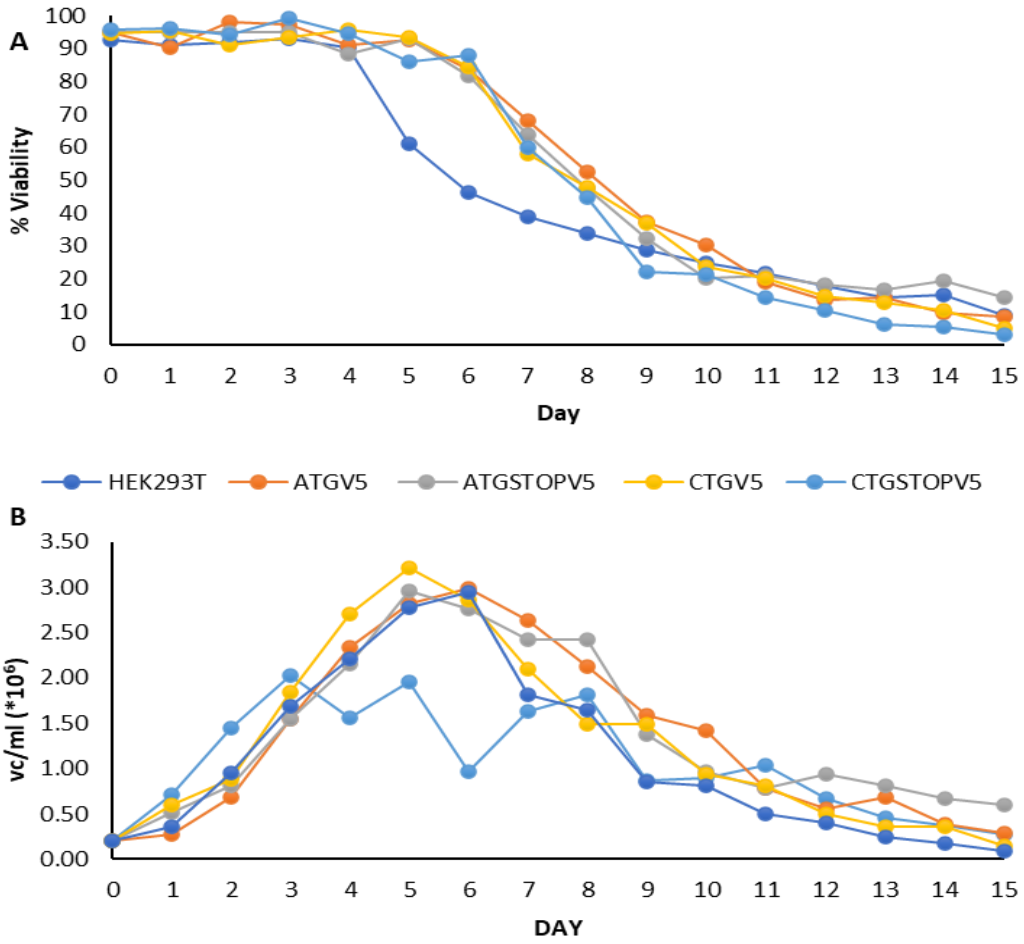

C

	HEK293T	ATGV5	ATGSTOPV5	CTGV5	CTGSTOPV5
Td (h)	21.73	23.58	25.30	23.66	22.65
Peak density (vc/ml) (x10⁶)	2.02	2.99	2.96	2.86	2.95

Figure 4.9 Viable cell concentration and culture viability of AAP expressing cell pools over a 15-day batch culture time course. A) Culture viability (% viable cells) of V5 tagged and untagged AAP expressing cell pool in comparison to the host HEK293T cell line. **(B)** Viable cell concentration of V5 tagged and untagged AAP expressing cell pools in comparison to the host HEK293T cell line. **(C)** Table showing the population doubling time (Td) in hours (h) of the host HEK293T cell line and the V5 tagged and untagged AAP cell pools (ATGV5, ATGSTOPV5, CTGV5 and CTGSTOPV5). The table also shows the peak cell densities (x10^6 vc/ml) achieved by the HEK293T cell line and AAP expressing cell pools. N=3

4.4.2 Analysis of AAP-V5 Expression in Stable Cell Pools via Western Blot Analysis

Over the batch culture growth curve described in section 4.4.1, cell pellets of 2x10^6 viable cells were harvested on culture days 3, 5 and 8 to determine if exogenous AAP expression fluctuated over time. The cell pellets from HEK293T, ATGV5 and CTGV5 cultures were lysed,

and the protein samples prepared as per Methods Section 2.5, respectively. Following development of the blot, there was clear evidence of V5 expression indicated by the presence of a band at approximately 25 kDa in the cell pool stably expressing ATGV5, as shown in Figure 4.10 A, B and C. Furthermore, the levels of AAP-V5 visually appeared to increase as the days of culture progressed when compared to the α-tubulin control (and assuming α -tubulin is constant across days). Meanwhile the CTGV5 samples did not have any detectable expression on day 3 (Fig 4.10), although protein was present on days 5 and 8 and the levels appeared visually to increase between days 5 and 8 (Fig 4.10) (assuming that tubulin levels remained consistent across the days with Tubulin amounts similar on days 5 and 8 although it is noted these are on different gels).

A 10-minute exposure also revealed evidence of V5 expression indicated by the presence of a band at approximately 25 kDa in both the cell pool stably expressing ATGV5 and the cell pool stably expressing CTG-AAP V5, as shown in Figure 4.10. As expected, there was no protein expression detected by the V5 antibody across the cell lysate samples from the HEK293T cell line as shown in Figure 4.10.

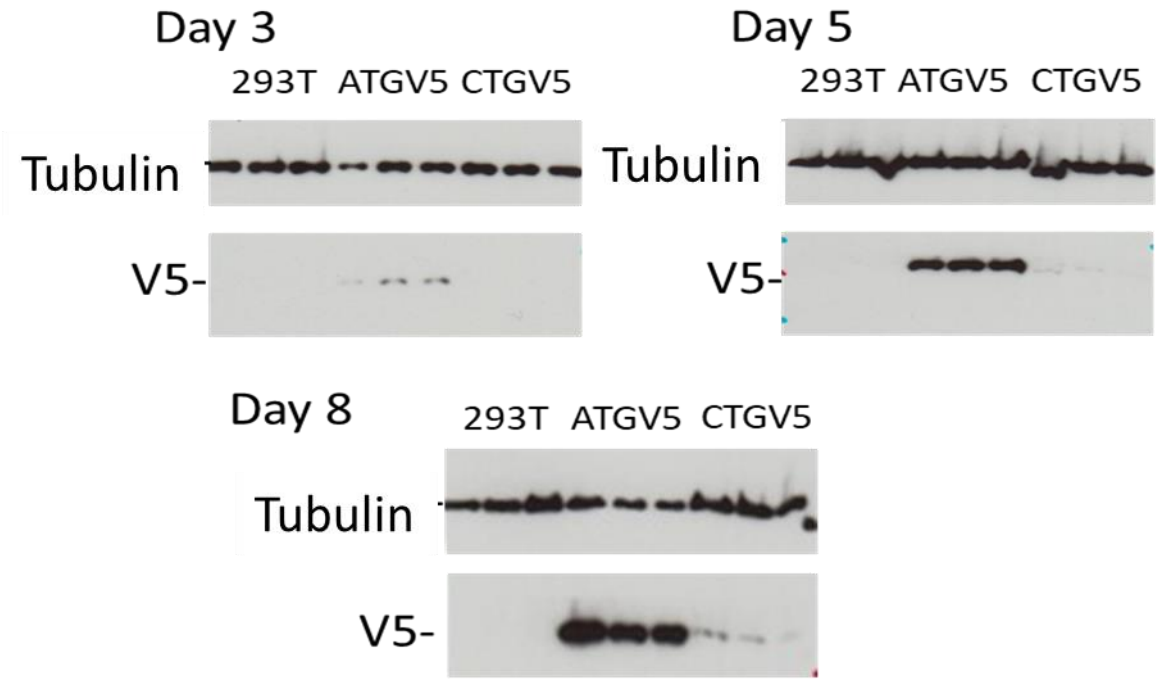

Figure 4.10 AAP-V5 expression analysis across different culture days by western blot. AAP expression was visualised using the anti-V5 antibody to detect the AAP expression in the ATG-AAP V5 cell pool (ATG V5) and the CTG-AAP V5 cell pool (CTG V5). The loading control alpha-tubulin can be seen across the blot at ~55 kDa while the AAP-V5 expression can be seen at ~25 kDa. Samples were harvested for protein analysis on days 3, 5 and 8 of batch culture.

4.4.3 Immunofluorescence analysis of AAP-V5 expressing cell pools

Immunofluorescence and confocal microscopy analysis was carried out as described in Methods sections 2.13 to analyse the localisation and compare the visual expression levels of the V5 tagged AAP proteins in the ATG-AAP V5 cell pool (ATG V5) to that of the CTG-AAP V5 cell pool (CTG V5). The nuclear stain DAPI was used to visualise the nucleus while the V5 primary antibody and the FITC labelled secondary antibody was used to visualise the V5 Tagged AAP. Since the HEK293T cell line does not have any V5 tagged proteins the lack of V5 fluorescence observed in Figure 4.11 A was expected. In Figure 4.11 B, there were what appears to be intense punctate spots of V5 protein aggregating in the nucleus/nucleolus of the cells. Furthermore, the number of these punctate V5 fluorescent spots varied in each of the cells imaged as would be expected for AAP engineered cell pools. As with the ATG V5 cell pool, V5 expression in the CTG V5 pool was also localised in the nucleus/nucleolus of the cells. However, in comparison to the ATG V5 cell pool, the CTG V5 cell pool had visually lower expression of the V5 tagged AAP with most cells showing only one punctate spot of AAP V5 expression and these were less intense than that of the ATGV5 expressing cell pool (Figure 4.11 C). Figure 4.11 B and C show a variety of V5 tagged AAP expression throughout the cell pools showing very heterogeneous expression between cells in the pools. This could lead to variability in any effect on cell growth or on AAV2 titre that might be observed as a result of AAP expression within a given cell.

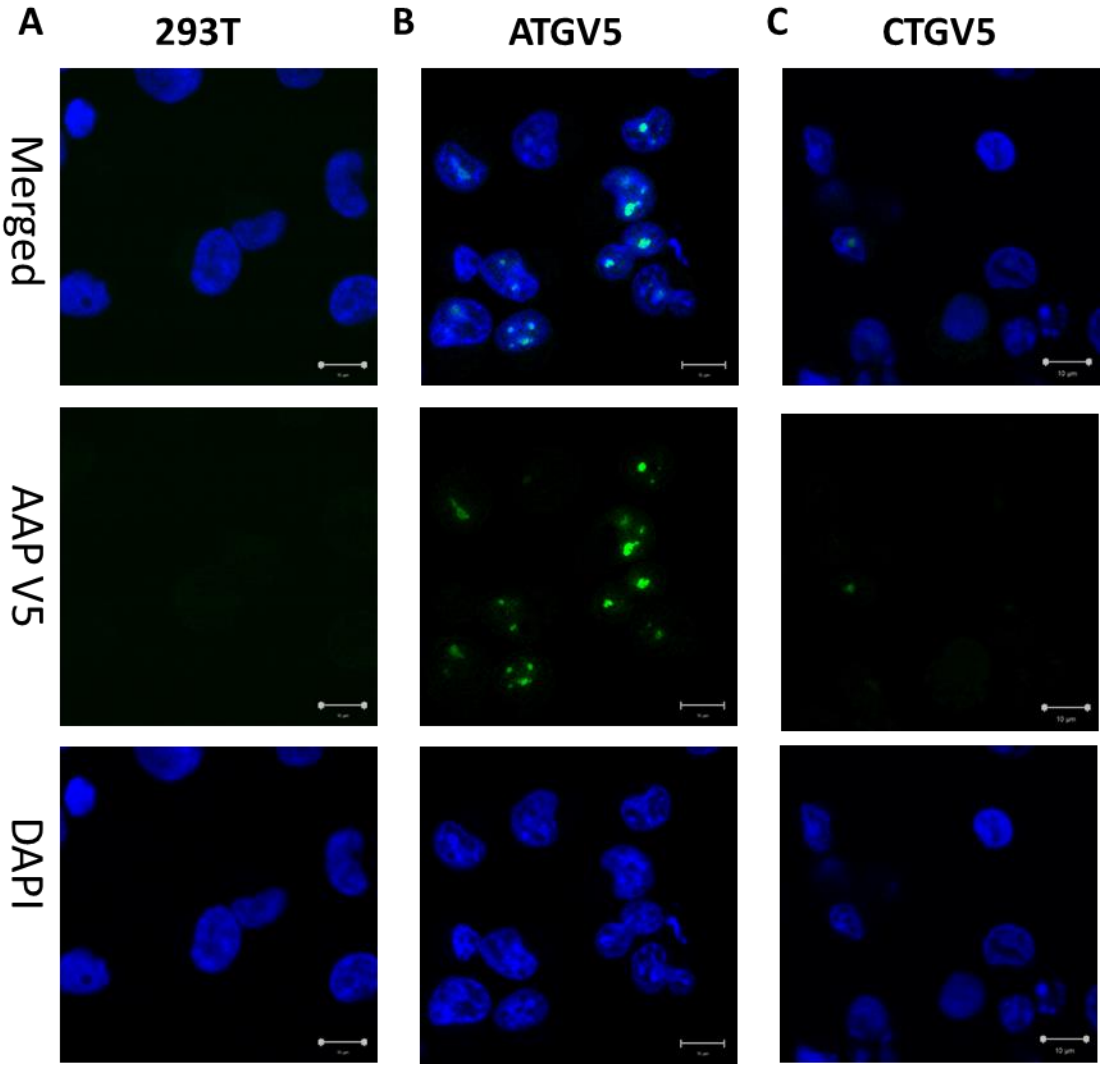

Figure 4.11 Immunofluorescence analysis of AAP-V5 expression and localisation in AAP V5 expressing cell pools as analysed by confocal microscopy. The nuclear stain DAPI was used to visualise the nucleus (Blue) while the V5 primary antibody and the FITC labelled secondary antibody was used to visualise the V5 Tagged AAP (Green). A) shows the merged, V5 tagged and DAPI stained cells for the HEK293T cell line, while B) shows the merged, V5 tagged and DAPI stained cells for the ATG-AAP expressing cell pools, and C) shows the merged, V5 tagged and DAPI stained cells for the CTG AAP expressing cell pool.

4.5 Assessing the Production of AAV2 in the HEK293T AAP Expressing Cell Pools

An initial rAAV2 production run was carried out in biological triplicate using the ATGV5 and CTGV5 cell pools, using the HEK293T suspension-adapted cell line as a control, to determine if there was any impact of stable AAP exogenous expression in the pools on subsequent AAV2 titre. rAAV2 vectors were produced as outlined in Methods section 2.4 by PEI co-transfection of three plasmids: pAAV-RC-Kan, pAAV-GFP-Kan and pHelper-Kan by transfection of 200,000 copies of each plasmid per cell. The viral particles were harvested 72 h post transfection using the Takara harvest method as described in Methods section 2.10.1 To determine total AAV2 particles present in the harvested samples, an ELISA was carried out using the commercially available Progen AAV2 titration ELISA kit as described in Methods Section 2.211. The error bars were determined based on the standard deviation of the triplicate results obtained. The number of particles released into the media was compared to those retained in the cells and the results from the ELISA assay are shown in Figure 4.12, capsid titre was determined based on the standard curve quantities. It was shown that the HEK293T cell line was producing an average $1.97x10^9$ total particles per mL of culture. The average viral particle yield for the ATGV5 expressing pool was $8.39x10^9$ total particles/mL in crude cell lysate although there was a large variation across the triplicate samples. Meanwhile, the CTGV5 cell pool achieved similar viral particle titres to that of the HEK293T cell line of $2.06x10^9$ total particles/mL. Error bars were generated as the standard deviation of each experimental repeat (n=3). There was variation in the data, most likely due to the pool nature

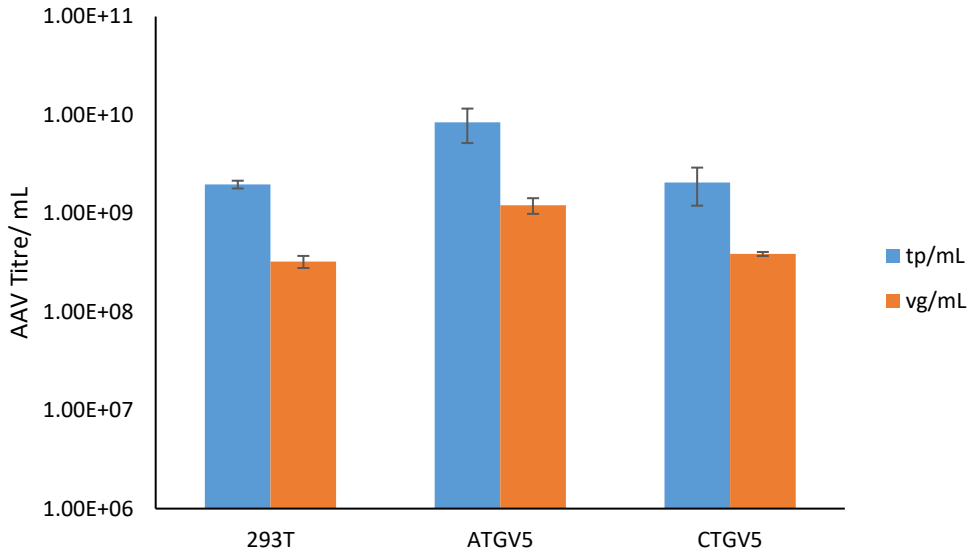

Figure 4.12 rAAV2 Titre Analysis 72 h post transfection. Total particle titre and genome titre per mL of transfected culture comparing titres from HEK293T cell line to the AAP expressing cell pools (ATGV5 and CTGV5). n=3

of the AAP expressing cell pools.

As described in results section 3.3.1, a model GFP transgene was utilised in the production of rAAV vectors. To determine the number of genome-containing particles harvested, a qPCR assay was carried out using the Takara AAVpro Titration kit (For Real Time PCR) as described in Methods Section 2.10. This assay targets the ITR regions of the genome which flank the GFP transgene. This involved the harvesting of samples, DNase treatment prior to lysis of capsids ensuring any residual plasmid material or non-packaged genome is degraded and that only encapsulated genome is measured. The viral genomes were extracted as described in methods section 2.10.2. Once the samples had been prepared for Real Time PCR a 96 well PCR plate was loaded as per methods section 2.10.3 and the plate was run using a BioRad thermocycler according to the protocol described in Methods Section 2.10.3. Technical triplicates of each sample were loaded into the qPCR plate. Error bars were determined from SD, n=3. The results obtained are shown in figure 4.12. Sample concentration was determined based on the standard curve quantities generated by serial dilution of the positive control supplied in the Takara kit. As shown in Figure 4.12, the ATGV5 cell pool had a higher proportion of genome packaged capsids, $1.21x10^9$ vg/mL, compared to that of the HEK293T cell line, $3.24x10^8$ vg/mL, and the CTGV5 cell pool, $3.87x10^8$ vg/mL. Through the analysis of both capsid and genome titre, it can be seen that the ATGV5 expressing cell pool appeared to have increased genome titre compared to the CTGV5 expressing cell pool. The CTGV5 expressing cell pool appeared to have little to no effect on capsid titre or genome titre with titres similar to that of the HEK293T host cell line observed.

4.6 Discussion

The aim of the work presented in this chapter was to generate AAP and AAP-V5 stably expressing HEK293T cell pools and characterise them for cell growth and ability to produce AAV2. AAP is a protein of interest in relation to the genome packaging efficiency during the capsid assembly as described in the introduction section of this chapter. In this chapter, the rAAV2 production of HEK293T cell pools stably expressing AAP from either the cryptic start codon CTG or the canonical start codon ATG was investigated. AAP cell pools were characterised for AAP-V5 expression and cell growth characteristics before determining their ability to produce rAAV2.GFP viral particles that were packaged with a model GFP genome.

To achieve this, vector constructs expressing the AAP protein either in frame, with a V5 tag or with a STOP codon preventing read through into the V5 tag were generated containing the mammalian selection marker for Hygromycin resistance to allow for the

selection/identification of the cells stably expressing AAP. As there are currently no commercially available antibodies for AAP, it was necessary to introduce a tag to AAP. The introduction of a tag to the Assembly Activating Protein to follow its expression is a common approach amongst AAP researchers, this circumvents the need for an antibody for AAP. Furthermore the tagging of AAP C-terminally suggests that this does not impact the biological function of AAP (Earley et al., 2017; Grosse et al., 2017; Maurer, Cepeda Diaz, & Vandenberghe, 2019).

Expression of the AAP from the plasmid vectors was initially studied by transient transfection into the HEK293T suspension adapted cell line. As seen in figure 4.8, there was V5 expression as shown by the presence of a band at approximately 25 kDa following western blot analysis in the samples where the AAP was in frame with the V5 tag (ATG V5 and CTG V5) and no expression when AAP contained a STOP codon (ATGSTOP and CTGSTOP) or in the HEK293T control samples. Based on these western blots, HEK293T cell pools stably expressing the different versions of AAP were established in the presence of Hygromycin B. As with the transient transfection analysis to test for expression, only the AAP-V5 cell pool and the CTG-V5 cell pool, show V5 expression as expected. However, the level of expression varied immensely between these two AAP cell pools with the ATG AAP-V5 expressing cell pools having much higher expression levels than that of the CTG AAP-V5 expressing cell pool. This is due to the difference in the efficiency of the start codons (Ivanov, Loughran, Sachs, & Atkins, 2010; Kearse & Wilusz, 2017). In a study by Ivanov *et al* (2010) it was shown that in HEK293T cell lines non-canonical start codons have varying initiation efficiencies in comparison to that of the conventional AUG start codon. They also showed that the CUG start codon was only a fifth as efficient as that of the conventional AUG start codon and the data here is in line with such observations. Furthermore, it has been shown that of the non-conventional start codons, the CUG start codon has a higher initiation efficiency than other non-convention start codons (Kearse & Wilusz, 2017). Based on these previous reports and the current study, the difference in the expression of AAP between the ATG and CTG cell pools is likely to be largely due to this difference in initiation efficiency (and the fact this is the only difference in these constructs). This gives a mechanism of 'titrating' or tuning protein expression simply by changing the start codon and may be important in the native virus where the AAP protein synthesis is initiated from a weaker CTG codon rather than a strong ATG codon.

Once the cell pools had been established, the batch culture growth profiles of these cell pools in comparison to that of the HEK293T control cell line were established to determine if AAP

expression impacted cell growth. As reported in Figure 4.9, the cell lines expressing AAP maintained a higher culture viability and correspondingly also reaching higher viable cell concentrations than those of the HEK293T cell line. Furthermore, the stably expressing AAP cell pools expressing the V5 tag exhibited a similar growth profile to those AAP pools generated where there was no V5 tag on the AAP protein. This indicates that the V5 tag has no detrimental/beneficial effects on the culture viability and viable cell concentration of these cell pools beyond that imparted as a result of expression of the AAP protein alone.

Along with analysing the growth profiles of the cell pools during batch culture, it was important to also assess expression of AAP in these pools across the culture. As shown in Figure 4.10, it appears that AAP expression increases over time, and again we observed that the CTG initiated constructs have lower expression levels than that of the ATG form. Based on the growth profiles though, the lower levels of AAP CTG expression seems to be sufficient to have a positive impact on the growth of the cells. However, the effects of AAP expression on cell growth was not investigated further.

Understanding localisation of the protein was also important as mis-localisation may impact/determine protein function (M. S. Scott, Calafell, Thomas, & Hallett, 2005). One of the best methods available to visualise protein localisation is confocal laser scanning microscopy. The benefit of this is that it allows for the observation of co-localisation of proteins (Miyashita, 2015). As shown in Figure 4.11, V5 tagged AAP was found to be localised to the nucleus. The localisation of AAP to the nucleus is consistent with findings reported in several studies. A study by Earley et al published in 2017, showed that FLAG-tagged AAP when transiently transfected into HeLa cells were found in the nucleus of the cell, this was the case in AAV serotypes 1-12 (Earley et al., 2017). A study by Gross et al published that same year demonstrated nuclear localisation of HA-tagged AAP in both HeLa and HEK293T cells via transient transfections (Grosse et al., 2017). The AAP-V5 protein appeared to be aggregating in a number of punctate spots inside the nucleus, this is clearly evident in Figure 4.11 B and to a lesser extent in Figure 4.11 C and is similar to what has been reported in other studies (Earley et al., 2015). The aggregation is not likely to be caused by the presence of the V5 tag as such spots of AAP localisation have also been reported in studies where the AAP protein was tagged with other tags including eGFP (Tse, Moller-Tank, Meganck, & Asokan, 2018), HA (Grosse et al., 2017) and FLAG (Earley et al., 2017). While the immunofluorescence work in this chapter only investigated the V5 tagged AAP expression with regard to nuclear localisation, the studies mentioned above looked at the localisation of the tagged AAP with the nucleus, but more specifically to the nucleolus. For example, the study by Earley *et al.*

(2015), used an anti-nucleostemin antibody to look at nucleolar localisation. Based on the results obtained in this chapter and work by others in this field, it is likely that the exogenous V5-tagged AAP is localising to the nucleolus. AAP nucleolar localisation corresponds to where AAV capsid morphogenesis occurs. AAP targets the VP proteins to the nucleolus, allowing for capsid assembly to occur here (Sonntag et al., 2010). Furthermore, as part of the ongoing characterisation of the AAP cell pools, the immunofluorescence work in this chapter also compared the AAP expression of the ATG start codon and the CTG start codon. As expected, the ATGV5 cells appeared to have more V5 tagged AAP expression than that of the CTGV5 cells, this difference in expression of AAP between the cell lines again being due to the different translation efficiencies of the start codons (Ivanov et al., 2010; Kearse & Wilusz, 2017).

Finally, it was important to study what effect, if any, AAP expression in the cell pools had on the actual production of rAAV2 total particles and viral genome packaging. As shown in Figure 4.12, the cell pools stably expressing ATG AAPV5 expression appeared to increase the total particles in comparison to that of the HEK293T control and that of the CTG AAPV5 expressing cell pool. The CTGV5 expressing cell pool produced approximately the same amount of total particles as that of the HEK293T cell line. Alongside particle expression, it was also important to investigate if the AAP expressing cell pools had an impact on genome packaging. We therefore compared the viral genome titre of the ATG-AAP and CTG-AAP (tagged and untagged) cell pools to that of the HEK293T control cell line. As shown in Figure 4.12, the ATG-AAP expressing cell pools had higher levels of genome as determined against a standard curve compared to those seen in the CTG-AAP cell pools and the HEK293T cell line.

As previously mentioned, the role of AAP is yet to be fully understood, but it is thought to be involved in the shuffling of the VP3 protein to the nucleolus. This role of APP was supported by findings reported by Earley *et al* (2015) who identified a nucleolar localisation signal at the C-terminus of AAP from serotype 2 (Earley et al., 2015). Another study by Naumer *et al* (2012) indicated that AAP2 can function as a scaffold nucleating capsid assembly, due to AAP's ability to induce a conformational change in VP3 (Naumer et al., 2012). Grosse *et al* (2017) published a study looking into the ability of AAP overexpression to impact AAV2 production in both mammalian cells and insect Sf9 cells. This study indicated that over expression of AAP2 is rate limiting to a point of saturation (Grosse et al., 2017). Nevertheless, the increase in the total particle titre observed in the ATGV5 cell pool here in HEK293T cells is different from that reported using baculovirus where AAP overexpression did not boost

AAV2 vector production (Grosse et al., 2017). While an increase in the particle and genome titre for the ATG-AAP-V5 pool on average was observed, there was also a wide range of variability based on the standard deviation of the titre. This variability could be caused by the variable nature of cell pools, these pools lacking clonality as seen in the immunofluorescence work in Figure 4.11 A, and there is a large variation in the AAP V5 expressed in individual cells within the cell pool with some cells containing much higher levels of AAP expression as visualised than others in the same pool.

One of the major factors associated with the work in this chapter was the levels of variability in AAP expression within the pools and subsequent impact on particle and genome titre. As previously mentioned, this variability was likely caused by the pool nature of the work, with every cell expressing differing AAP levels. The work described in this chapter suggests that the AAP expression in the ATGV5 cell pool had a positive impact on rAAV vector production and packaging. Therefore, this pool was selected for the work presented in Chapter 5 whereby clonal AAP-V5 expressing HEK293T cells were isolated and characterised from this ATGV5 pool.

Chapter 5

Generation and Characterisation of Clonal HEK293T Cells Stably Expressing Assembly Activating Protein (AAP) to Produce and Package Recombinant AAV2 Capsids

5.1 Introduction to the Work Described in this Chapter

Stable HEK293T AAP expressing cell pools were previously generated as described in Chapter 4. These pools were generated via antibiotic selection and will contain a mixed population of cells with a varying number of *AAP* copy numbers in different cells and AAP protein expression variable across individual cells. In stable mammalian cell lines such a mixed population of cells expressing different amounts of AAP can mean particular populations dominate and outgrow or perform other cells and populations making it difficult to determine the impact of AAP expression on AAV production. A polyclonal pool is also more likely to 'drift' or change over time than a monoclonal derived cell line meaning that the reproducibility from such a pool can also change over time. Furthermore, polyclonal pools cannot be reproduced, and each batch can differ. For this reason, researchers utilise monoclonal cell lines (Busby et al., 2016). Thus, single cell cloning of stable cell lines is often undertaken to overcome such variability issues that can arise from cell pools.

Single cell cloning gives rise to theoretically a homogenous population of cells derived from a single cell which reduces genetic instability and the heterogeneity within the cell population (Z.-G. Liu et al., 2018; Longo, Kavran, Kim, & Leahy, 2014). This approach has been used extensively for the identification of high recombinant protein producing mammalian cell lines for the production of biotherapeutics. Cell lines derived from a single cell are highly industrially relevant and a requirement of the regulators for the production of such biotherapeutics (Browne & Al-Rubeai, 2007). Single cell cloning can be carried out using a number of different methods, including limiting dilution, cloning rings, fluorescence activated cell sorting (FACS) and automated clone picking. Limiting dilution is one of the most commonly used methods being first described in 1955 (Puck & Marcus, 1955). Typically undertaken utilising micro-titre plates, a well containing a single cell is identified and the colony that grows from this is selected for further analysis (Browne & Al-Rubeai, 2007). Use of methods such as flow cytometry and cell sorting can be used to isolate a larger number of clones than possible with limiting dilution. The use of FACS is a widely established method of single cell cloning, it is a useful tool that results in the identification and purification of cell

populations to a high purity of 95-100%. Alongside the high degree of monoclonality this approach can deliver, it can be a useful method of single cell cloning when the cell populations express low levels of the identifying markers. Furthermore, FACS can be used to isolate cells based on granularity and size along with fluorescence. This method requires the use of fluorescently tagged monoclonal antibodies which will recognise surface markers on the desired cell line (Basu, Campbell, Dittel, & Ray, 2010). Cloning rings are a method of single cell cloning used if limiting dilution is not suitable. This method allows for the cloning process to be carried out at a higher cell concentration. Furthermore, cloning rings are a suitable method of single cell cloning for adherent cell lines. Cloning rings can often be ceramic or plastic hollow cylinders which surround single colonies, this isolates them from other cells in the cultures, unfortunately due to the nature of cloning rings they are a tedious time consuming method of single cell cloning (Mathupala & Sloan, 2009).

Once monoclonal cell lines were isolated, it was then sensible to assess the ability of these to produce genome packaged AAV, purify these and demonstrate their ability to transduce cells compared to the original HEK293T host cells. The upstream cell culture, transfection and harvest of the rAAVs was undertaken on the monoclonal cell lines as for the pools described in previous chapters. The downstream process, the purification of the rAAV, remains one of the most challenging aspects of rAAV production for gene therapy. There are a number of methods for the purification of AAV particles from cell culture. Adeno-Associated Virus serotypes 6, 7, 8 and 9 release their capsids into the supernatant, whereas the remainder of serotypes retain their capsids in the cell, this adds to the challenge, considerations and costs associated with the purification of AAV (W. Qu et al., 2015; Vandenberghe et al., 2010). A number of purification strategies utilise affinity chromatography, specifically AVB Sepharose which binds many serotypes of AAV making it a useful purification method over serotype specific methods (Nass et al., 2018b; O'Riordan, Lachapelle, Vincent, & Wadsworth, 2000; J. Zhou et al., 2011). AVB Sepharose is an affinity resin, this is a single chain antibody which has been conjugated to Sepharose beads. The AVB Sepharose beads have been shown to capture particles from AAV serotypes 1, 2, 3 and 5 and to capture baculovirus derived rAAV particles from serotypes 1-8, AAVrh.10 and 12. AAV binding affinity differs across the serotypes, due to a differing surface-exposed residue between the serotypes with high and low affinity for AVB Sepharose (Q. Wang et al., 2015).

The use of affinity chromatography is not without its disadvantages, it cannot distinguish between fully formed capsids and empty/incorrectly packaged capsids due to their identical amino acid structure. As previously discussed, serotypes such as AAV2 can contain

approximately 80% empty/incorrectly packaged particles (Nass et al., 2018b). In comparison to affinity binding chromatography, ion exchange chromatography has the capability to separate based on the charge difference between empty and full capsids (Dickerson et al., 2020; Nass et al., 2018b; G. Qu et al., 2007). Fully packaged particles have been successfully separated from empty rAAV particles using isocratic anion exchange chromatography by Dickerson and colleagues who have developed a method robust enough to suit production at a large scale. This approach utilises isocratic wash and elution steps. It utilises a combination of magnesium chloride and sodium chloride buffers during a gradient elution process. This isocratic method is advantageous to other more traditional methods due to its lower buffer consumption and smaller intermediate pool volumes. The method was able to give purity of 94% fully packaged rAAV at 9 mM $MgCl_2$, 50 mM NaCl, pH 9 (Dickerson et al., 2020).

5.2 Aims of the Chapter

The work presented in Chapter 4 developed and evaluated the potential of HEK293T cell pools engineered to stably express Assembly Activating Protein to produce AAV, comparing pools generated with a cryptic CTG start codon for AAP to those generated with an ATG start codon for AAP. Based on this work it was determined that the AAP expressing cell pools deriving from the ATG start codon construct showed the most potential for improving rAAV2 packaging compared to the original HEK293T cell host. The work in this chapter was focused on the generation of monoclonal HEK293T cell lines stably expressing AAP derived from the cell pools expressing AAP containing the ATG start codon and the subsequent evaluation of a number of AAP expressing monoclonal HEK293T cells in terms of the impact on recombinant AAV2 packaging efficiency. The work in this chapter also set out to investigate the transduction efficiency of the rAAV2 particles derived from the AAP expressing cell lines compared to both the original HEK293T host cell line and the ATGV5 cell pool from which they were derived.

The overall aims of the work described in this chapter were therefore to:

a. Generate monoclonal AAP expressing cell lines containing the ATG start codon via limiting dilution cloning.
b. Characterise the resulting AAP monoclonal cell lines specifically evaluating:
    I. Expression of C-terminally V5 tagged AAP in the clonal cell lines
    II. Growth characteristics of the monoclonal cell lines compared to that of the AAP pools and the HEK293T host cell line

c. Establish a rAAV2 production system using the monoclonal cell lines using commercially available qPCR and ELISA based assays to determine the effects of AAP overexpression on capsid formation and genome titre of the AAV2 expressing model transgene GFP.
d. Purify rAAV capsids derived from the generated AAP expressing monoclonal cell lines and pools, specifically investigating the ability of the rAAV2 particles to transduce HEK293T cells.

5.3 Generation and Characterisation of Recombinant HEK293T AAP Expressing Monoclonal Cell Lines via Limiting Dilution Cloning

5.3.1 Generation of Recombinant AAP Expressing HEK293T Monoclonal Cell Lines and Characterisation of their AAV-V5 Protein Expression

A selection of clonal cell lines were generated from the ATG-AAP V5 expressing cell pool generated in Chapter 4 by single cell cloning using limiting dilution as described in Methods section 2.7.1. Cloning was undertaken in Freestyle media with the addition of InstiGRO HEK supplement. Eight colonies grown from a single cell were identified (as determined by visual inspection under a microscope) and selected for further screening. These were termed **ATG06, ATG04, ATG02, ATG16, ATG36, ATG34, ATG33** and **ATG66** (for brevity also described as **A06, A04, A02, A16, A36, A34, A33** and **A66**, respectively)**.** These cell lines were then expanded, cell banks prepared and studied.

V5 tagged AAP expression was analysed via western blot. Cell pellets were harvested and lysed as per methods section 2.5 and probed using a commercially available V5 antibody and compared against that of the ATG-AAPV5 pool from which they originated **(ATGV5**), the ATG-AAPSTOP pool (**ATGSTOP**), and the original HEK293T control cell line (it is noted that the AAPSTOP and HEK293T control are negative controls with no V5-tagged protein expected to be present). As shown in figure 5.1 A, bands were observed in the ATG-AAPV5 pool and the ATG06, ATG04, ATG02, ATG16, ATG36, ATG34, ATG33, ATG66 samples at approximately 25 kDa, corresponding to the expected size for the V5 tagged AAP protein. As expected, neither the ATG-AAPSTOP pool nor the HEK293T control samples showed AAP-V5 tagged expression. The relative expression of AAP-V5 across all 11 cell pools and lines was determined by densitometry of the AAP-V5 band normalised to the tubulin loading control with all sample densitometries then shown relative to that observed in the ATGV5 pool sample. As shown in figure 5.1 A, there was varying AAP-V5 expression across the clones with the ATG66 clone appearing to have higher AAP-V5 expression than that of the original ATGV5 pool. Interestingly however, the other clones isolated tended to have a similar relative expression, to that observed in the original cell pool.

The expression of V5 tagged AAP was also investigated across different passages to study the stability of exogenous AAP-V5 expression over the time and passaging period experiments were generally undertaken. For this purpose, cell pellets from passage 6 and passage 17 were harvested and lysed and probed with the anti-V5 antibody. Once again, bands were observed in the ATG-AAPV5 pool and the ATG06, ATG04, ATG02, ATG16, ATG36, ATG34, ATG33, ATG66

clone samples at approximately 25 kDa (Figure 5.1 C). Densitometry was again undertaken on the bands and the expression relative to that of the ATGV5 cell pool determined. The pattern of V5 tagged AAP expression at passage 6 appeared different to that of the passage 17 samples. At the earlier passage both the ATG33 and ATG66 cell lines were expressing marginally more relative AAP-V5 than that in the ATGV5 pool whilst at the later passage the AATG33, ATG36 and AATG66 cell lines were all expressing approximately twice that of the ATGV5 pool. All the other cell lines expressed similar amounts of AAP-V5 relative to the ATGV5 pool at both passages (Figure 5.1 B and C).

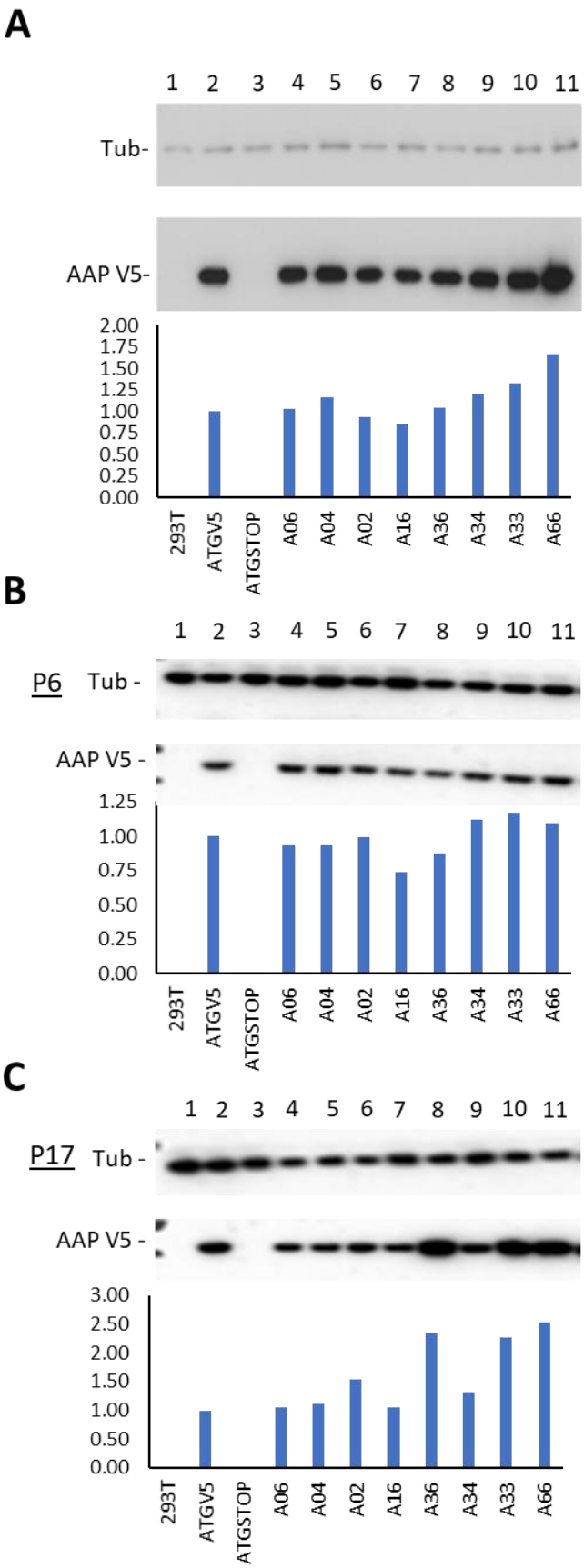

Figure 5.1 AAP-V5 expression of HEK293T cell lines stably expressing AAP-V5. (A) AAP-V5 expression was determined using an anti-V5 antibody to detect the AAPV5 expression in the ATGV5 cell pool in comparison to the cell lines stably expressing ATG-AAP-V5. The loading control alpha-tubulin can be seen at ~55 kDa with AAP-V5 expression visible at ~25 kDa. Densitometry analysis of the ATG-AAP-V5 expression levels relative to that of the ATGV5 cell pool. **(B and C)** AAP-v5 expression at passage 6 (B) and passage 17 (C). ATG-AAP V5 was visualised across the AAP-V5 stably expressing cell pools and clonal cell lines across two distinct passage days (P6 and P17) to determine if there were changes in expression over time. The graphs represent densitometry analysis of the ATG-AAP-V5 expression levels relative to that of the ATGV5 cell pool. 1= HEK293T, 2= ATGV5, 3= ATGSTOP, 4= ATG06, 5= ATG04, 6= ATG02, 7=ATG16, 8= ATG36, 9=ATG34, 10=ATG33 and 11= ATG66

5.3.2 Growth Characteristics of Clonal AAP-V5 Expressing Cell Lines Cultured Under Batch Culture Conditions

In order to establish the growth characteristics of the clonal AAP-V5 expressing cell lines in comparison to that of the HEK293T host cell line and ATGV5 and ATGSTOP cell pools, the clonal cell lines were cultured under batch conditions in 250 mL Erlenmeyer flasks as described in Methods Section 2.2.2. The growth profiles of the clonal cell lines were characterised in biological triplicate and compared against the HEK293T host cell line and the ATGV5 cell pool. The mean culture viability and cell concentrations reported in Figure 5.2 were generated from the biological triplicates. Figure 5.2 compares the growth profiles of the AAP expressing pools, ATGV5 and ATGSTOP to the HEK293T control cell line (Figure 5.2 A and D) and compares the AAP expressing clonal cell lines to the ATGV5 pool (Figure 5.2 B and D). The clonal cell lines all had a similar growth profile to that of the AAPV5 expressing cell pools. While the HEK293T host control cell line reached a higher viable cell concentration of 1.42 $x10^6$ viable cells (vc)/mL on day 2, the clonal cell line, ATG04, also reached a similar concentration to that of the HEK293T cell line on day 2. Both the HEK293T host cell line and ATGV5 pool attained their peak cell concentrations (Figure 5.2 A and B) on day 4, 2.65$x10^6$ vc/mL and 2.87$x10^6$ vc/mL respectively. The ATG36, ATG34, ATG33 and ATG66 cell lines attained their peak viable cell concentration on day 4 (2.84 $x10^6$ vc/mL, 2.29 $x10^6$ vc/mL, 2.16 $x10^6$ vc/mL and 2.24 $x10^6$ vc/mL respectively). The clonal cell lines ATG06, ATG04 and ATG02 reached their peak viable cell concentration on day 3 (2.30 $x10^6$ vc/mL, 2.49 $x10^6$ vc/mL and 2.90 $x10^6$ vc/ml). One clonal cell line, ATG16, did not attain its peak viable cell concentration until day 5, at this time reaching a concentration of 2.97$x10^6$ vc/mL, as displayed in Table 5.3-1 The viability of the HEK293T, ATGV5 and ATGSTOP pools all remained consistently high until day 3, after this point the culture viabilities dropped below 80% and rapidly declined to approximately 50% on day 5. All clonal cell lines remained at a high culture viability until the end of day 4, when the viability dropped below 80%.

The population doubling time was also determined based on the exponential growth phase of the cells. The majority of the clonal cell lines had a longer doubling time than the HEK293T control cell line and the ATGV5 pool which had a population doubling time of 21.26 h and 21.00 h respectively (Table 5.3-1). The clonal cell lines ATG16, ATG36, ATG34, ATG33 and ATG66 had population doubling times of 22.8 h, 21.59 h, 22.88 h, 22.15 h and 24.07 h respectively. However, the ATG06, ATG04 and ATG02 cell lines had a doubling time of 20.57 h, 19.75 h and 19.58 h respectively. However, based on statistical analysis via a one-way ANOVA there was no statistical significance between the AAP expressing cell lines and the

HEK293T control cell line nor between the AAP expressing clonal cell lines and the ATGV5 AAP expressing cell pool with regard to cell doubling times calculated.

Table 5.3-1 Population doubling time for AAP expressing cell lines compared to HEK293T control cell line.

	HEK293T	ATGV5	ATGSTOP	ATG06	ATG04	ATG02	ATG16	ATG36	ATG34	ATG33	ATG66
Td (h)	21.26	21.00	19.92	20.57	19.75	19.58	22.80	21.59	22.88	22.15	24.07
Td SD n=3	1.19	1.4	2.21	1.193	0.656	1.428	0.769	0.684	0.378	1.260	0.622
Peak viable cell concentration ($x10^6$)(vc/mL)	2.65	2.87	2.57	2.30	2.49	2.90	2.97	2.84	2.29	2.16	2.24
Peak viable cell concentration SD n=3	0.96	0.80	0.74	0.35	0.19	0.65	1.56	0.30	0.22	0.05	0.30

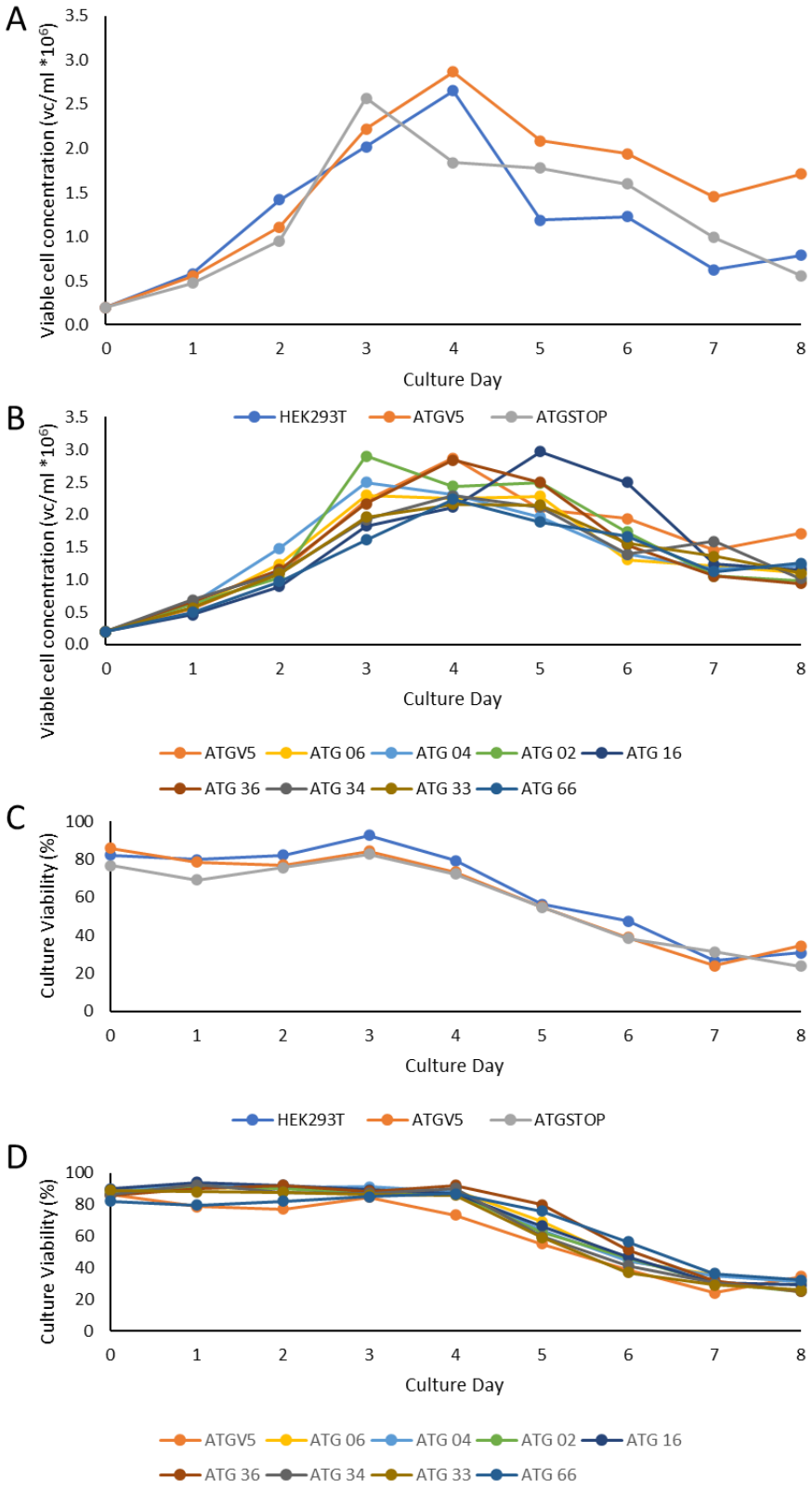

Figure 5.2 Viable cell concentration and culture viability profiles of AAP-V5 expressing clonal cell lines and control cell lines over an 8-day batch culture. (A) Viable cell concentration of V5 tagged AAP expressing cell pool in comparison to the host HEK293T cell line and the non-tagged ATGSTOP pool. **(B)** Viable cell concentration of the AAP expressing clonal cell lines in comparison to the ATGV5 cell pool **(C)** Culture viability of V5 tagged AAP expressing cell pool in comparison to the host HEK293T cell line and the non-tagged ATGSTOP pool. **(D)** Culture viability of the AAP expressing clonal cell lines in comparison to the ATGV5 cell pool. n=3

5.3.3 Production and Characterisation of Recombinant AAV2 in Clonal AAP Expressing Cell Lines

Following production of AAV2 in the monoclonal cell lines, the capsid and genome titres were determined as outlined in the methods section. An example of the titre data from a typical rAAV production undertaken in biological triplicate using the clonal and control cell lines is shown in Figure 5.3. The rAAV2 particles were harvested 72 h post transfection using the Takara harvest method as described in Methods Section 2.10.1. To determine the total AAV2 particles present in the harvested samples an ELISA assay was carried out using the commercially available Progen AAV2 titration ELISA kit as described in Methods Section 2.11. Error bars were determined based on the standard deviation of the triplicate cultures. The number of particles present per mL of crude cell lysate remained more-or-less consistent across the clonal cell lines and when compared to the HEK293T control cell line and the ATGV5 cell pool (Figure 5.3 A, blue bar). The average total particle yield ranged from $6.31x10^{10}$ total particles/mL (tp/mL) (ATG02) to $3.35x10^{10}$ tp/mL (ATG66) as seen in Table 5.4-1. Based on the total particle yields obtained a one-way ANOVA was carried out and using a post hoc Bonferroni test for multiple comparisons no statistical significance was shown when comparing all AAP expressing cell lines to that of the HEK293T control cell line. This suggests that engineering AAP expression does not influence the total number of particles that the cells can produce.

Table 5.4-1 Total particle yield for AAP expressing cell lines determined by ELISA.

Cell line	Total Particles (tp/mL)	Standard deviation (n=3)	Significance (One-way ANOVA)
HEK293T	$5.09x10^{10}$	$1.76x10^{10}$	
ATGV5	$5.18\ x10^{10}$	$1.81\ x10^{10}$	n.s.
ATG06	$3.49\ x10^{10}$	$2.30\ x10^{9}$	n.s.
ATG04	$3.58\ x10^{10}$	$8.86x10^{8}$	n.s.
ATG02	$6.31\ x10^{10}$	$6.10x10^{9}$	n.s.
ATG16	$3.37\ x10^{10}$	$2.07x10^{9}$	n.s.
ATG36	$3.50\ x10^{10}$	$1.61x10^{9}$	n.s.
ATG34	$6.28\ x10^{10}$	$6.38x10^{9}$	n.s.
ATG33	$3.49\ x10^{10}$	$2.03x10^{9}$	n.s.
ATG66	$3.35\ x10^{10}$	$1.77x10^{9}$	n.s.

A model GFP transgene was utilised in the production of recombinant AAV vectors. To determine the number of genome containing particles harvested (viral genomes, vg), qPCR assays were carried out using the Takara AAVpro Titration Kit (For Real Time PCR) as described in Methods Section 2.10. This assay targets the ITR regions of the genome which flank the GFP transgene. The average genome titre is shown alongside the capsid titre on figure 5.3 A (orange). The genome titre was determined based on serial dilution of a positive control. The average genome titre yield ranged between $3.05x10^{10}$ vg/mL (ATG66) of crude lysate to $1.35x10^{9}$ vg/mL (ATG34), as seen in Table 5.4-2. Based on statistical analysis of viral genome yields using a one-way ANOVA there was shown to be statistical differences across the means (*p* value= 0.01). Following a Bonferroni multiple comparisons post hoc test, it was determined that there was a significant difference between the ATG66 cell line when compared to that of the HEK293T host cell line (*p* values of 0.04, Table 5.4-2).

Table 5.4.2 Viral genome titre for AAP expressing cell lines.

Cell Line	Viral genome titre (vg/mL)	Standard Deviation (n=3)	Significance (One way ANOVA)
HEK293T	$6.10x10^9$	$5.90x10^9$	
ATGV5	$5.49x10^9$	$3.94 x10^9$	n.s.
ATG06	$8.66x10^9$	$7.10x10^9$	n.s.
ATG04	$7.74x10^9$	$4.39 x10^9$	n.s.
ATG02	$3.76x10^9$	$8.43 x10^8$	n.s.
ATG16	$6.86x10^9$	$5.27 x10^9$	n.s.
ATG36	$7.85x10^9$	$5.29 x10^8$	n.s.
ATG34	$1.35x10^9$	$1.00 x10^9$	n.s.
ATG33	$2.61x10^{10}$	$1.59 x10^{10}$	n.s.
ATG66	$3.05x10^{10}$	$1.77 x10^{10}$	* p= 0.04

As one of the major issues with manufacturing rAAV vectors is generating high yields of correctly packaged transgene into capsid particles, the percentage of packaged capsids was calculated based on the AAV titre analysis presented in Figure 5.3A. As shown in Figure 5.3B, the packaging efficiency varied greatly between the clonal cell lines and the HEK293T control cell line. The clonal cells ranged between 2.28% packaged particles (ATG34) and 91.07% packaged particles (ATG66), as shown in Table 5.4-3. There was variation between replicates, particularly for the higher packaging cell lines. Following statistical analysis via one-way ANOVA it was determined that there were significant differences across the mean percentage packaging (p value = 0.003). Following a Bonferroni's multiple comparison post hoc test, it was shown that there were significant differences in the percentage packaged by the AAP expressing clonal cell lines ATG33 and ATG66 compared to the HEK293T control cell line (p values of 0.014 and 0.008, respectively).

Table 5.4-3 Percentage of packaged particles for AAP expressing cell lines.

Cell Line	Percentage Packaged (%)	Standard Deviation (n=3)	Significance One way ANOVA
HEK293T	12.20	11.03	n.s.
ATGV5	10.68	7.50	n.s.
ATG06	24.07	19.19	n.s.
ATG04	21.97	13.01	n.s.
ATG02	5.90	0.87	n.s.
ATG16	19.87	14.43	n.s.
ATG36	22.26	1.17	n.s.
ATG34	2.28	1.85	n.s.
ATG33	86.36	50.82	p = 0.014 *
ATG66	91.07	54.98	p = 0.008 **

While the data presented in Figure 5.3A and B give a representative example of the data obtained from one production run, the data generated across three independent production runs (each run in biological triplicate giving 9 individual runs in total) throughout this work is presented in figure 5.3C and 5.3D. In order to compare the data across multiple production runs, the data was normalised to the HEK293T control cell line in each production run. As shown in figure 5.3C, the capsid titres (blue) across all production runs did not vary greatly from the HEK293T cell line capsid titres, in line with that shown in figure 5.3 A. The genome titres across all production runs normalised to HEK293T (Figure 5.3B orange) showed specific clonal cell lines tended to give a higher genome titre than that of the HEK293T control cell line. As shown in figure 5.3C, the ATG04 cell line across multiple production runs produced almost five times the genome titre of that of the HEK292T cell line. The clonal cell lines ATG06, ATG02, ATG16, ATG33 and ATG66 produced between 2 - 2.5 times the genome of the HEK293T. As across the production runs the data indicated that there were more transgenes made with better packaging efficiency from the clonal cell lines ATG04, ATG33 and ATG66, these clones were selected for further research (Figure 5.3 and 5.4).

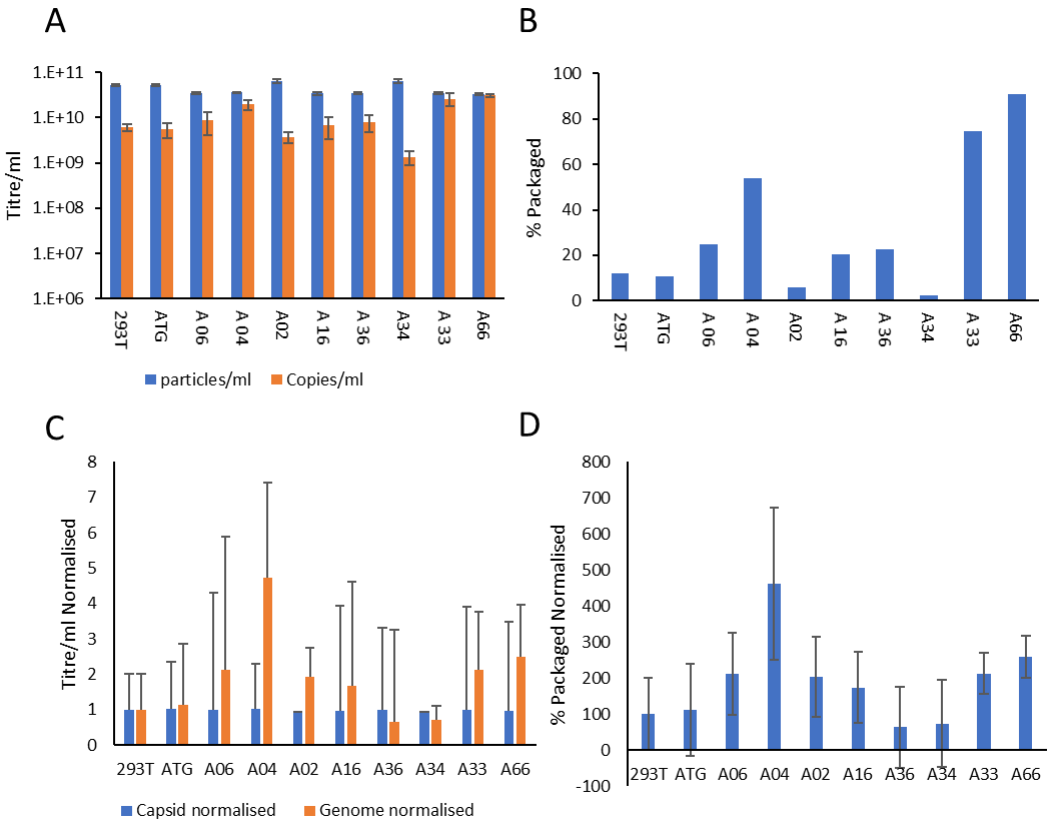

Figure 5.3 rAAV2 capsid and genome titre analysis from HEK293T and AAP engineered cell pools and lines. (A) An example of a typical rAAV2 production run using the HEK293T host cell line, the ATGV5 cell pool and the AAPV5 expressing cell lines A06, A04, A02, A16, A36, A34, A33 and A66 reporting total particles (tp) titre (tp/mL) (Blue) and viral genome (vg) titre (vg/mL) (Orange). The A66 cell line has a significant p value of p=0.035(*) based on Bonferroni's multiple comparisons test. Error bars = SD, n=3 **(B)** Percentage of particles packaged with genome across the cell lines and pools in A. Based on the post hoc Bonferroni's multiple comparisons test the % packaged particles generated in cell lines A33 and A66 are significant compared to the HEK293T control cell line with p values of p=0.014 (*) and p=0.008 (**), respectively. Error bars = SD, n=3 **(C)** rAAV titre data from 3 production runs normalised to the HEK293T host cell line. **(D)** Percentage of packaged capsids from 3 production runs normalised to the HEK293T cell line.

Finally, the relative expression of exogenous AAP-V5 present in the clonal cell lines was compared to that of the ATGV5 cell pool as indicated in Figure 5.4 A and B. Figure 5.4 A shows the relative V5 tagged AAP expression across the AAP expressing cell lines and pools. Expression above the line indicates AAP levels higher than that of the ATGV5 cell pool. As in Figure 5.1, all clonal cell lines had AAP expression levels similar to, or above that, of the ATGV5 pool. Figure 5.4 B shows the percentage of genome-packaged capsids as normalised to the HEK293T host cell line. These data show that while all higher packaging cell lines had AAP expression above that of the ATGV5 pool, the packaging wasn't solely based on the

exogenous AAP-V5 expression. For example, clones ATG04 and ATG16 have similar AAP-V5 expression (Figure 5.4 A) however the packaging efficiency varied greatly across these cell lines, suggesting that cell line specific constraints also determine packaging efficiency. Similarly, relatively high AAP-V5 expression in the ATG36, ATG33 and ATG66, was observed, however compared to ATG33 and ATG66 the clonal cell line ATG36 produced a low proportion of packaged capsids.

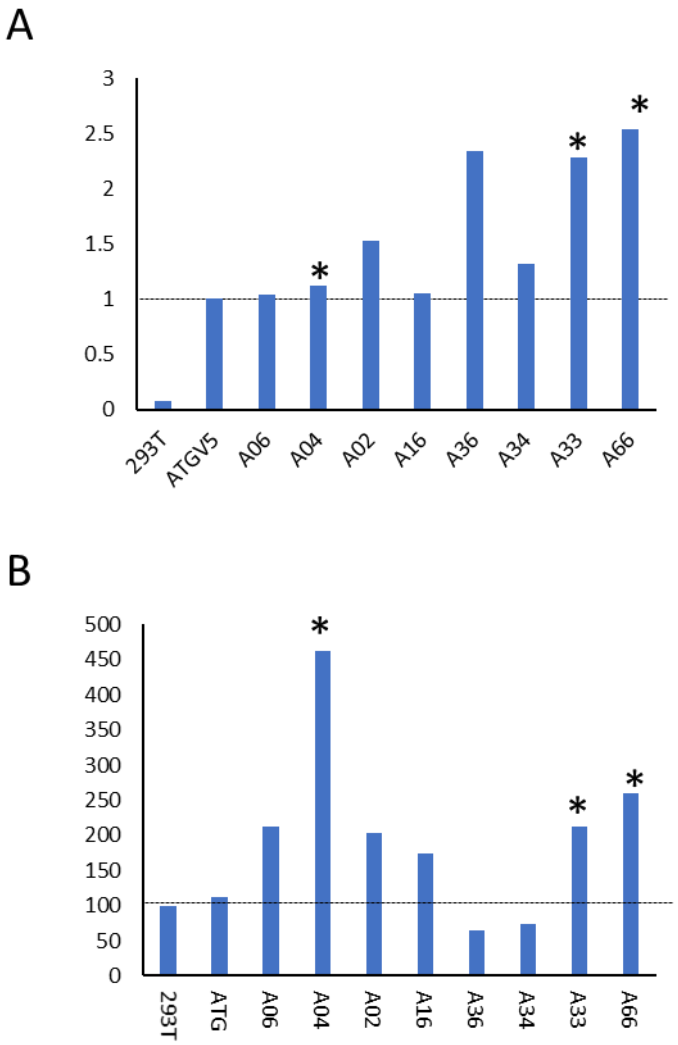

Figure 5.4 AAP-V5 expression analysis of HEK293T cell lines stably expressing AAP-V5 compared to the % of genome packaged capsids. (A) AAP-V5 expression in HEK293T and HEK293T cell lines stably expressing AAP-V5 (Figure 5.1). ATG-AAP V5 was determined by western blotting across the AAP stably expressing cell pools at P17 **(B)** % Packaged capsids normalised to capsids generated in the HEK293T host cell line. Cell lines selected for further work are annotated with an *.

5.3.4 Immunofluorescence Analysis of Selected AAP-V5 Expressing Clonal Cell Lines

Immunofluorescence confocal microscopy was carried out as described in Methods Section 2.13 to analyse the localisation of, and compare the visual expression levels of, the V5 tagged AAP proteins in the clonal cell lines ATG04, ATG33 and ATG66. The nuclear stain DAPI was used to visualise the nucleus while the V5 primary antibody and the FITC labelled secondary antibody was used to visualise the V5 tagged AAP. Figure 5.5 reports the expression of AAP-V5 in the three key clonal cell lines selected for further investigation. As with the work reported in Chapter 4, the localisation of the V5-AAP was in the nucleus as determined by co-localisation with DAPI. The AAP-V5 expression appeared consistent between each cell in each clonal cell line providing evidence of the clonality of these cell lines.

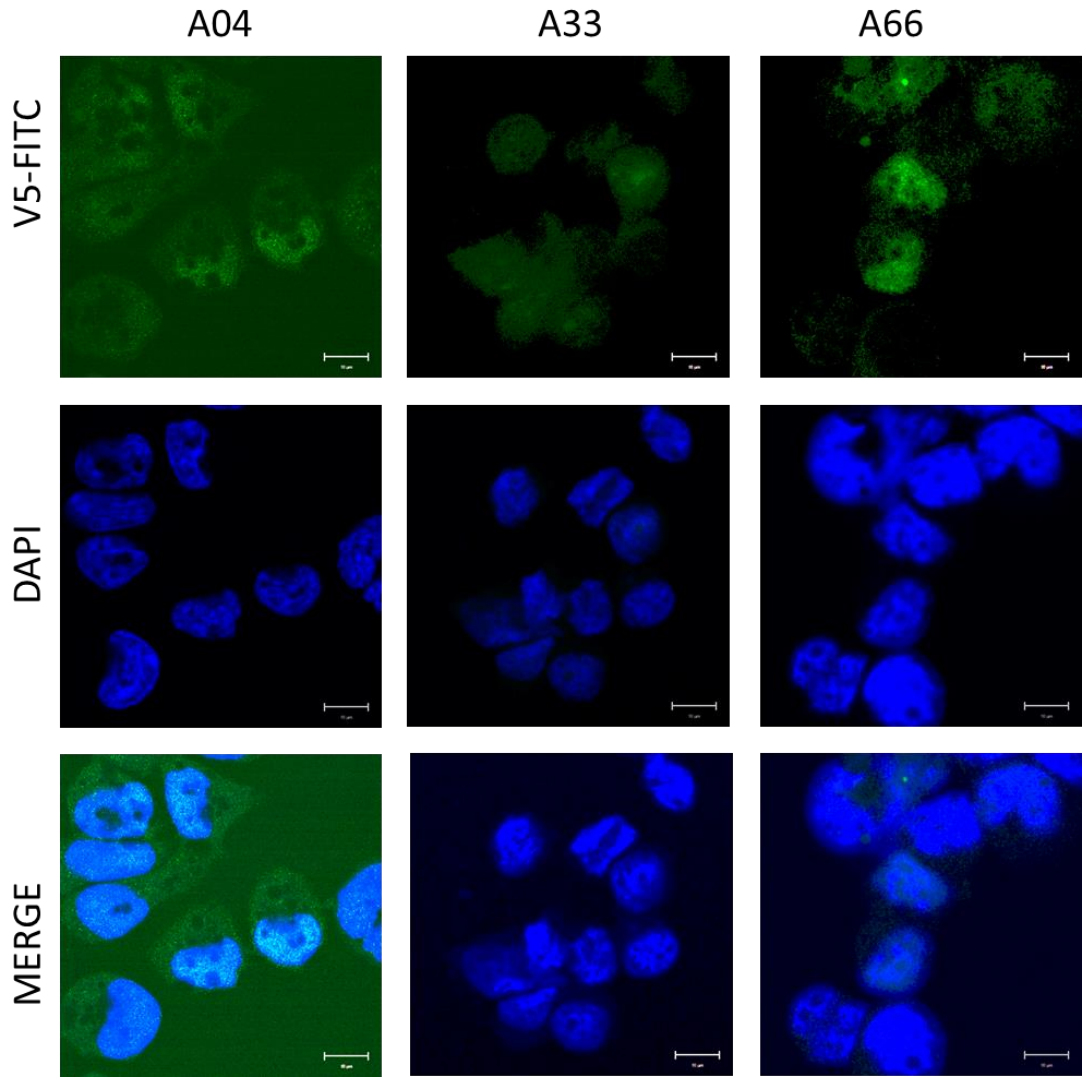

Figure 5.5 Immunofluorescence analysis of AAP-V5 expression and localisation in AAP V5 expressing clonal cell lines ATG04, ATG33 and ATG66 as analysed by confocal microscopy. The nuclear stain DAPI was used to visualise the nucleus (Blue) while the V5 primary antibody and the FITC labelled secondary antibody was used to visualise the V5 Tagged AAP (Green) across the ATG04, ATG33 and ATG66 clonal cell lines. Scale bar = 10 µm

5.4 Assessing and comparing the functionality of recombinant AAV2 derived from selected AAP-V5 expressing cell pools and clonal cell lines

5.4.1 Production of rAAV Capsids in Key AAP Expressing Clonal Cell Lines

To follow on from the work described in Section 5.3, further rAAV production runs were carried out in biological triplicate using the clonal cell lines ATG04, ATG33 and ATG66, and the total particle and genome titre compared to the HEK293T control cell line and the ATGV5 cell pool. As with the results shown in figure 5.6 and Table 5.6 the total particle titre ranged from $3.3x10^{10}$ tp/mL to $3.58x10^{10}$ tp/mL of crude lysate sample for this production run (Figure 5.6 A blue). Based on one-way ANOVA statistical analysis with a Bonferroni post hoc test there was no significant differences seen across the cell lines.

Table 5.6-1 Particle and genome titre comparing the AAP expressing cell lines and pool to the HEK293T host cell line.

Cell line	Total particles titre (tp/mL) +/-SD n=3	Viral genome (vg) titre (vg/mL) +/-SD n=3	tp p-values	vg p-values
HEK293T	$3.50x10^{10}$ +/- $6.99x10^{8}$	$6.10x10^{9}$ +/- $1.21x10^{9}$		
ATGV5	$3.57x10^{10}$ +/- $9.34x10^{8}$	$5.46x10^{9}$ +/- $2.07x10^{9}$	n.s.	n.s.
ATG04	$3.58x10^{10}$ +/- $8.86x10^{8}$	$1.94x10^{10}$ +/- $4.46x10^{9}$	n.s.	*** *P*= 0.0003
ATG33	$3.49x10^{10}$ +/- $2.03x10^{9}$	$2.61x10^{10}$ +/- $2.03x10^{9}$	n.s.	**** *P*= < 0.0001
ATG66	$3.35x10^{10}$ +/- $1.77x10^{9}$	$6.10x10^{10}$ +/- $1.79x10^{9}$	n.s.	**** *P*= < 0.0001

Figure 5.6 A (orange) reports the average viral genome titre from the biological triplicate cultures across the cell lines, ranging from $3.05x10^{10}$ vg/mL to $5.49x10^{9}$ vg/mL. The HEK293T control cell line gave an average of $6.10x10^{9}$ vg/mL and the ATGV5 cell pool gave an average of $5.49x10^{9}$ vg/mL. Meanwhile the clonal cell lines, ATG04, ATG33 and ATG66 gave $1.94x10^{10}$ vg/mL, $2.61x10^{10}$ vg/mL and $6.10x10^{10}$ vg/mL, respectively (Table 5.6-1). Following a one-way ANOVA, it was determined that there was statistically significant differences across the mean viral genomes (p value <0.0001). Using the Bonferroni multiple comparison post hoc test it

was determined that the viral genome titres from the AAP expressing clonal cell lines, ATG04, ATG33 and ATG66 were all statistically significant compared to the HEK293T control cell line with p values of 0.0003, <0.0001 and <0.0001, respectively (Table 5.6-1). Figure 5.6 B shows the genome packaging of the capsids generated. The HEK293T host cell line had an average of 17.43% packaging while the ATGV5 cell pool had an average of 15.39% packaged capsids. The AAP expressing clonal cell lines ATG04, ATG33 and ATG66 had 54.03%, 74.64% and 90.91% respectively. This data further shows that while the number of capsid particles generated was more-or-less the same across cell lines, the packaging efficiency varies across the cell lines and was increased in the monoclonal AAP expressing cells.

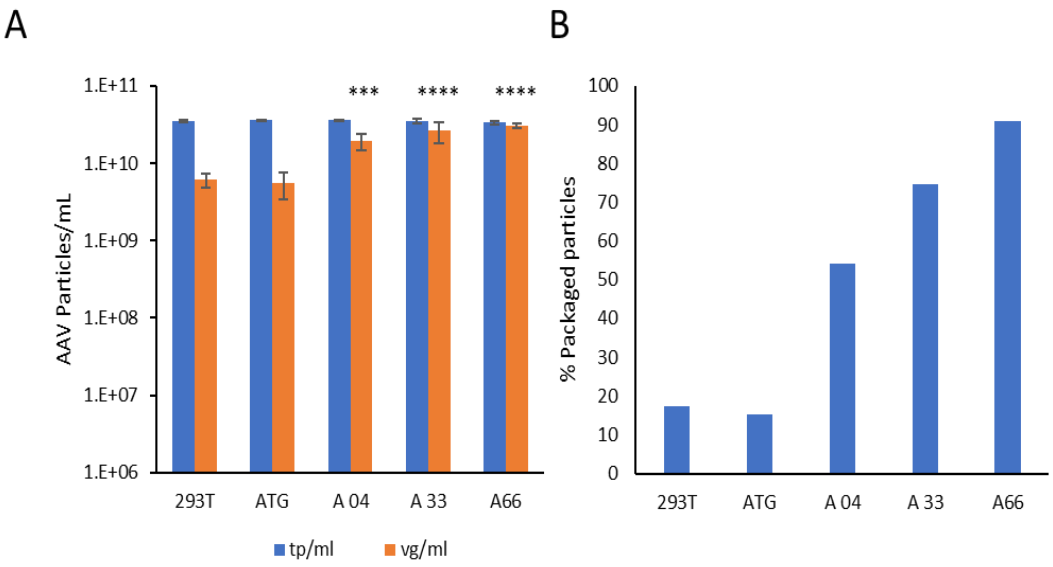

Figure 5.6 rAAV2 titre analysis from selected HEK293T cell lines. (A) An example of a rAAV2 production run using the HEK293T host cell line, the ATGV5 cell pool and the AAP expressing cell lines A04, A33 and A66, looking at both the capsid titre (Blue) and the genome titre (Orange). (B) Percentage of capsids packaged across the cell lines and pools in A. Error bars =SD where n=3, statistical analysis one-way ANOVA where *** = P value =0.0003 and **** = p value <0.0001 based on Bonferroni post hoc test.

5.4.2 Purification of rAAV Generated in Different HEK293T Cell Lines

Next the rAAV generated from the different cell lines developed during this study were purified so that the functionality of these could be investigated. For this purpose, a larger scale production run was initially carried out using the HEK293T cell line. This involved five CellBIND T25 flasks per cell line each transfected with 200,000 copies/cell of the pHelper-Kan, the pAAV-GFP-Kan and pAAV-RC-Kan plasmids. 72-hour post transfection the five cultures were combined to give a total culture volume 5x that of other production runs described in Chapters 3, 4 and 5. The rAAV capsid particles and genome upon harvest was determined to compare the pre- and post- purification genome titres of the larger scale HEK293T production run. Based on this larger scale production run (Figure 5.7) a total genome titre of $8.03x10^9$ vg/mL was measured from the crude lysate. Using the Takara AAVpro Purification kit, the capsids present in the crude lysate were purified and the genome titre calculated by qPCR. An average genome titre of $3.37x10^9$ vg/mL in the purified samples was observed.

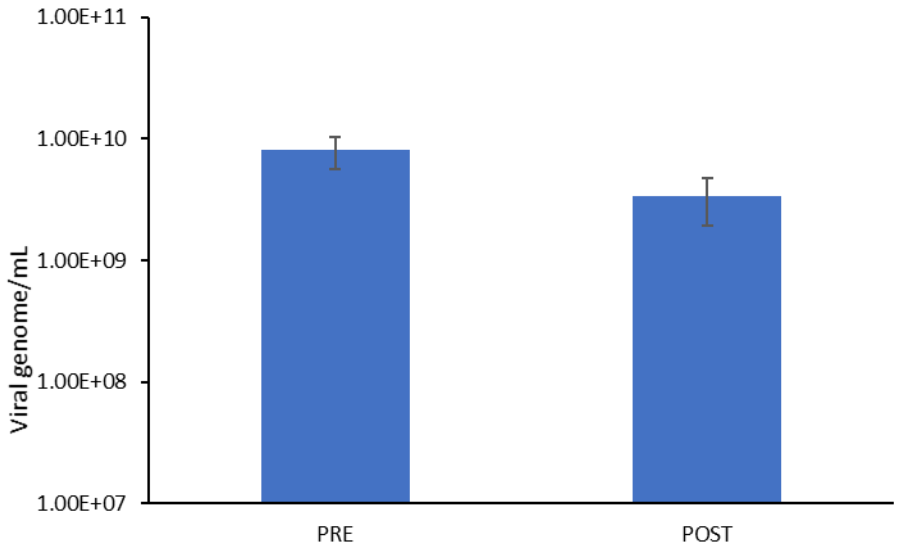

Figure 5.7 Comparison of HEK293T derived rAAV genome titres pre- and post-purification. Genome titre per mL of transfected culture was determined from samples both pre-purification and post purification. Error bars show standard deviation (n = 3).

5.4.3 Imaging of Purified rAAV2 Capsids by Electron Microscopy (EM)

In order to further characterise the purified rAAV2 capsids these were imaged by electron microscopy. Purified particles were negatively stained and imaged on an electron microscope as described in Methods Section 2.15. A representative selection of purified rAAV particles images are shown in figure 5.11. All images obtained from the different host

cell lines (HEK293T, ATGV5, ATG04, ATG33 and ATG66) showed hexagonal type structures indicative of purified rAAV of 20-25 nm in diameter. Black arrows indicate examples of these hexagonal structures. Many of these structures had electron density in the centre of the structures observed as dark areas inside the capsids, most likely "empty" or partially packaged capsids. On all images there were also smaller hexagonal structures measuring 10-12 nm in size as indicated by a Blue arrow (Figure 5.8), however these were not examined further but could be indicative of small VP3 only or contaminating ferritin particles based on other published work. A rAAV2 production run was carried out with HEK293T cell line, whereby the transgene was not co transfected. This was to allow the visualisation of purified "Empty" rAAV2 particles by way of electron microscopy. Imaging empty particles allows for the comparison of packaged particles to empty particles and can be used as a method of quantifying empty particles. As seen in Appendix Figure XVI, the rAAV2 particles that do not contain the GFP transgene have a dark electron dense core. Where the transgene plasmid has been co transfected we can see particles with both the electron dense core and with a lighter core. These particles are thought to range from empty to partially or fully packaged particles. Furthermore, the EM images obtained appear to show a lot of debris, which could indicate that the commercial purification kit would not be suitable for the purification of rAAV particles. It should also be noted that these samples underwent freeze thaw cycle and this could have resulted in the debris observed.

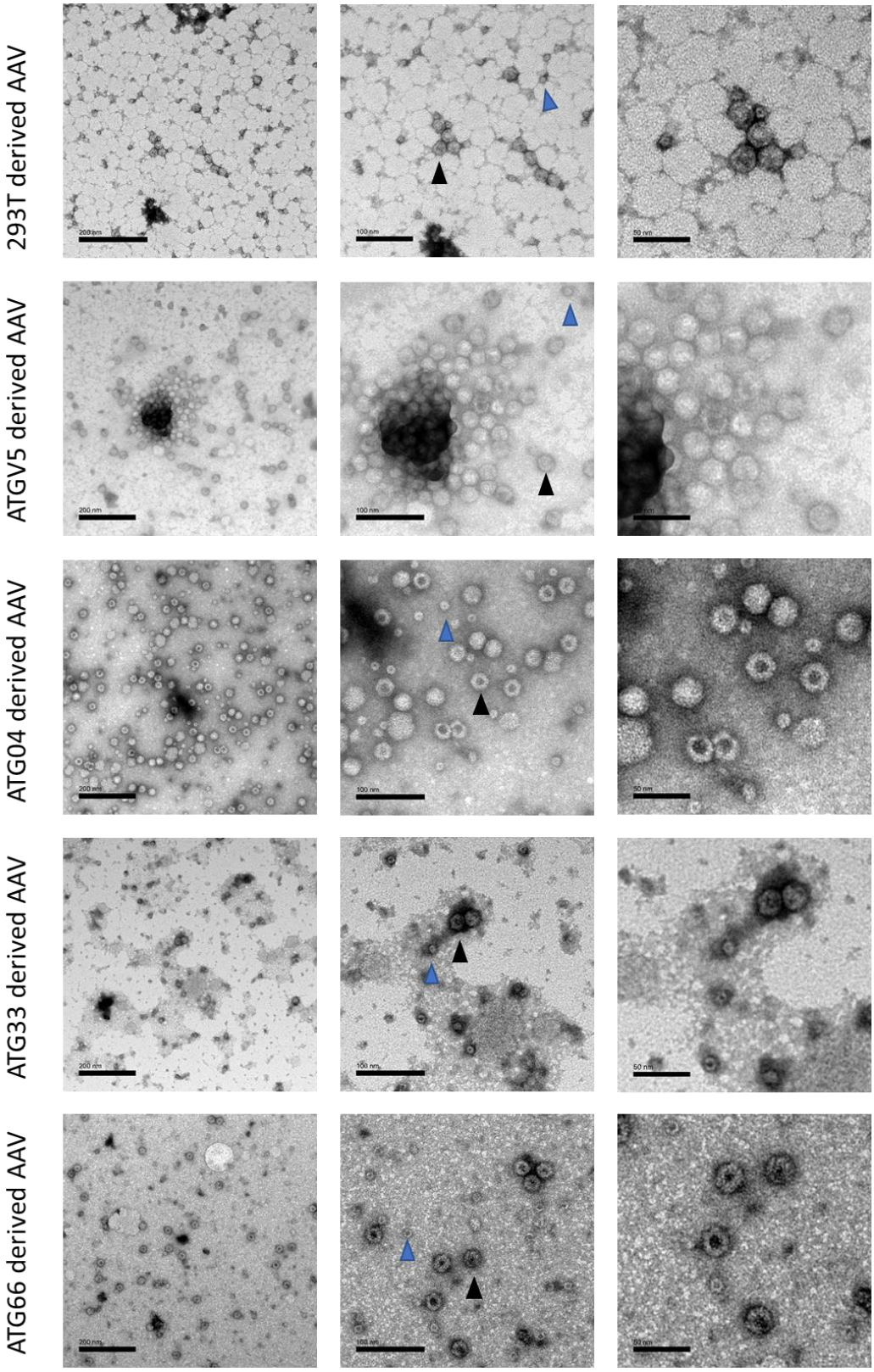

Figure 5.8 Electron microscope images of purified rAAV particles derived from the ATGV5 cell pool and the clonal cell lines HEK293T, ATG04, ATG33 and ATG66. AAV particles are observed as hexagonal structures between 20-25 nm (Black arrow). There was also a selection of smaller hexagonal structures identified that are approximately 11 nm in diameter (blue arrow). Bar represents scale = 200 nm (left hand column), 100 nm (middle column), 50 nm (right hand column).

5.4.4 Flow Cytometry Analysis of HEK2932T Cells Transduced with rAAV2 Particles Produced in HEK293T Cells

To study the transduction capability of rAAV2 particles derived from the HEK293T cell line and establish a transduction methodology, HEK293T cells were transduced with particles at a multiplicity of infection (MOI) of 100, 500 and 1000 vector genomes/cell. Transduction was carried out as described in Methods Section 2.14.1, and cells were analysed by flow cytometry 48 and 72 h post transduction as described in Methods Section 2.14.2. The threshold for auto-fluorescence and the gates M1, M2 and M3 were set based on non-transduced HEK293T cell lines (Figure 5.9 A and B). Any fluorescence lower than 10^1 FL1-H was considered cell autofluorescence, fluorescence between 10^1 and 10^2 in intensity was captured in an M1 gate, fluorescence between 10^2 and 10^3 was captured within an M2 gate and fluorescence between 10^3 and 10^4 was captured within an M3 gate.

Fluorescence across the different MOI at different timepoints post transduction are reported in Figure 5.9. The percentage of GFP positive fluorescing cells 48 and 72 h post transduction is reported in Figure 5.9 C and E. The data shows an increase in the percentage of fluorescing cells across the M1, M2 and M3 gates with increased MOI. Further, there was an increase in the percentage of cells fluorescing in the different gate threshold 72 h post-transduction compared to that at 48 h. At 48 h post transduction at 100 MOI the percentage of cells fluorescing across gates M1, M2 and M3 was 1.54, 0.15, 0.03 respectively. At 500 MOI there were 2.63%, 0.29% and 0.02% of cells fluorescing across gates M1, M2, and M3 and at an MOI of 1000 there was 5.48%, 0.60% and 0.02% of GFP positive cells 48 h post transduction across gates M1, M2 and M3 respectively. In comparison, 72 h post transduction, at an MOI of 100 there were 2.26%, 0.30 % and 0.01% of cells fluorescing across gates M1, M2 and M3, respectively while at an MOI of 500 there was 5.0%, 0.77% and 0.05% of cells fluorescing across the gates. Finally, at an MOI of 1000 there were 13.15%, 2.79% and 0.19% of cells fluorescing across gates M1, M2 and M3, respectively. Figure 5.9 D and F show the mean fluorescence across all cells for the different MOIs at 48 h and 72 h post transduction respectively. At 72 h post transduction there was an increase in the mean fluorescence at the different MOIs tested compared to the 48 h time point.

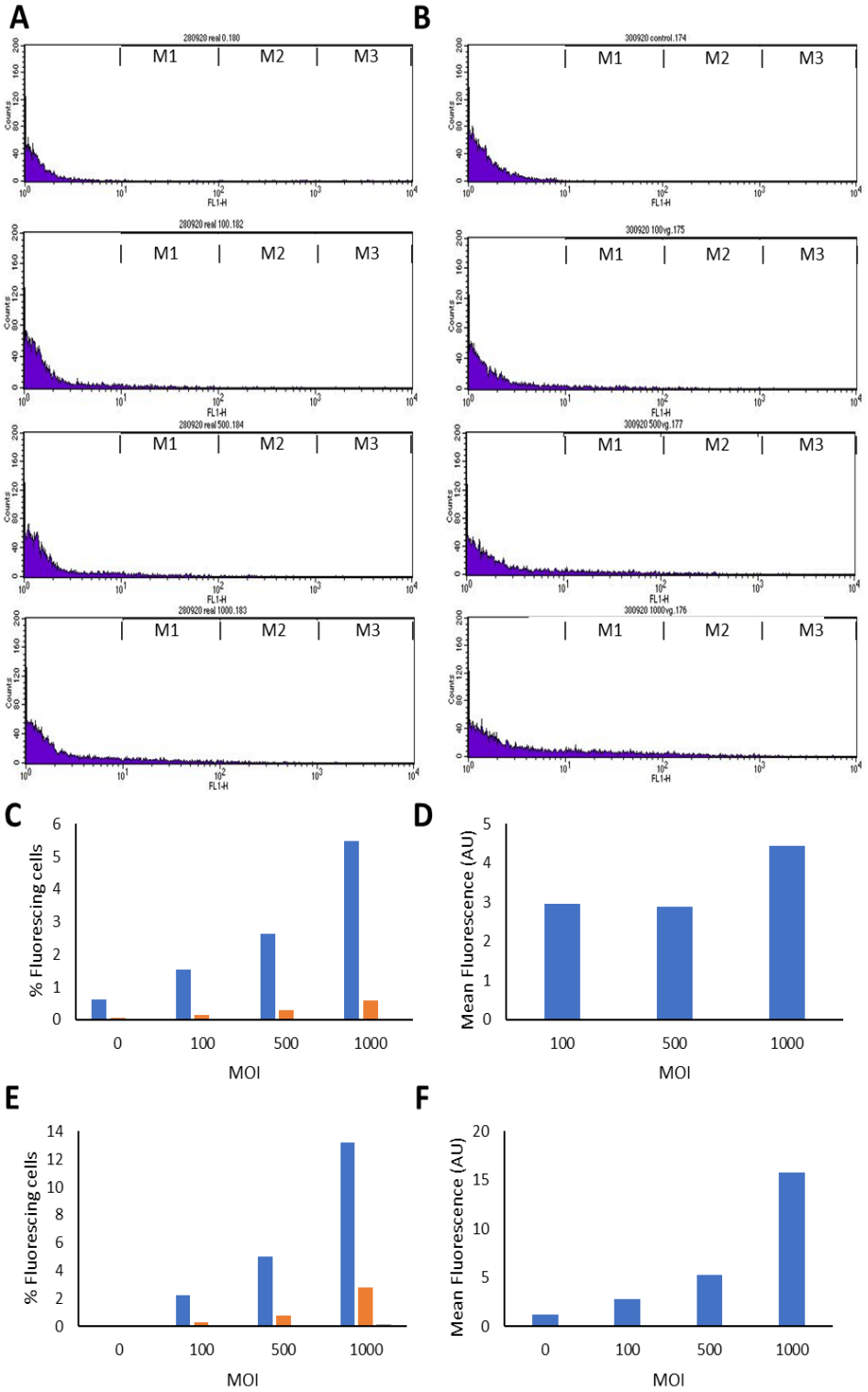

Figure 5.9 Flow cytometry analysis of HEK293T cells transduced with HEK293T derived rAAV2 particles. A) The number of fluorescence events across the gates M1, M2, and M3 and autofluorescence below the M1 gate for the control (top), 100, 500 and 1000 MOI (bottom) 48 h post transduction. B) The number of fluorescence events across the gates M1, M2, and M3 and autofluorescence below the M1 gate for the control (top), 100, 500 and 1000 MOI (bottom) 72 h post transduction. C) Percentage fluorescing cells 48 h post transduction across gate M1 (•), M2 (•) and M3(•). D) Mean fluorescence of HEK293T cells transduced with HEK293T derived rAAV2 particles 48 h post transduction. E) Percentage of fluorescing HEK293T cells 72 h post transduction across gates M1 (•), M2 (•) and M3(•). F) Mean fluorescing cells 72 h post transduction.

5.5 Assessment of the Functionality of rAAV Generated from Key AAP-V5 HEK293T Engineered Clonal Cell Lines

rAAV2 virus particles were purified from the selected AAP-V5 expressing clonal cell lines (ATG04, ATG33, ATG66) and the ATGV5 pool and HEK293T original host and then qPCR used to determine the genome copies present. Based on the genome copies purified, it was possible to determine the highest MOI possible to transduce HEK293T cells with. The cells were then transduced at an MOI of 1000, 2000 or 5000 except for the original HEK293T host where only sufficient material was available for transduction at 1000 and 2000 MOI. This reflected a low genome yield and provided further evidence that the AAP-V5 expressing cell lines produced higher genome titres. HEK293T cells were transduced and then analysed 72 h post transduction using fluorescent microscopy and flow cytometry.

5.5.1 Fluorescent Microscopy Analysis of HEK2932T Cells Transduced with Purified rAAV Viral Particles at a Range of MOIs

As outlined previously, the rAAV particles were produced with a genome containing a model GFP transgene. Fluorescent microscopy was therefore undertaken 72 h post-transduction to determine if the purified particles derived from the AAP-V5 expressing cell pool and clonal cell lines were functional and resulted in GFP expression when transduced into HEK293T cells. Images were obtained of all transduced and non-transduced cells and a typical selection are displayed in Figure 5.10. All cells that were transduced successfully appeared green, presumably as a result of GFP expression (Figure 5.10). Indeed, the rAAV derived from all cell lines, when transduce into HEK293T cells, gave rise to fluorescence 72 h post transduction, indicating the functionality of particles derived from all the AAP generated cell lines. As expected, the non-transduced HEK293T control cells did not fluoresce green.

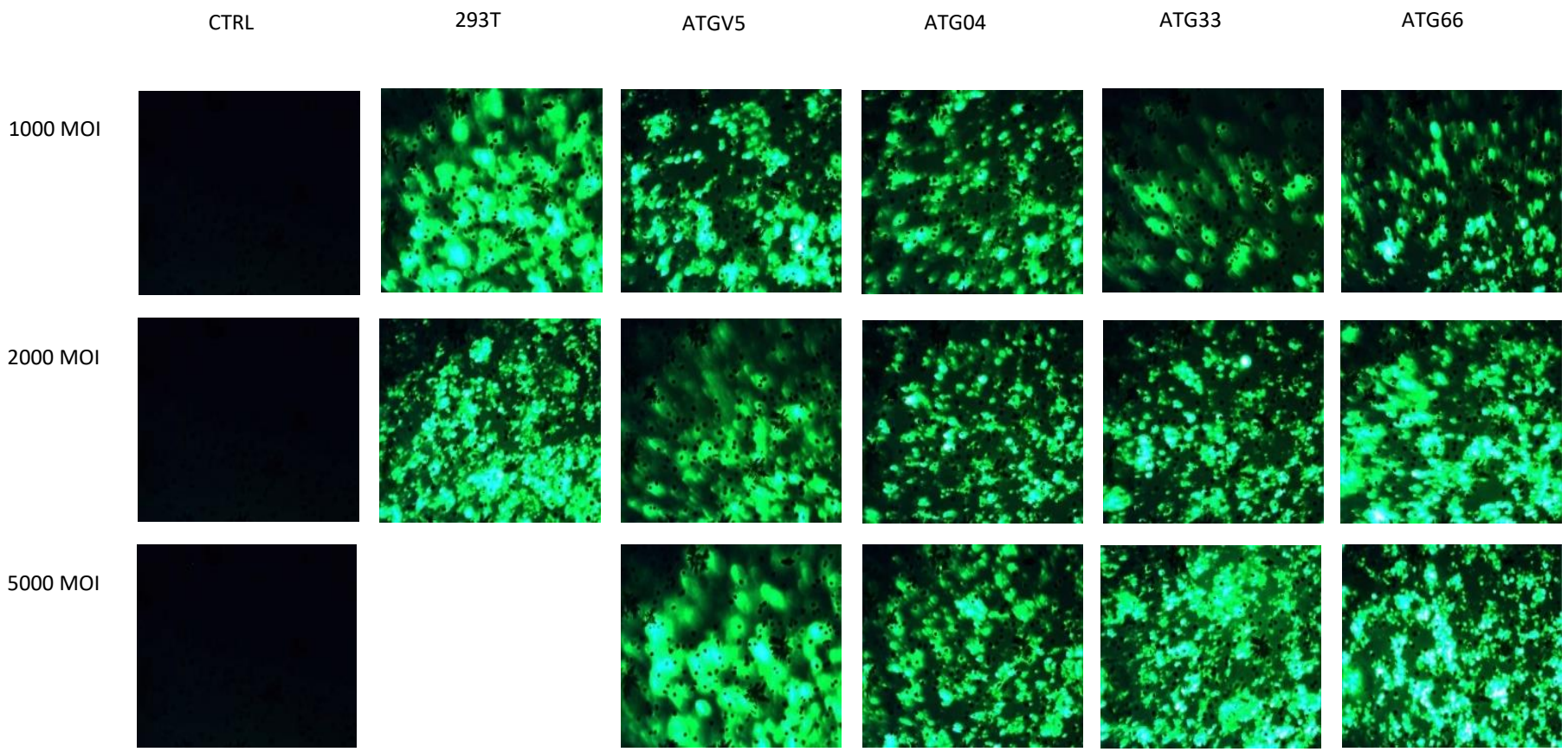

Figure 5.10 Fluorescent microscopy analysis of HEK293T cell lines transduced with either HEK293T, ATGV5, ATG04, ATG33 or ATG66 derived rAAV2 virus particles containing an eGFP genome. HEK293T cells were transduced with either 1000, 2000 or 5000 vector genomes per cell and visualised under the LEICA microscope 72 h post transduction with un-transduced HEK293T cells as a control.

5.5.2 Flow Cytometry Analysis of HEK293T Cells Transduced with rAAV Viral Particles Derived From Different Cell Lines

To further compare the functionality of the rAAV generated from the control and different HEK293T AAP-V5 expressing cell lines, the transduced HEK293T cells and non-transduced control were analysed by flow cytometry. As described in section 5.4.4 above, the threshold for autofluorescence was established from non-transduced cells and gates M1, M2 and M3 representing different intensity of fluorescence set. The percentage of GFP positive cells above the autofluorescence threshold in gates M1, M2 and M3 was then measured. As shown in Figure 5.9 A and Table 5.6-1, the percentage of GFP positive cells transduced with HEK293T derived rAAV increased with an increase in transduced particles across the three gates M1 (•), M2 (•) and M3(•). When transduced at 1000 MOI of HEK293T derived rAAV an average of 36.12%, 16.48% and 3.88% GFP positive cells across gates M1, M2 and M3, respectively was observed (Table 5.6-1). This was lower than that of the cells transduced at an MOI of 2000, where an average of 51.35%, 27.62% and 8.46% GFP positive cells across the M1, M2 and M3 gates, respectively was observed. The mean fluorescence across the MOIs was observed to almost double between an MOI of 1000 and 2000 (Figure 5.11 B, Table 5.6-1). Following a one-way ANOVA, it was determined by Bonferroni's post hoc multiple comparisons test, that there was a significant difference in the percentage of GFP positive cells in the M1 gate when comparing an MOI of 2000 to that of 1000 (p value= 0.011).

Table 5.6-2 Percentage of GFP positive cells across gates M1, M2 and M3 following transduction with HEK293T derived AAV2.GFP particles.(n=3)

MOI	M1 (% GFP +ve cells)	Significance between MOIs	M2 (% GFP +ve cells)	Significance between MOIs	M3 (% GFP +ve cells)	Significance between MOIs	Mean Fluorescence	Significance between MOIs
1000	36.12 +/- 19.01		16.48 +/- 9.05		3.88 +/-1.91		165.23 +/- 14.12	
2000	51.35 +/-6.90	* *P*= 0.0110	27.62 +/-5.29	n.s.	8.46 +/-2.36	n.s.	340.28 +/-100.77	n.s.

When transduced with ATGV5 derived rAAV at an MOI of 1000 an average of 45.49%, 23.63% and 7.35%% GFP positive cells across gates M1, M2 and M3, respectively were observed. This is compared to that observed with cells transduced at an MOI of 2000 where an average of 38.15%, 17.66% and 4.64% GFP positive cells across the M1, M2 and M3 gates, respectively were

observed and an average of 47.57%, 24.61% and 7.65% across gates M1, M2 and M3, respectively at an MOI of 5000 (Figure 5.11 A and Table 5.6-3). These data shows that there is no significant differences associated with an increase in the MOI, this is in line with the mean fluorescence remaining largely unchanged across the MOIs. This suggests that transduction is saturated (Figure 5.11 B, Table 5.6-3).

Table 5.6-3 Percentage of GFP positive cells across gates M1, M2 and M3 following transduction with ATGV5 derived AAV2.GFP particles (n=3). Significance was tested across the MOIs using ANOVA.

MOI	M1 (% GFP +ve cells)	Significant	M2 (% GFP +ve cells)	Significant	M3 (% GFP +ve cells)	Significant	Mean Fluorescence	Significant
1000	45.49 +/- 19.24		23.63 +/- 9.54		7.35 +/- 2.31		311.69 +/- 18.22	
2000	38.15 +/-16.31	n.s.	17.66 +/- 11.38	n.s.	4.64 +/- 4.60	n.s.	203.21 +/- 165.61	n.s.
5000	47.57 +/- 5.19	n.s.	24.61 +/- 4.05	n.s.	7.65 +/- 2.43	n.s.	316.27 +/-112.18	n.s.

When cells were transduced with ATG04 derived rAAVs an average of 39.90%, 19.11% and 5.91% GFP positive cells across gates M1, M2 and M3 was observed when using an MOI of 1000. When an MOI of 2000 was used, the percentage of GFP positive cells across gates M1, M2 and M3 averaged 42.49%, 19.66% and 5.34%. Unlike the ATGV5 derived rAAV transductions, the mean fluorescence across the ATG04 derived rAAVs transduced remained similar regardless of the MOI transduced, this plateau in mean fluorescence could be due to saturation across the MOI (Figure 5.11B, Table 5.6-4). Based on one-way ANOVA analysis, there was no significant differences across the MOIs.

Table 5.6-4 Percentage of GFP positive cells across gates M1, M2 and M3 following transduction with ATG04 derived rAAV.GFP particles (Error bars= SD, n=3). Significance was assessed using ANOVA,

MOI	M1 (% GFP +ve cells)	Significant	M2 (% GFP +ve cells)	Significant	M3 (% GFP +ve cells)	Significant	Mean Fluorescence	Significant
1000	39.90 +/- 5.59		19.11 +/- 4.25		5.91 +/- 2.12		252.44 +/- 164.47	
2000	42.49 +/- 13.31	n.s.	19.66 +/- 8.98	n.s.	5.34 +/- 3.55	n.s.	231.47 +/- 49.62	n.s.
5000	47.45 +/- 6.33	n.s.	23.14 +/- 4.71	n.s.	6.35 +/- 2.57	n.s.	268.55 +/- 54.44	n.s.

Based on the flow cytometry results obtained for the ATG33 derived rAAV transduction assay, an increase in MOI appears to both increase the percentage of GFP positive cells across the gates and increase the mean fluorescence across the MOIs (Figure 5.11 B). With 1000 MOI transduced an average of 24.14%, 10.11% and 2.30% GFP positive cells was observed across M1, M2 and M3 respectively. This was lower than the percentage of GFP positive cells when transduced with 2000 MOI, where there was an average of 34.03%, 15.98% and 4.57% GFP positive cells across the gates M1, M2 and M3, respectively. When transduced with 5000 MOI the highest amount of GFP positive cells across gates M1, M2 and M3 at 51.26%, 27.0% and 8.39% GFP positive cells was observed. The increase in the fluorescence associated with the increase in MOI was mirrored in the mean fluorescence reported in figure 5.11 B where the mean fluorescence increased from 100.56 to 190.86 to 370.42 as the MOI increased from 1000 to 2000 to 5000, respectively. One-way ANOVA analysis with post hoc tests were carried out via Tukey's multiple comparison test to determine significance across the range of MOI compared to that of the 1000 MOI. It was determined that at the M1 gate the MOI of 5000 was significantly different to 1000 MOI (p values < 0.0001). Furthermore, it was shown that there was significance in the % GFP positive cells at an MOI of 5000 compared to the MOI of 1000 across gate M2 (p value = 0.00.12). Finally, the mean fluorescence at MOI 5000 was significantly different to that of the MOI 1000 (p value= 0.0029) (Table 5.6-5).

Table 5.6-5 Percentage of GFP positive cells across gates M1, M2 and M3 following transduction with ATG33 derived AAV2.GFP particles (Error bars= SD, n=3). Significance was tested by ANOVA as described in the text.

MOI	M1 (% GFP +ve cells)	Significant	M2 (% GFP +ve cells)	Significant	M3 (% GFP +ve cells)	Significant	Mean Fluorescence	Significant
1000	24.14 +/- 4.81		10.11 +/- 3.51		2.30 +/- 1.68		100.56 +/- 70.17	
2000	34.03 +/- 12.39	n.s.	15.98 +/- 7.88	n.s.	4.57 +/- 3.71	n.s.	190.86 +/- 36.58	n.s.
5000	51.26 +/- 6.52	**** *p* <0.0001	27.00 +/- 4.74	** *p*= 0.0012	8.39 +/- 2.58	n.s.	370.42 +/- 60.20	** *p*= 0.0029

As for the ATG66 derived rAAV transduction, based on the flow cytometry analysis it can be seen that while there was only a small increase in the percentage of GFP positive cells across the MOIs there was an increase. At 1000 MOI transduction Figure 5.11 A shows that the percent GFP positive cells across gates M1, M2 and M3 was 42.14%, 19.47% and 5.67% respectively. When transduced with 2000 MOI the average percentage of GFP positive cells was 46.12%, 22.42% and 7.21% across gates M1, M2 and M3. The percentage of GFP positive cells at 5000 MOI was 49.12%, 25.58% and 8.50% across gates M1, M2 and M3 respectively (Table 5.6-6). This follows the pattern for the mean fluorescence observed as the transduced MOI increased. There was a mean fluorescence of 239.62 at 1000 MOI, 297.46 at 2000 MOI and 360.95 at 5000 MOI (Figure 5.11 B, Table 5.6-6). One-way ANOVA analysis with post hoc tests were carried out via Bonferroni (% GFP +ve cells) and Tukey's multiple comparison test (Mean fluorescence) to determine significance across the range of MOI compared to that of the 1000 MOI. It was determined that at the M1 gate both the MOI of 2000 and 5000 were significantly different to 1000 MOI (*p* values of 0.0266 and 0.0002, respectively). Furthermore, it was shown that there was significance in the % GFP positive cells at an MOI of 5000 compared to the MOI of 1000 across gate M2 (*p* value = 0.0008). Finally, the mean fluorescence at MOI 5000 was significantly different to that of the MOI 1000 (*p* value= 0.0198) (Table 5.6-6).

Table 5.6-6 Percentage of GFP positive cells across gates M1, M2 and M3 following transduction with ATG66 derived AAV2.GFP particles (Error bars=SD, n=3). Significance was tested using ANOVA as described in the text.

MOI	M1 (% GFP +ve cells)	Significant	M2 (% GFP +ve cells)	Significant	M3 (% GFP +ve cells)	Significant	Mean fluorescence	Significant
1000	42.14 +/- 0.98		19.47 +/- 0.74		5.67 +/- 0.07		239.62 +/- 53.73	
2000	46.12 +/- 8.29	* p = 0.0266	22.42 +/- 5.89	n.s.	7.21 +/- 3.71	n.s.	297.43 +/- 38.31	n.s.
5000	49.12 +/- 5.65	*** p= 0.0002	25.58 +/- 3.07	*** P= 0.0008	8.50 +/- 1.06	n.s.	360.95 +/- 10.57	* p= 0.0198

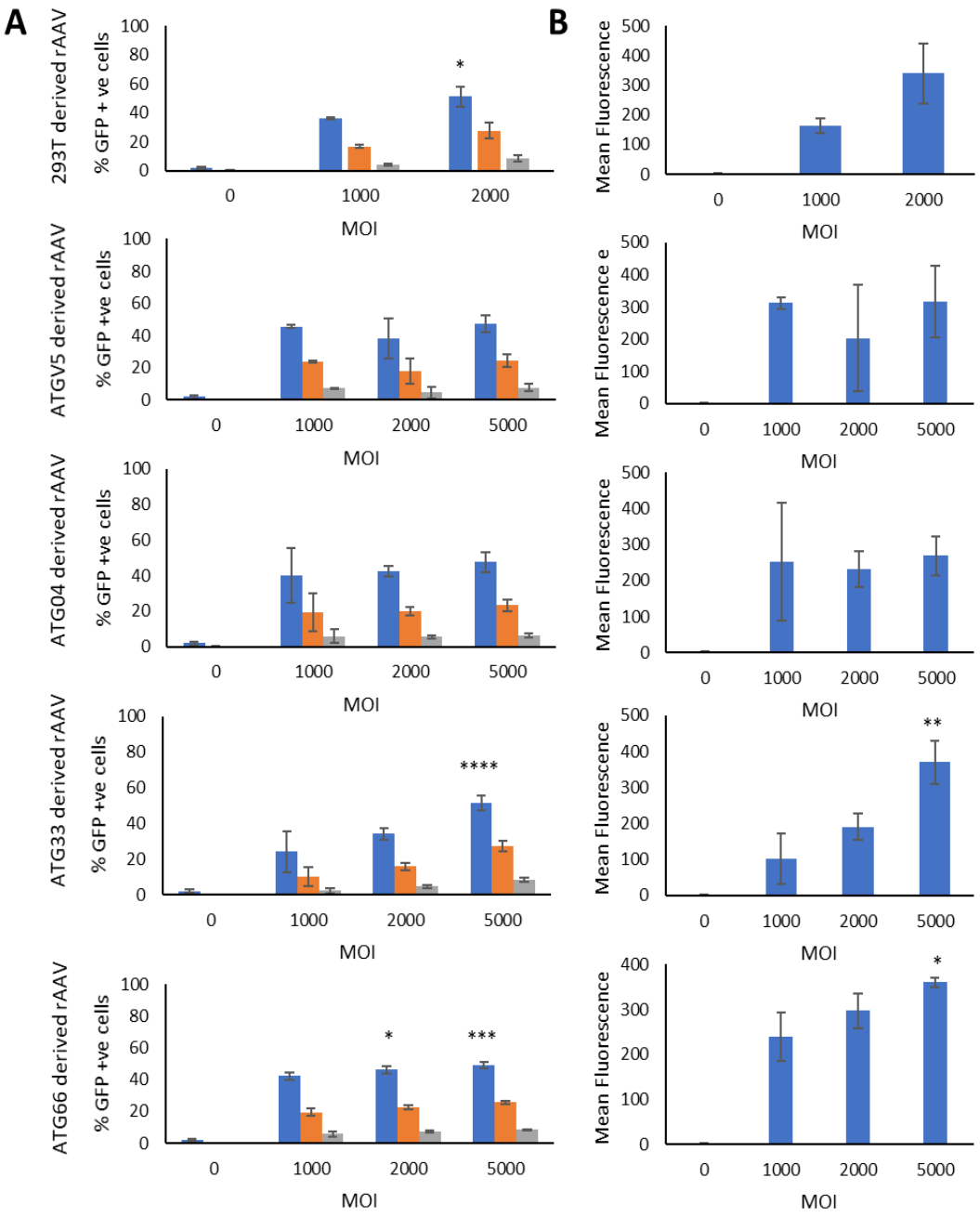

Figure 5.11 Flow cytometry analysis of HEK293T cells transduced with rAAV2 particles derived from HEK293T, ATGV5, ATG04, ATG33 or ATG66 cell lines 72 h post transduction at an MOI of either 1000, 2000 or 5000. A) % GFP positive cells 72 h post transduction across gate M1 (•), M2 (•) and M3(•). B) Mean fluorescence of HEK293T cells transduced with HEK293T, ATGV5, ATG04, ATG33 or ATG66 derived rAAV2 particles 72 h post transduction. Error bars show standard deviation, n=3. Statistical analysis carried out using one-way ANOVA.

Figure 5.12 A, C and E reports the percentage of GFP fluorescing cells after transduction of HEK293T cells with rAAV derived from either the HEK293T, ATGV5, ATG04, ATG33 or ATG66 cell lines at different MOIs (A=1000 MOI, C=2000 MOI and E=5000 MOI). Based on these data, the percentage of GFP positive cells

did not vary greatly across the different cell line derived rAAV transductions when compared across the MOIs (Table 5.6-7). Figure 5.12 B, D and F, shows the mean fluorescence observed after transduction of HEK293T cells with rAAV derived from the different cell lines at the different MOIs. Specifically, Figure 5.12 B reports the mean fluorescence across the HEK293T cells transduced at 1000 MOI, whereby the ATGV5 cell line derived rAAV gave rise to the highest mean fluorescence, followed closely by cells transduced with rAAV from the ATG04 and ATG66 cell lines. At an MOI of 1000 the ATG33 derived rAAV transduction gave the lowest mean fluorescence (Figure5.12, Table 5.6-7). Statistical analysis via a one-way ANOVA determined there was no significant differences across HEK293T cells when transduced with the particles derived from either the HEK293T, ATGV5, ATG04, ATG33 or ATG66 cell lines.

Table 5.6-7 Percentage of GFP positive cells and mean fluorescence across gates M1, M2 and M3 following transduction with ATG66 derived AAV2.GFP particles at an MOI 1000 (Error bars=SD, n=3). Significance was tested using ANOVA as described in the text.

Cell Line	M1 (% GFP +ve cells)	Significant	M2 (% GFP +ve cells)	Significant	M3 (% GFP +ve cells)	Significant	Mean fluorescence	Significant
293T	36.12 +/- 0.99		16.48 +/- 1.08		3.88 +/- 0.78		165.23 +/- 25.12	
ATG	45.49 +/- 0.98	n.s.	23.63 +/- 0.74	n.s.	7.35 +/- 0.07	n.s.	311.69 +/- 18.22	n.s.
A04	39.90 +/- 15.31	n.s.	19.11 +/- 10.54	n.s.	5.91 +/- 3.98	n.s.	252.44 +/- 164.47	n.s.
A33	24.14 +/- 11.59	n.s.	10.11 +/- 5.46	n.s.	2.30 +/- 1.63	n.s.	100.56 +/- 70.17	n.s.
A66	42.14 +/- 2.20	n.s.	19.47 +/- 2.53	n.s.	5.67 +/- 1.41	n.s.	239.62 +/- 53.73	n.s.

When an MOI of 2000 was transduced (Figure 5.12 D), the HEK293T derived rAAV gave rise to the highest mean fluorescence followed by the fluorescence observed after transduction with rAAV derived from the ATG66, ATG04, ATGV5 and finally ATG33 cell lines. Following analysis by a one-way ANOVA with a Bonferroni multiple comparisons test, it was shown that at an MOI of 2000 there was statistical differences between the 293T derived AAV2.GFP particles and the ATGV5 derived particles across gate M1 (p value =0.0085). Significant differences were also detected between the 293T derived particles and the ATG33 derived particles across gates M1 and M2 (p values of 0.0005 and 0.0234, respectively). However, while the ATGV5 and the ATG33 derived AAV2.GFP particles show significance across the gates, there was no statistical difference in the mean fluorescence across the different cell line derived particles (Table 5.6-8).

Table 5.6-8 Percentage of GFP positive cells and mean fluorescence across gates M1, M2 and M3 following transduction with ATG66 derived AAV2.GFP particles at an MOI 2000 (Error bars=SD, n=3). Significance was tested using ANOVA as described in the text.

Cell Line	M1 (% GFP +ve cells)	Significant	M2 (% GFP +ve cells)	Significant	M3 (% GFP +ve cells)	Significant	Mean fluorescence	Significant
293T	51.35 +/- 6.90		27.62 +/- 5.29		8.46 +/- 2.36		340.28 +/- 100.77	
ATG	38.15 +/- 12.39	** *p= 0.0085*	17.66 +/- 7.88	n.s.	4.67 +/- 3.71	n.s.	203.21 +/- 165.61	n.s.
A04	42.49 +/- 2.79	n.s.	19.66 +/- 2.39	n.s.	5.34 +/- 0.97	n.s.	231.47 +/- 49.62	n.s.
A33	34.02 +/- 3.08	*** *p= 0.0005*	15.98 +/- 2.07	* *p*= 0.0234	4.57 +/- 0.83	n.s.	190.86 +/- 36.58	n.s.
A66	46.12 +/- 2.24	n.s.	22.42 +/- 1.21	n.s.	7.21 +/- 0.72	n.s.	297.43 +/- 38.31	n.s.

Figure 5.12 F reports on mean fluorescence when the HEK293T cells were transduced with ATGV5 derived rAAV, ATG04 derived rAAV, ATG33 derived rAAV and ATG66 derived rAAV. These data show that the ATG33 derived rAAV and the ATG66 derived rAAV gave the highest mean fluorescence at 5000 MOI followed by the ATGV5 derived and then the ATG04 derived rAAV. However, there was no statistical difference between these data as determined by one-way ANOVA (Table 5.6.9).

Table 5.6-9 Percentage of GFP positive cells and mean fluorescence across gates M1, M2 and M3 following transduction with ATG66 derived AAV2.GFP particles at an MOI 2000 (Error bars=SD, n=3). Significance was tested by ANOVA as outlined in the text.

	M1 (% GFP +ve cells)	Significant	M2 (% GFP +ve cells)	Significant	M3 (% GFP +ve cells)	Significant	Mean fluorescence	Significant
ATG	47.57 +/- 5.19		24.61 +/- 4.05		7.65 +/- 2.43		316.27 +/- 112.18	
A04	47.45 +/- 5.65	n.s.	23.14 +/- 3.07	n.s.	6.35 +/- 1.06	n.s.	268.55 +/- 54.44	n.s.
A33	51.26 +/- 3.99	n.s.	27.00 +/- 3.01	n.s.	8.39 +/- 1.22	n.s.	370.42 +/- 60.20	n.s.
A66	49.12 +/- 1.97	n.s.	25.58 +/- 0.88	n.s.	8.50 +/- 0.17	n.s.	360.95 +/- 10.57	n.s.

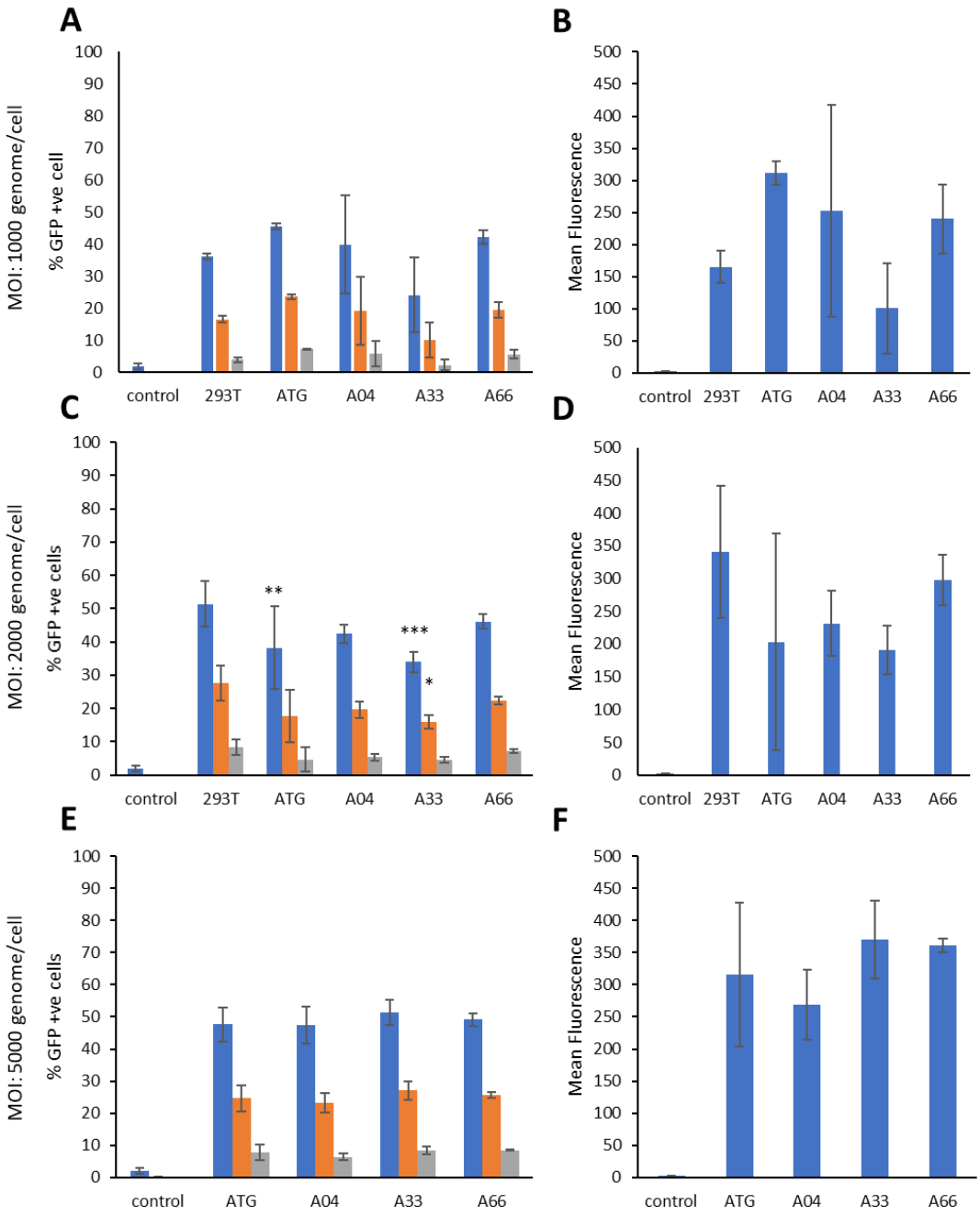

Figure 5.12 Flow cytometry analysis of HEK293T cells transduced with rAAV2 particles derived from HEK293T, ATGV5, ATG04, ATG33 or ATG66 cell lines 72 h post transduction at different MOI. A) percentage of GFP positive cells 72 h post transduction with an MOI of 1000 across gates M1 (•), M2 (•) and M3(•). B) Mean fluorescence of HEK293T cells transduced with1000 MOI HEK293T, ATGV5, ATG04, ATG33 or ATG66 derived rAAV2 particles 72 h post transduction. C) Percentage of GFP positive cells 72 h post transduction at 2000 MOI across gates M1 (•), M2 (•) and M3(•). D) Mean fluorescence of HEK293T cells transduced with 2000 MOI HEK293T, ATGV5, ATG04, ATG33 or ATG66 derived rAAV2 particles 72 h post transduction. E) Percentage of GFP positive cells 72 h post transduction at 5000 MOI across gates M1 (•), M2 (•) and M3(•). F) Mean fluorescence of HEK293T cells transduced at 5000 MOI of ATGV5, ATG04, ATG33 or ATG66 derived rAAV2 particles 72 h post transduction. Error bars determined based on SD, n=3. Statistical analysis was carried out using one-way ANOVA.

5.6 Discussion

The aim of the work presented in this chapter was to generate AAP stably expressing clonal cell lines by limiting dilution from the ATGV5 cell pool and then characterise the ability of these clonal cell lines to produce packaged rAAV particles. To investigate if stable expression of Assembly Activating Protein (AAP) in HEK293T cells impacted the packaging ability of the cells, clonal cell lines offer the ability to undertake studies whereby cells express similar amounts of AAP in the clonal population rather than as in a polyclonal population where the levels of expression may vary widely. AAP is postulated to play a role in packaging of AAV2 capsid particles (Maurer et al., 2018) and based on such reports, and the data presented in Chapter 4, cell lines that are highly likely to be monoclonal based on limiting dilution cloning were generated. The growth and packaging capabilities of these clonal cell lines was then investigated in comparison to both the HEK293T control cell line and the ATGV5 cell pool generated in Chapter 4. Finally, the work reported in this chapter moved towards identifying and focusing on the higher packaging clonal cell lines ATG04, ATG33 and ATG66. The rAAV2.GFP viral particles produced from these and the HEK293T and HEK293V5 pools were then further characterised by investigating the functionality of the capsid particles produced as assessed by the ability of purified particles to transduce the HEK293T host cell line.

The generation of stably exogenous gene expressing mammalian cell lines results in random integration of the transfected gene of interest (unless targeted integration approaches are utilised) along with variable copy numbers of the gene of interest, resulting in heterogeneity across the individual cells in the transfected cell pool (Lai, Yang, & Ng, 2013; Würtele, Little, & Chartrand, 2003; R. Yang et al., 2018). The variability of the work discussed in chapter 4 may, at least in part, be due to this heterogeneity within cell pools. It is this variability and heterogeneity which can be reduced by clonal cell line development. This of course does not reduce the inherent clone to clone variability that may arise but within a given clone more consistent results should be produced than when using a pool.

Identification of large numbers of cell lines with a particular phenotype by limiting dilution is a labour intensive task, which requires the screening of a large number of clones (Wurm, 2004). In this study, single cell cloning via limiting dilution was undertaken using the ATG-AAP-V5 expressing stable cell pool to overcome the variability of this cell pool and to isolate a number of clonal cell lines expressing AAP-V5. Following single cell cloning 8 clonal cell lines were eventually isolated and referred to as ATG06, ATG04, ATG02, ATG16, ATG36, ATG34, ATG33 and ATG66.

AAP expression in the clonal cell lines was analysed and compared to that of the original ATG-AAP pools using a commercially available V5 antibody due to the lack of commercially available AAP antibodies. As seen in Figure 5.1 A, there was V5- expression across all clonal cell lines as indicated by the presence of a band at approximately 25 kDa. Based on densitometry analysis and normalisation against the ATGV5 cell pool (Figure 5.1), the expression levels of V5 tagged AAP did vary across the different clonal cell lines although the range was quite narrow and not magnitudes different. This indicates isolation of cell lines with a variety of AAP expression levels, albeit a quite narrow range as expected from single cell cloning (Wurm, 2004). The narrow range suggests that higher expressing AAP-V5 cell lines either do not survive or are very rare and hence were not isolated in this study. When the stability of AAP expression across the clonal cell lines was followed, two clonal cell lines, ATG36 and ATG34, had variable expression levels of AAP over time, while the remaining clonal cell lines showed the same pattern of expression over time. The variability in the ATG36 and ATG34 clones could be due to a lack of clonality caused by limiting dilution or instability in these clones. Limiting dilution is a traditional and well utilised methods of single cell cloning, however issues such as cell clumping and limited plating efficiency can result in cells originating from more than one clone (Gross et al., 2015). This issue could be overcome by another round of sub cloning from these cells. It is also possible that the clonal variation in cell lines ATG36 and ATG34 is due to instability and non-genetic variation caused by epigenetics, promoter silencing, stochastic gene expression and changing environmental conditions (Grav et al., 2018; Pilbrough, Munro, & Gray, 2009).

Once the clonal cell lines had been established, the batch culture growth profiles in comparison to that of the HEK293T control host cell line and the ATGV5 cell pool were established to determine if the AAP-V5 expression impacted the growth of the cells. As shown in figures 5.2, 5.3 and 5.4, stable exogenous AAP-V5 expression did not have any detrimental impact on the growth of the cell lines when compared to that of the HEK293T cell line and the ATGV5 pool. Interestingly the clonal cell lines ATG06, ATG04, ATG02, ATG16, ATG36, ATG34 and ATG33 maintained a marginally higher culture viability on days 1 to 3 than that of the HEK293T control or the ATG-AAP expressing pools. The population doubling times did not vary greatly across the clonal cell lines, with the exception of clone ATG66 which had a population doubling time of over 24 h in comparison to that of the 19-22 h seen among other cell lines. Overall, the data suggest that the expression of exogenous AAP-V5 did not greatly impact the growth phenotypes of the cell lines investigated in this study under batch culture conditions.

Next, whether the stable expression of AAP impacted the titre or AAV packaging ability of the cell lines compared to the HEK293T control and pool was evaluated. It is important to note that

when producing rAAV2 particles by transfecting the RepCap plasmid into the cells, further transient AAP expression occurs above the stable AAP expression due to the presence of the *Cap* gene. Unfortunately, it was not possible to determine how much AAP is being produced by the transfection process due to a lack of commercially available antibodies. Thus, when studying the impact of AAP expression on rAAV2 titres and packaging in this chapter, it refers specifically to AAP expression by the stable cell lines and not that of the AAP produced by transfection of the Rep Cap plasmids.

Stable exogenous AAP-V5 expression appeared to impact the packaging of rAAV2 particles, although there was variability between the pool and different AAP-V5 expressing cell lines as to the magnitude of this effect. This suggests that whilst the amount of AAP being expressed in HEK293T cells influences packaging efficiency, packaging efficiency is not solely determined by AAP expression as might be expected. Other clone or pool specific limitations in the cellular machinery are also likely to exist. Nevertheless, the data suggest that the amount of AAP generated from the normal transient transfection approach is not sufficient to support higher packaging efficiency and thus can be overcome or improved by the exogenous expression of AAP in the host cell prior to transfection. As indicated by the total particle titres, an increase in AAP expression does not result in an increase in the particle titres. Based on work discussed in this chapter, there appears to be a trend showing that a number of the clonal cell lines gave rise to a greater number of packaged capsids of the total made (as indicated by % packing efficiency), specifically the ATG06, ATG04, ATG02, ATG16, ATG33 and ATG66, while the ATG36 and ATG34 cell lines gave lower packaged yields than their counterparts. It is interesting to note that the ATG36 and ATG34 cell lines both appeared to have a variability in AAP expression over time (Figure 5.1). Based on the average packaging efficiencies across the clonal cell lines, ATG04, ATG33 and ATG66 were selected as key cell lines of interest and taken forward for further research.

Further production runs were carried out on the key AAP clonal cell lines (ATG04, ATG33 and ATG66) (Figure 5.8). This work determined that there was a statistically significant increase in both the percentage packaging and the genome titre of the AAV expressing clonal cell line ATG33 and ATG66. To date, there are no studies which utilise AAP expressing HEK293T cell lines to produce rAAV. However, AAP overexpression and its effects on AAV titre has been studied in systems such as the baculovirus production system. In a study into the relevance of AAP by Stefanie Grosse and colleagues, it was shown that AAP overexpression did not impact the vector genome titres observed (Grosse et al., 2017)

Immunofluorescence and confocal laser scanning microscopy was carried out on clonal cell lines (ATG04, ATG33 and ATG66) to study AAP localisation across the cells. Earley and colleagues have identified both nuclear and nucleolar localisation signals (NLS and NoLS, respectively). These signals were identified at the carboxy-terminal region of the AAV2 AAP (AAP2) at amino acid position 144 to 184 (Earley et al., 2015). As shown in Figure 5.7, the V5 tagged AAP was found to be co-localised with the DAPI nuclear stain and so was shown to be localised in the nucleus, a finding that agrees with the findings in chapter 4 and from other reports (Earley et al., 2017; Grosse et al., 2017). Studies such as that by Earley et al and Grosse et al, utilised FLAG-tagged or HA-tagged AAP, respectively in HeLa and HEK293T cells. Earley et al, utilising a nucleostemin antibody showed localisation was specific to the nucleous which corresponds to when the production of AAV capsids occurs. The main function of AAP is reported to be to target the VP proteins to the nucleolus for assembly (Earley et al., 2015; Sonntag et al., 2010). Interestingly, the data presented in figure 5.7 shows the V5-tagged AAP to be more disperse throughout the nucleus than the ATGV5 cell line where punctate spots thought to correspond with the nucleolus were observed (Figure 4.11).

To further study the rAAV2.GFP capsid particles derived from the HEK293T or AAP expressing cell lines it was necessary to purify the particles. This was achieved utilising the commercial Takara AAVpro Purification kits. The kit utilises a Cold-active Nuclease prior to treatment with a precipitator, followed by filtration using a Millex-HV 0.45 µm filter before finally undergoing concentration using an Amicon Ultra-4 filter. Use of the commercially available kit negates the need for timely and cumbersome methods such as ultracentrifugation (Guo et al., 2012). The rAAV titres were compared pre- and post-purification to assess the effectiveness of this kit, unfortunately post purification the yield had dropped indicating that this purification method does not give a high recovery. Loss of rAAV2 post purification is not uncommon as many methods of rAAV purification show a high degree of loss (Burova & Ioffe, 2005; Guo et al., 2012; Zolotukhin et al., 1999). Zolotukhin and colleagues studied a range of purification methods and the percentage recovery obtained. Their study showed that use of iodixanol gradient purification can result in 75-80% purification of rAAV. In comparison to this, they showed that use of either heparin sulfate or sulfate cation exchange chromatography resulted in 40-70% recovery of the iodixanol fraction. However, use of CsCl gradients only yielded a 7% recovery of the material obtained from the iodixanol fraction (Zolotukhin et al., 1999).

Purified recombinant AAV particles derived from the AAP expressing cell lines were subjected to electron microscopy to further characterise these particles. As seen in figure 5.11, there are hexagonal particles present in the purified rAAVs derived from all AAP expressing cell lines.

These structures are 20-25 nm in diameter. This is the expected size of purified rAAV particles based on previous studies such as that by Zeltner et at who imaged AAV on an EM after staining with 2% uranyl acetate and showed wild type AAV and rAAV.GFP as hexagonal structures of approximately 20 nm in diameter (Zeltner, Kohlbrenner, Clément, Weber, & Linden, 2010). Several rAAV derived from our AAP expressing cell lines appeared to have a dark centre in the images obtained. A study by Zelter et al, compared the EM images of empty particles to wild type AAV2, reporting that the empty particles all contained a dark centre whereas the wild type AAV2 identified as 94% full had a small number of these darkened centres (Zeltner et al., 2010). The darker centre seen in empty AAV capsids is due to the electron dense centre (Lu et al., 2019)(Fu et al., 2019). The visual difference in the appearance between empty and full capsids when visualised with EM is thus reported in other work (Horowitz et al., 2013; Mostrom et al., 2019; Penaud-Budloo, François, Clément, & Ayuso, 2018). For example Horowitz et al, where full capsids are described as 25 nm solid structures and the empty capsids are described as having a donut like appearance of 25 nm (Horowitz et al., 2013). Interestingly, when purified rAAV were visualised on the EM, there was a number of similar hexagonal structures of approximately 10-15 nm in diameter which were morphologically similar to that of the rAAV. Grieger and colleagues also identified such structures of around 10-15 nm in diameter. This study identified these contaminating structures by way of mass spectrometry as consisting of ferritin. These contaminating ferritin structures were isolated from the rAAV particles by ion exchange chromatography (Grieger et al., 2016). Furthermore Blessing and colleagues identified similar structures in preparations purified by iodixanol gradient ultracentrifugation, again suggesting these structures were consisted of ferritin (Blessing et al., 2019).

Transduction assays were used to investigate the functionality of the purified capsids generated from the HEK293T, ATGV5, ATG04, ATG33 and ATG66 cell lines. Fisher et al used an MOI of 1000 (Fisher et al., 1996) for transduction assays and therefore MOIs around this were investigated here. HEK293T cells transduced with HEK293T derived rAAV underwent analysis by flow cytometry and the % of fluorescing GFP positive cells were measured across the gates M1, M2 and M3. As expected, the higher the MOI the more fluorescence observed.

HEK293T cells were transduced with purified rAAV derived from HEK293T, ATGV5, ATG04, ATG33 and ATG66 cell lines at an MOI of 1000, 2000 and where possible 5000 viral genomes/cell. Transduced cells were harvested 72 h post transfection and were analysed by fluorescent microscopy and flow cytometry. Fluorescent microscopy images are displayed in figure 5.12, and these show the purified rAAV particles when transduced give rise to GFP positive cells. The fluorescent microscopy images when taken alongside the flow cytometry results in figure 5.13

and 5.14 and these data indicate that the purified rAAV capsids generated from the AAP expressing cell lines are functional. Therefore, the cell lines used to generate these rAAV.GFP could be used to generate rAAV containing transgenes for use in gene therapies. Based on the mean fluorescence figures shown the 293T, ATG33 and ATG66 derived rAAV transduced with increasing MOI of 1000, 2000 and in the case of ATG33 and ATG66 an increase in the MOI results in an increase in the number of events or cells that have been transduced. For ATGV5 and ATG04, the amount of GFP positive cells did not appear to increase with MOI of 1000, 2000 and 5000 suggesting that perhaps a threshold has been reached and that after this point it does not matter what MOI is used for transduction no further GFP expression is observed.

Ultimately, the work in this chapter shows that it is possible to improve AAV packaging when utilising AAP expressing clonal HEK293T cell lines. Both the ATG66 and the ATG33 cell lines significantly increased the packaged genome titres, while having no effect on the total particles. Furthermore, the rAAV2 particles derived from these two cell lines could successfully transduce untransfected cells indicating their functionality. These rAAV particles had a similar transduction efficiency to particles derived from the original HEK293T cell line. Research into AAP and its effects on AAV packaging is a relatively recent field. While there are no published studies looking at AAP expressing cell lines, AAP overexpression studies have indicated that overexpression of AAP does not improve AAV packaging in the baculovirus system.

Chapter 6 General Discussion

6.1 Overall Discussion

Viral vectors and their potential as delivery mechanisms of nucleic acid, gene therapy-based therapeutics is a rapidly developing field. This is evidenced by the fact that there was over 2000 clinical trials carried out from 1989-2016 based on using viral vector technology (van der Loo & Wright, 2016). In the UK alone, there were 154 ongoing clinical trials in 2020 utilising cell and gene therapies(*Cell and Gene Therapy Catapult ATMP clinical trials report 2020*, 2020). As described in the introduction to this thesis, the non-enveloped Adeno Associated Virus (AAV) is one of the most predominant viral vectors used in gene therapy trials with 39% of trials in 2020 using this viral vector delivery system (*Cell and Gene Therapy Catapult ATMP clinical trials report 2020*, 2020). Again, as outlined in the introduction of this thesis, achieving AAV viral vector yields and quality sufficient to support the demands for both clinical trials and wider use remains a challenge that means these therapies are currently expensive to produce. Much research has therefore been undertaken into investigating the biology and bioprocesses that determine vector particle yields, thereby identifying approaches to improve the yields and genome packaging of particles. The overall aim of the work described in this thesis was to investigate the engineering of the HEK293T host cell line to over express AAV proteins and determine the effect of this on the impact of these cell lines to produce genome packaged recombinant AAV particles.

Although there are around 12 serotypes of AAV, recombinant AAV serotype 2 is one of the most widely studied serotypes and known to give high levels of empty particles during manufacturing, with some reports of at least 80% of rAAV2 particles being empty (D Grimm et al., 1999). One approach to increase the production and packaging of recombinant AAV vectors involves generating producer cell lines that stably express target proteins that enhance production (Yuan, Qiao, Hu, Li, & Xiao, 2011). Mammalian cell lines used for the production of rAAV traditionally include HEK293 or HEK293T cell lines. Cell lines such as these constitutively expresses the E1A/E1B helper genes required for the production of rAAV particles. As outlined in the introduction (see section 1.2.1 and 1.4.1) AAV replication is reliant on the coinfection of a helper virus, typically adenovirus. This helper virus supplies a number of genes required for AAV replication; E1A, E1B, E2a, E4 and VA RNA (K. Reed Clark et al., 1995; Xiao et al., 1998; Yuan et al., 2011).

The initial objectives of the work described in this thesis focused on the establishment of a rAAV production system using a HEK293T suspension adapted cell line, this acting as a baseline to use as a comparison for further work (Chapter 3). The work involved establishing methods for the

triple plasmid co-transfection of the HEK293T host cell line and subsequently determining particle and viral genome titre. Most published research utilises an ELISA assay to determine total particle titre (D Grimm et al., 1999), while quantitative real time PCR (qRT-PCR) is widely used to determine viral genome titre (D'Costa et al., 2016; Dobnik et al., 2019). Once established, these methods were the core analytical methods used for analysis in the work covered in chapters 4 and 5 to study the impact of HEK293T cell pools and cell lines engineered to express assembly activating protein (AAP) on AAV particle formation and genome packaging.

Cell line engineering to enhance the capacity of HEK293T cells to produce genome packaged rAAV was key to the work described in this thesis. The specific aim was to develop HEK293T cell lines expressing a selection of AAV proteins, including the Rep proteins (Rep 78, Rep 68, Rep 52 and Rep 40), the Cap proteins (VP1, VP2 and VP3) (Chapter 3) and the Assembly Activating Protein (AAP) with the ultimate goal to characterise and determine if the stable exogenous expression of these proteins impacted rAAV packaging (Chapters 4 and 5). As AAP expression is known to be required for the successful packaging of some serotypes of AAV, a particular focus was on the impact of stable expression of this protein. Initial work in the development of HEK293T engineered host cell lines required generation of plasmid vectors containing a mammalian selection marker to allow isolation of those cells whereby the plasmid had been stably integrated. Prior to the generation of stably engineered cell lines, transient expression of the constructs and expression of the target proteins was confirmed via western blotting (see Chapter 3). Once expression was confirmed, transfections for the generation of cell pools and lines stably expressing the AAV viral proteins were carried out.

The work discussed in the second half of chapter 3 describes the production of cell pools stably expressing either the Rep proteins alone or alongside the Cap proteins. The idea behind generation of these cell lines would be to reduce the number of plasmid vectors needing to be transfected when carrying out a production run and potentially reducing the stain on the cells when producing rAAV2. Throughout the work undertaken in this thesis, three plasmids are co-transfected for the production of rAAV2 capsids, pAAV-RC-Kan, pHelper-Kan and pAAV-GFP-Kan (see sections 2.2.4 and 3.3 for more detail on each of these plasmids). Co-transfection is a commonly used method for the production of proteins and viral vectors (Aricescu, Lu, & Jones, 2006; Baldi, Hacker, Meerschman, & Wurm, 2012; Dyson, 2016; Xiao et al., 1998). A cell line stably expressing the Rep and Cap proteins would reduce the number of plasmids required to be co-transfected and potentially allow a 'set amount' of Rep and/or Cap protein to be reproducibly and constitutively expressed in a host cell line (that could be selected from an initial pool) for 'optimal' rAAV production.

The establishment of stably expressing Rep and/or Cap HEK293T pools was unsuccessful. There are four rep proteins, Rep78, Rep68, Rep 52 and Rep40, non-structural proteins involved in AAV replication (Chiorini et al., 1996). There are also three Cap proteins, VP1, VP2 and VP3, structural proteins which form the AAV capsid in a ratio of 1:1:10 (Cassinotti, Weitzand, & Tratschin, 1988). Cells did not survive the selection process and no colonies grew out whilst cells that were transfected with a control plasmid containing no *Rep* or *Cap* gene did. This is likely due to Rep mediated cytotoxicity. In support of this hypothesis, Schmidt et al showed that expression of Rep 78 induces cell death by apoptosis, activating caspase 3 and the apoptosis signalling cascade (Schmidt et al., 2000). Due to this potential Rep protein mediated cytotoxicity, vector constructs were generated both with and without a CMV promoter region in an attempt to reduce the expression of the Rep proteins and hence any apoptotic effects of Rep78 or the other Rep proteins. Indeed, cell lines have been generated which express the Rep and Cap proteins in different systems used for recombinant AAV production. Clark and colleagues achieved this by generating an inducible cell line system, allowing for the expression of Rep and Cap proteins upon infection with adenovirus such that these were not constitutively expressed (K R Clark, Voulgaropoulou, & Johnson, 1996). In this way the cytotoxic impact is reduced by ensuring that the toxic proteins are only expressed when required for rAAV production.

Others have also reported similar approaches for adenovirus. Using both a HeLa host cell line and a HEK293 host cell line, Chadeuf and colleagues generated adenovirus inducible cell lines (Chadeuf et al., 2000). Collectively the results from this study in attempting to generate constitutively expressing Rep and Cap cell pools, alongside the inducible systems reported by others, it seems likely that the constitutive expression of some or all Rep and Cap proteins are toxic to HEK293T cells that cannot survive when these proteins are continually expressed. Inducible cell lines appear to be solutions to this problem. A further approach could be to generate cell lines expressing the non-toxic Rep and Cap proteins and introduce just the toxic protein(s) as part of the co-transfection approach. This is complicated by the nature of the transcripts and their overlapping sequence but could be achieved although the benefit to titre and packaging efficiency, if any, is difficult to predict. Regardless, as this approach to engineering the host was unsuccessful, the remainder of the work in the thesis focused on the development and analysis of cell pools and lines stably expressing the assembly activating protein (AAP) and the impact on rAAV2 production genome packaging.

In order to assess the impact of AAP expression in HEK293T cells on rAAV production and genome packaging, the generation of HEK293T AAP engineered cell pools and clonal cell lines was undertaken and these then characterised. Chapter 4 describes the development of 4

plasmid vector constructs with different translation start codons for AAP (ATG or CTG) and either with or without a V5-tag for detection at the protein level; pcDNA3.1 ATGV5, pcDNA3.1 ATG-AAP STOP, pcDNA3.1 CTGV5 and pcDNA3.1 CTG-AAP STOP. As outlined in the introduction chapter, AAP translation is initiated from an unconventional or cryptic CTG start codon (Sonntag et al., 2010). Two versions of the AAP plasmid vectors were designed and supplied by Cobra Biologics, one containing the CTG start codon and another containing the conventional ATG start codon. The ATG-AAP and CTG-AAP genes were ligated into a hygromycin containing plasmid in frame with a V5-tag or with a stop codon preventing readthrough to the V5 tag. V5 tagging is a well-established method used for identification of proteins with the V5 tag having a strong, specific antibody binding (Burg et al., 2016) and such antibodies do not generally detect cellular mammalian proteins (the V5 tag is viral in origin). It was necessary to generate constructs containing the V5 tag as there are currently no antibodies against AAP commercially available.

Tagging of AAP is a common method of AAP detection throughout research where C-terminally tagging of AAP does not appear to impact its biological function (Earley et al., 2017; Grosse et al., 2017; Le et al., 2019; Maurer et al., 2019, 2018). Initial transient experiments were carried out prior to stable cell line generation that confirmed the constructs resulted in expression of the AAP protein from HEK293T cells. Stable cell pools and lines were successfully generated from all four constructs by random integration into the HEK293T host cell line. The process initially resulted in the generation of cell pools with variable transgene expression. Having constructs which were either tagged or untagged allowed investigations into whether the tag itself was the cause of any differences observed in the phenotype of the engineered cells. The overall results from the work showed that it was possible to generate cell lines stably expressing AAP and that furthermore, the stable constitutive expression of AAP did not significantly impact cell growth. When studying the impact of stable AAP expression on AAV2 titres and packaging as a whole, there was variance as might be expected from heterogenous pools where cells expressed different amounts of AAP. Further characterisation of the generated cell pools via immunofluorescence confirmed that there was variance in the AAP expression levels across the population, this variance is a result of random integration (Kirchhoff et al., 2020). Nevertheless, a trend was clear whereby ATG-AAP expressing cell pools generally showed an increase in genome packaging.

To help overcome the variability with the ATG-AAP cell pool, clonal cell lines were generated by single cell limited dilution cloning. The work described in chapter 5 focused on the generation and characterisation of the ATG-AAP expressing clonal cell lines. The focus on ATG-AAP expression was based on the trends observed in the studies described in chapter 4 where ATG-

AAP expressing cell pools indicated an increase in genome packaging efficiency. Eight clonal cell lines were generated, ATG06, ATG04, ATG02, ATG16, ATG36, ATG34, ATG33 and ATG66, these cell lines had a range of AAP-V5 expression across the cell lines as determined by V5-western blotting, with the ATG66 cell line being a high expressing cell line and ATG16 being the lowest expressing cell line. Once again, growth analysis confirmed in the clonal cell lines that the expression of ATG-AAPV5 did not impact the growth characteristics of the cell lines compared to the host HEK293T cell line.

Upon analysis of the AAV2 titres from these AAP expressing cell lines, as with the ATG-AAP pools, there was no statistical impact on the AAP total particle titre, however, both the ATG33 and the ATG66 cell line resulted in a significant increase in the percentage of packaged particles. Furthermore, the particles generated from these cell lines were able to transduce cells effectively, indicating that the particles derived from these cell lines could be used successfully as a viral vector. It is also important to note that while the cell lines have been generated to express AAP, there will also be further AAP expressed as a result of the triple transient transfection from the pAAV-RC-Kan plasmid. As there are no commercially available antibodies against AAP, we were unable to determine how much of an impact transient AAP expression has on total AAP expression. AAP expression from transient expression must be sufficient to support a certain amount of genome packaging as observed in the original HEK293T cells. However, at least for some of the stably engineered AAP clonal cell lines, the increase in AAP likely enhancers the ability of these to efficiently package particles. The fact this was observed in several engineered clonal cell lines that expressed the highest exogenous AAP provides further evidence that the high amounts of stably expressed AAP in these cell lines does provide a positive impact on packaging and is not due to random clonal variation between cell lines in packaging ability. Thus, the amount of AAP produced from transient *Cap* gene expression is likely to be insufficient to sustain high genome packaging efficiency for the rAAV2 serotype at least. This hypothesis could be further tested by knocking down or out the expression of the AAP in the engineered hosts and observing the impact on genome packaging which would be expected to decrease to those observed in the original host. Further evidence that additional AAP can enhance AAV production comes from studies by Le and colleagues who showed that addition of purified recombinant AAP could be used to increase AAV and VP3 VLP (virus like particle) yields in an *Escherichia coli* AAV production system (Le et al., 2019).

Assembly activating protein is usually expressed from the cryptic start codon (Earley et al., 2017; Galli et al., 2017; Naumer et al., 2012). For a long time it was thought that eukaryotic translation was always initiated by the conventional AUG start codon, however, since the late 1980s

translation initiation from non-conventional start codons has been identified (Ivanov et al., 2017; Peabody, 1989). However, translation initiation from these non-conventional start codons is at a lower efficiency than that of the conventional AUG start codon. The work in this thesis focused on generation of AAP cell lines which contained either the non-conventional CTG start codon, present in wildtype AAP, or AAP containing the conventional start codon ATG. Use of the ATG start codon was used to increase the expression of AAP with the CTG codon being only 30-60% as efficient as the conventional ATG start codon in initiating translation (Kearse & Wilusz, 2017; Loughran et al., 2020; Mehdi, Ono, & Gupta, 1990). A similar approach was reported by Earley and colleagues to express AAP, showing that by utilising the strong ATG start codon it was possible to express steady levels of AAP (Earley et al., 2015, 2017). Furthermore, research carried out with AAV capsid chimeras utilised AAP plasmids vectors where the CTG start codon had been switched out for an ATG start codon, showing that for AAP6, titre improvements were observed only in the presence of the ATG canonical start codon and not in the presence of the CTG start codon (Viney et al., 2021). While this work was with AAP6, the findings are in line with what were observed with AAP2 in the current study.

As shown by immunofluorescence in chapters 4 and 5, AAP2 localises in the nucleus/nucleolus of the cell. This finding is in line with other works, which have shown through immunofluorescence that tagged AAP is localised to the nucleolus (Sonntag et al., 2010). The use of a tag for the visualisation and identification of AAP has been shown have no detrimental effects on the function of AAP with a number of tags being used in AAP research including the FLAG tag, His tag, C9 tag and AU1 tag (Earley et al., 2017; Le et al., 2019; Sonntag et al., 2011; Tse et al., 2018).

Interestingly, AAP expression varies across AAV serotypes 1-12. Earley and colleagues have mapped the nuclear and nucleolar localisation signals for AAP across the serotypes, identifying overlapping nuclear and nucleolar localisation signals near the C-terminus of AAP2 (Earley et al., 2015). As shown in the work reported in this thesis, immunofluorescence studies showed that for all AAV serotypes AAP expression was found in the nucleus. However, the nucleolar localisation was serotype specific. Earley's work studied a FLAG tagged AAP across serotypes 1-12 in HeLa cells (Earley et al., 2017). Based on the findings described in chapter 4, there was no indication that the V5 tag was impacting cell growth, however it was not possible from these data to determine if the tag was responsible for any impact on the packaging. To confirm the tag was not impacting packaging efficiency, the ATG-AAP STOP and CTG-AAP-STOP cell pools were also investigated, where a stop codon has been introduced prior to the V5 tag, these giving similar packaging efficiency to that of their tagged equivalents.

The data reported in this thesis has shown that rAAV2 generated in the AAP engineered HEK293T clonal cell lines transduced at efficiencies similar to that of rAAV produced in the original HEK293T host cell line. Thus, the AAP engineered host gave higher packaging efficiencies with similar transduction efficiencies meaning that more particles or doses can be generated. It is noted that the work here is solely focused on the AAP from serotype 2 (AAP2) and its impact on the production of recombinant AAV particles from serotype 2, cell lines expressing AAP from other serotypes or production of rAAV of other serotypes in the AAP2 engineered HEK293T hosts were not investigated. However, research has been carried out on AAP of other AAV serotypes and of AAV chimeras. One such study focusing on the impact of AAP6 on AAV capsid chimeras by Viney and colleagues showed that AAP expression can have an impact on the transduction efficiency of the AAV capsid chimeras (Viney et al., 2021) although this was not observed with the system (AAP2/rAAV2) investigated here.

As outlined above, the identification of AAP only was reported in 2010 by Sonntag and colleagues when they identified that a viral assembly factor promoted AAV serotype 2 formation (Sonntag et al., 2010). Since then, much research into AAP has been carried out, with most of the studies focusing on the role of AAP as a chaperone whereby it mediates and stabilizes AAV capsid formation. The protein structure of AAP has yet to be characterised fully and there has been no data published on the complete structure. It has been shown that AAP interacts with the capsid proteins (VP proteins) to traffic them to the nucleolus, while also providing some protection against degradation and stability of the monomers (Maurer et al., 2019). Quite how this function improves genome packaging is unclear, but it is possible that the presence of AAP helps in recruiting or 'feeding' of the genome into the formed capsid.

There are 12 other wild type AAV serotypes identified and over a hundred AAV hybrid serotypes and pseudo serotypes that have been engineered (Hammond, Leek, Richman, & Tjalkens, 2017). AAP has been shown to be essential for not only AAV2 capsid production but for all AAV serotypes with the exception of serotypes 4, 5 and 11 (Earley et al., 2017). Studies into capsid formation across the different serotypes have shown that AAP is essential for the particle production from serotypes 1, 8 and 9, however the AAP used was not specific to the serotype, Sonntag et al demonstrating it was possible to form AAV1/8/9 particles in the presence of AAP2 (Sonntag et al., 2011). This indicates that cross complementation of AAP is possible. It would be interesting to determine if the packaging of other serotypes such as 1, 8 and 9 can also be impacted using the AAP2 HEK293T expressing cell lines described in this thesis.

6.2 Future Work

The work described to generate a Rep or Rep-Cap expressing cell line were unsuccessful, likely due to the toxicity associated with the larger Rep proteins. At this point the work described in this thesis moved away from the Rep and Cap proteins and focus moved towards the Assembly Activating Protein. However, there are a number of avenues which could be investigated in order to generate Rep and Rep Cap expressing cell lines. Inducible mammalian cell lines are commonly used for the production of recombinant proteins. Cell lines have been successfully developed to inducibly express the AAV Rep and Cap proteins upon co-infection with adenovirus (K R Clark et al., 1996; X. Liu et al., 2000). As rAAV production has moved away from co-infecting with a helper virus and uses a helper plasmid instead, other methods of inducing expression could be investigated. Yang and colleagues have generated cell lines which can be induced to express the Rep proteins under the control of the metallothionein I promoter, this method of inducing Rep expression overcame the cytotoxic effects of Rep78 (Q Yang, Chen, & Trempe, 1994a). A further potential method used to generate inducible cell lines is Tetracycline-inducible cell lines (Chtarto et al., 2003; Gomez-Martinez, Schmitz, & Hergovich, 2013). Generation of an inducible Rep expressing cell line is one possible way to overcome the cytotoxicity associated with Rep 78, however other work has shown that generation of a Rep inducible cell line is not without its challenges. It is possible to regulate Rep78/68 expression by replacing the p5 promoter with an inducible promoter such as the tetracycline inducible system (Qiao, Li, et al., 2002). Generation of inducible cell lines is not the only avenue that could be investigated for the generation of stable cell lines, regulating the expression of the various rep genes. It has been shown that decreasing Rep 78 expression could reduce cytotoxicity (Dirk Grimm et al., 1998). However, such approaches would be similar to what has already been attempted. A more finely tuned inducible system that allowed different amounts of Rep proteins to be expressed, or that gave control of individual Rep proteins, would allow titration of the cytotoxic effect to determine an 'optimal' level of expression and time over which this could be tolerated by the cell before it became detrimental.

As a follow on from the work described in chapter 3 and chapter 4, the generation of an antibody against AAP would be useful. This would allow monitoring of the levels of AAP produced from transient co-transfection of the AAV plasmids used for AAV2 production, in comparison to the AAP produced by the stable cell pools and lines. Generation of such an AAP antibody could be utilised for further characterisation of the rAAV2 capsids, and the cell lines used to generate these particles. One further approach to characterise the cell lines could involve the generation of a Rep Cap plasmid vector where there is no expression of AAP, allowing determination as to

whether the effects on packaging observed in this thesis are solely due to the AAP expressed by the cell line or whether AAP from the transient transfection also is important when this is already stably expressed. Indeed, Maurer and colleagues showed that it is possible to introduce a stop codon into the *AAP* gene that hinders AAP expression from the Rep Cap plasmid vectors (Maurer et al., 2018). This would be a potential way to compare the impact of stable exogenous AAP in the presence of the AAP from the *Cap* gene during AAV production. This would also be a way of comparing the tagged AAP expression to the transient AAP expression without the need for an AAP antibody. Furthermore, introduction of a stop codon in the AAP sequence of the *Cap* gene has been shown to prevent rAAV2 capsid formation (Grosse et al., 2017). As previously mentioned for AAV serotypes 1, 8 and 9, AAP2 is sufficient in place of the serotype specific AAP to drive capsid formation (Sonntag et al., 2011). Based on this, it would be interesting to determine if AAV packaging of the other AAV serotypes, mainly AAV 1, 8 and 9, could be impacted by the use of the AAP2 expressing cell lines and pools.

While it has been shown that AAP is a rate limiting factor of AAV production, Grosse and colleagues suggested that overexpression of AAP does not result in an increase in AAV particles nor was there any indication that the AAP over expression would result in an increased viral genome yield (Grosse et al., 2017). The work described in this thesis is in direct contrast to these findings, showing an increase in the genome packaging of rAAV2 particles. It is possible there is a timing and threshold level of AAP required to elicit the increased packaging observed. This is further evidenced by the fact that when using the CTG start codon to make stable AAP expressing HEK293T cells, the amount of stable AAP expressed was much lower than from the ATG start codon and no increase in genome packaging was observed. Further, the generation of additional AAP upon transient transfection may 'tip' the balance towards favourable genome packaging compared to that observed in non-AAP expressing cell lines where there is a delay in achieving a threshold AAP level. Thus, it would be important in the future to define the kinetics of AAP expression in the stable and transfected cells and the generation of an AAP specific antibody would help in such studies.

A recent report by Yu and colleagues showed that AAV production can be increased in the Herpes simplex virus production system upon supplementation with KCl and NaCl. This study showed that when KCl and NaCl were supplemented 16 hours post infection a 10-fold increase in AAV vector production was observed when produced in the presence of HSV. Furthermore, this method of producing vectors resulted in increased packaging of the particles (Yu et al., 2021). Supplementation of media is a commonly used method of producing recombinant proteins and as such it would be worthwhile to study the impact of supplementation on the AAP

expressing cells during rAAV2 production. This would not be limited to KCl and NaCl, but other supplements which have been shown to increase protein production could also be investigated. For example, valproic acid, that inhibits histone deacetylase activity, has been shown to enhance recombinant protein expression levels in both HEK and CHO cell transient expression systems. Cervera and colleagues have shown that it is possible to increase GAG VLP production in HEK293 cells by addition of valproic acid (Backliwal et al., 2008; Cervera et al., 2015; Wulhfard, Baldi, Hacker, & Wurm, 2010). Addition of such histone deacetylase inhibitors could therefore be investigated to determine if these can enhance rAAV production and packaging.

Finally, the studies reported here have shown that AAP engineered HEK293T cells can be produced with increased genome packaging efficiency. However, an important next step would be to carry out industrially relevant large scale production runs using the AAP cell lines described in this thesis. The work described in this thesis used an adherent method for AAV production using CellBIND flask, however adherent methods are not as easy to scale up as suspension culture methods. Furthermore, suspension methods are more suitable at an industrial level for upstream processing. As such it would be essential to carry out a large-scale production run adherently but to also optimise the small-scale production run to suspension and compare to a large-scale production run. Systems such as CellSTACKs or CellCubes are suitable for large scale adherent cultures for the production of rAAV particles, have been shown to produce yields of 10^{14} -10^{15} rAAV particles (R. M. Kotin, 2011). The move to a suspension system traditionally involves the move away from serum media in a step wise manner while the cells are adapted to suspension. As the host cell line used in this study is a suspension adapted cell line which grows successfully in suspension cultures the complete adaption of this system to suspension would require the transfection protocol to be optimised for a suspension culture, this would require testing a range of DNA concentrations, plasmid ratios and PEI concentrations followed by analysis of AAV titre.

6.3 Limitations of the study

As previously described in Chapter 1, rAAV vectors are typically produced using HEK cell lines, including HEK293T (Grieger et al., 2016; Kimura et al., 2019). The HEK cell line was originally derived by the transformation of the primary cells with a fragment of Adenoviral DNA which encodes the *E1A* and *E1B* genes (W. C. Russell et al., 1977). From this, HEK293T cells were generated by the stable transfection of HEK293 cells with a plasmid encoding a temperature sensitive SV40 large T antigen(Bae et al., 2020; DuBridge et al., 1987). However, the presence of this SV40 large T antigen can potentially pose a safety risk for biological products produced in

cell lines such as HEK293T. SV40 large T antigens have been known to transform human cells both *in vitro* and *in vivo.* Furthermore, SV40 transformed cells can produce tumours in nude mice, thus the presence of the SV40 large T antigen protein or DNA in AAV vectors or other viral vectors is a safety risk and approving bodies such as the FDA are suggesting the move away from the use of HEK293T cells (Bae et al., 2020; Brooks et al., 1988; Reddel et al., 1993).

The work described in this thesis utilised HEK293T cells, and should the industrial collaborator Cobra Biologics wish to commercially use the cell lines generated in Chapter 5 of this thesis (e.g. A66), this would need to be taken into consideration. Despite this limitation, work has been carried out by other research groups to remove the SV40 large T antigen from the cells without impacting viral genome titres when producing viral vectors. Research by Bae and colleagues utilised a CRISPR-Cas9 system to remove any SV40 sequences from HEK293T cells using guide RNA targeting the beginning and end of the large T antigen. They showed that using the generated cells lacking the T antigen, it was possible to obtain lentiviral vectors and AAV vectors with titres similar to those of the T antigen containing cells(Bae et al., 2020). This shows promise that a method such as CRISPR could be used to remove the large T antigen from the AAP expressing cell lines discussed in chapter 5 with little impact on rAAV yields. It is worth noting, however, that the work described by Bae and colleagues utilised HEK293T cells grown in the presence of 10% FBS. A further approach would be to re-generate AAP expressing cells using the HEK293 host cell line that does not contain the T antigen.

One potential limitation with the work described in this thesis is the AAV production method, while the parental cell line, HEK293T, has been suspension adapted and is grown in the absence of serum, the physical production method currently occurs in an adherent manner. Adherent production systems are not ideal for large scale manufacturing. One reason for this is due to the difficulty in scaling out the manufacturing compared to suspension culture scale up. As the cells have already been adapted to serum free media, moving the transfection protocol to a suspension method would be more straightforward than if the cells needed to be suspension adapted first. Suspension adaption traditionally involves the gradual move away from serum containing media. This is done by reducing the percentage of FBS containing media gradually. Large scale manufacturing using adherent cultures typically takes place using multitrays/cell stacks or in roller bottles. This method is both time consuming and labour intensive at large scale. One method used to overcome the challenges of large scale adherent culture is transfecting in suspension, this is typically performed in flasks or stirred tank bioreactors which are much more manageable than that of their adherent counterparts. One unfortunate downside to the suspension method is the reduced transfection efficiency, which

can result in a reduced titre (Clément & Grieger, 2016). Thus, the move to a fully suspension production method would require studies to vary the concentration of both plasmids and transfection reagent to achieve similar yields to that of the adherent process described in this thesis

6.4 Conclusion

Overall, the work in this thesis has focused on the establishment of cell pools and lines for the production of rAAV2 particles, particularly investigating the impact of AAP expression, with the ultimate aim of increasing the genome packaging of rAAV particles. The generation of Assembly Activating Protein (AAP) expressing HEK293T cell lines, both pools and clonal in nature allowed the impact of expression of different amounts of AAP stable on rAAV production to be assessed. Cell pools were generated with cells stably expressing AAP from either the cryptic CTG start codon or an ATG start codon. The work described in chapter 4 indicated that the expression initiated at the ATG start codon appeared to have an impact on rAAV packaging by increasing the viral genome titres, in contrast to this the cell lines expressing the CTG initiated AAP, where AAP was expressed at much lower amounts, did not appear to have any impact on rAAV packaging. Based on immunofluorescence, ATG-AAP was expressed at much higher levels than that of the CTG-AAP. From this, a selection of relatively high, medium and low AAP expressing clonal HEK293T cell lines were isolated and characterised. The analysis of these showed that it was possible to generate ATG-AAP expressing cell lines which had a positive impact on the packaging of rAAV2 particles by increasing the percentage of packaged particles from less than 20% up to 50-80% packaged. Furthermore, this work showed that the rAAV2.GFP particles produced via the AAP expressing cell lines where rAAV2.GFP packaging was increased were functional at the same MOIs as the particles generated by the HEK293T host cell line. Thus, these cell lines at small scale indicate an improved viral genome titre for viral vectors produced in the high stably expressing AAP HEK293T cell lines.

Bibliography

(CDER), C. FOR D. EVALUATION AND R. (2019). Advancing Health Through Innovation New Drug Therapy Approvals 2018. *U.S. Food and Drug Administration (FDA)*, (January), 1–36.

AIHARA, H., & MIYAZAKI, J. (1998). Gene transfer into muscle by electroporation in vivo. *Nature Biotechnology*, **16**(9), 867–870.

AKIL, O., DYKA, F., CALVET, C., EMPTOZ, A., LAHLOU, G., NOUAILLE, S., … LUSTIG, L. R. (2019). Dual AAV-mediated gene therapy restores hearing in a DFNB9 mouse model. *Proceedings of the National Academy of Sciences*, **116**(10), 4496–4501.

AL-BATAINEH, O., JENNE, J., & HUBER, P. (2012). Clinical and future applications of high intensity focused ultrasound in cancer. *Cancer Treatment Reviews*, **38**(5), 346–353.

ALLAY, J. A., SLEEP, S., LONG, S., TILLMAN, D. M., CLARK, R., CARNEY, G., … GRAY, J. T. (2011). Good Manufacturing Practice Production of Self-Complementary Serotype 8 Adeno-Associated Viral Vector for a Hemophilia B Clinical Trial. *Human Gene Therapy*, **22**(5), 595–604.

ALVAREZ-ERVITI, L., SEOW, Y., YIN, H., BETTS, C., LAKHAL, S., & WOOD, M. J. A. (2011). Delivery of siRNA to the mouse brain by systemic injection of targeted exosomes. *Nature Biotechnology*, **29**(4), 341–345.

AMANAT, F., & KRAMMER, F. (2020). SARS-CoV-2 Vaccines: Status Report. *Immunity*, **52**(4), 583–589.

ANDERSON, R., MACDONALD, I., CORBETT, T., WHITEWAY, A., & PRENTICE, H. G. (2000). A method for the preparation of highly purified adeno-associated virus using affinity column chromatography, protease digestion and solvent extraction. *Journal of Virological Methods*, **85**(1–2), 23–34.

ANGUELA, X. M., & HIGH, K. A. (2019). Entering the Modern Era of Gene Therapy. *Annual Review of Medicine*, **70**, 273–288.

ARICESCU, A. R., LU, W., & JONES, E. Y. (2006). A time- and cost-efficient system for high-level protein production in mammalian cells. *Acta Crystallographica Section D Biological Crystallography*, **62**(10), 1243–1250.

ASHKTORAB, H., & SRIVASTAVA, A. (1989). Identification of nuclear proteins that specifically interact with adeno-associated virus type 2 inverted terminal repeat hairpin DNA. *Journal of Virology*, **63**(7), 3034–3039.

ASOKAN, A., SCHAFFER, D. V, & JUDE SAMULSKI, R. (2012). The AAV Vector Toolkit: Poised at the Clinical Crossroads. *Molecular Therapy*, **20**(4), 699–708.

ATCHISON, R. W., CASTO, B. C., & HAMMON, W. M. (1965). Adenovirus-Associated Defective Virus Particles. *Science*, **149**(3685), 754–755.

AUCOIN, M. G., PERRIER, M., & KAMEN, A. A. (2008). Critical assessment of current adeno-associated viral vector production and quantification methods. *Biotechnology Advances*, **26**(1), 73–88.

AURNHAMMER, C., HAASE, M., MUETHER, N., HAUSL, M., RAUSCHHUBER, C., HUBER, I., … BAIKER, A. (2012). Universal Real-Time PCR for the Detection and Quantification of Adeno-Associated Virus Serotype 2-Derived Inverted Terminal Repeat Sequences. *Human Gene Therapy Methods*, **23**(1), 18–28.

BABU, A., MURALIDHARAN, R., AMREDDY, N., MEHTA, M., MUNSHI, A., & RAMESH, R. (2016). Nanoparticles for siRNA-Based Gene Silencing in Tumor Therapy. *IEEE Transactions on NanoBioscience*, **15**(8), 849–863.

BACKLIWAL, G., HILDINGER, M., KUETTEL, I., DELEGRANGE, F., HACKER, D. L., & WURM, F. M. (2008). Valproic acid: A viable alternative to sodium butyrate for enhancing protein expression in mammalian cell cultures. *Biotechnology and Bioengineering*, **101**(1), 182–189.

BAE, D. H., MARINO, M., IAFFALDANO, B., FENSTERMAKER, S., AFIONE, S., ARGAW, T., … REISER, J. (2020). Design and Testing of Vector-Producing HEK293T Cells Bearing a Genomic Deletion of the SV40 T Antigen Coding Region. *Molecular Therapy - Methods & Clinical Development*, **18**, 631–638.

BALAKRISHNAN, B., & JAYANDHARAN, G. (2014). Basic Biology of Adeno-Associated Virus (AAV) Vectors Used in Gene Therapy. *Current Gene Therapy*, **14**(2), 1–15.

BALAZS, A. B., CHEN, J., HONG, C. M., RAO, D. S., YANG, L., & BALTIMORE, D. (2012). Antibody-based protection against HIV infection by vectored immunoprophylaxis. *Nature*, **481**(7379), 81–84.

BALAZS, A. B., & WEST, A. P. (2013). Antibody gene transfer for HIV immunoprophylaxis. *Nature Immunology*, **14**(1), 1–5.

BALDI, L., HACKER, D. L., MEERSCHMAN, C., & WURM, F. M. (2012). *Large-Scale Transfection of Mammalian Cells*.

BARTLETT, J. S., WILCHER, R., & SAMULSKI, R. J. (2000). Infectious Entry Pathway of Adeno-Associated Virus and Adeno-Associated Virus Vectors. *Journal of Virology*, **74**(6), 2777–2785.

BARTON, G. M., & MEDZHITOV, R. (2002). Retroviral delivery of small interfering RNA into primary cells. *Proceedings of the National Academy of Sciences*, **99**(23), 14943–14945.

BASU, S., CAMPBELL, H. M., DITTEL, B. N., & RAY, A. (2010). Purification of Specific Cell Population by Fluorescence Activated Cell Sorting (FACS). *Journal of Visualized Experiments*, (41).

BATCHU, R. B., SHAMMAS, M. A., WANG, J. Y., & MUNSHI, N. C. (1999). Interaction of adeno-associated virus Rep78 with p53: implications in growth inhibition. *Cancer Research*, **59**(15), 3592–3595.

BECERRA, S. P., KOCZOT, F., FABISCH, P., & ROSE, J. A. (1988). Synthesis of adeno-associated virus structural proteins requires both alternative mRNA splicing and alternative initiations from a single transcript. *Journal of Virology*, **62**(8), 2745–2754.

BELL, C. L., GURDA, B. L., VAN VLIET, K., AGBANDJE-MCKENNA, M., & WILSON, J. M. (2012). Identification of the Galactose Binding Domain of the Adeno-Associated Virus Serotype 9 Capsid. *Journal of Virology*, **86**(13), 7326–7333.

BERNS, K. I., & GIRAUD, C. (1996). *Biology of Adeno-associated Virus*.

BERNS, KENNETH I. (2020). The Unusual Properties of the AAV Inverted Terminal Repeat. *Human Gene Therapy*, **31**(9–10), 518–523.

BERRY, G. E., & ASOKAN, A. (2016). Cellular transduction mechanisms of adeno-associated viral vectors. *Current Opinion in Virology*, **21**, 54–60.

BERTHET, C., RAJ, K., SAUDAN, P., & BEARD, P. (2005). How adeno-associated virus Rep78 protein arrests cells completely in S phase. *Proceedings of the National Academy of Sciences*,

102(38), 13634–13639.

BIER, M., HAMMER, S. M., CANADAY, D. J., & LEE, R. C. (1999). Kinetics of sealing for transient electropores in isolated mammalian skeletal muscle cells. *Bioelectromagnetics*, **20**(3), 194–201.

BLEKER, S., PAWLITA, M., & KLEINSCHMIDT, J. A. (2006). Impact of Capsid Conformation and Rep-Capsid Interactions on Adeno-Associated Virus Type 2 Genome Packaging. *Journal of Virology*, **80**(2), 810–820.

BLESSING, D., VACHEY, G., PYTHOUD, C., REY, M., PADRUN, V., WURM, F. M., … DEGLON, N. (2019). Scalable Production of AAV Vectors in Orbitally Shaken HEK293 Cells. *Molecular Therapy - Methods & Clinical Development*, **13**, 14–26.

BOGGIO, A., KNOPPERS, B. M., ALMQVIST, J., & ROMANO, C. P. R. (2019). The Human Right to Science and the Regulation of Human Germline Engineering. *The CRISPR Journal*, **2**(3), 134–142.

BOREL, F., KAY, M. A., & MUELLER, C. (2014). Recombinant AAV as a Platform for Translating the Therapeutic Potential of RNA Interference. *Molecular Therapy*, **22**(4), 692–701.

BOREL, F., & MUELLER, C. (2019). *Design of AAV Vectors for Delivery of RNAi*.

BOSHTAM, M., ASGARY, S., RAHIMMANESH, I., KOUHPAYEH, S., NADERI, J., HEJAZI, Z., … KHANAHMAD, H. (2018). Display of human and rabbit monocyte chemoattractant protein-1 on human embryonic kidney 293T cell surface. *Research in Pharmaceutical Sciences*, **13**(5), 430.

BOUSSIF, O., LEZOUALC'H, F., ZANTA, M. A., MERGNY, M. D., SCHERMAN, D., DEMENEIX, B., & BEHR, J. P. (1995). A versatile vector for gene and oligonucleotide transfer into cells in culture and in vivo: polyethylenimine. *Proceedings of the National Academy of Sciences*, **92**(16), 7297–7301.

BRACEWELL, D. G., FRANCIS, R., & SMALES, C. M. (2015). The future of host cell protein (HCP) identification during process development and manufacturing linked to a risk-based management for their control. *Biotechnology and Bioengineering*, **112**(9), 1727–1737.

BRACEWELL, D. G., SMITH, V., DELAHAYE, M., & SMALES, C. M. (2021). Analytics of host cell proteins (HCPs): lessons from biopharmaceutical mAb analysis for Gene therapy products. *Current Opinion in Biotechnology*, **71**, 98–104.

BROOKS, S. E., ADACHI, M., HOFFMAN, L. M., STEIN, M. R., BROOKS, J., & SCHNECK, L. (1988). Induction of lymphomas and fibrosarcomas in nude mice after implantation of simian virus 40-transformed human meningioma. *Laboratory Investigation; a Journal of Technical Methods and Pathology*, **58**(5), 518–523.

BROWNE, S. M., & AL-RUBEAI, M. (2007). Selection methods for high-producing mammalian cell lines. *Trends in Biotechnology*, **25**(9), 425–432.

BULCHA, J. T., WANG, Y., MA, H., TAI, P. W. L., & GAO, G. (2021). Viral vector platforms within the gene therapy landscape. *Signal Transduction and Targeted Therapy*, **6**(1), 53.

BULLER, R. M. L., JANIK, J. E., SEBRING, E. D., & ROSE, J. A. (1981). Herpes Simplex Virus Types 1 and 2 Completely Help Adeno-Associated Virus Replication. *Journal of Virology*, **40**(1), 241–247.

BURG, L., ZHANG, K., BONAWITZ, T., GRAJEVSKAJA, V., BELLIPANNI, G., WARING, R., & BALCIUNAS, D. (2016). Internal epitope tagging informed by relative lack of sequence conservation. *Scientific Reports*, **6**(1), 36986.

BURNETT, J. R., & HOOPER, A. J. (2009). Alipogene tiparovec, an adeno-associated virus encoding the Ser(447)X variant of the human lipoprotein lipase gene for the treatment of patients with lipoprotein lipase deficiency. *Current Opinion in Molecular Therapy*, **11**(6), 681–691.

BUROVA, E., & IOFFE, E. (2005). Chromatographic purification of recombinant adenoviral and adeno-associated viral vectors: methods and implications. *Gene Therapy*, **12**(S1), S5–S17.

BUSBY, M., XUE, C., LI, C., FARJOUN, Y., GIENGER, E., YOFE, I., … GOREN, A. (2016). Systematic comparison of monoclonal versus polyclonal antibodies for mapping histone modifications by ChIP-seq. *Epigenetics & Chromatin*, **9**(1), 49.

Calcium phosphate–mediated transfection of eukaryotic cells. (2005). *Nature Methods*, **2**(4), 319–320.

CAPPELLA, M., CIOTTI, C., COHEN-TANNOUDJI, M., & BIFERI, M. G. (2019). Gene Therapy for ALS—A Perspective. *International Journal of Molecular Sciences*, **20**(18), 4388.

CARTON, J. M., SAUERWALD, T., HAWLEY-NELSON, P., MORSE, B., PEFFER, N., BECK, H., … SWEET, R. (2007). Codon engineering for improved antibody expression in mammalian cells. *Protein Expression and Purification*, **55**(2), 279–286.

CASSINOTTI, P., WEITZAND, M., & TRATSCHIN, J.-D. (1988). Organization of the adeno-associated virus (AAV) capsid gene: Mapping of a minor spliced mRNA coding for virus capsid protein. *Virology*, **167**(1), 176–184.

CAVAZZANA-CALVO, M. (2000). Gene Therapy of Human Severe Combined Immunodeficiency (SCID)-X1 Disease. *Science*, **288**(5466), 669–672.

Cell and Gene Therapy Catapult ATMP clinical trials report 2020. (2020).

CERVERA, L., FUENMAYOR, J., GONZÁLEZ-DOMÍNGUEZ, I., GUTIÉRREZ-GRANADOS, S., SEGURA, M. M., & GÒDIA, F. (2015). Selection and optimization of transfection enhancer additives for increased virus-like particle production in HEK293 suspension cell cultures. *Applied Microbiology and Biotechnology*, **99**(23), 9935–9949.

CERVERA, L., GUTIÉRREZ, S., GÒDIA, F., & SEGURA, M. M. (2011). Optimization of HEK 293 cell growth by addition of non-animal derived components using design of experiments. *BMC Proceedings*, **5**(Suppl 8), P126.

CHADEUF, G., FAVRE, D., TESSIER, J., PROVOST, N., NONY, P., KLEINSCHMIDT, J., … SALVETTI, A. (2000). Efficient recombinant adeno-associated virus production by a stable rep-cap HeLa cell line correlates with adenovirus-induced amplification of the integrated rep-cap genome. *The Journal of Gene Medicine*, **2**(4), 260–268.

CHAHAL, P. S., SCHULZE, E., TRAN, R., MONTES, J., & KAMEN, A. A. (2014). Production of adeno-associated virus (AAV) serotypes by transient transfection of HEK293 cell suspension cultures for gene delivery. *Journal of Virological Methods*, **196**, 163–173.

CHANG, L. S., SHI, Y., & SHENK, T. (1989). Adeno-associated virus P5 promoter contains an adenovirus E1A-inducible element and a binding site for the major late transcription factor. *Journal of Virology*, **63**(8), 3479–3488.

CHAO, H., LIU, Y., RABINOWITZ, J., LI, C., SAMULSKI, R. J., & WALSH, C. E. (2000). Several Log Increase in Therapeutic Transgene Delivery by Distinct Adeno-Associated Viral Serotype Vectors. *Molecular Therapy*, **2**(6), 619–623.

CHERIAN, D. S., BHUVAN, T., MEAGHER, L., & HENG, T. S. P. (2020). Biological Considerations in Scaling Up Therapeutic Cell Manufacturing. *Frontiers in Pharmacology*, **11**.

CHIORINI, J. A., WIENER, S. M., YANG, L., SMITH, R. H., SAFER, B., KILCOIN, N. P., … KOTIN, R. M. (1996). *The Roles of AAV Rep Proteins in Gene Expression and Targeted Integration*.

CHTARTO, A., BENDER, H. U., HANEMANN, C. O., KEMP, T., LEHTONEN, E., LEVIVIER, M., … TENENBAUM, L. (2003). Tetracycline-inducible transgene expression mediated by a single AAV vector. *Gene Therapy*, **10**(1), 84–94.

CLARK, K. REED, VOULGAROPOULOU, F., FRALEY, D. M., & JOHNSON, P. R. (1995). Cell Lines for the Production of Recombinant Adeno-Associated Virus. *Human Gene Therapy*, **6**(10), 1329–1341.

CLARK, K R, VOULGAROPOULOU, F., & JOHNSON, P. R. (1996). A stable cell line carrying adenovirus-inducible rep and cap genes allows for infectivity titration of adeno-associated virus vectors. *Gene Therapy*, **3**(12), 1124–1132.

CLÉMENT, N., & GRIEGER, J. C. (2016). Manufacturing of recombinant adeno-associated viral vectors for clinical trials. *Molecular Therapy - Methods & Clinical Development*, **3**, 16002.

COLELLA, P., RONZITTI, G., & MINGOZZI, F. (2018). Emerging Issues in AAV-Mediated In Vivo Gene Therapy. *Molecular Therapy - Methods and Clinical Development*, Vol. 8.

CÔTÉ, J., GARNIER, A., MASSIE, B., & KAMEN, A. (1998). Serum-free production of recombinant proteins and adenoviral vectors by 293SF-3F6 cells. *Biotechnology and Bioengineering*, **59**(5), 567–575.

COTRIM, A. P., & BAUM, B. J. (2008). Gene Therapy: Some History, Applications, Problems, and Prospects. *Toxicologic Pathology*, **36**(1), 97–103.

D'COSTA, S., BLOUIN, V., BROUCQUE, F., PENAUD-BUDLOO, M., FÇRANOIS, A., PEREZ, I. C., … AYUSO, E. (2016). Practical utilization of recombinant AAV vector reference standards: focus on vector genomes titration by free ITR qPCR. *Molecular Therapy - Methods and Clinical Development*, **5**.

DASHKOFF, J., LERNER, E. P., TRUONG, N., KLICKSTEIN, J. A., FAN, Z., MU, D., … HUDRY, E. (2016). Tailored transgene expression to specific cell types in the central nervous system after peripheral injection with AAV9. *Molecular Therapy - Methods & Clinical Development*, **3**, 16081.

DAYA, S., & BERNS, K. I. (2008). Gene Therapy Using Adeno-Associated Virus Vectors. *Clinical Microbiology Reviews*, **21**(4), 583–593.

DE LOS MILAGROS BASSANI MOLINAS, M., BEER, C., HESSE, F., WIRTH, M., & WAGNER, R. (2014). Optimizing the transient transfection process of HEK-293 suspension cells for protein production by nucleotide ratio monitoring. *Cytotechnology*, **66**(3), 493–514.

DEAN, D. A. (2006). Gene Delivery by Direct Injection (Microinjection) Using a Pulsed-Flow System. *Cold Spring Harbor Protocols*, **2006**(30), pdb.prot4653-pdb.prot4653.

DENET, A.-R., VANBEVER, R., & PRÉAT, V. (2004). Skin electroporation for transdermal and topical delivery. *Advanced Drug Delivery Reviews*, **56**(5), 659–674.

DIAS FLORENCIO, G., PRECIGOUT, G., BELEY, C., BUCLEZ, P.-O., GARCIA, L., & BENCHAOUIR, R. (2015). Simple downstream process based on detergent treatment improves yield and in vivo transduction efficacy of adeno-associated virus vectors. *Molecular Therapy - Methods & Clinical Development*, **2**, 15024.

DICKERSON, R., ARGENTO, C., PIERACCI, J., & BAKHSHAYESHI, M. (2020). Separating Empty and Full Recombinant Adeno-Associated Virus Particles Using Isocratic Anion Exchange

Chromatography. *Biotechnology Journal*, e2000015.

DiMattia, M. A., Nam, H.-J., Van Vliet, K., Mitchell, M., Bennett, A., Gurda, B. L., … Agbandje-McKenna, M. (2012). Structural Insight into the Unique Properties of Adeno-Associated Virus Serotype 9. *Journal of Virology*, **86**(12), 6947–6958.

Do Minh, A., Tran, M. Y., & Kamen, A. A. (2020). *Lentiviral Vector Production in Suspension Culture Using Serum-Free Medium for the Transduction of CAR-T Cells*.

Dobnik, D., Kogovšek, P., Jakomin, T., Košir, N., Tušek Žnidarič, M., Leskovec, M., … Ravnikar, M. (2019). Accurate Quantification and Characterization of Adeno-Associated Viral Vectors. *Frontiers in Microbiology*, **10**.

Domenger, C., & Grimm, D. (2019). Next-generation AAV vectors - don't judge a virus (only) by its cover. *Human Molecular Genetics*.

Dong, B., Duan, X., Chow, H. Y., Chen, L., Lu, H., Wu, W., … Xiao, W. (2014). Proteomics Analysis of Co-Purifying Cellular Proteins Associated with rAAV Vectors. *PLoS ONE*, **9**(2), e86453.

Drouin, L. M., & Agbandje-McKenna, M. (2013). Adeno-associated virus structural biology as a tool in vector development. *Future Virology*, **8**(12), 1183–1199.

DuBridge, R. B., Tang, P., Hsia, H. C., Leong, P. M., Miller, J. H., & Calos, M. P. (1987). Analysis of mutation in human cells by using an Epstein-Barr virus shuttle system. *Molecular and Cellular Biology*, **7**(1), 379–387.

Dull, T., Zufferey, R., Kelly, M., Mandel, R. J., Nguyen, M., Trono, D., & Naldini, L. (1998). A Third-Generation Lentivirus Vector with a Conditional Packaging System. *Journal of Virology*, **72**(11), 8463–8471.

Dumont, J., Euwart, D., Mei, B., Estes, S., & Kshirsagar, R. (2016). Human cell lines for biopharmaceutical manufacturing: history, status, and future perspectives. *Critical Reviews in Biotechnology*, **36**(6), 1110–1122.

Durocher, Y., Pham, P. L., St-Laurent, G., Jacob, D., Cass, B., Chahal, P., … Kamen, A. (2007). Scalable serum-free production of recombinant adeno-associated virus type 2 by transfection of 293 suspension cells. *Journal of Virological Methods*, **144**(1–2), 32–40.

Dyson, M. R. (2016). *Fundamentals of Expression in Mammalian Cells*.

Earley, L. F., Kawano, Y., Adachi, K., Sun, X.-X., Dai, M.-S., & Nakai, H. (2015). Identification and Characterization of Nuclear and Nucleolar Localization Signals in the Adeno-Associated Virus Serotype 2 Assembly-Activating Protein. *Journal of Virology*, **89**(6), 3038–3048.

Earley, L. F., Powers, J. M., Adachi, K., Baumgart, J. T., Meyer, N. L., Xie, Q., … Nakai, H. (2017). Adeno-associated Virus (AAV) Assembly-Activating Protein Is Not an Essential Requirement for Capsid Assembly of AAV Serotypes 4, 5, and 11. *Journal of Virology*, **91**(3).

Epstein, A., Marconi, P., Argnani, R., & Manservigi, R. (2005). HSV-1-Derived Recombinant and Amplicon Vectors for Gene Transfer and Gene Therapy. *Current Gene Therapy*, **5**(5), 445–457.

Farson, D., Harding, T. C., Tao, L., Liu, J., Powell, S., Vimal, V., … Donahue, B. A. (2004). Development and characterization of a cell line for large-scale, serum-free production of recombinant adeno-associated viral vectors. *The Journal of Gene Medicine*, **6**(12), 1369–1381.

FATAHI, A., RAHIMMANESH, I., MIRIAN, M., ROHANI, F., BOSHTAM, M., GHEIBI, A., … KOUHPAYEH, S. (2018). Construction and characterization of human embryonic kidney-(HEK)-293T cell overexpressing truncated α4 integrin. *Research in Pharmaceutical Sciences*, **13**(4), 353.

FELBERBAUM, R. S. (2015). The baculovirus expression vector system: A commercial manufacturing platform for viral vaccines and gene therapy vectors. *Biotechnology Journal*, **10**(5), 702–714.

FIRE, A., XU, S., MONTGOMERY, M. K., KOSTAS, S. A., DRIVER, S. E., & MELLO, C. C. (1998). Potent and specific genetic interference by double-stranded RNA in Caenorhabditis elegans. *Nature*, **391**(6669), 806–811.

FIRTH, A. E., & BRIERLEY, I. (2012). Non-canonical translation in RNA viruses. *Journal of General Virology*, **93**(7), 1385–1409.

FISHER, K. J., GAO, G. P., WEITZMAN, M. D., DEMATTEO, R., BURDA, J. F., & WILSON, J. M. (1996). Transduction with recombinant adeno-associated virus for gene therapy is limited by leading-strand synthesis. *Journal of Virology*, **70**(1), 520–532.

FOLEGATTI, P. M., BITTAYE, M., FLAXMAN, A., LOPEZ, F. R., BELLAMY, D., KUPKE, A., … GILBERT, S. (2020). Safety and immunogenicity of a candidate Middle East respiratory syndrome coronavirus viral-vectored vaccine: a dose-escalation, open-label, non-randomised, uncontrolled, phase 1 trial. *The Lancet Infectious Diseases*, **20**(7), 816–826.

FRAEFEL, C., MARCONI, P., & EPSTEIN, A. L. (2011). *Herpes Simplex Virus Type 1-Derived Recombinant and Amplicon Vectors*.

FRENKEL, V., & LI, K. C. (2006). Potential role of pulsed-high intensity focused ultrasound in gene therapy. *Future Oncology*, **2**(1), 111–119.

FU, X., CHEN, W.-C., ARGENTO, C., CLARNER, P., BHATT, V., DICKERSON, R., … PIERACCI, J. (2019). Analytical Strategies for Quantification of Adeno-Associated Virus Empty Capsids to Support Process Development. *Human Gene Therapy Methods*, **30**(4), 144–152.

FURUTA-HANAWA, B., YAMAGUCHI, T., & UCHIDA, E. (2019). Two-Dimensional Droplet Digital PCR as a Tool for Titration and Integrity Evaluation of Recombinant Adeno-Associated Viral Vectors. *Human Gene Therapy Methods*, **30**(4), 127–136.

GAJ, T., EPSTEIN, B. E., & SCHAFFER, D. V. (2016). Genome Engineering Using Adeno-associated Virus: Basic and Clinical Research Applications. *Molecular Therapy*, **24**(3), 458–464.

GALLI, A., DELLA LATTA, V., BOLOGNA, C., PUCCIARELLI, D., CIPRIANI, F., BACKOVIC, A., & CERVELLI, T. (2017). Strategies to optimize capsid protein expression and single-stranded DNA formation of adeno-associated virus in Saccharomyces cerevisiae. *Journal of Applied Microbiology*, **123**(2), 414–428.

GAO, G.-P., QU, G., FAUST, L. Z., ENGDAHL, R. K., XIAO, W., HUGHES, J. V., … WILSON, J. M. (1998). High-Titer Adeno-Associated Viral Vectors from a Rep/Cap Cell Line and Hybrid Shuttle Virus. *Human Gene Therapy*, **9**(16), 2353–2362.

GAO, G. P., LU, F., SANMIGUEL, J. C., TRAN, P. T., ABBAS, Z., LYND, K. S., … WILSON, J. M. (2002). Rep/cap gene amplification and high-yield production of AAV in an A549 cell line expressing rep/cap. *Molecular Therapy*.

GAO, GUANG-PING, LU, F., SANMIGUEL, J. C., TRAN, P. T., ABBAS, Z., LYND, K. S., … WILSON, J. M. (2002). Rep/Cap Gene Amplification and High-Yield Production of AAV in an A549 Cell Line Expressing Rep/Cap. *Molecular Therapy*, **5**(5), 644–649.

GAO, GUANGPING, VANDENBERGHE, L. H., ALVIRA, M. R., LU, Y., CALCEDO, R., ZHOU, X., & WILSON, J. M. (2004). Clades of Adeno-Associated Viruses Are Widely Disseminated in Human Tissues. *Journal of Virology*, **78**(12), 6381–6388.

GAO, K., LI, M., ZHONG, L., SU, Q., LI, J., LI, S., … GAO, G. (2014). Empty virions in AAV8 vector preparations reduce transduction efficiency and may cause total viral particle dose-limiting side effects. *Molecular Therapy - Methods & Clinical Development*, **1**, 9.

GERASHCHENKO, M. V., SU, D., & GLADYSHEV, V. N. (2010). CUG Start Codon Generates Thioredoxin/Glutathione Reductase Isoforms in Mouse Testes. *Journal of Biological Chemistry*, **285**(7), 4595–4602.

GHADERI, D., TAYLOR, R. E., PADLER-KARAVANI, V., DIAZ, S., & VARKI, A. (2010). Implications of the presence of N-glycolylneuraminic acid in recombinant therapeutic glycoproteins. *Nature Biotechnology*, **28**(8), 863–867.

GHEBREMEDHIN, B. (2014). Human adenovirus: Viral pathogen with increasing importance. *European Journal of Microbiology and Immunology*, **4**(1), 26–33.

GHOSH, S., BROWN, A. M., JENKINS, C., & CAMPBELL, K. (2020). Viral Vector Systems for Gene Therapy: A Comprehensive Literature Review of Progress and Biosafety Challenges. *Applied Biosafety*, **25**(1), 7–18.

GIARD, D. J., AARONSON, S. A., TODARO, G. J., ARNSTEIN, P., KERSEY, J. H., DOSIK, H., & PARKS, W. P. (1973). In Vitro Cultivation of Human Tumors: Establishment of Cell Lines Derived From a Series of Solid Tumors2. *JNCI: Journal of the National Cancer Institute*, **51**(5), 1417–1423.

GINN, S. L., AMAYA, A. K., ALEXANDER, I. E., EDELSTEIN, M., & ABEDI, M. R. (2018). Gene therapy clinical trials worldwide to 2017: An update. *The Journal of Gene Medicine*, **20**(5), e3015.

GLOVER, D. J., LIPPS, H. J., & JANS, D. A. (2005). Towards safe, non-viral therapeutic gene expression in humans. *Nature Reviews Genetics*, **6**(4), 299–310.

GOMEZ-MARTINEZ, M., SCHMITZ, D., & HERGOVICH, A. (2013). Generation of Stable Human Cell Lines with Tetracycline-inducible (Tet-on) shRNA or cDNA Expression. *Journal of Visualized Experiments*, (73).

GONÇALVES, G. A. R., & MELO ALVES PAIVA, R. DE. (2017). Gene therapy: advances, challenges and perspectives. *Einstein (Sao Paulo)*, **15**(3), 369–375.

GONÇALVES, G. A. R., & PAIVA, R. DE M. A. (2017). Gene therapy: advances, challenges and perspectives. *Einstein (São Paulo)*, **15**(3), 369–375.

GRAHAM, F. L. (1987). Growth of 293 Cells in Suspension Culture. *Journal of General Virology*, **68**(3), 937–940.

GRAHAM, S. P., MCLEAN, R. K., SPENCER, A. J., BELIJ-RAMMERSTORFER, S., WRIGHT, D., ULASZEWSKA, M., … LAMBE, T. (2020). Evaluation of the immunogenicity of prime-boost vaccination with the replication-deficient viral vectored COVID-19 vaccine candidate ChAdOx1 nCoV-19. *Npj Vaccines*, **5**(1), 69.

GRASSO, R. J., HELLER, R., COOLEY, J. C., & HALLER, E. M. (1989). Electroffusion of individual animal cells directly to intact corneal epithelial tissue. *Biochimica et Biophysica Acta (BBA) - Biomembranes*, **980**(1), 9–14.

GRAV, L. M., SERGEEVA, D., LEE, J. S., MARIN DE MAS, I., LEWIS, N. E., ANDERSEN, M. R., … KILDEGAARD, H. F. (2018). Minimizing Clonal Variation during Mammalian Cell Line Engineering for Improved Systems Biology Data Generation. *ACS Synthetic Biology*, **7**(9), 2148–2159.

GREGORY-EVANS, K., M.A. EMRAN BASHAR, A., & TAN, M. (2012). Ex Vivo Gene Therapy and Vision. *Current Gene Therapy*, **12**(2), 103–115.

GRIEGER, J. C., SOLTYS, S. M., & SAMULSKI, R. J. (2016). Production of Recombinant Adeno-associated Virus Vectors Using Suspension HEK293 Cells and Continuous Harvest of Vector From the Culture Media for GMP FIX and FLT1 Clinical Vector. *Molecular Therapy*, **24**(2), 287–297.

GRIMM, D, KERN, A., PAWLITA, M., FERRARI, F. K., SAMULSKI, R. J., & KLEINSCHMIDT, J. A. (1999). Titration of AAV-2 particles via a novel capsid ELISA: packaging of genomes can limit production of recombinant AAV-2. *Gene Therapy*, **6**(7), 1322–1330.

GRIMM, DIRK. (2002). Production methods for gene transfer vectors based on adeno-associated virus serotypes. *Methods*, **28**(2), 146–157.

GRIMM, DIRK, KERN, A., RITTNER, K., & KLEINSCHMIDT, J. A. (1998). Novel Tools for Production and Purification of Recombinant Adenoassociated Virus Vectors. *Human Gene Therapy*, **9**(18), 2745–2760.

GRIMM, DIRK, & KLEINSCHMIDT, J. A. (1999). Progress in Adeno-Associated Virus Type 2 Vector Production: Promises and Prospects for Clinical Use. *Human Gene Therapy*, **10**(15), 2445–2450.

GRIMM, DIRK, STREETZ, K. L., JOPLING, C. L., STORM, T. A., PANDEY, K., DAVIS, C. R., … KAY, M. A. (2006). Fatality in mice due to oversaturation of cellular microRNA/short hairpin RNA pathways. *Nature*, **441**(7092), 537–541.

GROSS, A., SCHOENDUBE, J., ZIMMERMANN, S., STEEB, M., ZENGERLE, R., & KOLTAY, P. (2015). Technologies for Single-Cell Isolation. *International Journal of Molecular Sciences*, **16**(8), 16897–16919.

GROSSE, S., PENAUD-BUDLOO, M., HERRMANN, A.-K., BÖRNER, K., FAKHIRI, J., LAKETA, V., … GRIMM, D. (2017). Relevance of Assembly-Activating Protein for Adeno-associated Virus Vector Production and Capsid Protein Stability in Mammalian and Insect Cells. *Journal of Virology*, **91**(20).

GUO, P., EL-GOHARY, Y., PRASADAN, K., SHIOTA, C., XIAO, X., WIERSCH, J., … GITTES, G. K. (2012). Rapid and simplified purification of recombinant adeno-associated virus. *Journal of Virological Methods*, **183**(2), 139–146.

GUY, H. M., MCCLOSKEY, L., LYE, G. J., MITROPHANOUS, K. A., & MUKHOPADHYAY, T. K. (2013). Characterization of Lentiviral Vector Production Using Microwell Suspension Cultures of HEK293T-Derived Producer Cells. *Human Gene Therapy Methods*, **24**(2), 125–139.

HAMMOND, S. L., LEEK, A. N., RICHMAN, E. H., & TJALKENS, R. B. (2017). Cellular selectivity of AAV serotypes for gene delivery in neurons and astrocytes by neonatal intracerebroventricular injection. *PLOS ONE*, **12**(12), e0188830.

HANDA, H., SHIROKI, K., & SHIMOJO, H. (1977). Establishment and characterization of KB cell lines latently infected with adeno-associated virus type 1. *Virology*, **82**(1), 84–92.

HERMENS, W. T. J. M. C., BRAKE, O. TER, DIJKHUIZEN, P. A., SONNEMANS, M. A. F., GRIMM, D., KLEINSCHMIDT, J. A., & VERHAAGEN, J. (1999). Purification of Recombinant Adeno-Associated Virus by Iodixanol Gradient Ultracentrifugation Allows Rapid and Reproducible Preparation of Vector Stocks for Gene Transfer in the Nervous System. *Human Gene Therapy*, **10**(11), 1885–1891.

HERMONAT, P. L. (1989). The adeno-Associated virus Rep78 gene inhibits cellular transformation induced by bovine papillomavirus. *Virology*, **172**(1), 253–261.

HERNANDEZ, Y. J., WANG, J., KEARNS, W. G., LOILER, S., POIRIER, A., & FLOTTE, T. R. (1999). Latent Adeno-Associated Virus Infection Elicits Humoral but Not Cell-Mediated Immune Responses in a Nonhuman Primate Model. *Journal of Virology*, **73**(10), 8549–8558.

HIRSCH, M. L. (2015). Adeno-associated virus inverted terminal repeats stimulate gene editing. *Gene Therapy*, **22**(2), 190–195.

HOGGAN, M. D., BLACKLOW, N. R., & ROWE, W. P. (1966). Studies of small DNA viruses found in various adenovirus preparations: physical, biological, and immunological characteristics. *Proceedings of the National Academy of Sciences*, **55**(6), 1467–1474.

HOLKERS, M., MAGGIO, I., HENRIQUES, S. F. D., JANSSEN, J. M., CATHOMEN, T., & GONÇALVES, M. A. F. V. (2014). Adenoviral vector DNA for accurate genome editing with engineered nucleases. *Nature Methods*, **11**(10), 1051–1057.

HOLKERS, M., MAGGIO, I., LIU, J., JANSSEN, J. M., MISELLI, F., MUSSOLINO, C., … GONÇALVES, M. A. F. V. (2013). Differential integrity of TALE nuclease genes following adenoviral and lentiviral vector gene transfer into human cells. *Nucleic Acids Research*, **41**(5), e63–e63.

HÖLSCHER, C., KLEINSCHMIDT, J. A., & BÜRKLE, A. (1995). High-level expression of adeno-associated virus (AAV) Rep78 or Rep68 protein is sufficient for infectious-particle formation by a rep-negative AAV mutant. *Journal of Virology*, **69**(11), 6880–6885.

HOROWITZ, E. D., RAHMAN, K. S., BOWER, B. D., DISMUKE, D. J., FALVO, M. R., GRIFFITH, J. D., … ASOKAN, A. (2013). Biophysical and Ultrastructural Characterization of Adeno-Associated Virus Capsid Uncoating and Genome Release. *Journal of Virology*, **87**(6), 2994–3002.

HUANG, X., HARTLEY, A.-V., YIN, Y., HERSKOWITZ, J. H., LAH, J. J., & RESSLER, K. J. (2013). AAV2 production with optimized N/P ratio and PEI-mediated transfection results in low toxicity and high titer for in vitro and in vivo applications. *Journal of Virological Methods*, **193**(2), 270–277.

Human Gene Therapy for Rare Diseases- Guidance for Industry. (2020).

IANNITTI, T., SCARROTT, J. M., LIKHITE, S., COLDICOTT, I. R. P., LEWIS, K. E., HEATH, P. R., … AZZOUZ, M. (2018). Translating SOD1 Gene Silencing toward the Clinic: A Highly Efficacious, Off-Target-free, and Biomarker-Supported Strategy for fALS. *Molecular Therapy - Nucleic Acids*, **12**, 75–88.

IM, D.-S., & MUZYCZKA, N. (1990). The AAV origin binding protein Rep68 is an ATP-dependent site-specific endonuclease with DNA helicase activity. *Cell*, **61**(3), 447–457.

INOUE, N., & RUSSELL, D. W. (1998). Packaging Cells Based on Inducible Gene Amplification for the Production of Adeno-Associated Virus Vectors. *Journal of Virology*, **72**(9), 7024–7031.

IVANOV, I. P., LOUGHRAN, G., SACHS, M., & ATKINS, J. F. (2010). Initiation context modulates autoregulation of eukaryotic translation initiation factor 1 (eIF1). *Proceedings of the National Academy of Sciences*, **107**(42), 18056–18060.

IVANOV, I. P., WEI, J., CASTER, S. Z., SMITH, K. M., MICHEL, A. M., ZHANG, Y., … SACHS, M. S. (2017). Translation Initiation from Conserved Non-AUG Codons Provides Additional Layers of Regulation and Coding Capacity. *MBio*, **8**(3).

JIN, L., ZENG, X., LIU, M., DENG, Y., & HE, N. (2014). Current progress in gene delivery technology based on chemical methods and nano-carriers. *Theranostics*, Vol. 4, pp. 240–255.

KALUDOV, N., HANDELMAN, B., & CHIORINI, J. A. (2002). Scalable Purification of Adeno-Associated Virus Type 2, 4, or 5 Using Ion-Exchange Chromatography. *Human Gene Therapy*, **13**(10), 1235–1243.

KEARSE, M. G., & WILUSZ, J. E. (2017). Non-AUG translation: a new start for protein synthesis in eukaryotes. *Genes & Development*, **31**(17), 1717–1731.

KENDALL, M., RISHWORTH, S., CARTER, F., & MITCHELL, T. (2004). Effects of Relative Humidity and Ambient Temperature on the Ballistic Delivery of Micro-Particles to Excised Porcine Skin. *Journal of Investigative Dermatology*, **122**(3), 739–746.

KHALIL, I. A., KOGURE, K., AKITA, H., & HARASHIMA, H. (2006). Uptake Pathways and Subsequent Intracellular Trafficking in Nonviral Gene Delivery. *Pharmacological Reviews*, **58**(1), 32–45.

KHLEIF, S. N., MYERSZ, T., CARTER, B. J., & TREMPE, J. P. (1991). Inhibition of Cellular transformation by the adeno-associated virus rep gene. *Virology*, **181**(2), 738–741.

KIMBALL, K. J., PREUSS, M. A., BARNES, M. N., WANG, M., SIEGAL, G. P., WAN, W., … ALVAREZ, R. D. (2010). A Phase I Study of a Tropism-Modified Conditionally Replicative Adenovirus for Recurrent Malignant Gynecologic Diseases. *Clinical Cancer Research*, **16**(21), 5277–5287.

KIMURA, T., FERRAN, B., TSUKAHARA, Y., SHANG, Q., DESAI, S., FEDOCE, A., … BACHSCHMID, M. M. (2019). Production of adeno-associated virus vectors for in vitro and in vivo applications. *Scientific Reports*, **9**(1), 13601.

KIRCHHOFF, J., SCHIERMEYER, A., SCHNEIDER, K., FISCHER, R., AINLEY, W. M., WEBB, S. R., … SCHILLBERG, S. (2020). Gene expression variability between randomly and targeted transgene integration events in tobacco suspension cell lines. *Plant Biotechnology Reports*, **14**(4), 451–458.

KLEINSCHMIDT, J. A., WISTUBA, A., STEINBACH, S., & BOCK, T. (1997). Assembly of adeno-associated virus type 2 capsids in vitro. *Journal of General Virology*, **78**(6), 1453–1462.

KOHLBRENNER, E., HENCKAERTS, E., RAPTI, K., GORDON, R. E., LINDEN, R. M., HAJJAR, R. J., & WEBER, T. (2012). Quantification of AAV Particle Titers by Infrared Fluorescence Scanning of Coomassie-Stained Sodium Dodecyl Sulfate–Polyacrylamide Gels. *Human Gene Therapy Methods*, **23**(3), 198–203.

KOST, T. A., CONDREAY, J. P., & JARVIS, D. L. (2005). Baculovirus as versatile vectors for protein expression in insect and mammalian cells. *Nature Biotechnology*, **23**(5), 567–575.

KOTIN, R. M. (2011). Large-scale recombinant adeno-associated virus production. *Human Molecular Genetics*, **20**(R1), R2–R6.

KOTIN, R M, SINISCALCO, M., SAMULSKI, R. J., ZHU, X. D., HUNTER, L., LAUGHLIN, C. A., … BERNS, K. I. (1990). Site-Specific integration by adeno associated virus. *PNAS*, **87**(6), 2211–2215.

KOTIN, ROBERT M., MENNINGER, J. C., WARD, D. C., & BERNS, K. I. (1991). Mapping and direct visualization of a region-specific viral DNA integration site on chromosome 19q13-qter. *Genomics*, **10**(3), 831–834.

KRAMMER, F. (2020). SARS-CoV-2 vaccines in development. *Nature*, **586**(7830), 516–527.

KUCK, D., KERN, A., & KLEINSCHMIDT, J. A. (2007). Development of AAV serotype-specific ELISAs using novel monoclonal antibodies. *Journal of Virological Methods*, **140**(1–2), 17–24.

KULKARNI, J. A., CULLIS, P. R., & VAN DER MEEL, R. (2018). Lipid Nanoparticles Enabling Gene

Therapies: From Concepts to Clinical Utility. *Nucleic Acid Therapeutics*, **28**(3), 146–157.

KUZMIN, D. A., SHUTOVA, M. V., JOHNSTON, N. R., SMITH, O. P., FEDORIN, V. V., KUKUSHKIN, Y. S., … JOHNSTONE, E. C. (2021). The clinical landscape for AAV gene therapies. *Nature Reviews Drug Discovery*, **20**(3), 173–174.

KYÖSTIÖ, S. R., OWENS, R. A., WEITZMAN, M. D., ANTONI, B. A., CHEJANOVSKY, N., & CARTER, B. J. (1994). Analysis of adeno-associated virus (AAV) wild-type and mutant Rep proteins for their abilities to negatively regulate AAV p5 and p19 mRNA levels. *Journal of Virology*, **68**(5), 2947–2957.

LAI, T., YANG, Y., & NG, S. (2013). Advances in Mammalian Cell Line Development Technologies for Recombinant Protein Production. *Pharmaceuticals*, **6**(5), 579–603.

LANA, M. G., & STRAUSS, B. E. (2020). *Production of Lentivirus for the Establishment of CAR-T Cells*.

LAROCCA, C., & SCHLOM, J. (2011). Viral Vector-Based Therapeutic Cancer Vaccines. *The Cancer Journal*, **17**(5), 359–371.

LAUGHLIN, C A, JONES, N., & CARTER, B. J. (1982). Effect of deletions in adenovirus early region 1 genes upon replication of adeno-associated virus. *Journal of Virology*, **41**(3), 868–876.

LAUGHLIN, CATHERINE A., TRATSCHIN, J.-D., COON, H., & CARTER, B. J. (1983). Cloning of infectious adeno-associated virus genomes in bacterial plasmids. *Gene*, **23**(1), 65–73.

LE BEC, C., POULARD, K., ALLO, V., RIVIÈRE, C., DENÈFLE, P., & DOUAR, A.-M. (2008). Adeno-Associated Viral Vector Based on ITR of Serotype 5 Ameliorates Gene Transfer in Mouse Skeletal Muscle. *Molecular Therapy*, **16**, S346.

LE, D. T., RADUKIC, M. T., & MÜLLER, K. M. (2019). Adeno-associated virus capsid protein expression in Escherichia coli and chemically defined capsid assembly. *Scientific Reports*, **9**(1), 1–10.

LEE, C. S., BISHOP, E. S., ZHANG, R., YU, X., FARINA, E. M., YAN, S., … HE, T.-C. (2017). Adenovirus-mediated gene delivery: Potential applications for gene and cell-based therapies in the new era of personalized medicine. *Genes & Diseases*, **4**(2), 43–63.

LEE, J. H., WANG, J. H., CHEN, J., LI, F., EDWARDS, T. L., HEWITT, A. W., & LIU, G. S. (2019). Gene therapy for visual loss: Opportunities and concerns. *Progress in Retinal and Eye Research*.

LENNAERTZ, A., KNOWLES, S., DRUGMAND, J.-C., & CASTILLO, J. (2013). Viral vector production in the integrity® iCELLis® single-use fixed-bed bioreactor, from bench-scale to industrial scale. *BMC Proceedings*, **7**(S6), P59.

LEONARD, C. J., & BERNS, K. I. (1994). *Adeno-associated Virus Type 2: A Latent Life Cycle*.

LI, C., & SAMULSKI, R. J. (2020). Engineering adeno-associated virus vectors for gene therapy. *Nature Reviews Genetics*, **21**(4), 255–272.

LI, H., YANG, Y., HONG, W., HUANG, M., WU, M., & ZHAO, X. (2020). Applications of genome editing technology in the targeted therapy of human diseases: mechanisms, advances and prospects. *Signal Transduction and Targeted Therapy*, **5**(1), 1.

LI, S., QI, Z., LI, H., HU, J., WANG, D., WANG, X., & FENG, Z. (2015). Conditionally replicating oncolytic adenoviral vector expressing arresten and tumor necrosis factor-related apoptosis-inducing ligand experimentally suppresses lung carcinoma progression. *Molecular Medicine Reports*, **12**(2), 2068–2074.

LIANG, H.-D., TANG, J., & HALLIWELL, M. (2010). Sonoporation, drug delivery, and gene therapy. *Proceedings of the Institution of Mechanical Engineers, Part H: Journal of Engineering in Medicine*, **224**(2), 343–361.

LINDSKOG, E. K. (2018). The Upstream Process: Principal Modes of Operation. In *Biopharmaceutical Processing* (pp. 625–635).

LIU, X. L., CLARK, K. R., & JOHNSON, P. R. (1999). Production of recombinant adeno-associated virus vectors using a packaging cell line and a hybrid recombinant adenovirus. *Gene Therapy*, **6**(2), 293–299.

LIU, X., VOULGAROPOULOU, F., CHEN, R., JOHNSON, P. R., & CLARK, K. R. (2000). Selective Rep-Cap Gene Amplification as a Mechanism for High-Titer Recombinant AAV Production from Stable Cell Lines. *Molecular Therapy*, **2**(4), 394–403.

LIU, Z.-G., DING, W.-F., XIE, S.-C., SUN, N., ZHANG, X., LI, X., & FENG, Y. (2018). Establishment and characterization of cell clones from the Papilio cell line RIRI-PaDe-3 by a high-efficiency clonal method. *Cytotechnology*, **70**(4), 1235–1245.

LOCK, M., ALVIRA, M. R., CHEN, S.-J., & WILSON, J. M. (2014). Absolute Determination of Single-Stranded and Self-Complementary Adeno-Associated Viral Vector Genome Titers by Droplet Digital PCR. *Human Gene Therapy Methods*, **25**(2), 115–125.

LOMBARDO, A., GENOVESE, P., BEAUSEJOUR, C. M., COLLEONI, S., LEE, Y.-L., KIM, K. A., … NALDINI, L. (2007). Gene editing in human stem cells using zinc finger nucleases and integrase-defective lentiviral vector delivery. *Nature Biotechnology*, **25**(11), 1298–1306.

LONGO, P. A., KAVRAN, J. M., KIM, M.-S., & LEAHY, D. J. (2014). *Single Cell Cloning of a Stable Mammalian Cell Line*.

LOU, E. (2003). Oncolytic Herpes Viruses as a Potential Mechanism for Cancer Therapy. *Acta Oncologica*, **42**(7), 660–671.

LOUGHRAN, G., ZHDANOV, A. V., MIKHAYLOVA, M. S., ROZOV, F. N., DATSKEVICH, P. N., KOVALCHUK, S. I., … ANDREEV, D. E. (2020). Unusually efficient CUG initiation of an overlapping reading frame in POLG mRNA yields novel protein POLGARF. *Proceedings of the National Academy of Sciences*, **117**(40), 24936–24946.

LOWE, S. W., RULEY, H. E., JACKS, T., & HOUSMAN, D. E. (1993). p53-dependent apoptosis modulates the cytotoxicity of anticancer agents. *Cell*, **74**(6), 957–967.

LU, X., BAKHSHAYESHI, M., BHATT, V., BERGELSON, S., FU, X., DICKERSON, R., … ARGENTO, C. (2019). Analytical Strategies for Quantification of Adeno-Associated Virus Empty Capsids to Support Process Development. *J*, **30**(4).

LUAN, X., SANSANAPHONGPRICHA, K., MYERS, I., CHEN, H., YUAN, H., & SUN, D. (2017). Engineering exosomes as refined biological nanoplatforms for drug delivery. *Acta Pharmacologica Sinica*, **38**(6), 754–763.

LUNDSTROM, K. (2018). Viral Vectors in Gene Therapy. *Diseases*, **6**(2), 42.

MAEDER, M. L., & GERSBACH, C. A. (2016, March 1). Genome-editing technologies for gene and cell therapy. *Molecular Therapy*, Vol. 24, pp. 430–446.

MALI, S. (2013). Delivery systems for gene therapy. *Indian Journal of Human Genetics*, **19**(1), 3.

MALM, M., SAGHALEYNI, R., LUNDQVIST, M., GIUDICI, M., CHOTTEAU, V., FIELD, R., … ROCKBERG, J. (2020). Evolution from adherent to suspension: systems biology of HEK293 cell line

development. *Scientific Reports*, **10**(1), 18996.

MARCONI, P., ARGNANI, R., EPSTEIN, A. L., & MANSERVIGI, R. (2008). HSV as a vector in vaccine development and gene therapy. *Human Vaccines*, **4**(2), 91–105.

MARCONI, P., FRAEFEL, C., & EPSTEIN, A. L. (2015). *Herpes Simplex Virus Type 1 (HSV-1HSV-1)-Derived Recombinant Vectorsvectors for Gene Transfergene transfer and Gene Therapygene therapy*.

MARQUEZ LOZA, L., YUEN, E., & MCCRAY, P. (2019). Lentiviral Vectors for the Treatment and Prevention of Cystic Fibrosis Lung Disease. *Genes*, **10**(3), 218.

MARTINI, S. V., ROCCO, P. R. M., & MORALES, M. M. (2011). Adeno-associated virus for cystic fibrosis gene therapy. *Brazilian Journal of Medical and Biological Research*, **44**(11), 1097–1104.

MASON, J. M., GRANDE, D. A., BARCIA, M., GRANT, R., PERGOLIZZI, R. G., & BREITBART, A. S. (1998). Expression of human bone morphogenic protein 7 in primary rabbit periosteal cells: potential utility in gene therapy for osteochondral repair. In *Gene Therapy* (Vol. 5).

MATHUPALA, S. P., & SLOAN, A. E. (2009). An agarose-based cloning-ring anchoring method for isolation of viable cell clones. *BioTechniques*, **46**(4), 305–307.

MATSUSHITA, T., OKADA, T., INABA, T., MIZUKAMI, H., OZAWA, K., & COLOSI, P. (2004). The adenovirus E1A and E1B19K genes provide a helper function for transfection-based adeno-associated virus vector production. *Journal of General Virology*, **85**(8), 2209–2214.

MATTHEWS, K. S., ALVAREZ, R. D., & CURIEL, D. T. (2009). Advancements in adenoviral based virotherapy for ovarian cancer. *Advanced Drug Delivery Reviews*, **61**(10), 836–841.

MAURER, A. C., CEPEDA DIAZ, A. K., & VANDENBERGHE, L. H. (2019). Residues on Adeno-associated Virus Capsid Lumen Dictate Interactions and Compatibility with the Assembly-Activating Protein. *Journal of Virology*, **93**(7).

MAURER, A. C., PACOURET, S., CEPEDA DIAZ, A. K., BLAKE, J., ANDRES-MATEOS, E., & VANDENBERGHE, L. H. (2018). The Assembly-Activating Protein Promotes Stability and Interactions between AAV's Viral Proteins to Nucleate Capsid Assembly. *Cell Reports*, **23**(6), 1817–1830.

MEHDI, H., ONO, E., & GUPTA, K. C. (1990). Initiation of translation at CUG, GUG, and ACG codons in mammalian cells. *Gene*, **91**(2), 173–178.

MEHIERHUMBERT, S., & GUY, R. (2005). Physical methods for gene transfer: Improving the kinetics of gene delivery into cells. *Advanced Drug Delivery Reviews*, **57**(5), 733–753.

MELLOTT, A. J., FORREST, M. L., & DETAMORE, M. S. (2013). Physical Non-Viral Gene Delivery Methods for Tissue Engineering. *Annals of Biomedical Engineering*, **41**(3), 446–468.

MENA, J. A., AUCOIN, M. G., MONTES, J., CHAHAL, P. S., & KAMEN, A. A. (2010). Improving adeno-associated vector yield in high density insect cell cultures. *The Journal of Gene Medicine*, **12**(2), 157–167.

MERCADO, N. B., ZAHN, R., WEGMANN, F., LOOS, C., CHANDRASHEKAR, A., YU, J., … BAROUCH, D. H. (2020). Single-shot Ad26 vaccine protects against SARS-CoV-2 in rhesus macaques. *Nature*, **586**(7830), 583–588.

MERKEL, S. F., ANDREWS, A. M., LUTTON, E. M., MU, D., HUDRY, E., HYMAN, B. T., … RAMIREZ, S. H. (2017). Trafficking of adeno-associated virus vectors across a model of the blood-brain barrier; a comparative study of transcytosis and transduction using primary human brain

endothelial cells. *Journal of Neurochemistry*, **140**(2), 216–230.

MERTEN, O. W., GENY-FIAMMA, C., & DOUAR, A. (2005). Current issues in adeno-associated viral vector production. *Gene Therapy*, *12*, S51–S61.

MEYER, N. L., HU, G., DAVULCU, O., XIE, Q., NOBLE, A. J., YOSHIOKA, C., … CHAPMAN, M. S. (2019). Structure of the gene therapy vector, adeno-associated virus with its cell receptor, AAVR. *ELife*, **8**.

MIDOUX, P., PICHON, C., YAOUANC, J.-J., & JAFFRÈS, P.-A. (2009). Chemical vectors for gene delivery: a current review on polymers, peptides and lipids containing histidine or imidazole as nucleic acids carriers. *British Journal of Pharmacology*, **157**(2), 166–178.

MIETZSCH, M., JOSE, A., CHIPMAN, P., BHATTACHARYA, N., DANESHPARVAR, N., MCKENNA, R., & AGBANDJE-MCKENNA, M. (2021). Completion of the AAV Structural Atlas: Serotype Capsid Structures Reveals Clade-Specific Features. *Viruses*, **13**(1), 101.

MILIOTOU, A. N., & PAPADOPOULOU, L. C. (2018). CAR T-cell Therapy: A New Era in Cancer Immunotherapy. *Current Pharmaceutical Biotechnology*, **19**(1), 5–18.

MINGOZZI, F., ANGUELA, X. M., PAVANI, G., CHEN, Y., DAVIDSON, R. J., HUI, D. J., … HIGH, K. A. (2013). Overcoming Preexisting Humoral Immunity to AAV Using Capsid Decoys. *Science Translational Medicine*, **5**(194), 194ra92-194ra92.

MINGOZZI, FEDERICO, & HIGH, K. (2007). Immune Responses to AAV in Clinical Trials. *Current Gene Therapy*, **7**(5), 316–324.

MIYASHITA, T. (2015). *Confocal Microscopy for Intracellular Co-localization of Proteins*.

MOCELLIN, S., & PROVENZANO, M. (2004). RNA interference: learning gene knock-down from cell physiology. *Journal of Translational Medicine*, **2**(39).

MOÇO, P. D., DE ABREU NETO, M. S., FANTACINI, D. M. C., & PICANÇO-CASTRO, V. (2020). *Optimized Production of Lentiviral Vectors for CAR-T Cell*.

MORENWEISER, R. (2005). Downstream processing of viral vectors and vaccines. *Gene Therapy*, **12**, S103–S110.

MOSTROM, J., LESKOVEC, M., KOŠIR, N., ŽNIDARIČ, M., DOBNIK, D., LEE, H., … KOGOVŠEK, P. (2019). Accurate quantification and characterization of adeno-associated viral vectors. *J*, **10**(JULY).

MOULLIER, P., & SNYDER, R. O. (2008). International Efforts for Recombinant Adeno-associated Viral Vector Reference Standards. *Molecular Therapy*, **16**(7), 1185–1188.

MOURBY, M., & MORRISON, M. (2020). Gene therapy regulation: could in-body editing fall through the net? *European Journal of Human Genetics*, **28**(7), 979–981.

MULLARD, A. (2021). FDA approves fourth CAR-T cell therapy. *Nature Reviews Drug Discovery*, **20**(3), 166–166.

MURUVE, D. A. (2004). The Innate Immune Response to Adenovirus Vectors. *Human Gene Therapy*, **15**(12), 1157–1166.

MYERS, M. W., & CARTER, B. J. (1980). Assembly of adeno-associated virus. *Virology*, **102**(1), 71–82.

NALDINI, L. (2015). Gene therapy returns to centre stage. *Nature*, **526**(7573), 351–360.

NASO, M. F., TOMKOWICZ, B., PERRY, W. L., & STROHL, W. R. (2017). Adeno-Associated Virus (AAV) as a Vector for Gene Therapy. *BioDrugs*, **31**(4), 317–334.

NASS, S. A., MATTINGLY, M. A., WOODCOCK, D. A., BURNHAM, B. L., ARDINGER, J. A., OSMOND, S. E., … O'RIORDAN, C. R. (2018a). Universal Method for the Purification of Recombinant AAV Vectors of Differing Serotypes. *Molecular Therapy - Methods and Clinical Development*, **9**.

NASS, S. A., MATTINGLY, M. A., WOODCOCK, D. A., BURNHAM, B. L., ARDINGER, J. A., OSMOND, S. E., … O'RIORDAN, C. R. (2018b). Universal Method for the Purification of Recombinant AAV Vectors of Differing Serotypes. *Molecular Therapy - Methods & Clinical Development*, **9**, 33–46.

NAUMER, M., SONNTAG, F., SCHMIDT, K., NIETO, K., PANKE, C., DAVEY, N. E., … KLEINSCHMIDT, J. A. (2012). Properties of the Adeno-Associated Virus Assembly-Activating Protein. *Journal of Virology*, **86**(23), 13038–13048.

NEGRETE, A., & KOTIN, R. M. (2007). Production of recombinant adeno-associated vectors using two bioreactor configurations at different scales. *Journal of Virological Methods*, **145**(2), 155–161.

NEGRINI, M., WANG, G., HEUER, A., BJÖRKLUND, T., & DAVIDSSON, M. (2020). AAV Production Everywhere: A Simple, Fast, and Reliable Protocol for In-house AAV Vector Production Based on Chloroform Extraction. *Current Protocols in Neuroscience*, **93**(1).

NEUMANN, E., SCHAEFER-RIDDER, M., WANG, Y., & HOFSCHNEIDER, P. H. (1982). Gene transfer into mouse lyoma cells by electroporation in high electric fields. *The EMBO Journal*, **1**(7), 841–845.

NGUYEN, T. N. T., SHA, S., HONG, M. S., MALONEY, A. J., BARONE, P. W., NEUFELD, C., … BRAATZ, R. D. (2021). Mechanistic model for production of recombinant adeno-associated virus via triple transfection of HEK293 cells. *Molecular Therapy - Methods & Clinical Development*, **21**, 642–655.

NIRENBERG, M. W. (1967). Will Society be Prepared. *Science*, **157**(3789).

NITZAHN, M., ALLEGRI, G., KHOJA, S., TRUONG, B., MAKRIS, G., HÄBERLE, J., & LIPSHUTZ, G. S. (2020). Split AAV-Mediated Gene Therapy Restores Ureagenesis in a Murine Model of Carbamoyl Phosphate Synthetase 1 Deficiency. *Molecular Therapy*, **28**(7), 1717–1730.

O'RIORDAN, C. R., LACHAPELLE, A. L., VINCENT, K. A., & WADSWORTH, S. C. (2000). Scaleable chromatographic purification process for recombinant adeno-associated virus (rAAV). *The Journal of Gene Medicine*, **2**(6), 444–454.

PARRIS, T. Z., VIZLIN-HODZIC, D., SALMELA, S., & FUNA, K. (2019). Tumorigenic effects of <scp> *TLX* </scp> overexpression in HEK 293T cells. *CANCER REPORTS*, **2**(5).

PEABODY, D. S. (1989). Translation Initiation at Non-AUG Triplets in Mammalian Cells. *The Journal of Biological Chemistry*, **264**, 5031–5035.

PEAR, W. S., NOLAN, G. P., SCOTT, M. L., & BALTIMORE, D. (1993). Production of high-titer helper-free retroviruses by transient transfection. *Proceedings of the National Academy of Sciences*, **90**(18), 8392–8396.

PEI, X., EARLEY, L. F., HE, Y., CHEN, X., HALL, N. E., SAMULSKI, R. J., & LI, C. (2018). Efficient Capsid Antigen Presentation From Adeno-Associated Virus Empty Virions In Vivo. *Frontiers in Immunology*, **9**.

PEI, X., HAN, M., & ZHANG, L. (2019). Advances of adeno-associated virus applied in gene therapy

to hemophilia from bench work to the clinical use. *Blood Science*, **1**(2), 130–136.

PENAUD-BUDLOO, M., FRANÇOIS, A., CLÉMENT, N., & AYUSO, E. (2018, March 16). Pharmacology of Recombinant Adeno-associated Virus Production. *Molecular Therapy - Methods and Clinical Development*, Vol. 8, pp. 166–180.

PEREIRA, D. J., MCCARTY, D. M., & MUZYCZKA, N. (1997). The adeno-associated virus (AAV) Rep protein acts as both a repressor and an activator to regulate AAV transcription during a productive infection. *Journal of Virology*, **71**(2), 1079–1088.

PFEIFER, A. M., COLE, K. E., SMOOT, D. T., WESTON, A., GROOPMAN, J. D., SHIELDS, P. G., … TRUMP, B. F. (1993). Simian virus 40 large tumor antigen-immortalized normal human liver epithelial cells express hepatocyte characteristics and metabolize chemical carcinogens. *Proceedings of the National Academy of Sciences*, **90**(11), 5123–5127.

PILBROUGH, W., MUNRO, T. P., & GRAY, P. (2009). Intraclonal Protein Expression Heterogeneity in Recombinant CHO Cells. *PLoS ONE*, **4**(12), e8432.

PILDER, S., MOORE, M., LOGAN, J., & SHENK, T. (1986). The adenovirus E1B-55K transforming polypeptide modulates transport or cytoplasmic stabilization of viral and host cell mRNAs. *Molecular and Cellular Biology*, **6**(2), 470–476.

PILLAY, S., ZOU, W., CHENG, F., PUSCHNIK, A. S., MEYER, N. L., GANAIE, S. S., … CARETTE, J. E. (2017). Adeno-associated Virus (AAV) Serotypes Have Distinctive Interactions with Domains of the Cellular AAV Receptor. *Journal of Virology*, **91**(18).

POLAND, G. A., OVSYANNIKOVA, I. G., CROOKE, S. N., & KENNEDY, R. B. (2020). SARS-CoV-2 Vaccine Development: Current Status. *Mayo Clinic Proceedings*, **95**(10), 2172–2188.

POWELL, S. K., RIVERA-SOTO, R., & GRAY, S. J. (2015). Viral expression cassette elements to enhance transgene target specificity and expression in gene therapy. *Discovery Medicine*, **19**(102), 49–57.

POWERS, A. D., PIRAS, B. A., CLARK, R. K., LOCKEY, T. D., & MEAGHER, M. M. (2016). Development and Optimization of AAV hFIX Particles by Transient Transfection in an iCELLis ® Fixed-Bed Bioreactor. *Human Gene Therapy Methods*, **27**(3), 112–121.

PRAUSNITZ, M. R. (2004). Microneedles for transdermal drug delivery. *Advanced Drug Delivery Reviews*, **56**(5), 581–587.

PRAUSNITZ, M. R., & LANGER, R. (2008). Transdermal drug delivery. *Nature Biotechnology*, **26**(11), 1261–1268.

PRIDDY, F. H., LEWIS, D. J. M., GELDERBLOM, H. C., HASSANIN, H., STREATFIELD, C., LABRANCHE, C., … JOHNSON, P. (2019). Adeno-associated virus vectored immunoprophylaxis to prevent HIV in healthy adults: a phase 1 randomised controlled trial. *The Lancet HIV*, **6**(4), e230–e239.

PUCK, T. T., & MARCUS, P. I. (1955). A RAPID METHOD FOR VIABLE CELL TITRATION AND CLONE PRODUCTION WITH HELA CELLS IN TISSUE CULTURE: THE USE OF X-IRRADIATED CELLS TO SUPPLY CONDITIONING FACTORS. *Proceedings of the National Academy of Sciences*, **41**(7), 432–437.

QIAO, C., LI, J., SKOLD, A., ZHANG, X., & XIAO, X. (2002). Feasibility of Generating Adeno-Associated Virus Packaging Cell Lines Containing Inducible Adenovirus Helper Genes. *Journal of Virology*, **76**(4), 1904–1913.

QIAO, C., WANG, B., ZHU, X., LI, J., & XIAO, X. (2002). A Novel Gene Expression Control System and Its Use in Stable, High-Titer 293 Cell-Based Adeno-Associated Virus Packaging Cell Lines.

Journal of Virology, **76**(24), 13015–13027.

QIN, J. Y., ZHANG, L., CLIFT, K. L., HULUR, I., XIANG, A. P., REN, B.-Z., & LAHN, B. T. (2010). Systematic Comparison of Constitutive Promoters and the Doxycycline-Inducible Promoter. *PLoS ONE*, **5**(5), e10611.

QU, G., BAHR-DAVIDSON, J., PRADO, J., TAI, A., CATANIAG, F., MCDONNELL, J., … WRIGHT, J. F. (2007). Separation of adeno-associated virus type 2 empty particles from genome containing vectors by anion-exchange column chromatography. *Journal of Virological Methods*, **140**(1–2), 183–192.

QU, W., WANG, M., WU, Y., & XU, R. (2015). Scalable Downstream Strategies for Purification of Recombinant Adeno- Associated Virus Vectors in Light of the Properties. *Current Pharmaceutical Biotechnology*, **16**(8).

RAMAMOORTH, M., & NARVEKAR, A. (2015). Non viral vectors in gene therapy- an overview. *Journal of Clinical and Diagnostic Research : JCDR*, **9**(1), GE01-6.

RAMBOER, E., DE CRAENE, B., DE KOCK, J., BERX, G., ROGIERS, V., VANHAECKE, T., & VINKEN, M. (2015). Development and characterization of a new human hepatic cell line. *EXCLI Journal*, **14**, 875–889.

RAPER, S. E., CHIRMULE, N., LEE, F. S., WIVEL, N. A., BAGG, A., GAO, G., … BATSHAW, M. L. (2003). Fatal systemic inflammatory response syndrome in a ornithine transcarbamylase deficient patient following adenoviral gene transfer. *Molecular Genetics and Metabolism*, **80**(1–2), 148–158.

REDDEL, R. R., SALGHETTI, S. E., WILLEY, J. C., OHNUKI, Y., KE, Y., GERWIN, B. I., … HARRIS, C. C. (1993). Development of tumorigenicity in simian virus 40-immortalized human bronchial epithelial cell lines. *Cancer Research*, **53**(5), 985–991.

REED, S. E., STALEY, E. M., MAYGINNES, J. P., PINTEL, D. J., & TULLIS, G. E. (2006). Transfection of mammalian cells using linear polyethylenimine is a simple and effective means of producing recombinant adeno-associated virus vectors. *Journal of Virological Methods*, **138**(1–2), 85–98.

REGULATION (EC) No 1394/2007 OF THE EUROPEAN PARLIAMENT AND OF THE COUNCIL of 13 November 2007 on advanced therapy medicinal products and amending Directive 2001/83/EC and Regulation (EC) No 726/2004. (2007). *Official Journal of the European Union*.

REUS, J. B., TRIVINO-SOTO, G. S., WU, L. I., KOKOTT, K., & LIM, E. S. (2020). SV40 Large T Antigen Is Not Responsible for the Loss of STING in 293T Cells but Can Inhibit cGAS-STING Interferon Induction. *Viruses*, **12**(2), 137.

ROBERTS, L. (1989). Human gene transfer test approved. *Science*, **243**(4890), 473–473.

RODRIGUEZ-ESTEVEZ, L., ASOKAN, P., & BORRÁS, T. (2020). Transduction optimization of AAV vectors for human gene therapy of glaucoma and their reversed cell entry characteristics. *Gene Therapy*, **27**(3–4), 127–142.

ROHR, U.-P., HEYD, F., NEUKIRCHEN, J., WULF, M.-A., QUEITSCH, I., KROENER-LUX, G., … KRONENWETT, R. (2005). Quantitative real-time PCR for titration of infectious recombinant AAV-2 particles. *Journal of Virological Methods*, **127**(1), 40–45.

ROHR, U.-P., WULF, M.-A., STAHN, S., STEIDL, U., HAAS, R., & KRONENWETT, R. (2002). Fast and reliable titration of recombinant adeno-associated virus type-2 using quantitative real-

time PCR. *Journal of Virological Methods*, **106**(1), 81–88.

ROLLING, F., & SAMULSKI, R. J. (1995). AAV as a viral vector for human gene therapy. *Molecular Biotechnology*, **3**(1), 9–15.

ROOIJ, J. DE, DECONTO, J., SCHAENZLER, G., BAUER, D., BARRE, K., DUSKIN, M., … WATANABE, K. (2019). https://insights.bio/cell-and-gene-therapy-insights/journal/articles/pros-and-cons-of-suspension-culture-systems-in-lvv-upstream-bioprocessing/. *Cell and Gene Therapy Insights*, **5**(S5), 1017–1029.

ROSENBERG, S. A., AEBERSOLD, P., CORNETTA, K., KASID, A., MORGAN, R. A., MOEN, R., … ANDERSON, W. F. (1990). Gene Transfer into Humans — Immunotherapy of Patients with Advanced Melanoma, Using Tumor-Infiltrating Lymphocytes Modified by Retroviral Gene Transduction. *New England Journal of Medicine*, **323**(9), 570–578.

RUMACHIK, N. G., MALAKER, S. A., POWELEIT, N., MAYNARD, L. H., ADAMS, C. M., LEIB, R. D., … PAULK, N. K. (2020). Methods Matter: Standard Production Platforms for Recombinant AAV Produce Chemically and Functionally Distinct Vectors. *Molecular Therapy - Methods & Clinical Development*, **18**, 98–118.

RUSSELL, S., BENNETT, J., WELLMAN, J. A., CHUNG, D. C., YU, Z.-F., TILLMAN, A., … MAGUIRE, A. M. (2017). Efficacy and safety of voretigene neparvovec (AAV2-hRPE65v2) in patients with RPE65 -mediated inherited retinal dystrophy: a randomised, controlled, open-label, phase 3 trial. *The Lancet*, **390**(10097), 849–860.

RUSSELL, W. C., GRAHAM, F. L., SMILEY, J., & NAIRN, R. (1977). Characteristics of a Human Cell Line Transformed by DNA from Human Adenovirus Type 5. *Journal of General Virology*, **36**(1), 59–72.

RYABOVA, L. A., POOGGIN, M. M., & HOHN, T. (2002). *Viral strategies of translation initiation: Ribosomal shunt and reinitiation*.

SALVETTI, A., ORÈVE, S., CHADEUF, G., FAVRE, D., CHEREL, Y., CHAMPION-ARNAUD, P., … MOULLIER, P. (1998). Factors Influencing Recombinant Adeno-Associated Virus Production. *Human Gene Therapy*, **9**(5), 695–706.

SAMULSKI, R. J., BERNS, K. I., TAN, M., & MUZYCZKA, N. (1982). Cloning of adeno-associated virus into pBR322: rescue of intact virus from the recombinant plasmid in human cells. *Proceedings of the National Academy of Sciences*, **79**(6), 2077–2081.

SAMULSKI, R. JUDE, & MUZYCZKA, N. (2014). AAV-Mediated Gene Therapy for Research and Therapeutic Purposes. *Annual Review of Virology*, **1**(1), 427–451.

SAMULSKI, R J, ZHU, X., XIAO, X., BROOK, J. D., HOUSMAN, D. E., EPSTEIN, N., & HUNTER, L. A. (1991). Targeted integration of adeno-associated virus (AAV) into human chromosome 19. *The EMBO Journal*, **10**(12), 3941–3950.

SAMULSKI, RICHARD J., SRIVASTAVA, A., BERNS, K. I., & MUZYCZKA, N. (1983). Rescue of adeno-associated virus from recombinant plasmids: Gene correction within the terminal repeats of AAV. *Cell*, **33**(1), 135–143.

SANCHO-ALBERO, M., MEDEL-MARTÍNEZ, A., & MARTÍN-DUQUE, P. (2020). Use of exosomes as vectors to carry advanced therapies. *RSC Advances*, **10**(40), 23975–23987.

SANDERS, J. W., & PONZIO, T. A. (2017). Vectored immunoprophylaxis: an emerging adjunct to traditional vaccination. *Tropical Diseases, Travel Medicine and Vaccines*, **3**(1), 3.

SANFORD, JOHN, C., KLEIN, T. M., WOLF, E. D., & ALLEN, N. (1987). Delivery of Substances into Cells

and Tissues Using a Particle Bombardment Process. *Particulate Science and Technology*, **5**(1), 27–37.

SATKUNANATHAN, S., WHEELER, J., THORPE, R., & ZHAO, Y. (2014). Establishment of a Novel Cell Line for the Enhanced Production of Recombinant Adeno-Associated Virus Vectors for Gene Therapy. *Human Gene Therapy*, **25**(11), 929–941.

SAUDAN, P. (2000). Inhibition of S-phase progression by adeno-associated virus Rep78 protein is mediated by hypophosphorylated pRb. *The EMBO Journal*, **19**(16), 4351–4361.

SCHERER, W. F., SYVERTON, J. T., & GEY, G. O. (1953). STUDIES ON THE PROPAGATION IN VITRO OF POLIOMYELITIS VIRUSES. *Journal of Experimental Medicine*, **97**(5), 695–710.

SCHMIDT, M., AFIONE, S., & KOTIN, R. M. (2000). Adeno-Associated Virus Type 2 Rep78 Induces Apoptosis through Caspase Activation Independently of p53. *Journal of Virology*, **74**(20), 9441–9450.

SCHMIDT, M., GROT, E., CERVENKA, P., WAINER, S., BUCK, C., & CHIORINI, J. A. (2006). Identification and Characterization of Novel Adeno-Associated Virus Isolates in ATCC Virus Stocks. *Journal of Virology*, **80**(10), 5082–5085.

SCHNEIDER, C. A., RASBAND, W. S., & ELICEIRI, K. W. (2012). NIH Image to ImageJ: 25 years of image analysis. *Nature Methods*, **9**(7), 671–675.

SCHULTZ, B. R., & CHAMBERLAIN, J. S. (2008). Recombinant Adeno-associated Virus Transduction and Integration. *Molecular Therapy*, **16**(7), 1189–1199.

SCHWARZ, H., ZHANG, Y., ZHAN, C., MALM, M., FIELD, R., TURNER, R., … CHOTTEAU, V. (2020). Small-scale bioreactor supports high density HEK293 cell perfusion culture for the production of recombinant Erythropoietin. *Journal of Biotechnology*, **309**, 44–52.

SCOTT, L. J. (2015). Alipogene Tiparvovec: A Review of Its Use in Adults with Familial Lipoprotein Lipase Deficiency. *Drugs*, **75**(2), 175–182.

SCOTT, M. S., CALAFELL, S. J., THOMAS, D. Y., & HALLETT, M. T. (2005). Refining Protein Subcellular Localization. *PLoS Computational Biology*, **1**(6), e66.

SENIOR, M. (2017). After Glybera's withdrawal, what's next for gene therapy? *Nature Biotechnology*, **35**(6), 491–492.

SHAHRYARI, A., SAGHAEIAN JAZI, M., MOHAMMADI, S., RAZAVI NIKOO, H., NAZARI, Z., HOSSEINI, E. S., … LICKERT, H. (2019). Development and Clinical Translation of Approved Gene Therapy Products for Genetic Disorders. *Frontiers in Genetics*, **10**.

SHARMA, A., TANDON, M., BANGARI, D., & MITTAL, S. (2009). Adenoviral Vector-Based Strategies for Cancer Therapy. *Current Drug Therapy*, **4**(2), 117–138.

SHEN, C., BUCK, A. K., LIU, X., WINKLER, M., & RESKE, S. N. (2003). Gene silencing by adenovirus-delivered siRNA. *FEBS Letters*, **539**(1–3), 111–114.

SHIRLEY, J. L., DE JONG, Y. P., TERHORST, C., & HERZOG, R. W. (2020). Immune Responses to Viral Gene Therapy Vectors. *Molecular Therapy*, **28**(3), 709–722.

SMALLEY, E. (2017). First AAV gene therapy poised for landmark approval. *Nature Biotechnology*, **35**(11), 998–999.

SOHN, R. L., MURRAY, M. T., SCHWARZ, K., NYITRAY, J., PURRAY, P., FRANKO, A. P., … DULCHAVSKY, S. A. (2001). In-vivo particle mediated delivery of mRNA to mammalian tissues: ballistic and biologic effects. *Wound Repair and Regeneration*, **9**(4), 287–296.

SOMMER, J. M., SMITH, P. H., PARTHASARATHY, S., ISAACS, J., VIJAY, S., KIERAN, J., … WRIGHT, J. F. (2003). Quantification of adeno-associated virus particles and empty capsids by optical density measurement. *Molecular Therapy*, **7**(1), 122–128.

SONNTAG, F., KOTHER, K., SCHMIDT, K., WEGHOFER, M., RAUPP, C., NIETO, K., … KLEINSCHMIDT, J. A. (2011). The Assembly-Activating Protein Promotes Capsid Assembly of Different Adeno-Associated Virus Serotypes. *Journal of Virology*, **85**(23), 12686–12697.

SONNTAG, F., SCHMIDT, K., & KLEINSCHMIDT, J. A. (2010). A viral assembly factor promotes AAV2 capsid formation in the nucleolus. *Proceedings of the National Academy of Sciences*, **107**(22), 10220–10225.

STEEGENGA, W. T., RITECO, N., JOCHEMSEN, A. G., FALLAUX, F. J., & BOS, J. L. (1998). The large E1B protein together with the E4orf6 protein target p53 for active degradation in adenovirus infected cells. *Oncogene*, **16**(3), 349–357.

STEPANENKO, A. A., & HENG, H. B. (2017). Transient and stable vector transfection: pitfalls, off-target effects and artifacts. *Mutation Research*, **773**, 91–103.

STOCKER, A. G., KREMER, K. L., KOLDEJ, R., MILLER, D. S., ANSON, D. S., & PARSONS, D. W. (2009). Single-dose lentiviral gene transfer for lifetime airway gene expression. *The Journal of Gene Medicine*, **11**(10), 861–867.

STROBEL, B., ZUCKSCHWERDT, K., ZIMMERMANN, G., MAYER, C., EYTNER, R., RECHTSTEINER, P., … LAMLA, T. (2019). Standardized, Scalable, and Timely Flexible Adeno-Associated Virus Vector Production Using Frozen High-Density HEK-293 Cell Stocks and CELLdiscs. *Human Gene Therapy Methods*, **30**(1), 23–33.

STROES, E. S., NIERMAN, M. C., MEULENBERG, J. J., FRANSSEN, R., TWISK, J., HENNY, C. P., … KUIVENHOVEN, J. A. (2008). Intramuscular Administration of AAV1-Lipoprotein Lipase S447X Lowers Triglycerides in Lipoprotein Lipase–Deficient Patients. *Arteriosclerosis, Thrombosis, and Vascular Biology*, **28**(12), 2303–2304.

SUMMERFORD, C., & SAMULSKI, R. J. (1998). Membrane-Associated Heparan Sulfate Proteoglycan Is a Receptor for Adeno-Associated Virus Type 2 Virions. *Journal of Virology*, **72**(2), 1438–1445.

SUNG, Y., & KIM, S. (2019). Recent advances in the development of gene delivery systems. *Biomaterials Research*, **23**(1), 8.

SWIECH, K., PICANÇO-CASTRO, V., & COVAS, D. T. (2012). Human cells: New platform for recombinant therapeutic protein production. *Protein Expression and Purification*, **84**(1), 147–153.

TAKAHASHI, T., & SUZUKI, T. (2011). Function of Membrane Rafts in Viral Lifecycles and Host Cellular Response. *Biochemistry Research International*, **2011**, 1–23.

TAKATA, M., SASAKI, M. S., SONODA, E., MORRISON, C., HASHIMOTO, M., UTSUMI, H., … TAKEDA, S. (1998). Homologous recombination and non-homologous end-joining pathways of DNA double-strand break repair have overlapping roles in the maintenance of chromosomal integrity in vertebrate cells. *The EMBO Journal*, **17**(18), 5497–5508.

TENENBAUM, L., LEHTONEN, E., & MONAHAN, P. (2003). Evaluation of Risks Related to the Use of Adeno-Associated Virus-Based Vectors. *Current Gene Therapy*, **3**(6), 545–565.

TERMINI, J. M., SILVER, Z. A., CONNOR, B., ANTONOPOULOS, A., HASLAM, S. M., DELL, A., & DESROSIERS, R. C. (2017). HEK293T cell lines defective for O-linked glycosylation. *PLOS ONE*, **12**(6),

e0179949.

TERWILLIGER, E. F., GODIN, B., SODROSKI, J. G., & HASELTINE, W. A. (1989). Construction and use of a replication-competent human immunodeficiency virus (HIV-1) that expresses the chloramphenicol acetyltransferase enzyme. *Proceedings of the National Academy of Sciences*, **86**(10), 3857–3861.

THOMAS, C. E., EHRHARDT, A., & KAY, M. A. (2003). Progress and problems with the use of viral vectors for gene therapy. *Nature Reviews Genetics*, **4**(5), 346–358.

TODO, T. (2002). Oncolytic Virus Therapy Using Genetically Engineered Herpes Simplex Viruses. *Human Cell*, **15**(3), 151–159.

TOMAR, R. S., MATTA, H., & CHAUDHARY, P. M. (2003). Use of adeno-associated viral vector for delivery of small interfering RNA. *Oncogene*, **22**(36), 5712–5715.

TRATSCHIN, J. D., WEST, M. H., SANDBANK, T., & CARTER, B. J. (1984). A human parvovirus, adeno-associated virus, as a eucaryotic vector: transient expression and encapsidation of the procaryotic gene for chloramphenicol acetyltransferase. *Molecular and Cellular Biology*, **4**(10), 2072–2081.

TSE, L. V., MOLLER-TANK, S., MEGANCK, R. M., & ASOKAN, A. (2018). Mapping and Engineering Functional Domains of the Assembly-Activating Protein of Adeno-associated Viruses. *Journal of Virology*, **92**(14).

URA, T., OKUDA, K., & SHIMADA, M. (2014). Developments in Viral Vector-Based Vaccines. *Vaccines*, **2**(3), 624–641.

URABE, M., DING, C., & KOTIN, R. M. (2002). Insect Cells as a Factory to Produce Adeno-Associated Virus Type 2 Vectors. *Human Gene Therapy*, **13**(16), 1935–1943.

URABE, M., XIN, K.-Q., OBARA, Y., NAKAKURA, T., MIZUKAMI, H., KUME, A., … OZAWA, K. (2006). Removal of Empty Capsids from Type 1 Adeno-Associated Virus Vector Stocks by Anion-Exchange Chromatography Potentiates Transgene Expression. *Molecular Therapy*, **13**(4), 823–828.

VALSALAKUMARI, J., BABY, J., BIJIN, E., CONSTANTINE, I., MANJILA, S., & PRAMOD, K. (2013). Novel gene delivery systems. *International Journal of Pharmaceutical Investigation*, **3**(1), 1.

VAN DER LOO, J. C. M., & WRIGHT, J. F. (2016). Progress and challenges in viral vector manufacturing. *Human Molecular Genetics*, **25**(R1), R42–R52.

VAN DOREMALEN, N., LAMBE, T., SPENCER, A., BELIJ-RAMMERSTORFER, S., PURUSHOTHAM, J. N., PORT, J. R., … MUNSTER, V. J. (2020). ChAdOx1 nCoV-19 vaccine prevents SARS-CoV-2 pneumonia in rhesus macaques. *Nature*, **586**(7830), 578–582.

VAN VLIET, K. M., BLOUIN, V., BRUMENT, N., AGBANDJE-MCKENNA, M., & SNYDER, R. O. (2008). *The Role of the Adeno-Associated Virus Capsid in Gene Transfer*.

VANDENBERGHE, L. H., XIAO, R., LOCK, M., LIN, J., KORN, M., & WILSON, J. M. (2010). Efficient Serotype-Dependent Release of Functional Vector into the Culture Medium During Adeno-Associated Virus Manufacturing. *Human Gene Therapy*, **21**(10), 1251–1257.

VANNUCCI, L., LAI, M., CHIUPPESI, F., CECCHERINI-NELLI, L., & PISTELLO, M. (2013). Viral vectors: a look back and ahead on gene transfer technology. *The New Microbiologica*, **36**(1), 1–22.

VARGHESE, S., & RABKIN, S. D. (2002). Oncolytic herpes simplex virus vectors for cancer virotherapy. *Cancer Gene Therapy*, **9**(12), 967–978.

VENKATAKRISHNAN, B., YARBROUGH, J., DOMSIC, J., BENNETT, A., BOTHNER, B., KOZYREVA, O. G., … AGBANDJE-MCKENNA, M. (2013). Structure and Dynamics of Adeno-Associated Virus Serotype 1 VP1-Unique N-Terminal Domain and Its Role in Capsid Trafficking. *Journal of Virology*, **87**(9), 4974–4984.

VINEY, L., BÜRCKSTÜMMER, T., EDDINGTON, C., MIETZSCH, M., CHOUDHRY, M., HENLEY, T., & AGBANDJE-MCKENNA, M. (2021). Adeno-associated Virus (AAV) Capsid Chimeras with Enhanced Infectivity Reveal a Core Element in the AAV Genome Critical for both Cell Transduction and Capsid Assembly. *Journal of Virology*.

VIRELLA-LOWELL, I., POIRIER, A., CHESNUT, K. A., BRANTLY, M., & FLOTTE, T. R. (2000). Inhibition of recombinant adeno-associated virus (rAAV) transduction by bronchial secretions from cystic fibrosis patients. *Gene Therapy*, **7**(20), 1783–1789.

VOYSEY, M., CLEMENS, S. A. C., MADHI, S. A., WECKX, L. Y., FOLEGATTI, P. M., ALEY, P. K., … ZUIDEWIND, P. (2020). Safety and efficacy of the ChAdOx1 nCoV-19 vaccine (AZD1222) against SARS-CoV-2: an interim analysis of four randomised controlled trials in Brazil, South Africa, and the UK. *The Lancet*.

WALTHER, W., & STEIN, U. (2000). Viral Vectors for Gene Transfer. *Drugs*, **60**(2).

WANG, B., LI, J., FU, F. H., CHEN, C., ZHU, X., ZHOU, L., … XIAO, X. (2008). Construction and analysis of compact muscle-specific promoters for AAV vectors. *Gene Therapy*, **15**(22), 1489–1499.

WANG, D., TAI, P. W. L., & GAO, G. (2019). Adeno-associated virus vector as a platform for gene therapy delivery. *Nature Reviews Drug Discovery*, Vol. 18.

WANG, F., CUI, X., WANG, M., XIAO, W., & XU, R. (2013). A reliable and feasible qPCR strategy for titrating AAV vectors. *Medical Science Monitor Basic Research*, **19**, 187–193.

WANG, Q., LOCK, M., PRONGAY, A. J., ALVIRA, M. R., PETKOV, B., & WILSON, J. M. (2015). Identification of an adeno-associated virus binding epitope for AVB sepharose affinity resin. *Molecular Therapy - Methods & Clinical Development*, **2**, 15040.

WANG, X. S., PONNAZHAGAN, S., & SRIVASTAVA, A. (1996). Rescue and replication of adeno-associated virus type 2 as well as vector DNA sequences from recombinant plasmids containing deletions in the viral inverted terminal repeats: selective encapsidation of viral genomes in progeny virions. *Journal of Virology*, **70**(3), 1668–1677.

WANG Y, L. C., WANG L, L. Y., & ASLANIDI GV, J. G. (2015). The Adeno-Associated Virus Genome Packaging Puzzle. *Journal of Molecular and Genetic Medicine*, **09**(03).

WEITZMAN, M. D., KYOSTIO, S. R., KOTIN, R. M., & OWENS, R. A. (1994). Adeno-associated virus (AAV) Rep proteins mediate complex formation between AAV DNA and its integration site in human DNA. *Proceedings of the National Academy of Sciences*, **91**(13), 5808–5812.

WILMOTT, P., LISOWSKI, L., ALEXANDER, I. E., & LOGAN, G. J. (2019). A User's Guide to the Inverted Terminal Repeats of Adeno-Associated Virus. *Human Gene Therapy Methods*, **30**(6), 206–213.

WIRTH, T., PARKER, N., & YLÄ-HERTTUALA, S. (2013). History of Gene Therapy. *Gene*, **525**(2), 162–169.

WISTUBA, A., KERN, A., WEGER, S., GRIMM, D., & KLEINSCHMIDT, J. A. (1997). Subcellular compartmentalization of adeno-associated virus type 2 assembly. *Journal of Virology*, **71**(2), 1341–1352.

WOLD, W. S. M., & TOTH, K. (2013). Adenovirus vectors for gene therapy, vaccination and cancer gene therapy. *Current Gene Therapy*, **13**(6), 421–433.

WRIGHT, J. (2014). Product-Related Impurities in Clinical-Grade Recombinant AAV Vectors: Characterization and Risk Assessment. *Biomedicines*, **2**(1), 80–97.

WRIGHT, J. FRASER. (2009). Transient Transfection Methods for Clinical Adeno-Associated Viral Vector Production. *Human Gene Therapy*, **20**(7), 698–706.

WRIGHT, J F. (2008). Manufacturing and characterizing AAV-based vectors for use in clinical studies. *Gene Therapy*, **15**(11), 840–848.

WRIGHT, J FRASER. (2014). AAV Empty Capsids: For Better or for Worse? *Molecular Therapy*, **22**(1), 1–2.

WU, J., ZHAO, W., ZHONG, L., HAN, Z., LI, B., MA, W., … SRIVASTAVA, A. (2007). Self-Complementary Recombinant Adeno-Associated Viral Vectors: Packaging Capacity And The Role of Rep Proteins in Vector Purity. *Human Gene Therapy*, **18**(2), 171–182.

WU, X., DONG, X., WU, Z., CAO, H., NIU, D., QU, J., … HOU, Y. (2001). A novel method for purification of recombinant adenoassociated virus vectors on a large scale. *Chinese Science Bulletin*, **46**(6), 485–488.

WU, Z., HIRIYANNA, S., QIAN, H., MOOKHERJEE, S., CAMPOS, M. M., GAO, C., … SWAROOP, A. (2015). A long-term efficacy study of gene replacement therapy for RPGR-associated retinal degeneration. *Human Molecular Genetics*, **24**(14), 3956–3970.

WULHFARD, S., BALDI, L., HACKER, D. L., & WURM, F. (2010). Valproic acid enhances recombinant mRNA and protein levels in transiently transfected Chinese hamster ovary cells. *Journal of Biotechnology*, **148**(2–3), 128–132.

WURM, F. M. (2004). Production of recombinant protein therapeutics in cultivated mammalian cells. *Nature Biotechnology*, **22**(11), 1393–1398.

WÜRTELE, H., LITTLE, K. C. E., & CHARTRAND, P. (2003). Illegitimate DNA integration in mammalian cells. *Gene Therapy*, **10**(21), 1791–1799.

XIAO, X. (2010). Adeno-Associated Viral Vectors Found Free in Media. *Human Gene Therapy*, **21**(10), 1221–1222.

XIAO, X., LI, J., & SAMULSKI, R. J. (1998). Production of High-Titer Recombinant Adeno-Associated Virus Vectors in the Absence of Helper Adenovirus. *Journal of Virology*, **72**(3), 2224–2232.

XU, X., CAO, DENG, WEI, SU, YANG, … YU. (2011). Encapsulation of plasmid DNA in calcium phosphate nanoparticles: stem cell uptake and gene transfer efficiency. *International Journal of Nanomedicine*, 3335.

YAN, Z., ZAK, R., ZHANG, Y., & ENGELHARDT, J. F. (2005). Inverted Terminal Repeat Sequences Are Important for Intermolecular Recombination and Circularization of Adeno-Associated Virus Genomes. *Journal of Virology*, **79**(1), 364–379.

YANG, N. S., BURKHOLDER, J., ROBERTS, B., MARTINELL, B., & MCCABE, D. (1990). In vivo and in vitro gene transfer to mammalian somatic cells by particle bombardment. *Proceedings of the National Academy of Sciences*, **87**(24), 9568–9572.

YANG, Q, CHEN, F., & TREMPE, J. P. (1994a). Characterization of cell lines that inducibly express the adeno-associated virus Rep proteins. *Journal of Virology*, **68**(8), 4847–4856.

YANG, Q, CHEN, F., & TREMPE, J. P. (1994b). Characterization of cell lines that inducibly express

the adeno-associated virus Rep proteins. *Journal of Virology*, **68**(8), 4847–4856.

YANG, QICHENG, CHEN, F., ROSS, J., & TREMPE, J. P. (1995). Inhibition of Cellular and SV40 DNA Replication by the Adeno-Associated Virus Rep Proteins. *Virology*, **207**(1), 246–250.

YANG, R., LEMAÎTRE, V., HUANG, C., HADDADI, A., MCNAUGHTON, R., & ESPINOSA, H. D. (2018). Monoclonal Cell Line Generation and CRISPR/Cas9 Manipulation via Single-Cell Electroporation. *Small*, **14**(12), 1702495.

YEI, S., MITTEREDER, N., TANG, K., O'SULLIVAN, C., & TRAPNELL, B. C. (1994). Adenovirus-mediated gene transfer for cystic fibrosis: quantitative evaluation of repeated in vivo vector administration to the lung. *Gene Therapy*, **1**(3), 192–200.

YLÄ-HERTTUALA, S. (2012). Endgame: glybera finally recommended for approval as the first gene therapy drug in the European union. *Molecular Therapy : The Journal of the American Society of Gene Therapy*, **20**(10), 1831–1832.

YOON, C. S., & PARK, J. H. (2010). Ultrasound-mediated gene delivery. *Expert Opinion on Drug Delivery*, **7**(3), 321–330.

YOUNG, S. M., & SAMULSKI, R. J. (2001). Adeno-associated virus (AAV) site-specific recombination does not require a Rep-dependent origin of replication within the AAV terminal repeat. *Proceedings of the National Academy of Sciences*, **98**(24), 13525–13530.

YU, C., TRIVEDI, P. D., CHAUDHURI, P., BHAKE, R., JOHNSON, E. J., CATON, T., … CLÉMENT, N. (2021). Sodium Chloride and Potassium Chloride Mediate Log-increase in AAV Viral Vector Particle and Infectious Titers in a Specific and Timely Manner when Using the HSV Production Platform. *Molecular Therapy - Methods & Clinical Development*.

YUAN, Z., QIAO, C., HU, P., LI, J., & XIAO, X. (2011). A Versatile Adeno-Associated Virus Vector Producer Cell Line Method for Scalable Vector Production of Different Serotypes. *Human Gene Therapy*, **22**(5), 613–624.

ZAMORE, P. D., TUSCHL, T., SHARP, P. A., & BARTEL, D. P. (2000). RNAi. *Cell*, **101**(1), 25–33.

ZELENIN, A., KOLESNIKOV, V., TARASENKO, O., SHAFEI, R., ZELENINA, I., MIKHAILOV, V., … BARANOVAND, V. (1997). Bacterial β-galactosidase and human dystrophin genes are expressed in mouse skeletal muscle fibers after ballistic transfection. *FEBS Letters*, **414**(2), 319–322.

ZELTNER, N., KOHLBRENNER, E., CLÉMENT, N., WEBER, T., & LINDEN, R. M. (2010). Near-perfect infectivity of wild-type AAV as benchmark for infectivity of recombinant AAV vectors. *Gene Therapy*, **17**(7), 872–879.

ZHANG, C., & ZHOU, D. (2016). Adenoviral vector-based strategies against infectious disease and cancer. *Human Vaccines & Immunotherapeutics*, **12**(8), 2064–2074.

ZHANG, HAN, FENG, Q., GONG, J., & MA, J. (2018). Anticancer effects of isofraxidin against A549 human lung cancer cells via the EGFR signaling pathway. *Molecular Medicine Reports*.

ZHANG, HONGWEI, YANG, B., MU, X., AHMED, S. S., SU, Q., HE, R., … GAO, G. (2011). Several rAAV Vectors Efficiently Cross the Blood–brain Barrier and Transduce Neurons and Astrocytes in the Neonatal Mouse Central Nervous System. *Molecular Therapy*, **19**(8), 1440–1448.

ZHAO, H., LEE, K.-J., DARIS, M., LIN, Y., WOLFE, T., SHENG, J., … MEISEN, W. H. (2020). Creation of a High-Yield AAV Vector Production Platform in Suspension Cells Using a Design-of-Experiment Approach. *Molecular Therapy - Methods & Clinical Development*, **18**, 312–320.

ZHOU, J., YANG, X., WRIGHT, J. F., HIGH, K. A., COUTO, L., & QU, G. (2011). PEG-modulated column chromatography for purification of recombinant adeno-associated virus serotype 9. *Journal of Virological Methods*, **173**(1), 99–107.

ZHOU, Q., TIAN, W., LIU, C., LIAN, Z., DONG, X., & WU, X. (2017). Deletion of the B-B' and C-C' regions of inverted terminal repeats reduces rAAV productivity but increases transgene expression. *Scientific Reports*, **7**.

ZHU, F.-C., LI, Y.-H., GUAN, X.-H., HOU, L.-H., WANG, W.-J., LI, J.-X., … CHEN, W. (2020). Safety, tolerability, and immunogenicity of a recombinant adenovirus type-5 vectored COVID-19 vaccine: a dose-escalation, open-label, non-randomised, first-in-human trial. *The Lancet*, **395**(10240), 1845–1854.

ZITOMER, R. S., WALTHALL, D. A., RYMOND, B. C., & HOLLENBERG, C. P. (1984). Saccharomyces cerevisiae ribosomes recognize non-AUG initiation codons. *Molecular and Cellular Biology*, **4**(7), 1191–1197.

ZOLOTUKHIN, S., BYRNE, B. J., MASON, E., ZOLOTUKHIN, I., POTTER, M., CHESNUT, K., … MUZYCZKA, N. (1999). Recombinant adeno-associated virus purification using novel methods improves infectious titer and yield. *Gene Therapy*, **6**(6), 973–985.

Appendix

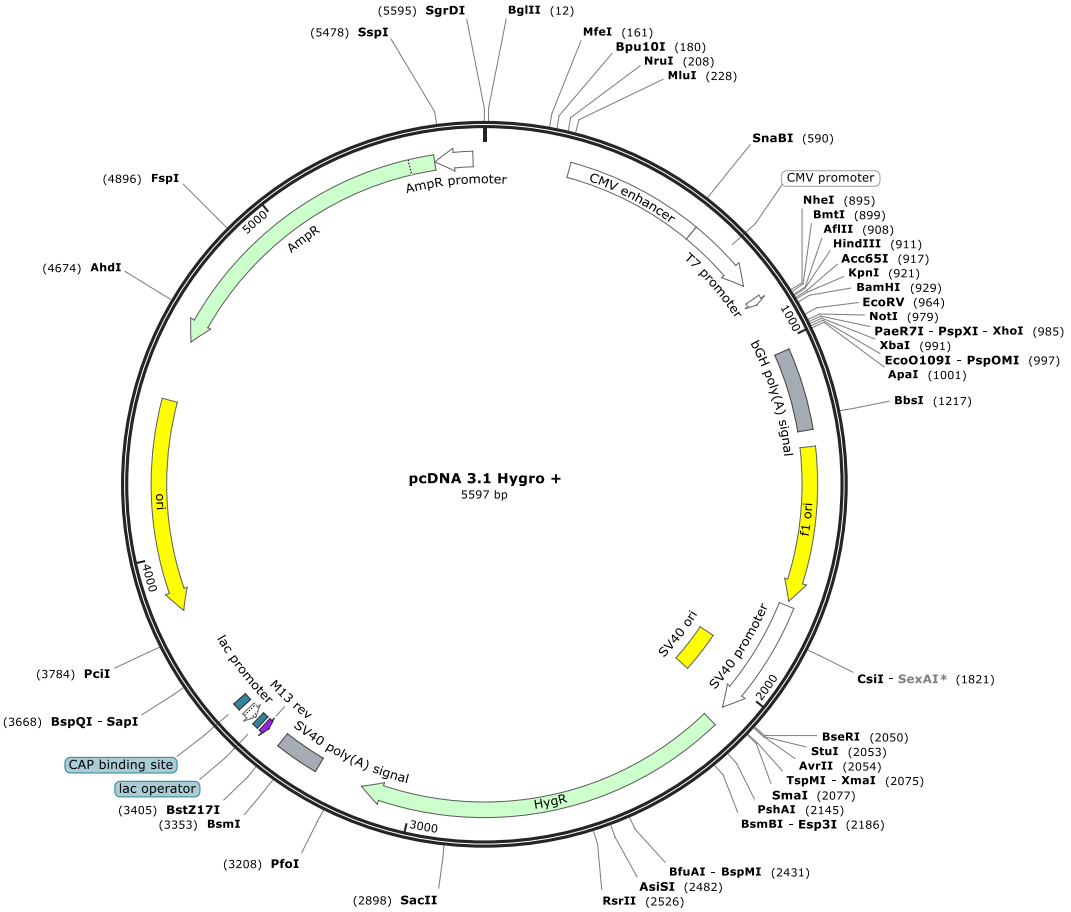

Appendix Figure I Schematic showing the vector map for the cloning vector pcDNA3.1 Hygro.

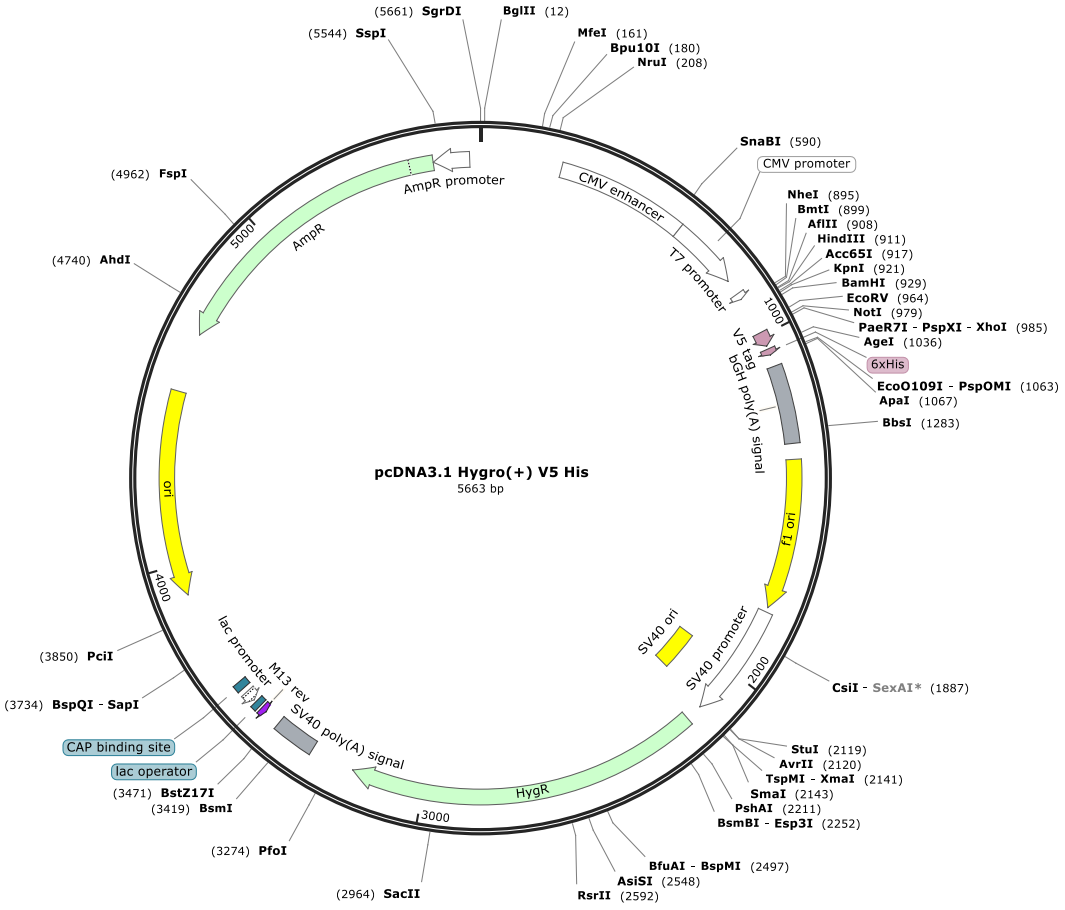

Appendix Figure II Schematic showing the vector map for the cloning vector pcDNA3.1 Hygro (+) V5 His.

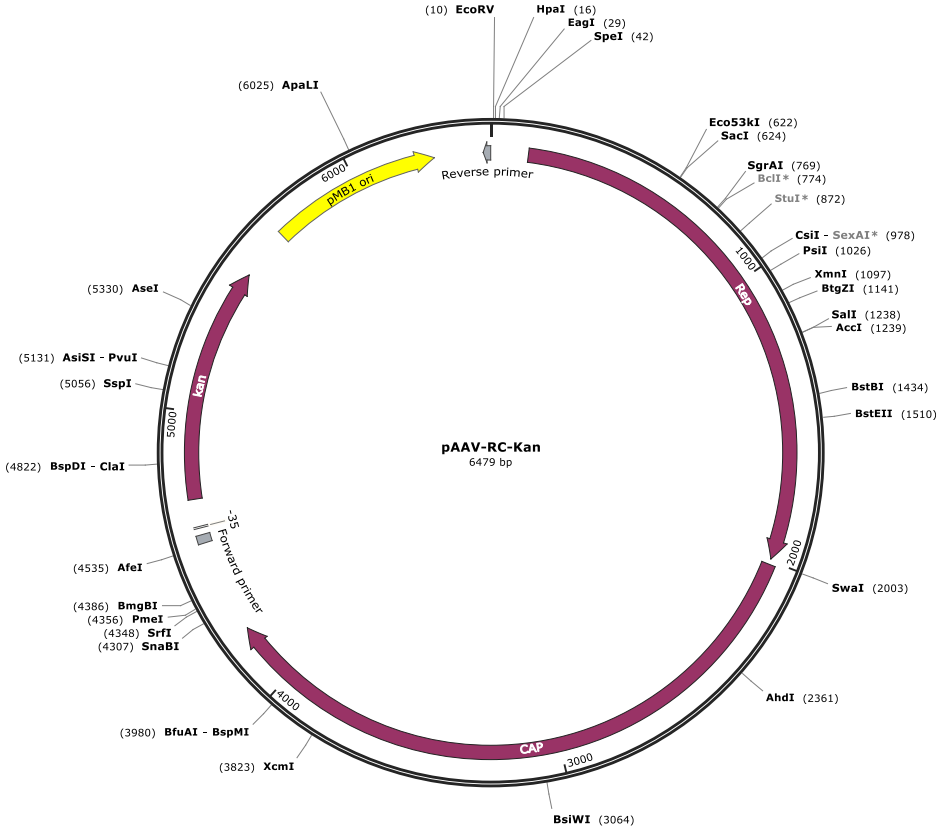

Appendix Figure III Schematic showing the vector map for the cloning vector pAAV-RC-Kan. Supplied by Cobra Biologics.

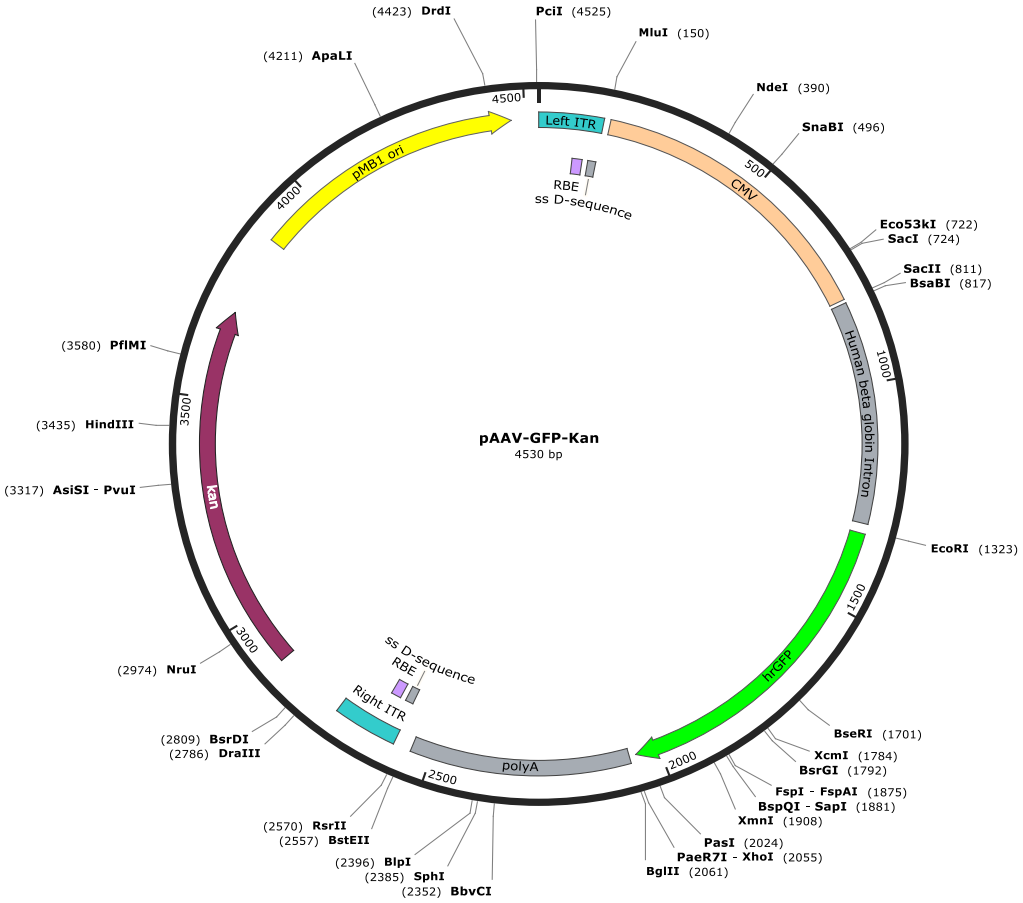

Appendix Figure IV Schematic showing the vector map for the cloning vector pAAV-GFP-Kan. Supplied by Cobra Biologics.

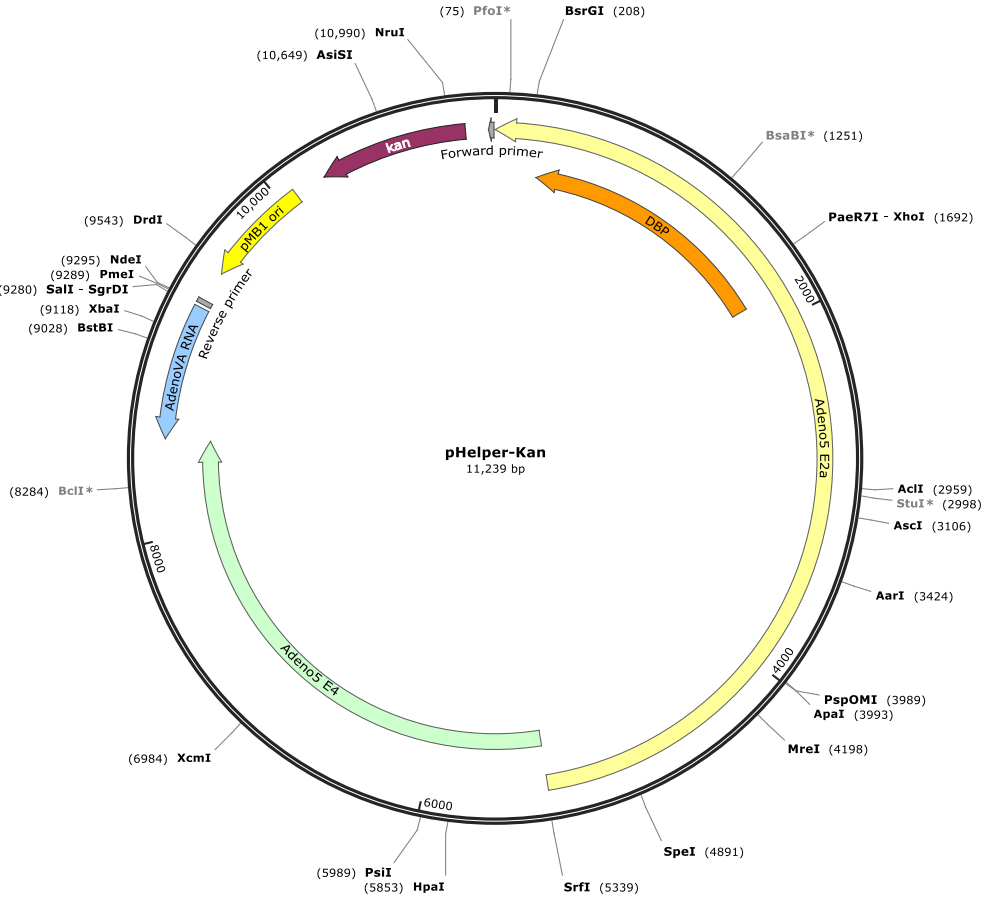

Appendix Figure V Schematic showing the vector map for the cloning vector pHelper-Kan. Supplied by Cobra Biologics.

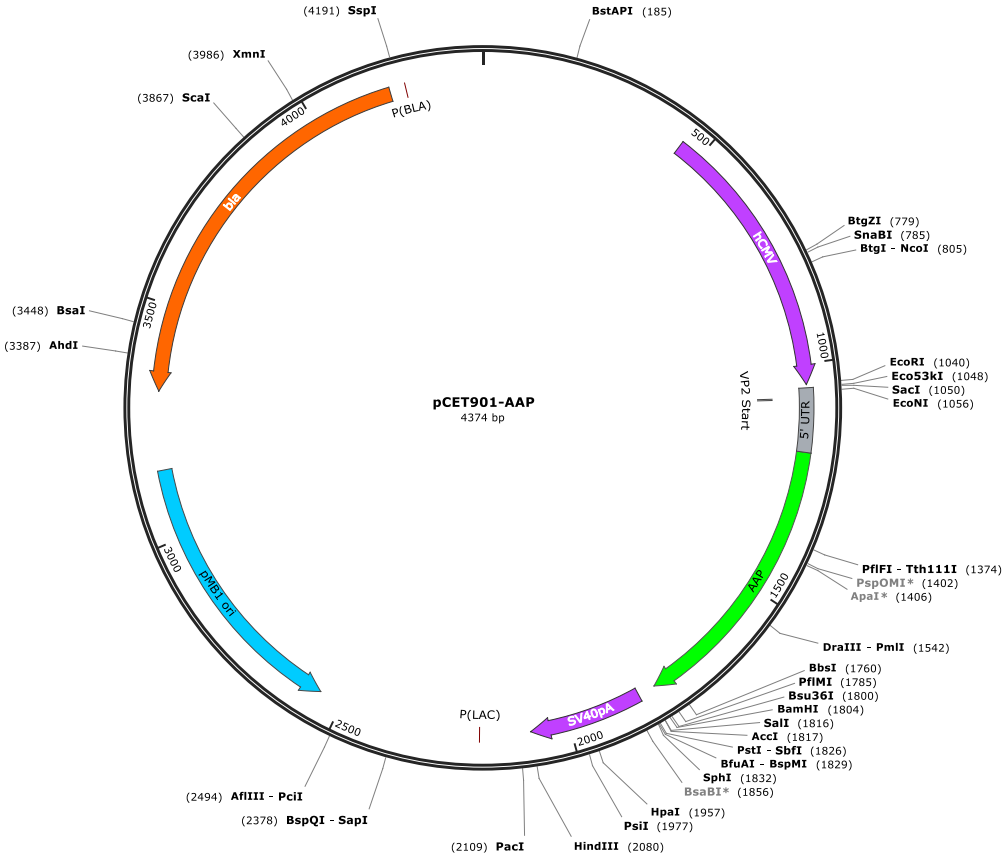

Appendix Figure VI Schematic showing the vector map for the cloning vector pCET901-AAP. Supplied by Cobra Biologics.

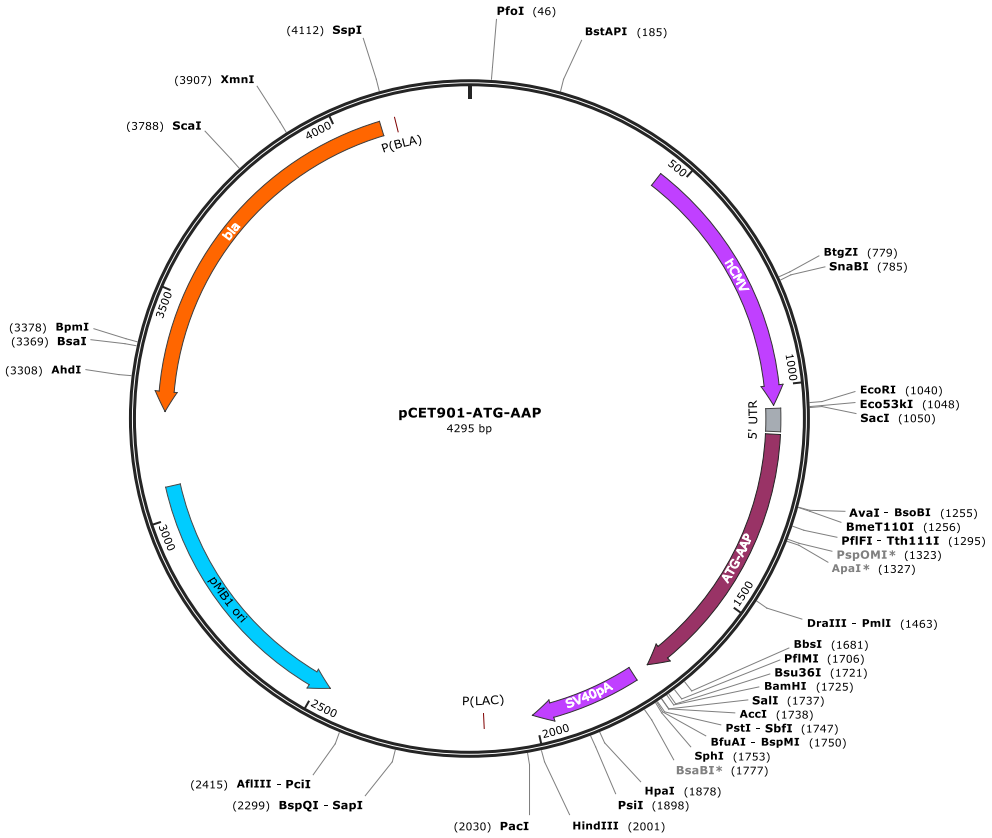

Appendix Figure VII Schematic showing the vector map for the cloning vector pCET901-ATG-AAP. Supplied by Cobra Biologics.

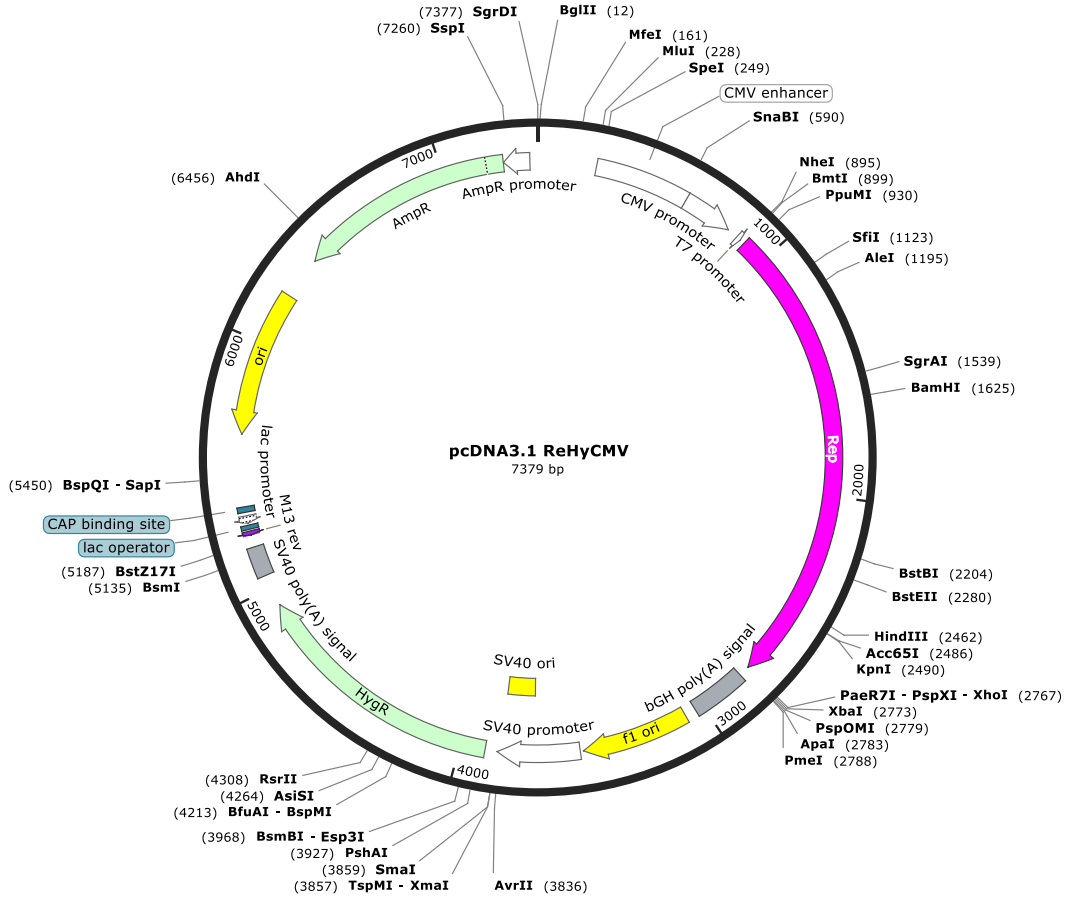

Appendix Figure VIII Schematic showing the vector map for the cloning vector pcDNA3.1 ReHyCMV.

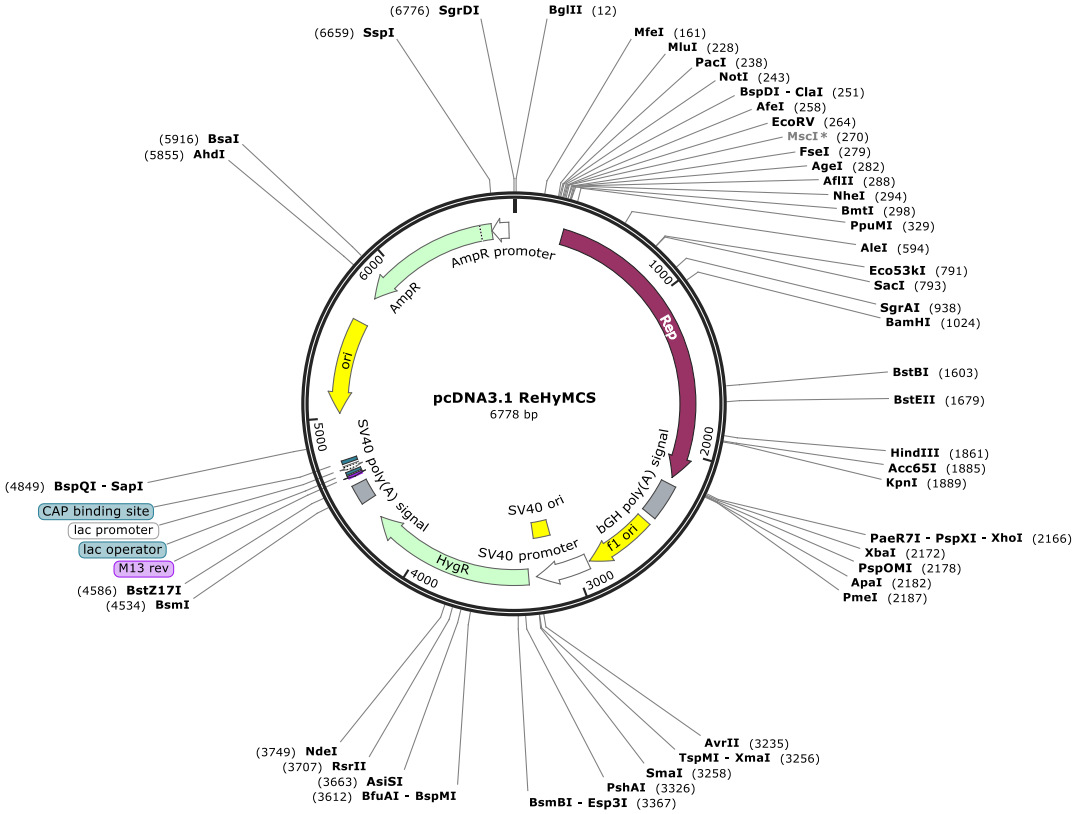

Appendix Figure IX Schematic showing the vector map for the cloning vector pcDNA3.1 ReHyMCS.

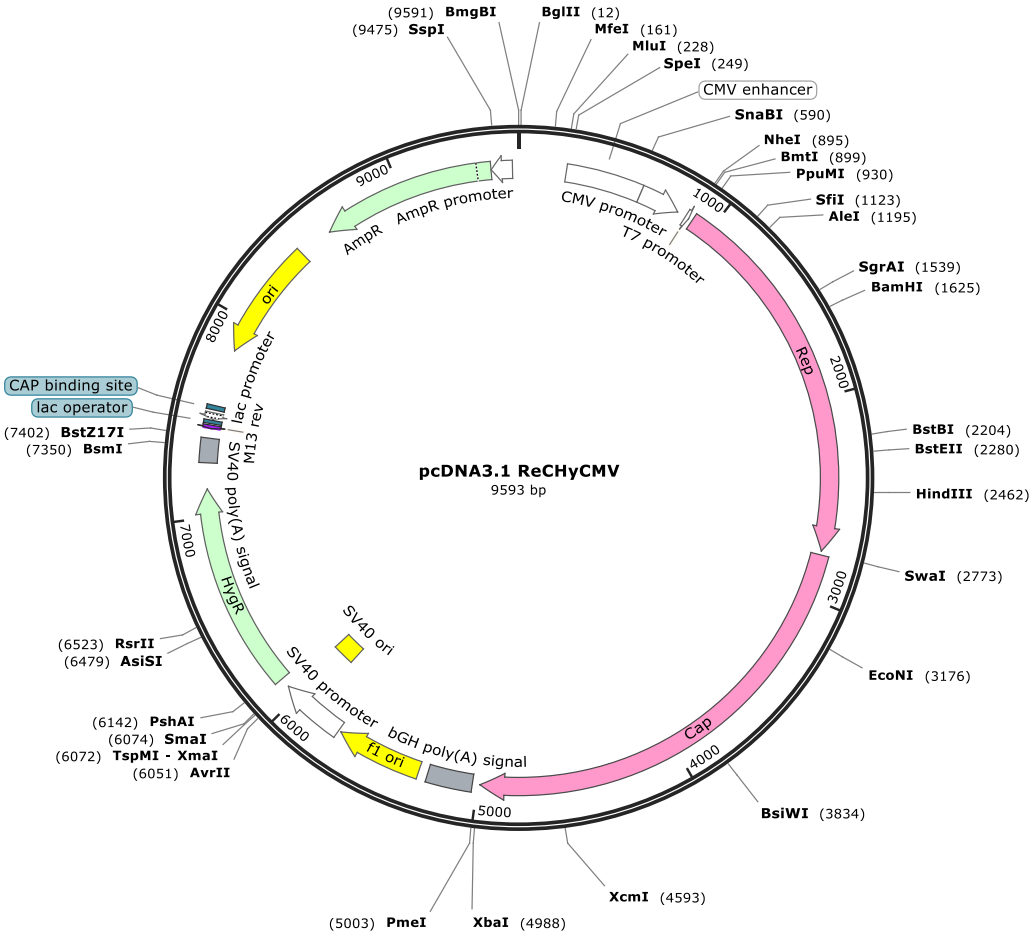

Appendix Figure X Schematic showing the vector map for the cloning vector pcDNA3.1 ReCHyCMV.

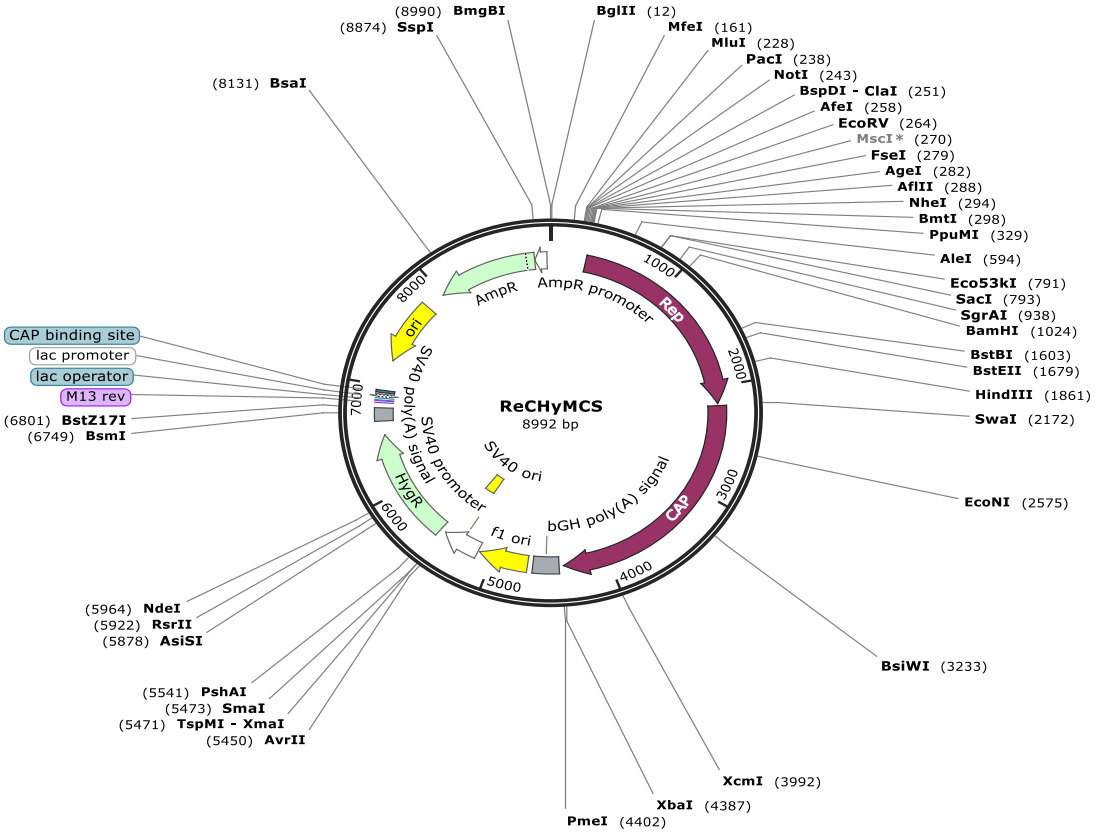

Appendix Figure XI Schematic showing the vector map for the cloning vector pcDNA3.1 ReCHyMCS.

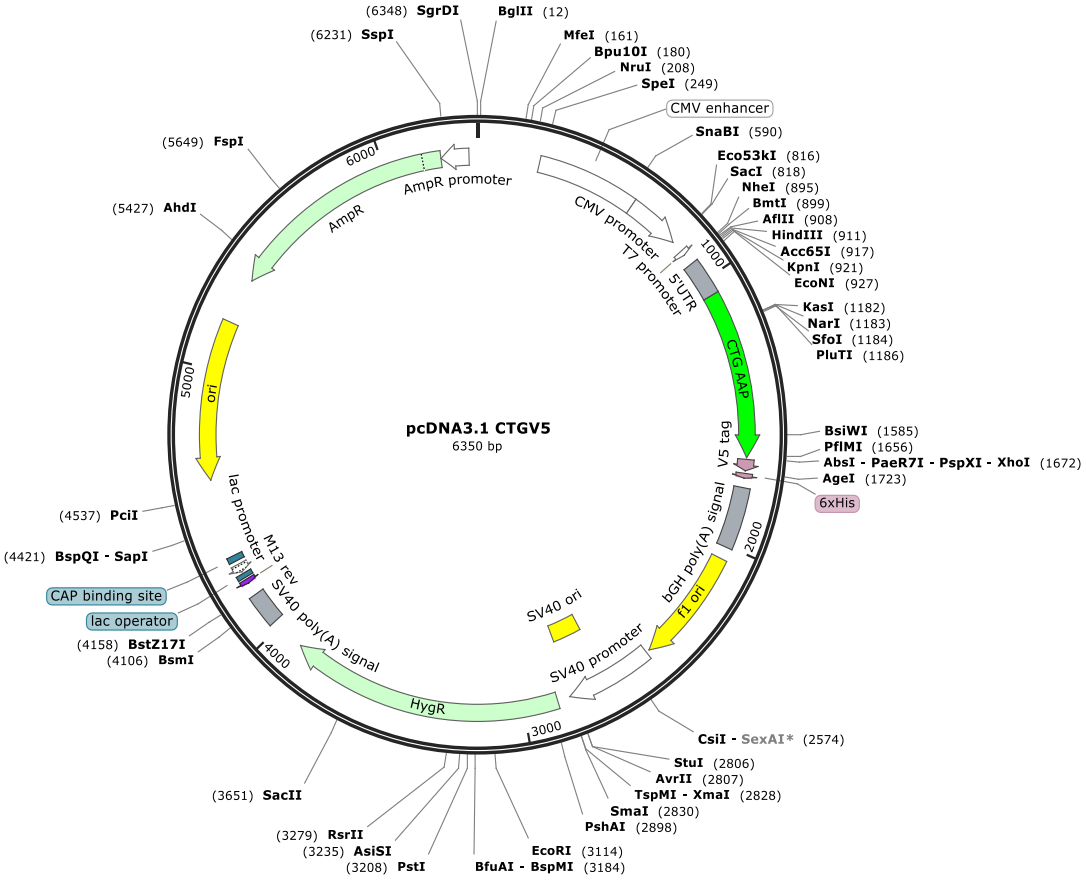

Appendix Figure XII Schematic showing the vector map for the cloning vector pcDNA3.1 CTGV5.

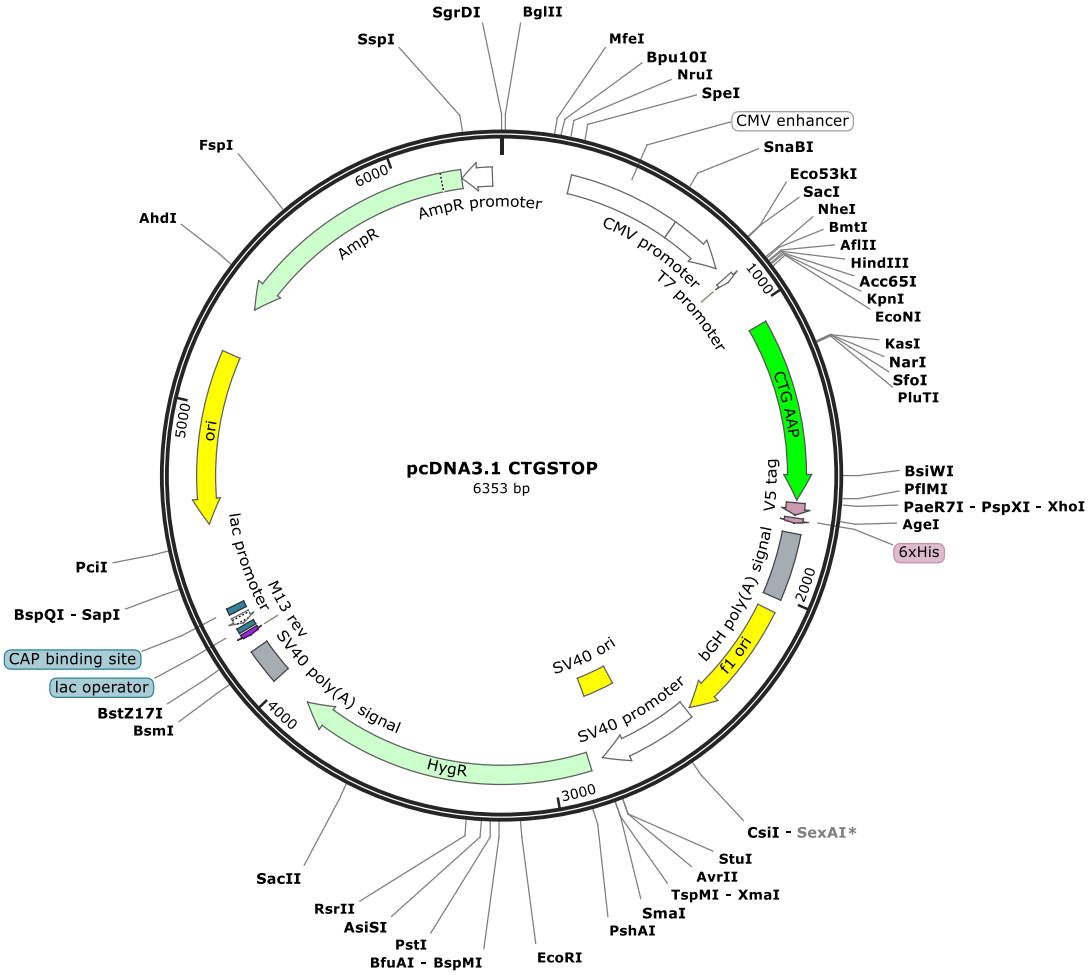

Appendix Figure XIII Schematic showing the vector map for the cloning vector pcDNA3.1 CTGSTOP.

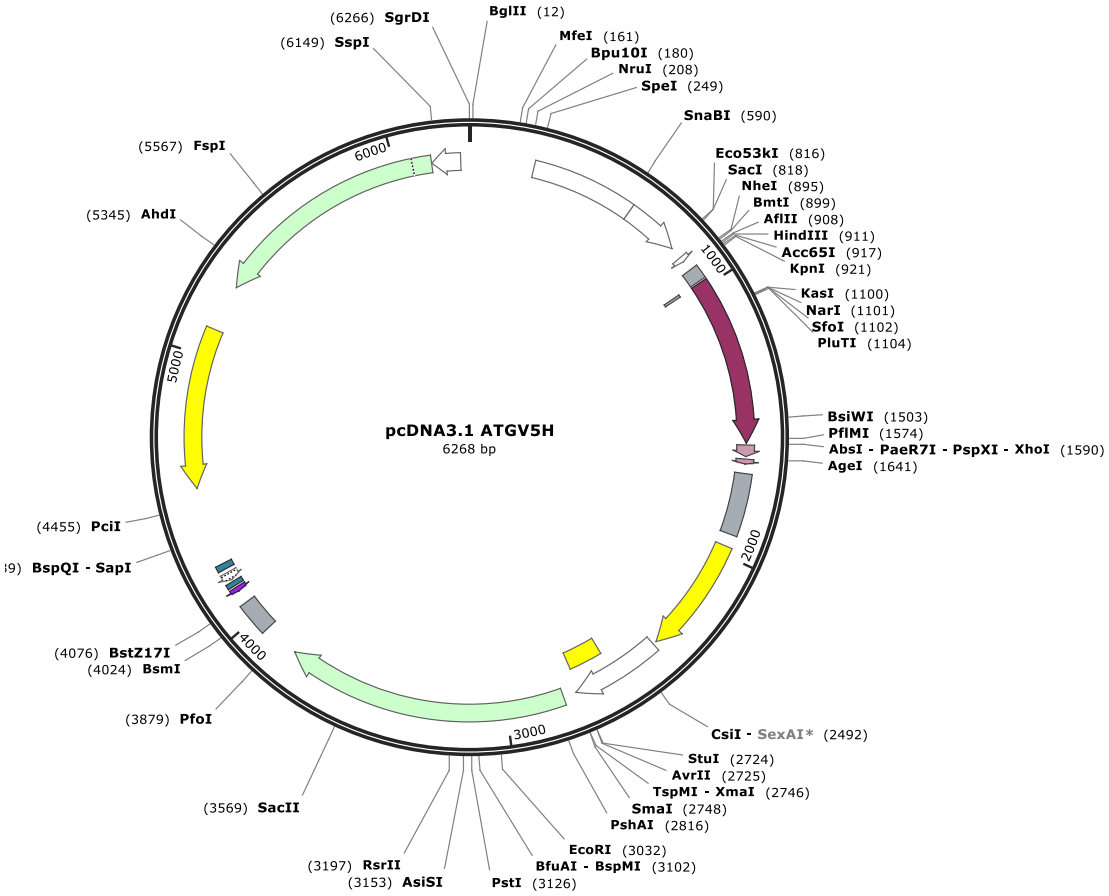

Appendix Figure XIV Schematic showing the vector map for the cloning vector pcDNA3.1 ATGV5.

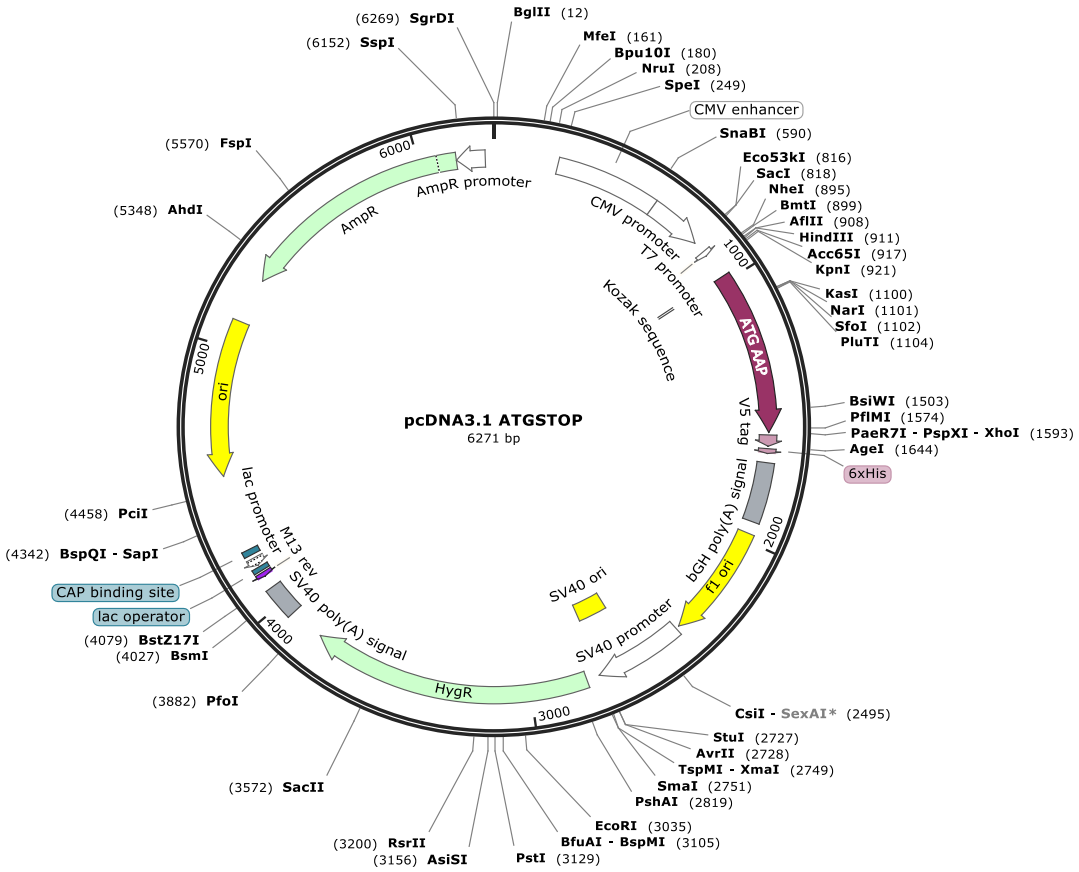

Appendix Figure XV Schematic showing the vector map for the cloning vector pcDNA3.1 ATGSTOP.

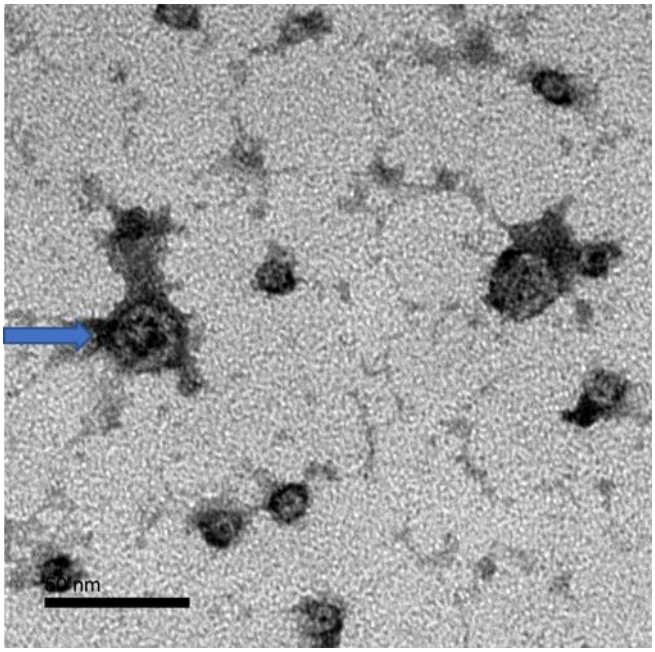

Appendix Figure XVI Electron microscopy of purified “Empty” rAAV particles lacking a transgene (Blue Arrow).